REPORT NO. FAA-RD-77-76

ENGINEERING SUMMARY OF POWERPLANT ICING TECHNICAL DATA

G. D. Pfeifer and G. P. Maier

JULY 1977

FINAL REPORT

Prepared for

U.S. DEPARTMENT OF TRANSPORTATION
FEDERAL AVIATION ADMINISTRATION
Systems Research & Development Service
Washington, D.C. 20590

NOTICE

This document is disseminated under the sponsorship of the Department of Transportation in the interest of information exchange. The United States Government assumes no liability for its contents or use thereof.

Technical Report Documentation Page

1. Report No.	2. Government Accession No.	3. Recipient's Catalog No.
FAA-RD-77-76		

4. Title and Subtitle	5. Report Date
ENGINEERING SUMMARY OF POWERPLANT ICING TECHNICAL DATA	July 1977
	6. Performing Organization Code
	8. Performing Organization Report No.

7. Author(s)	8. Performing Organization Report No.
G. D. Pfeifer and G. P. Maier	PWA-5522

9. Performing Organization Name and Address	10. Work Unit No. (TRAIS)
Commercial Products Division Pratt & Whitney Aircraft Group United Technologies Corporation East Hartford, Connecticut 06108	11. Contract or Grant No. DOT-FA76WA-3840
	13. Type of Report and Period Covered Final Report

12. Sponsoring Agency Name and Address	14. Sponsoring Agency Code
U. S. Department of Transportation Federal Aviation Administration Systems Research and Development Service Washington, D. C. 20591	

15. Supplementary Notes

16. Abstract

The problem of aircraft engine icing is caused by the existence of liquid water droplets in atmospheric clouds at temperatures below freezing. The disturbance resulting from an airplane flying through these supercooled droplets causes the formation of ice on the impinging surfaces. Aircraft engines ingest these droplets in concentrations of roughly fifty percent greater than the cloud concentration, and the first few stages of the engine compressor are subject to icing. Engine icing can be prevented, or at least kept within tolerable limits, by engine design procedures which utilize: the tendency of the rotor to shed ice by centrifugal effects before it gets too thick, the tendency of the fan to create warmer temperatures by compression, and various designs of active anti-icing systems.

This report provides the aircraft engine designer with appropriate backgound information, and with sufficient equations and design charts, and instructions regarding their use, such that a logical approach to the complex problem of engine ice prevention can be established and understood. A technical data review and discussion of current practices of test verification procedures are presented to give visibility to those areas of atmospheric icing phenomena which can be realistically simulated by experiments, and to point out those areas in which more research is needed.

17. Key Words	18. Distribution Statement
Aircraft Engine Icing Information Icing Protection Systems Design Anti-icing Data Review Test Verification Procedures	Document is available to the U.S. public through the National Technical Information Service, Springfield, Virginia 22161.

19. Security Classif. (of this report)	20. Security Classif. (of this page)	21. No. of Pages	22. Price
		210	

Form DOT F 1700.7 (8-72) Reproduction of completed page authorized

410116 LB

METRIC CONVERSION FACTORS

Approximate Conversions to Metric Measures

Symbol	When You Know	Multiply by	To Find	Symbol
	LENGTH			
in	inches	*2.5	centimeters	cm
ft	feet	30	centimeters	cm
yd	yards	0.9	meters	m
mi	miles	1.6	kilometers	km
	AREA			
in^2	square inches	6.5	square centimeters	cm^2
ft^2	square feet	0.09	square meters	m^2
yd^2	square yards	0.8	square meters	m^2
mi^2	square miles	2.6	square kilometers	km^2
	acres	0.4	hectares	ha
	MASS (weight)			
oz	ounces	28	grams	g
lb	pounds	0.45	kilograms	kg
	short tons (2000 lb)	0.9	tonnes	t
	VOLUME			
tsp	teaspoons	5	milliliters	ml
Tbsp	tablespoons	15	milliliters	ml
fl oz	fluid ounces	30	milliliters	ml
c	cups	0.24	liters	l
pt	pints	0.47	liters	l
qt	quarts	0.95	liters	l
gal	gallons	3.8	liters	l
ft^3	cubic feet	0.03	cubic meters	m^3
yd^3	cubic yards	0.76	cubic meters	m^3
	TEMPERATURE (exact)			
°F	Fahrenheit temperature	5/9 (after subtracting 32)	Celsius temperature	°C

*1 in = 2.54 (exactly). For other exact conversions and more detailed tables, see NBS Misc. Publ. 286, Units of Weights and Measures, Price $2.25, SD Catalog No. C13.10:286.

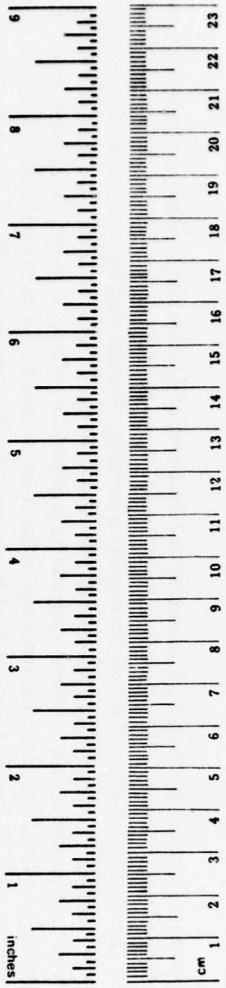

Approximate Conversions from Metric Measures

Symbol	When You Know	Multiply by	To Find	Symbol
	LENGTH			
mm	millimeters	0.04	inches	in
cm	centimeters	0.4	inches	in
m	meters	3.3	feet	ft
m	meters	1.1	yards	yd
km	kilometers	0.6	miles	mi
	AREA			
cm^2	square centimeters	0.16	square inches	in^2
m^2	square meters	1.2	square yards	yd^2
km^2	square kilometers	0.4	square miles	mi^2
ha	hectares (10,000 m^2)	2.5	acres	
	MASS (weight)			
g	grams	0.035	ounces	oz
kg	kilograms	2.2	pounds	lb
t	tonnes (1000 kg)	1.1	short tons	
	VOLUME			
ml	milliliters	0.03	fluid ounces	fl oz
l	liters	2.1	pints	pt
l	liters	1.06	quarts	qt
l	liters	0.26	gallons	gal
m^3	cubic meters	35	cubic feet	ft^3
m^3	cubic meters	1.3	cubic yards	yd^3
	TEMPERATURE (exact)			
°C	Celsius temperature	9/5 (then add 32)	Fahrenheit temperature	°F

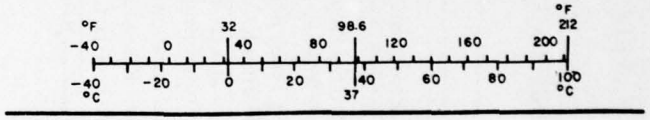

TABLE OF CONTENTS

TABLE OF CONTENTS (Cont'd)

TABLE OF CONTENTS (Cont'd)

LIST OF ILLUSTRATIONS

LIST OF ILLUSTRATIONS (Cont'd)

LIST OF ILLUSTRATIONS (Cont'd)

LIST OF ILLUSTRATIONS (Cont'd)

LIST OF ILLUSTRATIONS (Cont'd)

LIST OF TABLES

CHAPTER I INTRODUCTION, SUMMARY, AND RECOMMENDED PROCEDURES

1.1 INTRODUCTION

The intent of this report is to provide a technical reference document which can be used by aircraft powerplant design engineers as a guide in designing powerplant ice protection systems. A similar document, FAA Technical Report No. ADS-4 (Reference 1), was issued in 1964 to serve the needs of airframe anti-icing designers, but contained no information specifically for powerplants. This report supplements the ADS-4 report by providing an engineering summary of powerplant icing technical information, and thereby greatly enhances the FAA library of technical design anti-icing summaries for the total flying machine.

The user of this report should keep in mind that the overall subject of atmospheric icing is a highly complex technical field in which unresolved questions and puzzling phenomena continue to be researched by various organizations in industry and government. Recently-available research results have been incorporated, whenever possible, into the body of this report in order to make the recommended analytical and test procedures as up-to-date as possible at the present time. The incorporation of such up-dates during the preparation of this report has required examination of past procedures - - analytical and test, as well as field experience. What has been found is similar to detailed examination of any scientific procedure. Simplifying assumptions are required to make analyses possible, imperfect simulations are required in demonstration tests, and field service data are not always sufficiently specific or well correlated. Thus, engineering judgement must be used to provide the conservative approaches required in both analysis and test to compensate for uncertainties. Although the procedures set forth in this report to assess powerplant icing are deemed proper, the results of this contract investigation may lead to future recommendations to improve some specific approaches.

The overall procedure recommended in this report is to assess by analysis which parts do and which parts do not require anti-icing protection. Those parts which are marginal should be tested for determination. In addition to icing tests, ice ingestion tests are recommended to ensure that the powerplant installation can safely withstand ice breakup and ingestion. Thus, the overall procedure, while not completely definable with design analytical calculations, provides thorough ice protection designs for the powerplant parts as required for severe meterological icing conditions. For more severe, yet statistically rare conditions, the powerplant should be designed and demonstrated to be sufficiently tolerant to withstand ice buildup and subsequent ingestion. The industry has now amassed considerable experience in the techniques of avoiding ice accumulation and flight-safety incidents as demonstrated in millions of hours of actual flight. This is in part due to inherent conservation in the analyses, tests and operating procedures. Thus, a significant part of the design process should always be judgement which takes into account not only analysis and test but also field experience and knowledge of the limitations of the overall system.

In accordance with the foregoing introductory remarks, the body of the report which follows presents the current state-of-the-art of powerplant icing technical information, including analysis of NACA atmospheric icing condition data for design-point selection, recommended analytical tools and techniques for assessing engine icing and designing anti-icing systems, and a discussion of test verification procedures.

1.2 SUMMARY

The problem of aircraft engine icing is caused by the existence of liquid water droplets in atmospheric clouds at temperatures below freezing. The disturbance of an airplane flying through these supercooled droplets causes the formation of ice on the impinging surfaces. Aircraft engines ingest these droplets in concentrations of roughly fifty percent greater than the cloud concentration, and the first few stages of the engine compressor are subject to icing. Engine icing can be avoided, or at least kept within tolerable limits, by engine design procedures which utilize: (a) the tendency of the fan to create warmer temperatures by compression effects, (b) various designs of active anti-icing systems, and (c) the tendency of the rotor to shed ice by centrifugal effects before it gets too thick.

This report is intended to provide the aircraft engine designer with appropriate background information, and with sufficient equations, design charts, and instructions regarding their use, such that a logical approach to the complex problem of engine ice prevention can be established and understood. A technical data review and discussion of current practices of test verification procedures are presented to give visibility to those areas of atmospheric icing phenomena which can be realistically simulated by experiments, and to point out those areas in which more research is needed.

The following section constitutes an outline of recommended procedures for the anti-icing design engineer. This section includes several subsections:

Atmospheric Environmental Design Points
Engine Water Ingestion Rates
Water Droplet Impingement on Engine Surfaces
Assessment of Whether or Not Anti-Icing is Required
Ice Accumulation Calculations and Ice Accumulation Limits
Design of Anti-Iced Parts
Test Verification

Detailed discussion of these subjects is covered in later chapters. A flow-chart summary of the recommended analytical design procedure is presented on Figure 1-1. This procedure is applicable for small to large powerplants installed in fixed and rotary-wing aircraft.

1.3 RECOMMENDED PROCEDURES OUTLINE

The following recommended procedures represent the present-day state-of-the-art design guide established as a result of the extensive study and literature review performed during the preparation of this report. Recently available improvements to past procedures have been incorporated into this list, and some of the items may be subject to updating revisions as future research data becomes available. It is also expected that modifications to suit specific installations and unique requirements may be appropriate in some instances as dictated by engineering judgement.

1.3.1 Atmospheric Environmental Design Points

1. The general atmospheric Icing Conditions parametric charts defined by FAR Part 25 Appendix C (Appendix A of this report) should be used for engine icing design.

    a. Icing in ice-crystal atmospheres, including snow, is not included in the FAR Part 25, Appendix C, and is not considered to be an engine problem.

    b. Icing in the atmospheric condition classed as "Instantaneous Maximum Icing", which can be occasionally experienced for short (5 second) time durations, is not included in the FAR Part 25, but may be a minor design consideration for engine icing.

2. The atmospheric temperature versus altitude "Single Operating Line" shown in this report on Figure 2-14 should be used to define a suitable "Icing Day" for design purposes. A Standard Day atmospheric Pressure versus Altitude curve is considered adequate.

3. A mean effective water droplet diameter (as specified by the FAA in Advisory Circular AC No. 20-73, Reference 3, and defined by d_m in the Nomenclature of this report) of 20 microns is recommended for all engine water ingestion, water impingement, and other icing design calculations, except for the establishment of the extent of wetted surface impingment limits, and except for Freezing Rain design calculations.

    a. To determine the geometric extent of water impingement, a conservative 40 micron mean effective droplet diameter should be used.

    b. Design values of atmospheric liquid water content (LWC) should be obtained from the Cumuliform Cloud LWC curves of Figure 2-16, read at the temperatures of the Single Operating Line, and at 20 micron droplet diameter. Exceptions to this are the same as those noted in Recommendation 6.

    c. Freezing rain atmospheric water droplet characteristic diameters are not well defined. Values of 20, 30, or 40 microns are all considered suitable assumptions for engine icing design calculations.

4. In general, engine icing design calculations should be based on continuous flight through cumuliform clouds (i.e., steady-state operation through cloud liquid water contents corresponding to the Intermittent Maximum atmospheric icing conditions of Figure 2-16).

5. In conjunction with Recommendation 4, the general recommended values of the liquid water content (LWC) horizontal-extent correction factor (Figure A-6) is 1.0, in spite of the longer horizontal extents implied by Recommendation 4.

6. There are three recommended exceptions to Recommendations 4 and 5.

   a. For ice-accumulation calculations over extensive time periods, it is considered appropriate to base such calculations on the Stratiform Cloud atmospheric icing conditions of Figure 2-17.

   b. For short-time duration transient ice accumulation calculations, the appropriate values of LWC correction factors greater than 1.0 on Figure A-6 should be applied to the LWC values of Figure 2-16.

   c. For gound level freezing rain and other low-altitude icing design work, the Stratiform Cloud atmospheric icing conditions of Figure 2-17 are recommended.

7. Recommendations 1 through 6 constitute the recommended Atmospheric Environment Design Points to be used in engine icing designs.

1.3.2 Engine Water Ingestion Rates

8. It is recommended that basic engine inlet water ingestion rates should be based on the NACA TN 4268 data shown on Figure 3-2, unless specific more precise data can be obtained. Typical in-flight liquid water contents in the basic inlet range from 0.6 to 1.5 times the liquid water content of the atmosphere.

9. It is further recommended that engine water ingestion rates in the flow splitter duct behind the fan should also be based on the NACA TN 4268 data of Figure 3-2, with the approaching streamline areas determined from the aerodynamic flow-split considerations discussed in Section 3.1.1.1. (This recommendation also can be replaced by specific more precise data, if available.) Typical liquid water contents in the splitter duct are 1.5 times the liquid water content of the basic inlet.

10. In order to obtain a non-trivial numerical solution for water ingestion rates when Recommendation 8 is applied to ground-static engine operation, it is recommended that a free-stream wind velocity of 30 mph be assumed. Resulting inlet liquid water contents are about ½ of ambient liquid water content.

1.3.3 Water Droplet Impingement on Engine Surfaces

11. For design calculations on any engine surface, it is recommended that the water droplet temperature be held at its atmospheric free-stream value, regardless of ram effects and compression effects on engine air temperature.

12. Liquid water droplet impingement rates on engine surfaces should be calculated by using the standard analytical techniques which employ either the "total impingement efficiency," (E_m), or the "local impingement efficiency," (β).

13. It is recommended that the wealth of experimental data which is available in the literature for E_m on airplane wing airfoils should be disregarded in engine analyses. It is considered that differences in droplet trajectory behavior around wings, as opposed to engine compressor airfoils, are too pronounced for valid interpolation of these data.

14. It is recommended that engine airfoil water droplet impingement rates should be calculated based on the local impingement efficiency β, which is conservatively assumed to be 1.0 at the foil stagnation region and decreases with the cosine of the local surface inclination angle thereafter, as shown on Figure 3-18.

15. It is recommended that engine nose-cap water droplet impingement rates should be based upon appropriate interpolation and/or extrapolation among various data presented on Figures 3-10 through 3-17, which summarize representative literature data for either E_m or β on spheres, ellipsoids, and cones. According to Reference 18, typical overall impingement efficiencies of nose caps are about 0.12 for a moderately slender shape, and about 0.03 for a blunted shape.

16. It is considered that engine nose-cap water impingement rates, calculated in accordance with Recommendation 15, can be applied with equal accuracy to both rotating spinners and non-rotating nose caps. (It is noted here that there are many icing considerations which show vast differences between rotating and non-rotating nose caps, but the water impingement rate itself does not appear to be one of them.)

1.3.4 Assessment of Whether or Not Anti-Icing is Required

17. The determination of whether a given part of the engine will or will not require active anti-icing depends upon the combined effects of the atmospheric environment icing Design Points, and the water ingestion and heat-of-compression effects of the engine at various power levels. Hence flight cycle analyses are required.

18. The use of the popular and easily-calculated "Datum Temperature" method for determining engine wetted surface temperatures should be restricted to preliminary flight cycle analyses only. Un-heated engine surfaces which show only marginal freedom from excessive icing should be reanalyzed with more accurate detailed flight-cycle calculations.

19. The "Datum Temperature" procedure in the preliminary flight-cycle analysis is considered an adequate and advantageously fast method of identifying those engine surfaces which definitely will require active anti-icing, and those surfaces which are sufficiently far back in the engine so as to definitely not require anti-icing.

20. Detailed flight cycle analyses should be performed with accurate, specially generated, engine aerodynamic performance tables which correspond to operation on the "Icing Day" Single Operating Line. These performance tables should include points of intermittent engine rev-up during ground idle, and powered descents.

21. Detailed flight cycle analyses should use the true equilibrium wetted surface heat balance equations to assess the temperature of non-anti-iced surfaces, and to assess the required heat load of anti-iced surfaces.

1.3.5 Ice Accumulation Calculations and Ice Accumulation Limits

22. Ice accumulation on any surface is considered to be adequately calculated by simple integrations of the various water impingement rates over the flight cycle time duration for which the surface is below freezing, The ice freezing-fraction term available from the true equilibrium wetted surface heat balance equation may be incorporated if desired, and will increase the accuracy but decrease the conservatism.

23. Rotating nose caps (spinners) may, or may not require active anti-icing, depending upon the ice accumulation/shedding characteristics of the spinner, the engine structural ability to ingest a sudden release, and engine tolerance to unbalance due to non-uniform accumulation and shedding characteristics. For design purposes, recommended ice-accumulation limits for spinners are the lesser of:

    a. A total non-shedding accumulation, over the flight cycle icing time duration, of less thickness than is actually ingested in proof-testing of engine ingestion experiments, or

    b. A total non-shedding accumulation, over the flight cycle time duration, of less thickness than that which could induce a rotor vibration problem.

    This recommendation can be replaced by demonstration tests to show that the spinner in question always sheds its ice well before the accumulation has reached either of the above limits.

24. Fan blades and other rotating compressor blades have demonstrated over many years of flight experience that their ice accumulation/ice shedding characteristics are compatible with engine tolerance to ice ingestion. No recommendation regarding the calculation of ice accumulation or the evaluation of the magnitude of icing limits on fan blades and other compressor rotating foils is available at the present time.

25. Non-rotating nose caps generally require an active anti-icing system. The system may be sized to allow some ice to accumulate during short-term "worst icing" transients. Allowable ice accumulation during such transients should be limited to a thickness or chunk size less than is readily ingested without engine damage as proven during demonstration testing.

26. Engine compressor inlet guide vanes located upstream of the fan generally require an active anti-icing system. The system may be sized to allow some ice to accumulate during short term "worst-icing" transients. Allowable ice accumulation during such transients is the lesser of:

a. same limit as for non-rotating nose caps, applied to the total of all vanes.

b. the thickness and/or location that would impair aerodynamic performance. (This limit is usually different for each engine model.)

27. Compressor stator vanes located downstream of the fan may, or may not require active anti-icing, depending on whether or not the heat of compression is adequate to preclude intolerable icing. Some ice may be allowed to accumulate during short-term "worst-icing" transients, and ice accumulation limits for compressor stator vanes are the same as items 26a and b, applied to stator vanes.

28. For engine probes on which icing could affect flight safety, icing should in general be limited to zero accumulation, unless the probe is equipped with a de-icing system to completely remove ice in the event of sensor malfunction. For probes on which icing does not affect flight safety, the accumulation limit is the maximum ice chunk size of safe ingestion.

1.3.6 Design of Anti-Iced Parts

29. For anti-iced parts, the recommended heated surface temperature is 35°F, with corresponding heat fluxes sufficient to establish a "running wet" condition.

30. Final selection of the optimum Design Point for anti-iced surfaces should be deduced from detailed heat-balance calculations of required heat loads at each point of the flight cycle.

a. For electrical anti-icing systems, it appears that the mid-climb region of the flight cycle represents the worst anti-icing condition, and is the recommended optimum Design Point for sizing electric current capacity requirements.

b. For hot-air compressor-bleed anti-icing systems, the worst anti-icing condition generally occurs during the mid-descent region of the flight cycle.

c. Powered descents are generally recommended in severe icing conditions. Recommendation 30b is still true, even for powered descents.

d. Intermittent power rev-ups during ground-idle appear to be a necessity in severe freezing rain.

e. For hot-air compressor-bleed anti-icing systems, the next worst anti-icing condition is apt to be a long time duration holding condition of the flight cycle.

f. For hot air compressor bleed anti-icing systems, the recommended optimum Design Point for sizing the system is either power descent or a conservatively modified holding condition, depending on detail design considerations.

31. The final anti-icing system design should be analyzed for heat-available versus heat-required over the entire flight cycle. Regions of likely icing should be further assessed to assure that any ice accumulation is, indeed, tolerable.

1.3.7 Test Verification

32. Acceptable means of compliance for FAA icing certification tests are usually agreed to on an engine-by-engine basis with the manufacturer.

33. Ice ingestion demonstration tests should be performed, with sheet ice and chunk ice samples which simulate the sizes of probable in-flight encounters. It is noted here that ingestion tests of hailstones (one or two inches diameter) are mandatory under FAR Part 33.77, which is reproduced as Appendix E in this report.

34. The engine test facility should incorporate sufficient distance between the water spray nozzles and the engine inlet, in order to assure adequate cool-down of the water droplets. Water spray nozzles should produce a mean effective droplet diameter equal to that specified in the Regulation Specs. (normally 20 microns).

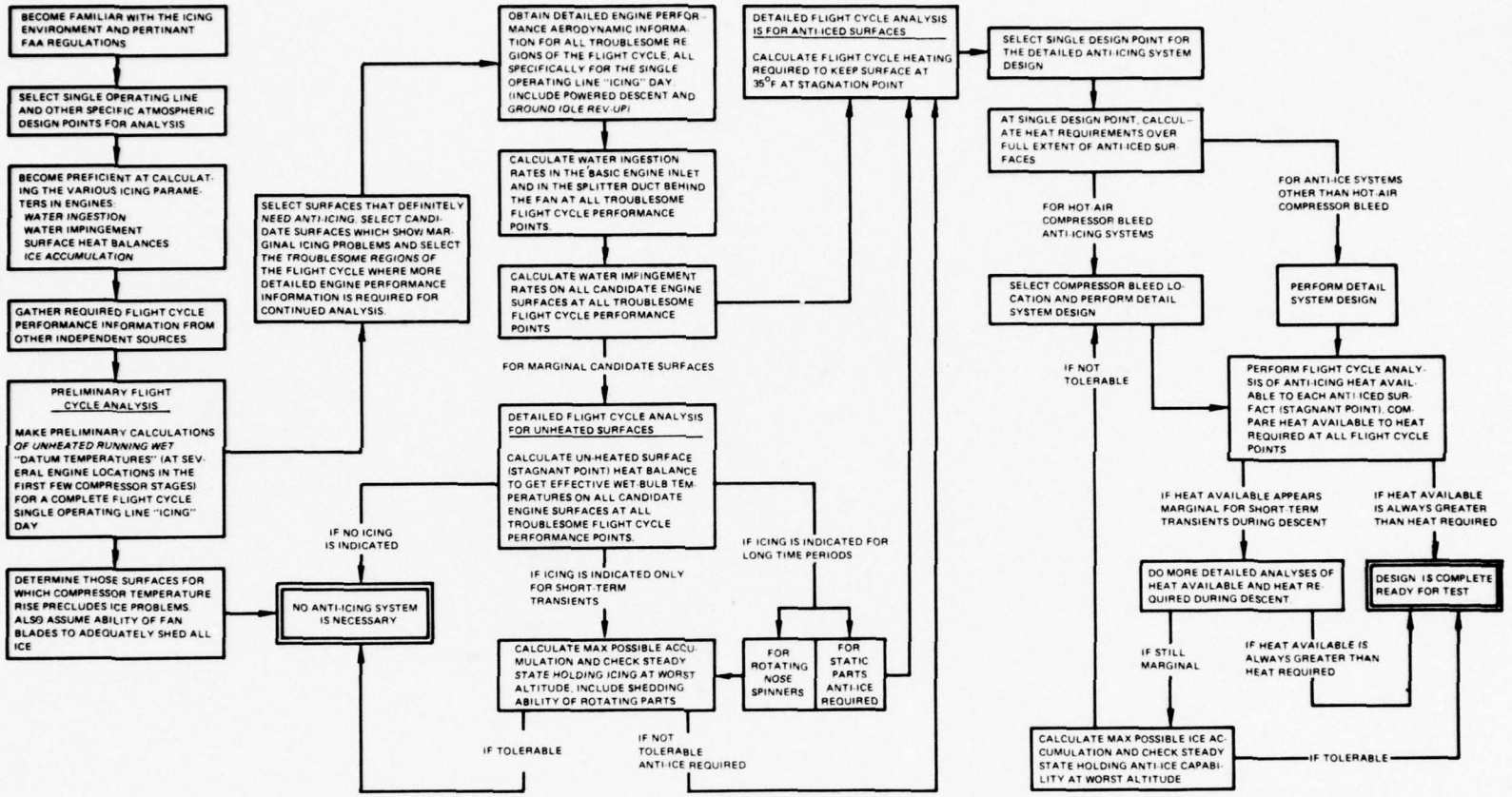

Figure 1-1 Aircraft Engine Icing Protection, Analytic Design System Summary

CHAPTER II DESIGN POINT SELECTION

This section presents details on atmospheric icing condition analyses required to ascertain suitable design points. Whereas the presentation of Atmospheric Icing Conditions in Section 2.1 is essentially a repeat of the statistical data already documented in Reference 1, it is considered appropriate to include the summary in this report so that various powerplant-related items pertaining to design point selection can be conveniently presented in their proper context.

2.1 ATMOSPHERIC ICING CONDITIONS

The fundamental atmospheric condition which causes aircraft icing is the occasional presence of small water droplets which exist as supercooled liquid in air at below-freezing temperatures. Because supercooled liquid is a thermodynamic state of metastable equilibrium, a significant physical disturbance such as a flying aircraft causes the droplets to rapidly change to the stable-equilibrium state of ice on the impinging surfaces. There are three major types of atmospheric environments in which supercooled liquid droplets are known to exist in nature.

(a) Stratiform clouds (or layer clouds). These clouds have relatively low to moderate liquid water content and long horizontal extent associated with continuous icing.

(b) Cumuliform clouds. These clouds have moderate to high liquid water content and relatively short horizontal extent associated with intermittent severe icing.

(c) Freezing rain and other low-altitude icing.

The icing characteristics of these three types of environments has been the subject of many years of research, performed primarily in the United States by the National Advisory Committee for Aeronautics (now NASA), and various other cooperating groups. These data describe the important environmental icing parameters of temperature, water concentration, and droplet size, but because they necessarily incorporate probability complexities of scientifically characterizing cloud formations, the data are statistical in nature and involve considerations of the probability of natural simultaneous occurrence of the aforementioned parameters at various altitudes. Fortunately, the NACA statistical data have already been summarized into working charts of design standards, currently in use by the FAA as part of their Federal Aviation Regulations documents - - i.e., FAR Part 25. Whereas the recommended procedure in this powerplant icing report is to use the FAR charts directly to obtain design input parameters of atmospheric icing conditions, it is of interest to first briefly discuss the statistical data upon which the charts are based. (The brief statistical data discussion which follows is essentially a condensed version of a more detailed similar discussion in ADS-4, Chapter 1.)

2.1.1 The NACA Statistical Data

2.1.1.1 Stratiform Clouds

Stratiform clouds are characterized by low to moderate liquid water content (LWC-0.1 to 0.8 gm/m^3), maximum probable cloud depth of 6500 feet above the cloud base, mean effective droplet diameters (dm) of 10 to 40 microns, temperatures of 32°F to -22°F, cloud-base altitudes of 3000 ft to 22,000 ft., and horizontal extents of 20 miles to 200 miles. Figure 2-1, taken directly from ADS-4, shows that the "liquid water content" of interest for aircraft icing exists only when the free air temperature is below the dew point. Hence, LWC values, commonly expressed in grams of liquid water per cubic meter of air, include only the water in supercooled droplet form and do not include any water in vapor form. The LWC in stratiform clouds tends to increase uniformly as ambient air temperature decreases with cloud height. It is observed that stratiform icing encounters in flight are most likely to occur at altitudes from 3,000 to 6,000 ft. Icing encounters above 22,000 ft. are rare, and the minimum icing temperature appears to be about -22°F.

2.1.1.2 Cumuliform Clouds

Typical isolated cumuliform clouds may vary from two to six miles in horizontal extent at altitudes from 4,000 to 24,000 ft., with moderate to high LWC of 0.2 to 2.5 gm/m^3 or more, and mean droplet diameters of 15 to 50 microns or larger. However, statistical data indicates that maximum values of drop size and LWC are not likely to occur simultaneously. Figures 2-2a and 2-2b, also taken directly from ADS-4, shows properties of two separate cumuliform clouds. Inspection of Figure 2-2a and -b shows that these cumuliform cloud depths are about 5,000 ft., and the liquid water content distribution with cloud depth is not as uniform as was previously observed in stratiform clouds. Whereas Figure 2-2a shows an ambient temperature range from 30°F to 28°F, other cumuliform cloud data indicates that icing conditions have been observed at temperatures around -15°F. The minimum temperature established by laboratory tests for the existence of supercooled water droplets is -40°F. Cumuliform icing encounters tend to be of relatively short time duration (about 1 minute) because the cloud horizontal extent is short, but can be about two to three times as severe as stratiform icing because of high liquid water content. Cumuliform icing encounters are most likely to occur at altitudes from 8,000 to 12,000 ft. Although icing encounters above 22,000 ft., are rare, and the minimum icing temperature appears to be about -22°F, there is some evidence that these apparent limits should be extended to 30,000 ft. and -40°F.

2.1.1.3 Freezing Rain and Other Low-Altitude Icing

Although reports from aircraft that have encountered freezing rain are not a rarity, quantitative atmospheric data on freezing rain are virtually non-existent. According to NACA TN 1855 (Reference 6), freezing rain is characterized by some large droplets (up to 1000 microns), temperatures of 32°F to 25°F, altitudes from 0 to 5,000 ft., and liquid water content of about 0.15 gm/m^3 (which corresponds to a rain-fall rate of about 0.1 inch per hour). Horizontal extent may be as much as 100 miles. Supplementary freezing rain data (Reference 1-22 of ADS-4) seem to suggest that these conditions represent realistic values for design purposes.

Other low-altitude icing data is presented on Figure 2-3, taken directly from ADS-4. These data show that the liquid water content is reduced below stratiform-cloud values in low altitude icing environments. Thus, design use of the liquid water contents for normal stratiform clouds will produce systems that are more than adequate for very low altitude operation.

2.1.1.4 Icing Envelopes and Classes of Clouds

For the stratiform and cumuliform cloud environments characterized in the preceding paragraphs, the available NACA data includes charts of temperature versus altitude which show the relative frequency of icing-condition occurrences observed at the various temperature and altitude coordinates. These charts are shown on Figures 2-4 and 2-5, taken directly from NACA TN 2569. These charts are very useful for defining the boundaries of atmospheric "icing envelopes", i.e., bounding the range of atmospheric air temperatures in which icing conditions have been observed at various altitudes. For example, Figure 2-5 shows that an airplane flying through cumuliform clouds at 10,000 ft. can expect icing conditions to be prevalent if the free air temperature is between 26°F and -7°F, with the most frequent occurrences at 14°F.

In addition to characterizing the three major types of icing environments (a), (b) and (c) above, the NACA data classifies the relative severity of icing conditions which may be expected in the various environments. The class distinctions are shown in Table 2-I, taken directly from NACA TN 1855. On this figure, the Class I and Class II severities (Instantaneous and Intermittent icing) pertain to cumuliform cloud environments, and the continuous encounters of Class III severity pertain to stratiform cloud environments. The Class IV freezing rain encounters do not include the low-altitude data of Figure 2-3 which was not available until a later date. One observation that can be made from Table 2-I is that, within each class at a given temperature, the liquid water content tends to decrease as the droplet diameter increases. This appears to be a basic characteristic of all clouds, and is due to the very low probability that maximum droplet size and maximum LWC will occur simultaneously within the cloud formation. Another observation from Table 2-I is that the liquid-water content for short-duration encounters is substantially higher than the LWC for long-duration encounters. This observation is shown more completely on Figure 2-6 taken directly from NACA TN 2738. This figure shows the probable change of liquid water content in cumulus clouds and layer clouds as their respective horizontal extents vary from a characteristic average. The data shown on this figure incorporates probability analyses as denoted by the symbol P_e. According to NACA 2738 (Reference 8), P_e is the "probability that any random icing encounter will be characterized by a combination of values of the variables (LWC, T, dm) in which each variable must, respectively, equal or exceed a specified value of that variable".

Specific exceedance probability curves for the various icing parameter of LWC, droplet diameter, ambient temperature, and distance flown in icing, are presented in Figures 2-7 thru 2-10. These figures, taken directly from ADS-4, show data taken by the ADS-4 authors from the NACA and NASA reports referenced thereon. To read Figure 2-7, for example, consider a liquid water content of, say, 0.8 gm/m^3. The figure indicates that the exceedance probability of this LWC in cumulus clouds is 45 percent (i.e., in cumulus clouds, the actual LWC will be greater than 0.8 gm/m^3 in 45 out of 100 icing encounters). The corresponding exceedance probability for layer clouds is somewhere between 4 percent and less-than-one percent, depending on the data source.

TABLE 2-I

RECOMMENDED VALUES OF METEOROLOGICAL FACTORS FOR CONSIDERATION IN THE DESIGN OF AIRCRAFT ICE-PREVENTION EQUIPMENT

(COPIED FROM TABLE I OF NACA TN 1855, REF. 6)

Class	Item	Air Temp. (°F)	Liquid Water Content (g/m^3)	Drop Diameter (Microns)	Pressure Altitude (ft)	Remarks
I-M Instantaneous Maximum	1	32	5.0	25	18,000 to 20,000	Horizontal extent: ½ mile. Duration at 180 mph: 20 seconds. Characteristic: *Very high liquid water content.* Applicable to: Any part of the airplane, such as guide vanes in inlet ducts, where a sudden large mass of supercooled water would be critical, even though of short duration. Example: Induction systems, particularly turbine-engine inlets.
	2	14	4.0	25	22,000 to 25,000	
	3	- 4	3.0	25	25,000 to 30,000	
	4	-22	2.0	20	20,000 to 30,000	
	5	-40	0.5	15	20,000 to 30,000	
I-N Instantaneous Normal	6	32	1.0	20	10,000 to 20,000	
	7	14	1.0	20	10,000 to 25,000	
	8	- 4	0.6	18	12,000 to 30,000	
	9	-22	0.2	15	15,000 to 30,000	
	10	-40	<0.1	13	15,000 to 30,000	
II-M Intermittent Maximum	11	32	2.5		10,000 to 15,000	Horizontal extent: 3 miles Duration at 180 mph: 1 minute Characteristic: High liquid water content Applicable to: Any critical component of the airplane where ice conditions, even though slight and of short duration could not be tolerated. Example: Induction systems, windshields when continuous visibility is required.
	12	14	2.2		10,000 to 20,000	
	13	- 4	1.7	20	12,000 to 30,000	
	14	-22	1.0		15,000 to 30,000	
	15	-40	0.2		15,000 to 30,000	
	16	32	1.3		8,000 to 15,000	
	17	14	1.0		8,000 to 20,000	
	18	- 4	0.8	30	10,000 to 30,000	
	19	-22	0.5		15,000 to 30,000	
	20	-40	0.1		15,000 to 30,000	
	21	32	0.4		8,000 to 15,000	
	22	14	0.3		8,000 to 20,000	
	23	—	0.2	50	10,000 to 30,000	
	24	-22	0.1		15,000 to 30,000	
	25	-40	<0.1		15,000 to 30,000	
II-N Intermittent Normal	26	32	0.8	20	8,000 to 12,000	
	27	14	0.6	20	8,000 to 15,000	
	28	- 4	0.4	18	12,000 to 20,000	
	29	-22	0.1	15	15,000 to 25,000	
	30	-40	<0.1	13	15,000 to 25,000	
III-M Continuous Maximum	31	32	0.8		3,000 to 20,000	Horizontal extent and duration: Continuous. Characteristic: Moderate to low liquid water content for an indefinite period of time. Applicable to: All components of the airplane: that is, every part of the airplane should be examined with the question in mind, "Will this part be affected seriously by accretions during continuous flight in icing conditions?" Example: Wings and tail surfaces.
	32	14	0.6			
	33	- 4	0.3	15		
	34	-22	0.2			
	35	-40	0.05			
	36	32	0.5			
	37	14	0.3			
	38	- 4	0.15	25		
	39	-22	0.10			
	40	-40	0.03			
	41	32	0.15			
	42	14	0.10			
	43	- 4	0.06	40		
	44	-22	0.04			
	45	-40	0.01			
III-N Continuous Normal	46	32	0.3			
	47	14	0.2	15		
	48	- 4	0.1			
	49	-22	<0.1			
IV-M Freezing Rain	50	25 to 32	0.15	1000	0 to 5,000	Horizontal extent: 100 miles. Duration at 180 mph: 30 minutes. Characteristic: Very large drops at near-freezing temperatures and low values of liquid water content. Applicable to: Components of the airplane for which no protection would be supplied after considering classes I, II, and III. Example: Fuselage static pressure airspeed tests.

For this report, it is suggested that one simply consider that the term P_e on Figure 2-6 represents the probability that the three variables (LWC, T, and dm) will all three depart from a specified set of (LWC, T, dm) simultaneously - - i.e., three at a time, while the curves of Figures 2-7 thru 2-10 represent the specific probability that any one of the variables within a set will be individually exceeded - - i.e., one at a time. In this way, one can get some appreciation of the scientific uncertainties associated with the ultimate definitions of atmospheric icing conditions.

For a more thorough understanding of the NACA probability and statistical data, the reader is referred to the specific NACA reports referenced. The main purpose for presenting the brief summary of these data in the preceding paragraphs is to afford the reader a cursory appreciation of the complexities and uncertainties which are implicitly contained in the culmination of the foregoing data, i. e. in the Federal Aviation regulatory design standards for defining atmospheric icing conditions.

2.1.2 Regulatory Design Standards

2.1.2.1 The FAR Part 25 Design Standards

The Federal Aviation Regulations for design standards to define atmospheric icing parameter ranges of temperature, liquid water content, and droplet size, at various altitudes for various horizontal extents of stratiform and cumuliform clouds are documented in FAR Part 25, Appendix C. This Appendix is included in its entirety in this report as Appendix A. The first page contains instructions on how to use the charts. The charts of Figures A-1 and A-4 are based upon the NACA data previously tabulated in Table 2-I for the Continuous Maximum and Intermittent Maximum Classes of clouds. The icing envelope charts of Figure A-2 and A-5 are based on the bounding envelopes of the NACA data of Figures 2-4 and 2-5. The LWC correction factors of Figures A-3 and A-6 are based on Figure 2-6, from NACA 2738.

Whereas these charts adequately define the ranges of icing parameters, they do not specify which combinations of these parameters will produce the most severe icing condition at a given flight condition. For example, consider an aircraft for which it is known that ascents and descents through an altitude of 14,000 ft. will occur regularly. Figure A-5 specifies that intermittent protection must be adequately designed for all temperatures from -22°F to 19°F, and Figure A-4 provides a large range of possible LWC values at each of these limiting temperatures. A similar dilemma occurs with the charts for stratiform clouds. Thus, it is left up to the designer to select a few discrete points which represent maximum icing, thereby assuring the integrity of ice protection over the full parametric range without performing multitudinous calculations, or tests, at all possible combinations of parameters. Recommended procedures for doing this are presented in Section 2.2 of this chapter. However, before proceeding to that discussion, it is of interest to first compare the FAA design standard charts of Figures A-1 thru A-6 to corresponding design standard charts used by the United States Military and to similar charts used by England and Canada, including various design standard definitions of freezing rain and other low-altitude icing conditions.

2.1.2.2 U. S. Military Design Standards

The United States Military design standard charts for defining atmospheric icing conditions are shown on Figures 2-11 and 2-12 taken directly from MIL-E-5007D (Reference 10). These charts show only minor deviations from the FAA charts, and for all practical purposes may be considered identical, except that the military does not concern itself with the horizontal-extent factors on liquid water content.

2.1.2.3 British Design Standards

The atmospheric icing charts used by Great Britain are completely identical to the FAA charts in Appendix A. They are available for inspection in Reference 11, but are not repeated in this report.

Even though the Great Britian icing environment charts per se are identical to those of the United States FAA, there are a couple of additional atmospheric condition requirements which are apparently mandatory in Great Britian but are not mentioned in the FAR documents. These additional conditions are demonstrated in Table 2-II and 2-III, taken directly from ADS-4. Referring first to Table 2-II, it is seen that the British apparently require design consideration of the "Instantaneous Maximum" class of clouds originally specified in NACA 1855 and previously shown in this report in Table 2-I. As classified in Table 2-I, this class of cloud has a very high liquid water content, but the characteristic horizontal extent is only ½ mile. A modern aircraft flying at Mach 0.5, for example, would flash through such a cloud in about 5 seconds or less, which probably corresponds to negligible ice accumulation. The other atmospheric phenomenon which is considered by the British is ice crystal conditions. Table 2-III, taken directly from ADS-4 (originally from a Canadian document issued in 1961) is a good summary of ice crystals, and indicates in Note 2 that this condition can present icing problems for engines and intakes. However, a 1975 British Civil Aviation Authority Airworthiness Requirements document (Reference 11) states that engines with "pitot" type intakes have not proved to be susceptible to ice crystal difficulties, and the Authority will not normally require tests on engines of such layout. Engines designed with reverse flow intakes, or with intakes involving considerable changes of air flow direction, may be susceptible to ice crystal conditions. These two sentences, stated by the British, appear to endorse the position taken in this Powerplant Icing Report regarding ice crystal conditions, i.e., if ice crystals are a problem at all, they affect primarily the inlet design, which in this report is considered to be part of the airframe, not the engine. It is therefore considered acceptable to ignore ice crystal conditions in powerplant ice protection designs.

2.1.2.4 Freezing Rain and Other Low Altitude Icing Condition Design Standards

As previously mentioned in the discussion of the NACA statistical data, there is very little data upon which a definite low altitude icing condition design standard can be based. As a consequence, suitable design standards have to be inferred from the limited NACA data and from various test-specification documents in which attempts are made to specify a model of a low-altitude or ground level icing environment. A summary of the various possibilities is listed in Table 2-IV, all of which are considered to be acceptable design standards.

TABLE 2-II

BRITISH CIVIL AIRWORTHINESS REQUIREMENTS
(COPIED FROM TABLE I-5 OF ADS-4, REF. 1)

Table 1-5
British Civil Airworthiness Requirements
(Reference 1-29)
Continuous Maximum (D 4-7 & D 5-5)

Temperature °C	LWC - gm/m^3	Drop Size Microns	Altitude - ft.
0	0.8	20	SL - 20,000
-10	0.6	20	3,000 - 27,500
-20	0.3	20	3,000 - 30,000
-30	0.2	20	3,000 - 30,000

Icing layer thickness is 6,500 ft. maximum
(Note: Continuous maximum values are identical to Table 1-1, Class III-M, except that droplet size is 20 microns instead of 15).

Intermittent Maximum (D 5-5)

Temperature °C	LWC - gm/m^3	Drop Size Microns	Altitude - ft.
0	2.5	20	10,000 - 20,000
-10	2.2	20	10,000 - 27,500
-20	1.7	20	15,000 - 30,000
-30	1.0	20	15,000 - 35,000
-40	0.2	20	15,000 - 40,000

Up to 30,000 ft. - three mi. duration, with three-mi. gaps of "continuous maximum" condition. Between 30,000 and 40,000 ft. the gaps are 20 mi. of clear air. (Note: Intermittent maximum values are identical to Table 1-1, Class II-M values)

For powerplant, 30 min. of operation is required in a combination of "intermittent" and "continuous" maximum icing, with one-half mile at approximately double the LWC of the "intermittent" condition (see following tabulation).

Instantaneous Maximum

Temperature °C	LWC - gm/m^3	Drop Diameter Microns	Altitude Feet	Horizontal Extent Miles
0	5.0	20	10,000 - 20,000	Continuous For
-10	4.0	20	10,000 - 27,500	½ Mile
-20	3.0	20	15,000 - 30,000	
-30	2.0	20	15,000 - 35,000	
-40	0.5	20	15,000 - 40,000	

TABLE 2-III

ICE CRYSTAL STANDARDS (CANADA)

(COPIED FROM TABLE 1-6 OF ADS-4, REF. 1)

Ice Crystal Concentration Standards
(Supplied by the National Research Council of Canada)

Ambient Temperature °C	Altitude 1,000 Ft.	Maximum Total Concentration (ice crystals plus LWC) gm/m^3	Maximum Concentration In Liquid Form gm/m^3	Extent Mi.
0 to -20	10 to 30	8	1	0.5
		5	1	3
		2	1	50
		1	0.5	Indef.
-20 to -40	15 to 40	5	0	3
		2	0	10
		1	0	50
		0.5	0	Indef.
-40 to -60	20 to 45	2	0	3
		1	0	10
		0.25	0	Indef.
-60 to -80	30 to 60	1	0	3
		0.50	0	10
		0.10	0	Indef.

Thirty minutes exposure is considered for the "indefinite" extent.

NOTES (Ref 1-29)

1. In the present state of knowledge, it is not possible to say how much of the "total free water contents" tabulated exist in the form of water and how much as ice crystals, because supercooled water has been shown to exist at temperatures down to -40°C. Furthermore the percentage of ice crystals and water may vary considerably in any one cloud.
2. From present information it appears that the worst condition for engine and intake icing in mixed water/ice crystals occurs when there is a small quantity of water present.
3. The following assumptions may reasonably be made for design purposes:
   a. Below -20°C all the water present may be assumed to be in the form of ice crystals.
   b. Of the total free water shown in the 0°C to -20°C range, not more than 1 gm/m^3 should be taken as water and the remainder as ice crystals, except where the total water content is shown as 1 gm/m^3, when half should be considered as water and half ice crystals.
   c. When the extent of the condition is shown as "indefinite", it is acceptable to show that the airplane functions satisfactorily during 30 minutes continuous exposure to the conditions.

TABLE 2-IV

FREEZING RAIN & LOW-ALTITUDE ICING ENVIRONMENTS

Environment Number	Data Source	Icing Environment & Altitude Range	Liquid Water Content gm/m^3	Ambient Temperature °F	Droplet Diameter Microns
1	NACA TN 1855 Table 2-I	Freezing Rain 0 to 5000 ft.	0.15 (rainfall of 0.1 inch/hour)	25 to 32	1000
2	Unpublished NASA Data (Ref. 1-18 of ADS-4) (shown on Fig. 2-3).	Low-Altitude layer clouds 0 to 5000 ft.	0.05 At Ground, 0.80 At 5000 ft.	Unavailable	Unavailable
3	Test Requirement: FAR Part 33 (Reference 2)	Ground Level Icing	0.6	29	40
4	Test Suggestion: FAA Advisory Circular AC #20-73 (Ref. 3)	Ground Fog	2.0 (note: This unjustifiably high value was later ammended to the 0.6 value of FAR Part 33)	29	40
5	Test Requirement: Mil Spec Mil-E-5007D (Ref. 10)	Low-Altitude Icing 0 to 500 ft.	0.4	23	30
6	British Test Requirement: (Ref 11)	Ground Level Icing	0.3	28.4	20
7	British Civil Airworthiness Requirements: (Ref. 1-29 of ADS-4) shown on Table 2-II.	Continuous Maximum icing,	0.8	32	20

It is also considered acceptable to simply use the stratiform-cloud conditions of Figure A-1 for ground and low-altitude icing environments from 25 to 32°F. The fact that the LWC of Environment Number 2 is always less than the LWC of Fig. A-1 suggests that this figure may be conservative when applied at low altitudes.

The foregoing discussion completes the presentation of material from ADS-4 which, for the most part, applies to both airframe anti-icing and powerplant anti-icing. The remainder of this chapter discusses recommended procedures for selecting appropriate "worst-icing" environmental design points for powerplant icing studies.

2.2 THE SINGLE OPERATING LINE AND RECOMMENDED ENVIRONMENTAL DESIGN POINTS

As previously mentioned in the discussion of the FAA design standards for atmospheric icing conditions (Appendix A), these charts do not specify which combinations of icing parameters will produce the most severe icing condition at a given flight condition. The selection of these worst-icing environmental combinations is somewhat different for engines than for airframes because many of the engine surfaces which are likely to experience icing are located within the engine itself, where the heat of compression of the air flow can neutralize an otherwise formidable icing environment, or can fail to neutralize free stream environments of lesser icing potential. Furthermore, when engine surfaces such as inlet guide vanes are provided with an active anti-icing system, the internal heating source is usually compressor bleed air. Thus, the engine power level also affects the heating capability of an anti-icing system. Variations of the heating capability of the compressed air are just as important as variations of the icing capability of the external environment. This dependence of worst-icing free stream conditions upon heat-of-compression in the engine requires that the designer consider a double set of design points:

> Environmental Design Points: These are selected probable-worst-icing atmospheric environmental conditions within the atmospheric icing charts of Appendix A. Their selection involves general considerations of engine heat-of-compression, and are the subject matter of this section of the report.
>
> Flight Cycle Design Points: These design points involve the detailed determination of discreet portions of an aircraft flight cycle for which "worst-icing" occurs. These design points may, or may not, occur at the most severe Environmental Design Points, and will be discussed subsequently in the Flight Cycle Analysis section of this report, Chapter IV.

The engine power level (or heat of compression) is not the only consideration affecting engine surface icing potential and/or anti-icing potential. The heat of compression merely creates a ΔT relative to $T_{atmosphere}$, whereas the real quantity of interest is the magnitude of the compressed air temperature relative to 32°F. Hence, the value of free-stream atmospheric air temperature must be considered in conjunction with engine power level. It will be shown later (in the Flight Cycle Analysis section) that many other engine performance characteristics eventually enter into the complete icing design calculations. However, the task at hand in this section is simply to recommend selected atmospheric design points on

the free-air icing-environment charts of Appendix A, and to that end the foregoing general introduction of the concepts of engine performance considerations combined with free-stream ambient temperature considerations is sufficient information upon which to proceed.

2.2.1 The Single Operating Line

Directing attention now specifically to Figures A-2 and A-5 (which are the icing envelope temperature vs. altitude charts), it is ovserved that the coordinates of these two charts are the same coordinates as are commonly used by aircraft performance analysts to define the various design model atmospheres (i.e., "Hot Day", "Cold Day", "Standard Day", etc.) upon which they base their aircraft-performance calculations. Figure 2-13 shows two such design model atmospheres (an "Artic Day" and a "Standard Day") superimposed on a combined graph of the icing envelopes of Figure A-2 thru A-5. The "most probable icing temperature versus altitude" line for these icing envelopes is also shown, and will be used for future reference. In examining Figure 2-13 it should be kept in mind that even though the performance-atmosphere lines and the icing-environment envelopes plot nicely on a common set of coordinates, the lines and the envelopes are usually used for two different purposes -- the lines solely for performance, and the envelopes solely for icing. The obvious conclusion from this observation is that, since the icing design calculations are going to be dependent upon engine-performance calculations at various ambient temperatures of icing environments, it would be very convenient to collapse the icing envelopes into a single line which would be representative of the icing envelopes and would also serve as a temperature vs. altitude "icing day" line upon which performance calculations could be based. Because the performance calculations in question will be performed specifically for the purpose of assessing the engine compressor behavior relative to icing-condition air temperature at various altitudes (rather than for the more usual purposes of assessing the extremes of engine behavior at various altitudes relative to rotor speed matching, internal pressures, thrust, etc.), the resultant "icing day" line need not necessarily be coincident with any of the usual model atmosphere lines. It is also not necessary for the proposed "icing day" line to coincide with the "most probable icing temperature" line because this line does not necessarily correspond to worst icing, as is ultimately proved in the concluding paragraph of Chapter IV. The "icing day" line can therefore be generated solely by the collapsing of the icing envelopes into a single line which is representative of the most severe atmospheric icing conditions, and which corresponds to realistically cold values of ambient temperature vs. altitude such that the compressor heats of compression produce compressed air temperature values likely to be experienced in actual flight. Such a line is referred to in this report as the "Single Operating Line". It is the same line as the "severe icing operating line" of Reference 18, and is a simultaneous most-severe balance of the severe free-atmosphere icing potentials and the most difficult free air temperatures for compressor transformations to values sufficiently above 32°F for potential anti-icing capabilities.

The proposed location of the "single operating line" is deduced from the following observations regarding Figure 2-13.

(a) It has been previously demonstrated that the cumuliform cloud envelope corresponds to icing conditions which are generally more severe than those in the stratiform cloud envelope, primarily because of a significantly higher level of liquid water

content. Whereas the ADS-4 document for airframe anti-icing downplays this observation for airframes on the basis that cumuliform cloud icing encounters are not continuous and can therefore be quickly escaped if they start to overtax the airframe anti-icing systems, one cannot afford the luxury of such a statement when designing engine anti-icing. It is recommended that engine anti-icing design studies should be based on cumuliform cloud icing conditions, and the location of the "single operating line" should therefore lie somewhere within the cumuliform cloud envelope.

(b) Examination of the boundaries of the cumuliform cloud envelope on Figure 2-13, particularly the sloping left-edge boundary and the sloping right-edge boundary, indicates that there will be some difficulty in deciding which of these boundaries should be favored for predicting worst atmospheric icing conditions. If the sloping right-edge boundary is favored, then a given flight altitude will correspond to considerably warmer free air temperatures than would result if the sloping left-edge boundary were favored, but the warmer right-edge boundary temperature at a given altitude corresponds to a greater liquid water content (cf. Figure A-4) than would be associated with the colder left-edge boundary temperature at the same altitude. Since atmospheric icing severity is intuitively assumed to increase with decreasing temperature and increasing liquid water content, the foregoing comparison of envelope boundaries is judged inconclusive for cursorily predicting which boundary will correspond to the more severe icing condition at a given altitude. However, there are a couple of other considerations which can help resolve this dilemma. First of all, based on verbal contacts with various cognizant individuals, it seems that most of the high altitude icing-incident reports gathered from pilots in actual flight come from geographic areas where the typical climatic conditions are normally closer to a typical Arctic Day rather than a typical Standard Day. This observation also seems to be intuitively logical. It is therefore suggested that the proposed single operating line position should favor the sloping left-edge boundary of the cumuliform cloud envelope, at least for high altitudes. The fact that this suggestion disagrees with the high-altitude trend of the "most probable icing temperature" line on Figure 2-13 is not considered to be important, because that line applies only to the probability of encountering icing per se, not necessarily the most severe icing. The second consideration which will help locate the "single operating line" within the envelope boundaries is an observation about low-altitude and ground level freezing rain icing probabilities. From the limited information available in the references regarding low-altitude icing and freezing rain, it appears to be a general consensus of opinion that this type of icing is severe only when the ambient air temperature is around 25 to 32°F. This observation is substantiated by Table 2-IV, (previously presented), which shows that the test-specification requirements from various cognizant agencies recommend that low altitude icing and freezing rain icing protection should be proof-tested at temperature levels in the neighborhood of 25 to 32°F. On this basis, it is therefore suggested that the proposed "single operating line" position on Figure 2-13 should also favor the sloping left-edge boundary of the cumuliform cloud envelope for low altitudes, because a hypothetical linear extension of this sloping boundary intersects the zero-altitude temperature ordinate at 27°F, which is deemed reasonable for freezing rain worst-icing.

(c) The third and final point of rationale which establishes the position of the proposed single operating line is to recall the comments made previously regarding the influence of compressor heat-of-compression on both icing potential of the gas path around airfoils and on anti-icing potential of compressor bleed air. The net conclusion from that discussion was that it tends to enhance design conservatism if the "icing day" ambient temperatures are a reasonable minimum for the particular altitude in question. The obvious means of satisfying this objective without violating either of the previous recommendations of (a) or (b) above, is to locate the proposed single operating line directly on the sloping left-edge of the cumuliform cloud icing envelope, with a linear extension to 27°F at sea level.

The recommended Single Operating Line, thusly located, is shown on Figure 2-14. For convenience, a Standard Day atmospheric pressure scale is included along the abscissa altitude scale. It is noted here, and also later on in this report, that the Figure 2-14 location of the Single Operating Line always corresponded to more severe icing conditions than a Standard Day temperature line, for all of several icing points that were checked at both locations during the preparation of this report.

2.2.2 Recommended Environmental Design Points

Having defined a worst-icing operating line upon which to base the forth-coming flight cycle analyses, it is now convenient to focus attention on the other atmospheric icing parameters - - namely Figures A-1 and A-4 - - to examine the possibilities of logically reducing the parametric range of the water-content versus droplet diameter sets of values which can be associated with each of the temperature values along the Single Operating Line of Figure 2-14. Whereas the Single Operating Line was defined primarily to account for icing in cumuliform clouds, there may be a few occasions during the flight cycle, (e.g. low-altitudes, ground idle, and perhaps others) where the Stratiform Cloud water-contents may be more suitable for assessing realistic icing in the engine. For this reason, both Figure A-1 and A-4 are to be considered in the following discussion of parametric-range reduction.

Inspection of the overall trends of Figure A-1 and A-4 shows that, at any specified temperature, as the droplet diameter increases the liquid water content decreases. This observation, however, is simply a characteristic of clouds (as has been previously mentioned in the discussion of the NACA statistical data), and is of no help for assessing worst-icing conditions. Intuitively, one would suspect that icing severity would tend to increase as liquid-water content increases, but a corresponding intuitive comment about the effects of droplet diameter are not obvious. It therefore becomes necessary to pursue other approaches in order to condense the range of these parameters for design purposes. The approach selected is to review the available literature to determine what simplifications are made as a matter of common design practice. The best source of literature on this subject appears to be the various engine test-specification requirements of the FAA and other regulatory agencies. The cognizant regulatory agencies which write these test specifications have no doubt given this matter considerable thought. It would be unreasonable to write test specs which required testing over the full range of LWC vs. droplet diameter, and each of the various regulatory agencies has specified one or two droplet diameters to be used in a few tests to demonstrate suitable compliance over the entire range

of droplet diameters shown on Figures A-1 and A-4. This is precisely what the designer desires to do in design analyses, so if it can be shown that the recommendations of the various regulatory agencies are in substantial agreement with each other, then the problem will be considered to be resolved.

Figure 2-15 shows that there is indeed good agreement among the various regulatory agencies. For all flight-icing simulations a droplet diameter of 15 to 25 microns is specified, with the majority of the specs falling on the 20 micron diameter line. For freezing rain, the recommended droplet diameters vary from 20 to 40 microns.

Although Figure 2-15 clearly shows uniformity in droplet diameter specifications, the graph is somewhat confusing in other respects, and deserves a little explanation. Basically, the graphs are plots of LWC versus dm, with temperature as a parameter. However, many of the test specification points do not plot nicely on this graph because the specified combinations of (LWC, T, dm) of each of the spec points are consistent with the graph in only two of the three variables. For example, it seems to be popular to write a test point with, say T and dm plottable on the graph, but the test-specified value of LWC is set conservatively high. Therefore, the test specification points have been plotted as "bubbles" with arrows to indicate the specified values of dm, LWC and T associated with each test-spec. bubble.

The final recommended values of droplet diameter to be used for design purposes are shown on Figures 2-16 and 2-17. These values are in substantial agreement with the recommendations contained in the ADS-4 document, as regards droplet diameter.

Because engine ice-protection must be conservatively designed, it is recommended that all-in-flight design calculations should be performed on the basis of continuous long-term exposures to the Cumuliform cloud liquid water contents of Figure 2-16. Thus, for any flight condition at an altitude of, say, 9000 feet, the designer would consult Figure 2-14 to determine that the design atmospheric temperature is $-4°F$. Then entering Figure 2-16 at a droplet diameter of 20 microns, he would read a corresponding design atmospheric liquid water content of 1.7 grams per cubic meter. The liquid water content horizontal-extent correction factors specified in the FAR Part 25 graph of Figure A-6 should be ignored when the indicated correction factor is less than unity, and it is considered that using a correction factor value greater than unity is unjustified for the conservative assumption of continuous operation in intermittent Cumuliform clouds. The normal correction factor from Figure A-6 is Therefore 1.0.

There are three recommended exceptions to the above general recommendation:

(a) For ice-accumulation calculations during short-time transients, the appropriate values of liquid water correction factors greater than 1.0 from Figure A-6 should be applied.

(b) For ice-accumulation calculations over extensive time periods, it is considered permissible to base such calculations on the Stratiform Cloud atmospheric icing conditions of Figure 2-17, with the appropriate liquid water correction factors applied from the FAR curve of Figure A-3.

(c) For ground level freezing rain and other low-altitude icing design calculations, the Stratiform Cloud liquid water contents of Figure 2-17 are recommended, with a correction factor of 1.0.

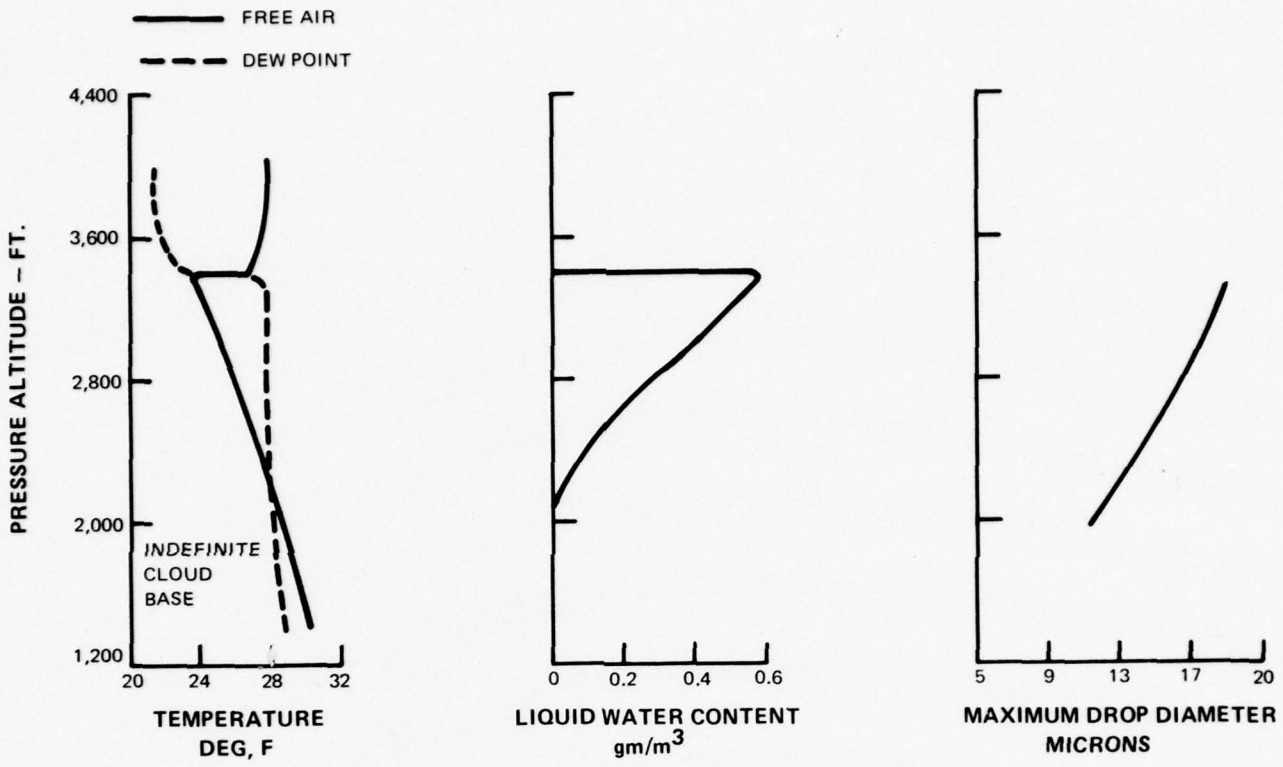

PROPERTIES OF TYPICAL NON-CYCLONIC STRATUS CLOUDS
(FROM FIG. 3a, NACA TN1391)

Figure 2-1 Properties of Stratiform Clouds

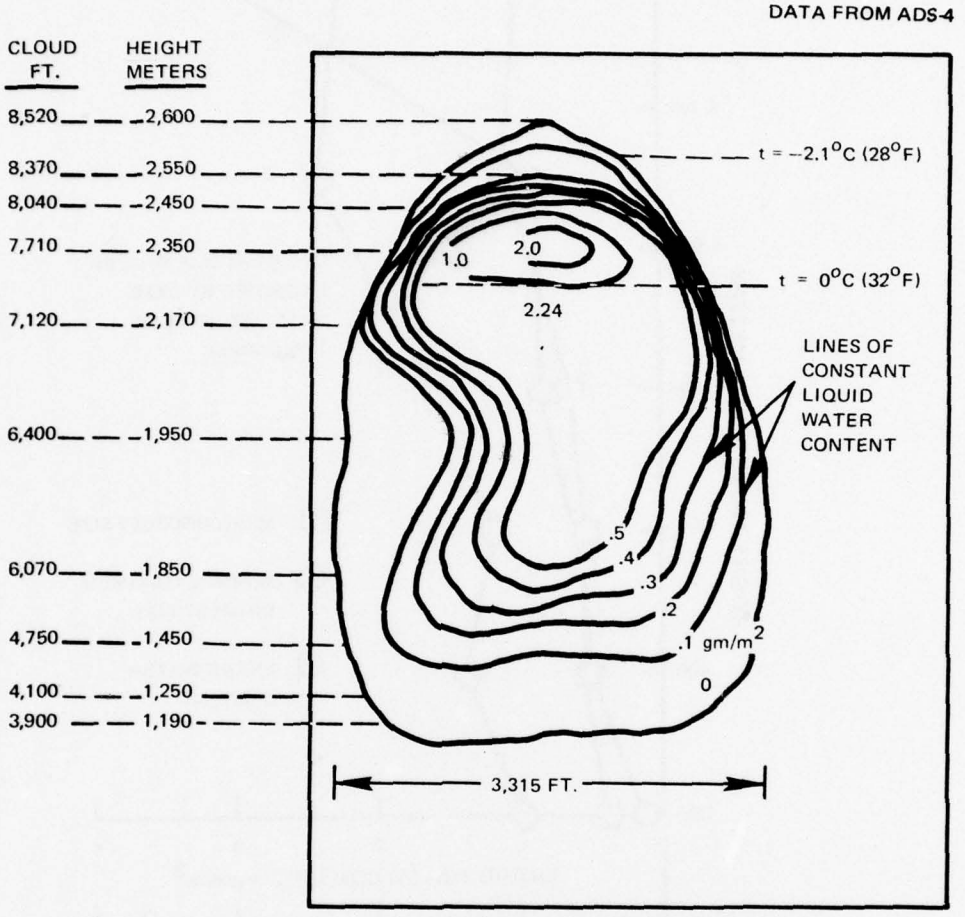

Figure 2-2a Properties of Cumuliform Clouds

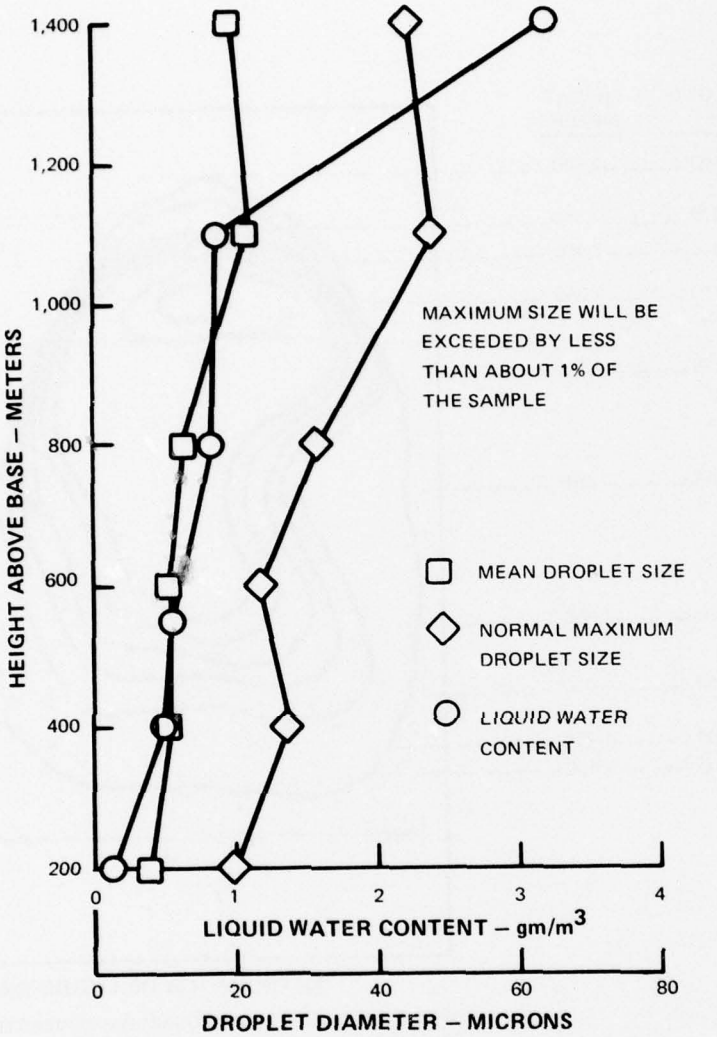

PROPERTIES OF TYPICAL CUMULUS CONGESTUS CLOUDS – LWC, DROP SIZE, TEMPERATURE, VERTICAL AND HORIZONTAL DIMENSIONS. (FROM ADS-4).

Figure 2-2b Cumuliform Clouds, Droplet Size and Liquid Water Content

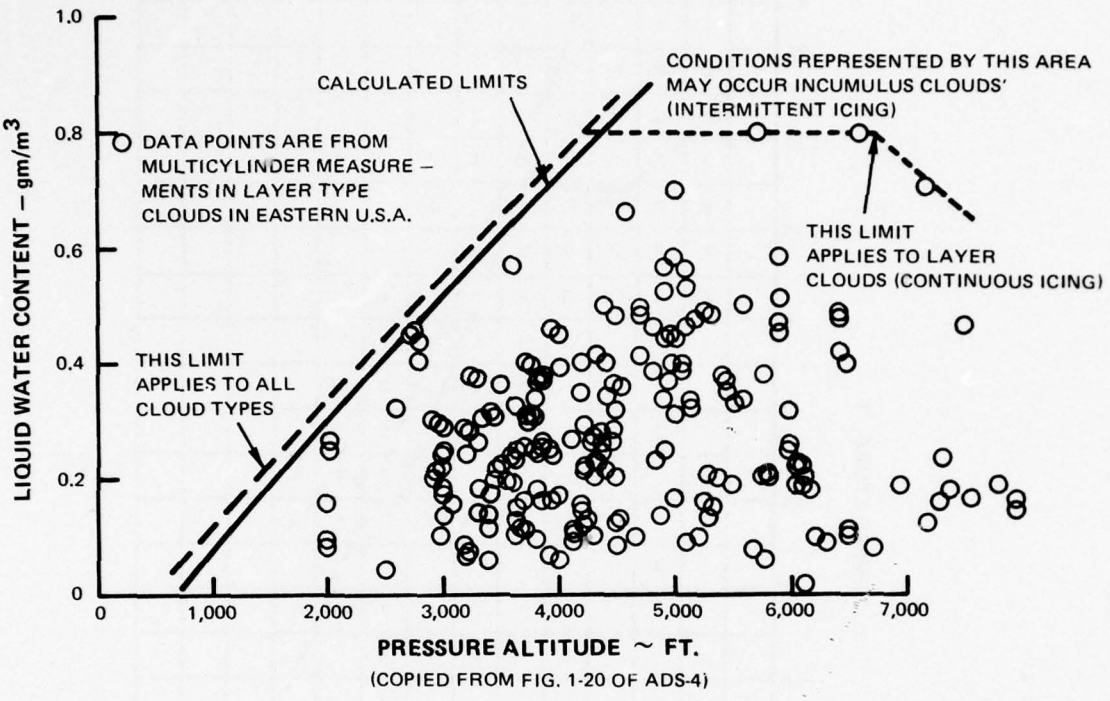

Figure 2-3 Cloud LWC Limits at Low Altitudes

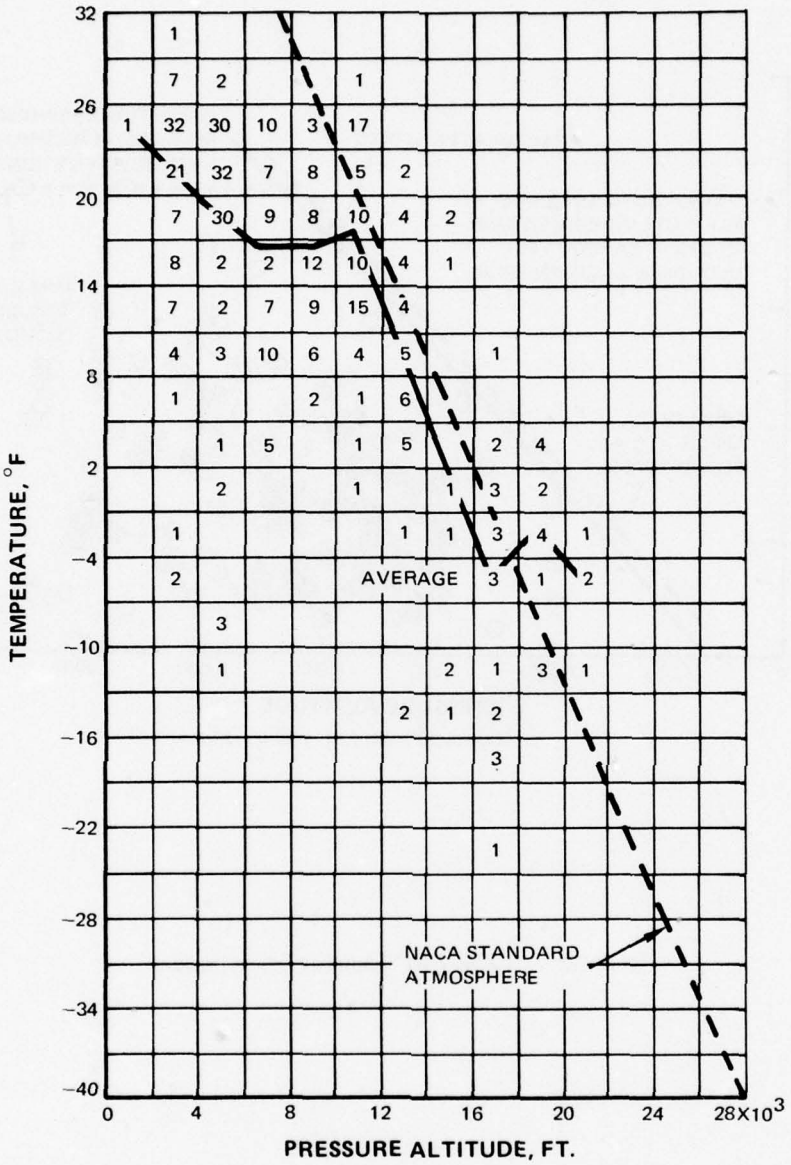

(COPIED FROM FIG. 4 OF NACA TN 2569)

Figure 2-4 *Stratiform Clouds, Frequency Distribution of Icing Observations For Various Increments of Temperature and Pressure Altitude*

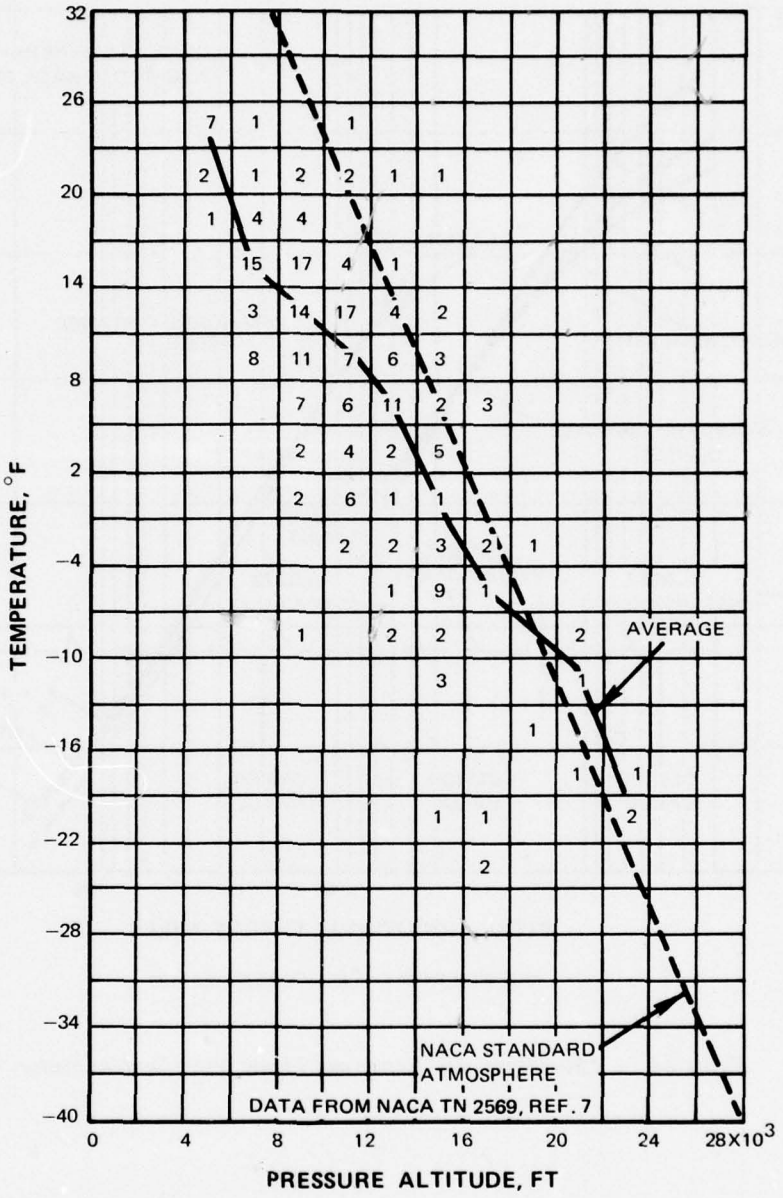

(COPIED FROM FIG. 4 OF NACA TN 2569)

Fig. 2-5 Cumuliform Clouds, Frequency Distribution of Icing Observations for Various Increments of Temperature and Pressure Altitude

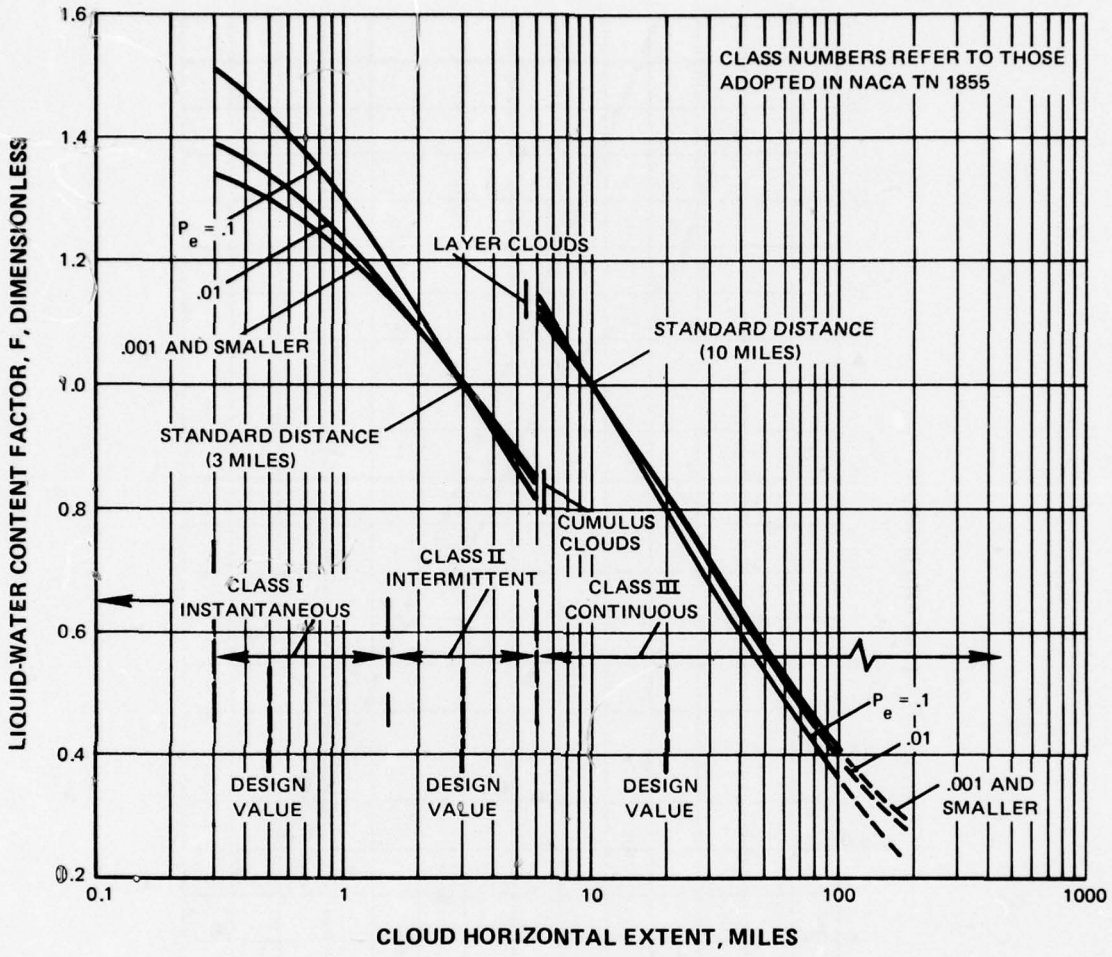

Figure 2-6 Cloud Horizontal Extent and Liquid Water Content Factor

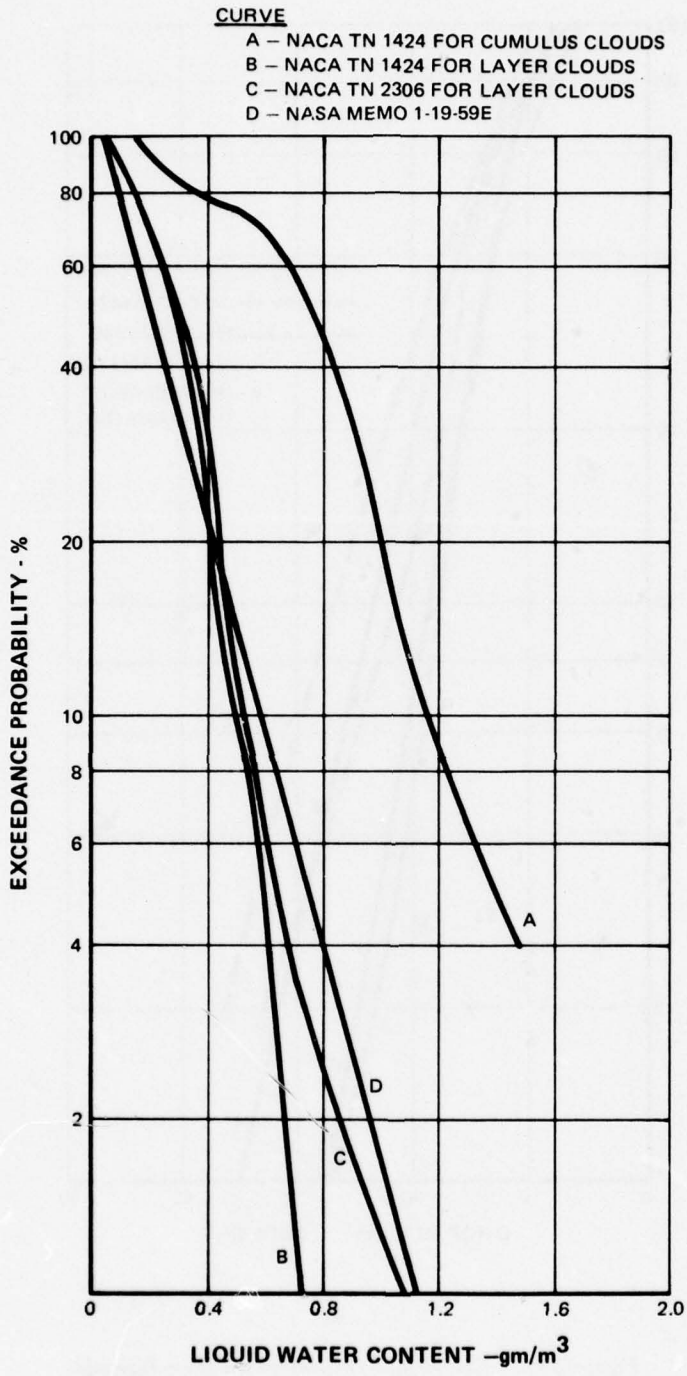

Figure 2-7 Exceedance Probability for Liquid Water Content

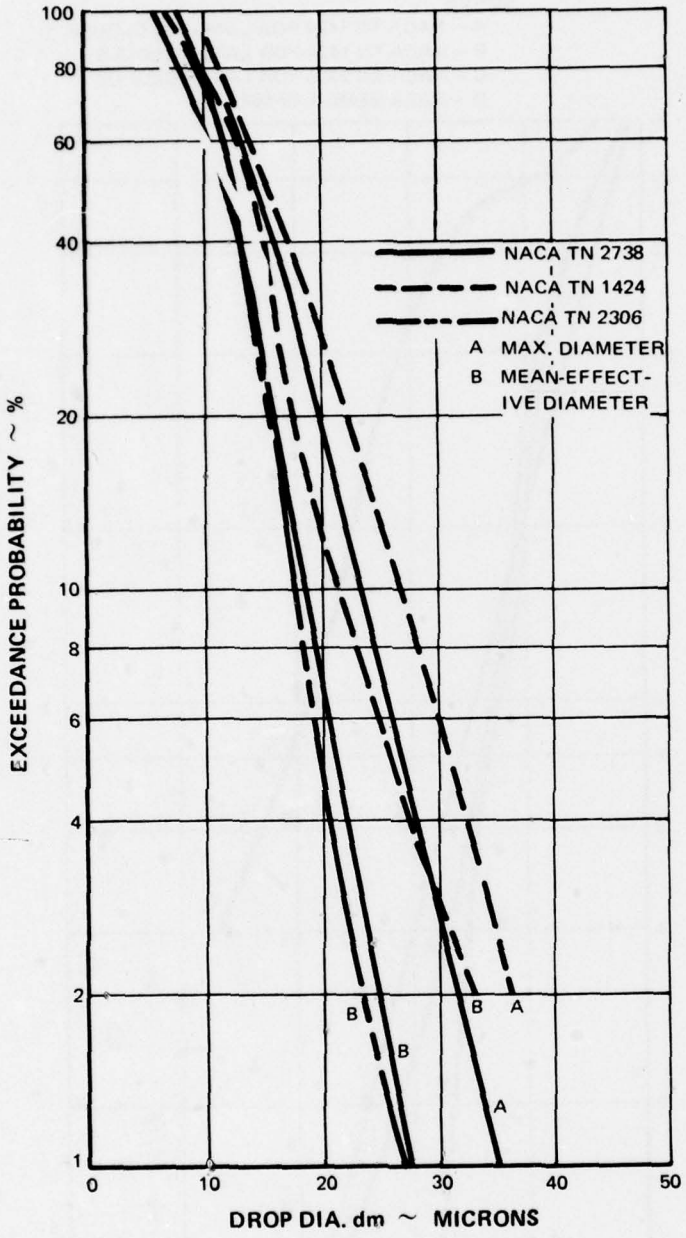

Figure 2-8 Exceedance Probability for Drop Dameter

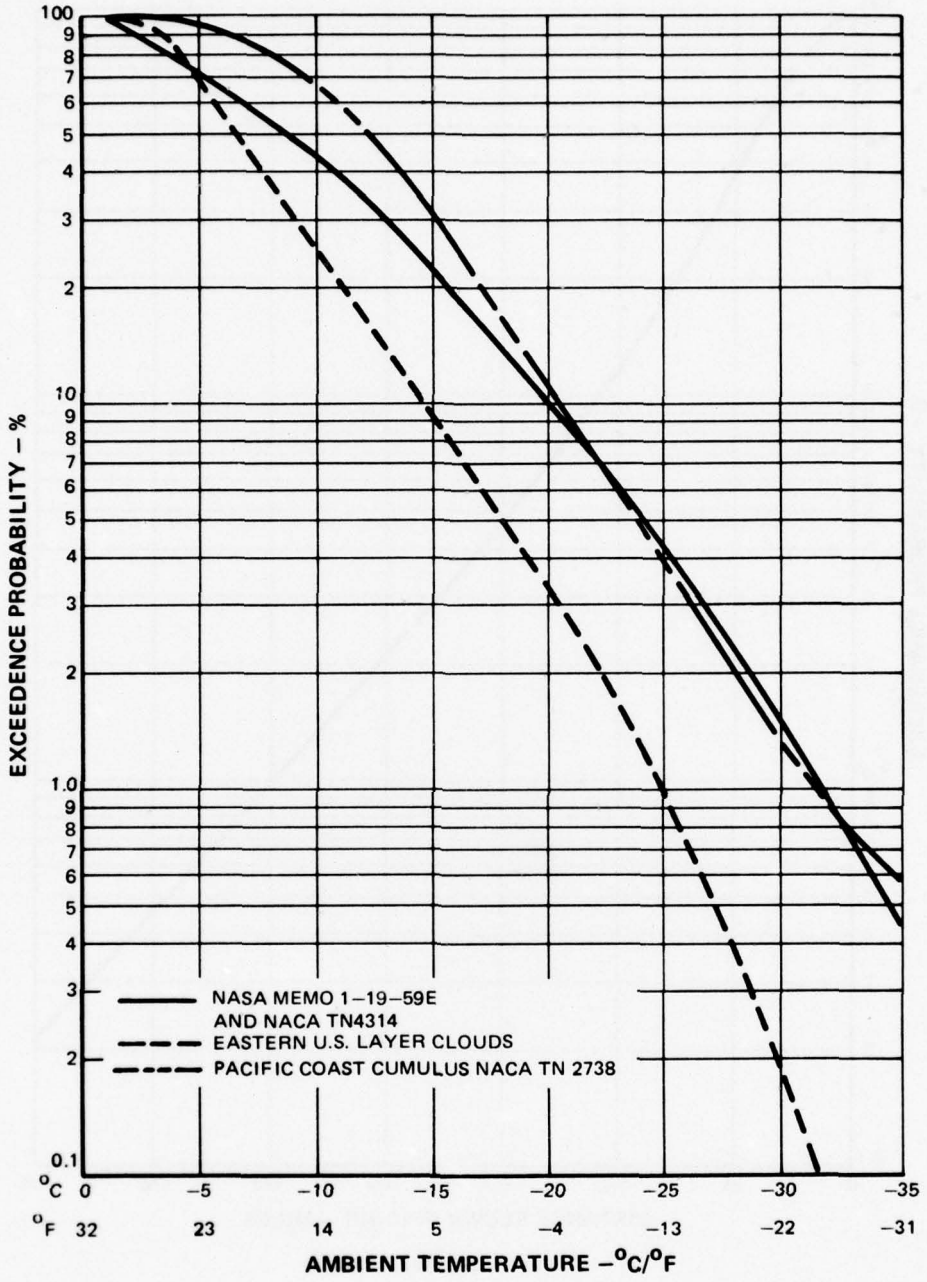

Figure 2-9 Probability of Cloud Icing Temperature

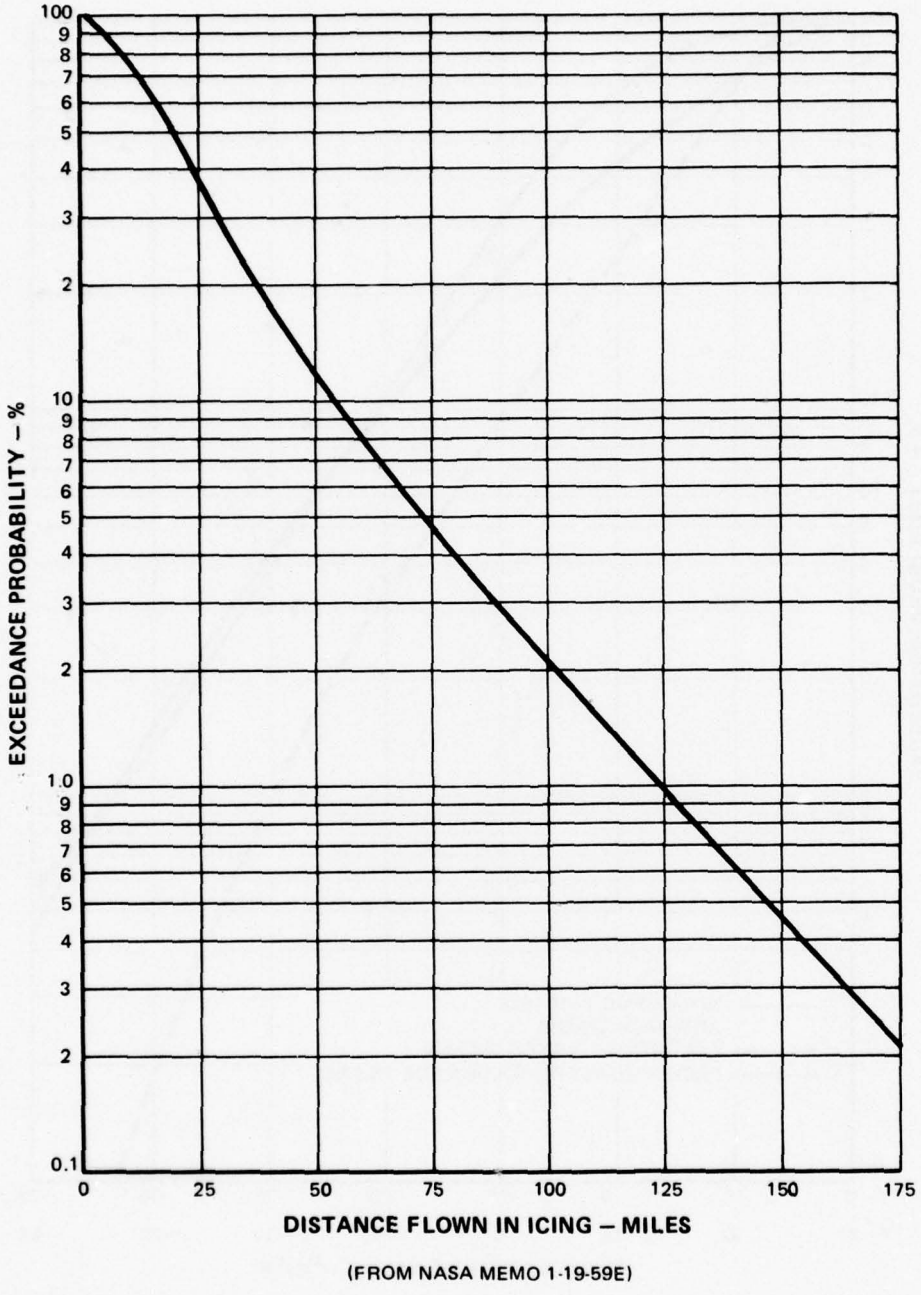

Figure 2-10 Probability of Distance Flown in Icing

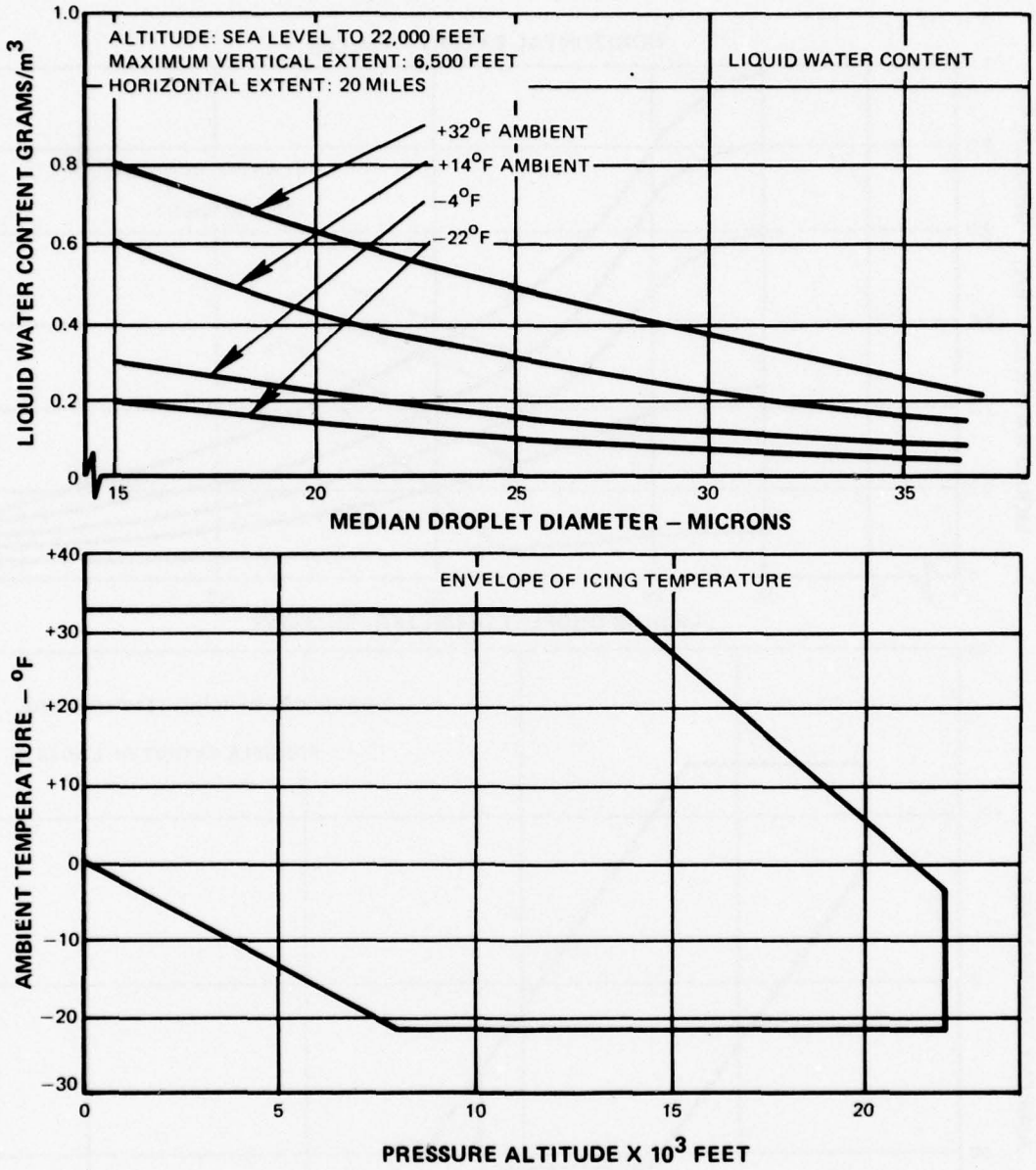

(FROM FIG. 11 OF MIL-E-5007D)

Figure 2-11 U. S. Military Icing Environments, Continuous Maximum

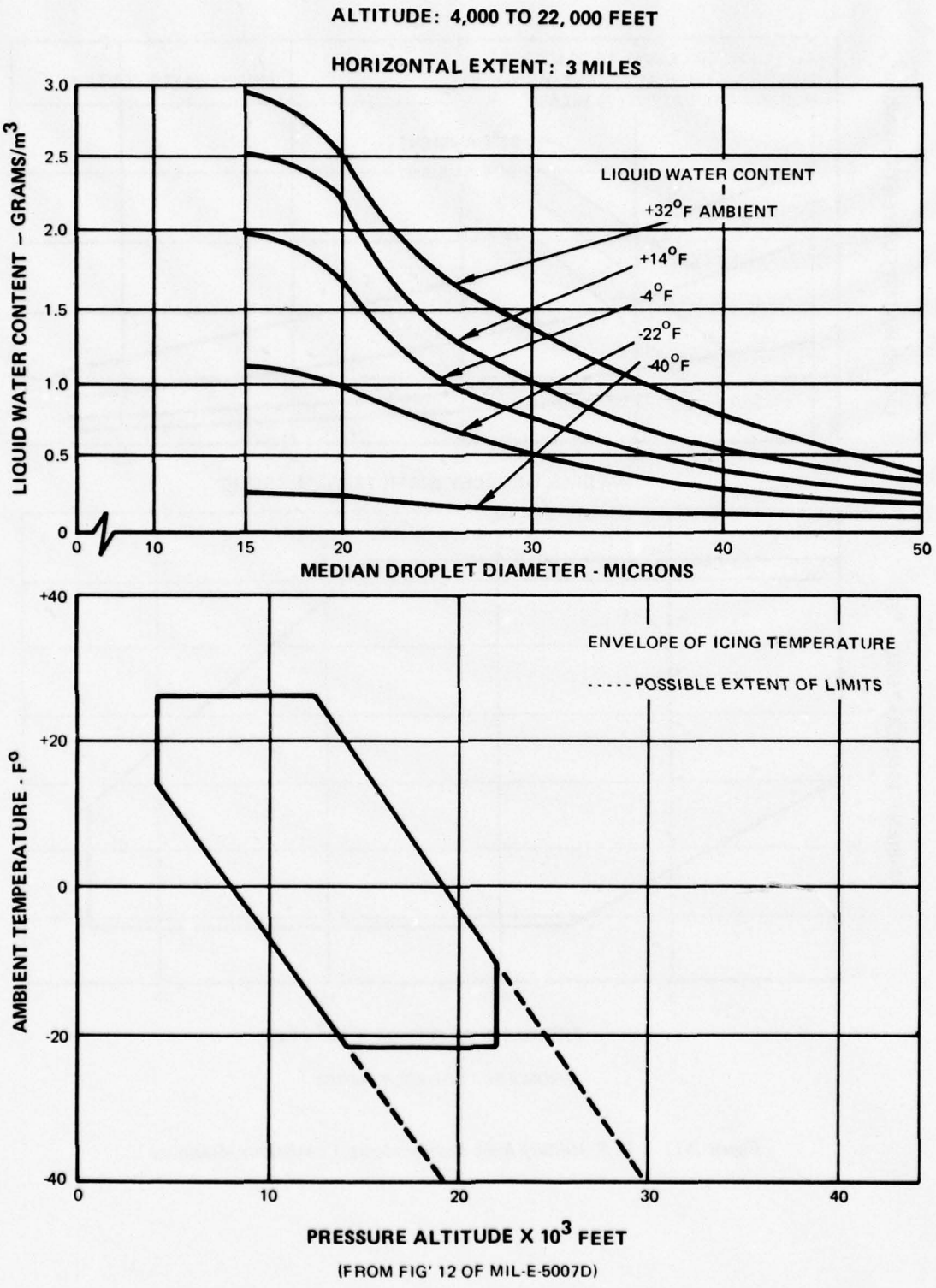

Figure 2-12 U. S. Military Icing Environments, Intermittent Maximum

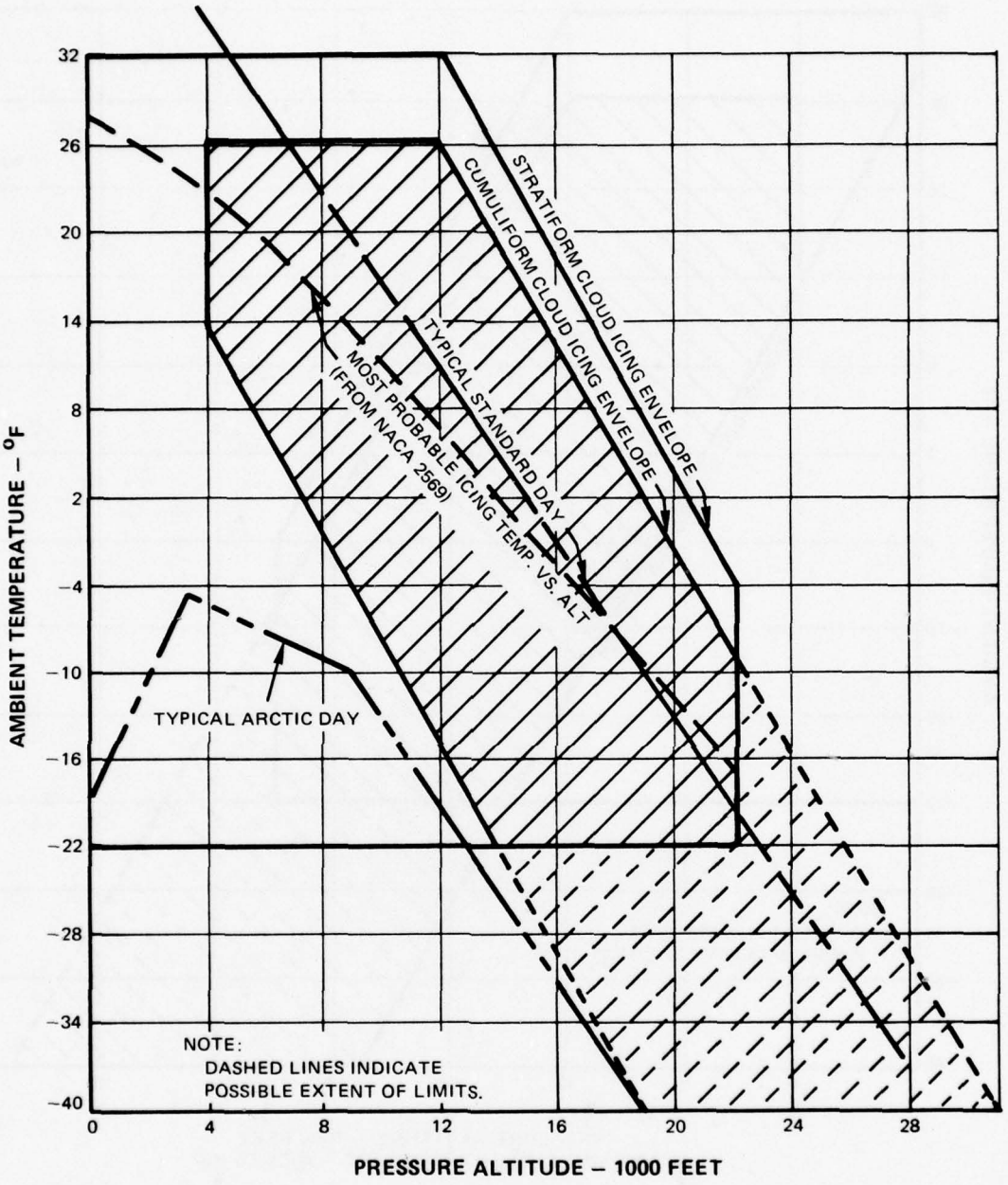

Figure 2-13 Atmospheric Icing Envelopes and Two Model Atmospheres

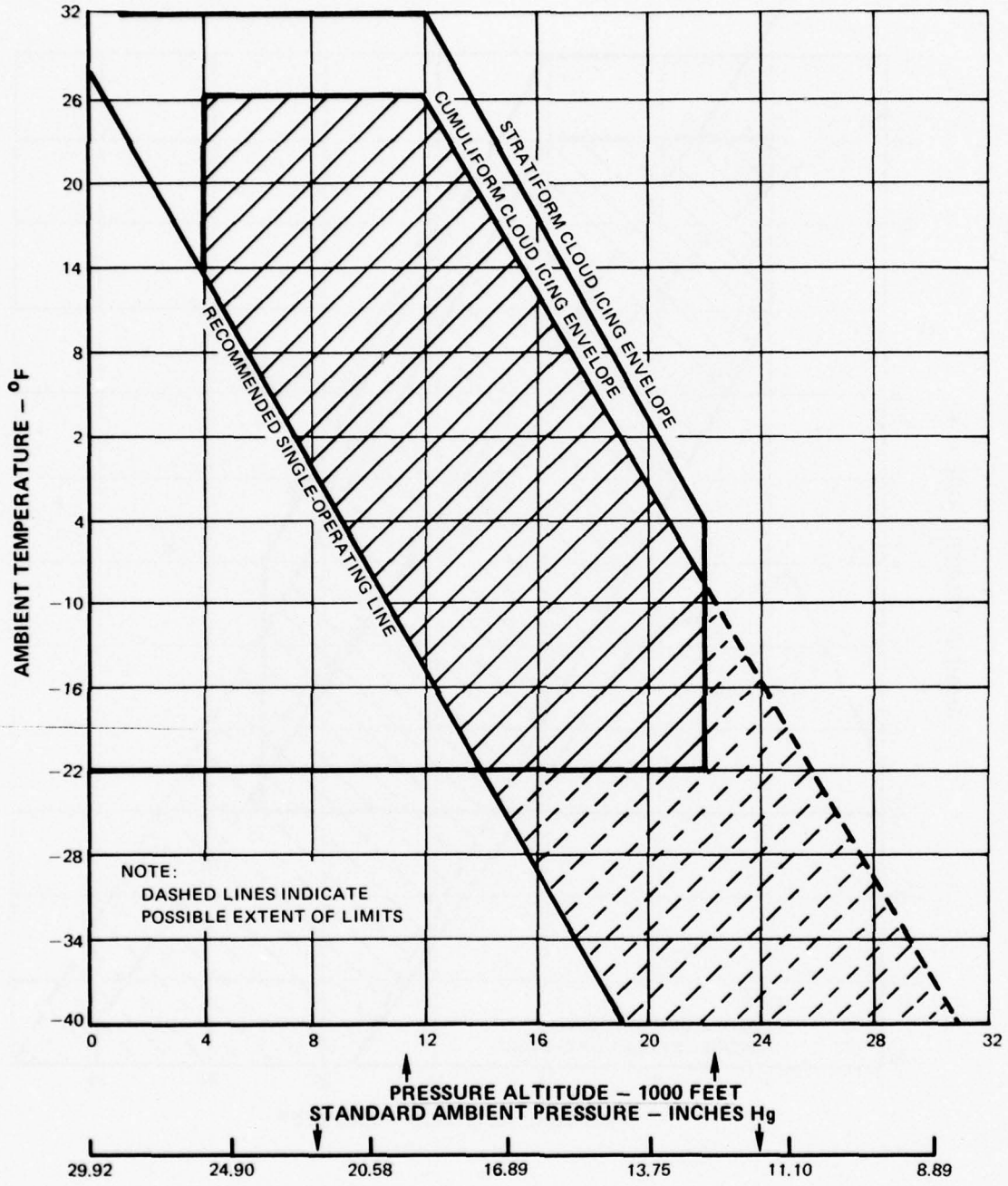

Figure 2-14 Recommended Single Operating Line

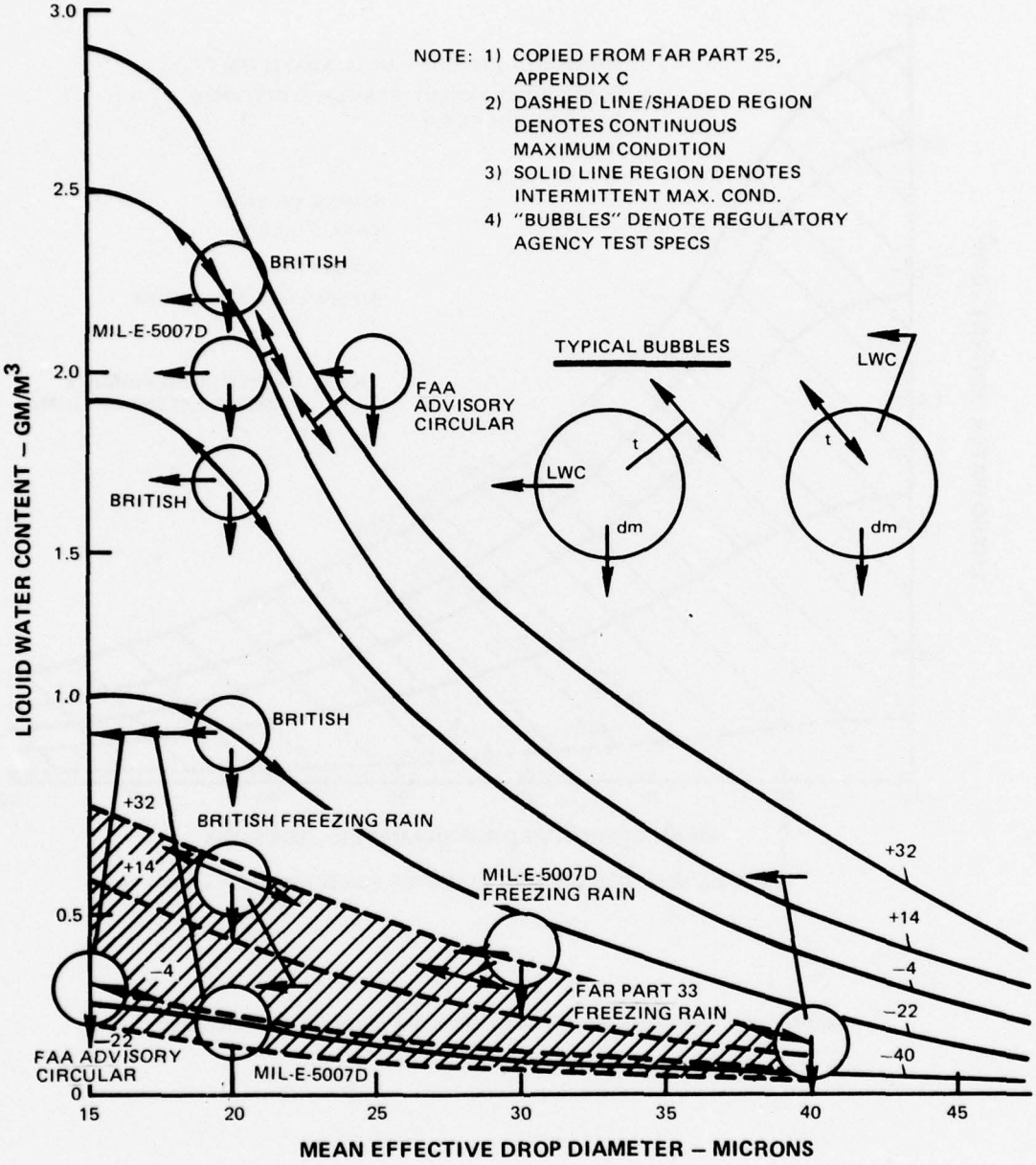

Figure 2-15 *Liquid Water Content and Mean Effective Drop Diameter, Comparison of Various Specifications*

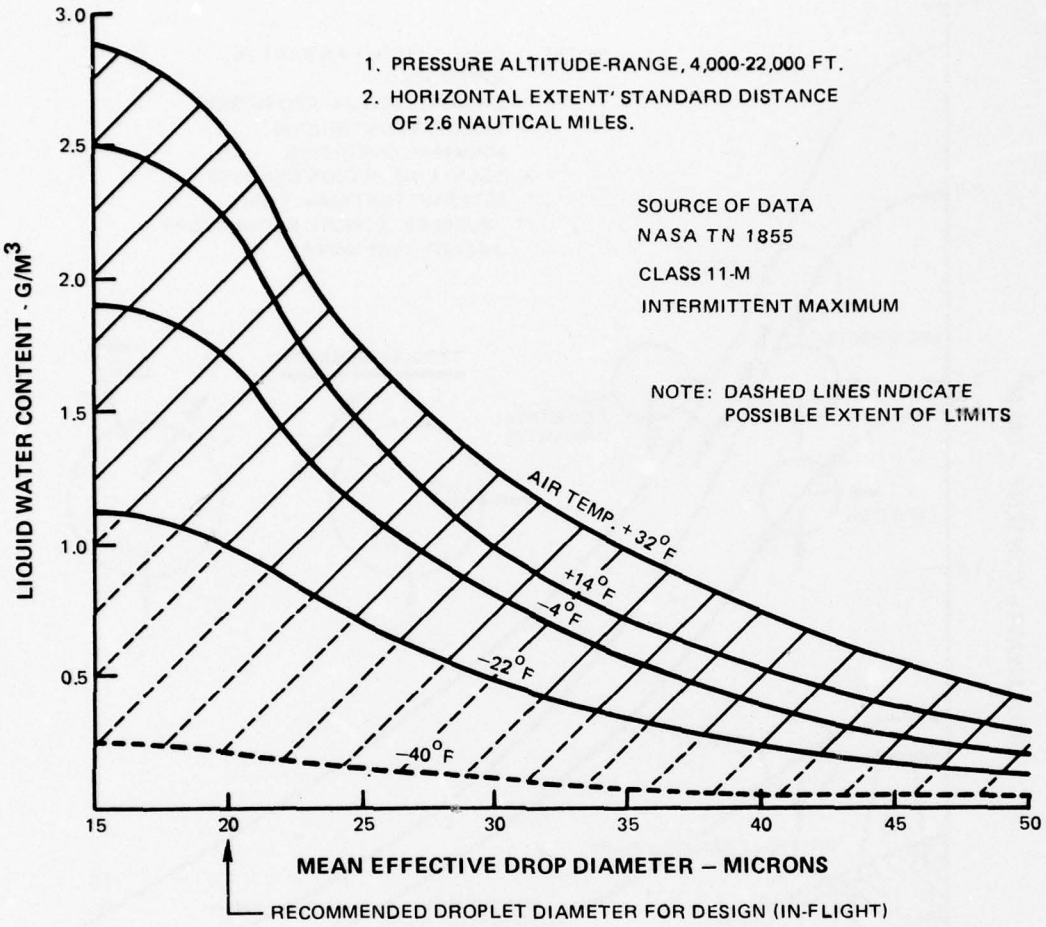

Figure 2-16 Recommended Droplet Diameter for In-Flight Conditions

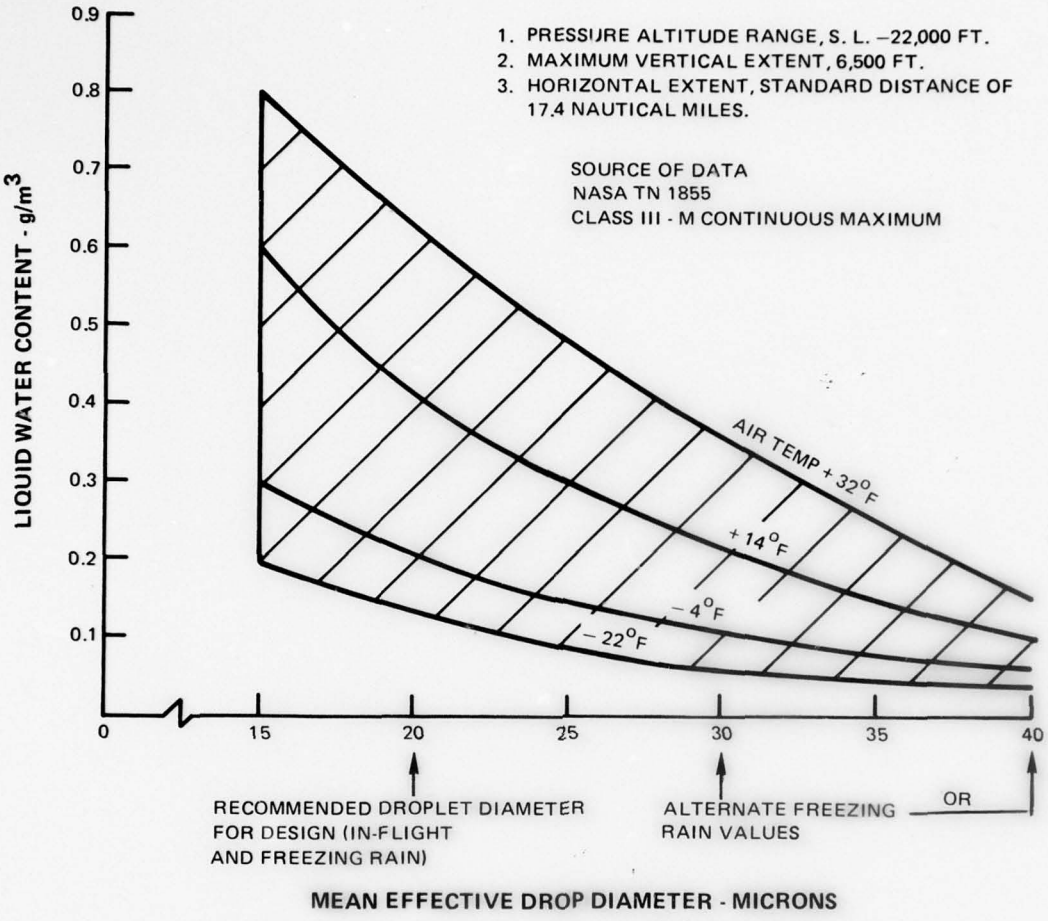

Figure 2-17 Recommended Droplet Diameter For Freezing Rain Conditions

CHAPTER III ANALYTICAL SOLUTION FOR ENGINE ANTI-ICING

Having established the recommended environmental conditions in the previous chapter, considerations of icing engine conditions are the next concepts presented for the complete analysis of engine anti-icing.

3.1 ICING PARAMETERS IN ENGINES

The icing conditions existing within the engine at various points in its flight cycle are dependent upon both the atmospheric conditions of Chapter II, and the engine aerodynamic performance conditions. The engine aerodynamic performance characteristics affect the manner in which the important icing parameters, i.e., liquid water concentration, impingement rates, temperature; are transformed from external environmental properties to internal ice-accumulation conditions or anti-icing heat load requirements within the engine.

It is helpful to define and discuss the various important icing parameters which exist in an engine at any given point in a flight cycle.

3.1.1 Water Ingestion Rates

Water ingestion rate is the time rate at which water is ingested (in droplet form, units of mass/time) by an engine inlet, and is dependent upon the inlet geometry, the ratio of inlet air velocity to free-stream air velocity (Vi/Vo), water droplet size (dm), and the liquid water content $(LWC)_\infty$ in the free stream (cloud).

The dependence of engine water ingestion rates on inlet geometry poses a minor problem to the engine anti-icing design, in that the inlet duct geometry design and inlet duct anti-icing design are the responsibility of the airframe manufacturer. However, many inlets are of the straight ram type, and the calculation of water-ingestion in this type of inlet is a fairly straightforward procedure. It is recommended in this report that the engine anti-ice designer should assume a straight ram-type inlet of the same diameter as the engine front face, and proceed with his own calculations. If better information becomes available later from the airframe manufacturer on an inlet of different geometry, the engine water ingestion rates can be altered accordingly.

In a typical fan engine, there are three areas of concern within the inlet for which the designer will need to calculate water ingestion rates. These three areas are designated on Figure 3-1, and are analyzed as follows:

3.1.1.1 Water Ingestion Into the Basic Inlet

The inlet to free stream velocity ratio V_i/V_o is a function of whether the engine is "gulping" or "spilling" air, and defines the shape of air streamlines upstream of the inlet. Atmospheric icing design curves of Figure 2-16 or -17 are used to define mean effective droplet size and liquid water content of the free stream, at various temperature selected from the Single Operating Line of Figure 2-14. Consideration of the droplet size allows one to deduce the general shape of droplet streamlines relative to the air streamlines so that limiting values of

the inlet water ingestion rates can be calculated. NACA TN 4268 presents actual water ingestion data, for a given inlet, as determined experimentally by wind tunnel tests using a dye-tracer technique and compares it with analytical predictions (NACA TN 3593) solving the droplet equations of motion.

Figure 3-2 taken from NASA TN4268 shows schematically the possible shapes of air streamlines ahead of the inlet and summarizes the basic inlet ingestion data in terms of the total concentration factor C_t (also known as scooping ratio) versus inlet velocity ratio. The fact that the nose cone on Figure 3-2 extends beyond the inlet plane A_i is immaterial, because A_i is calculated for the full unobstructed cowl area. The factor C_t is defined as the ratio of water ingested by the engine inlet plane area A_i to the water contained in a hypothetically-extended free-stream tube of the same A_i cross section. Limiting values of C_t can be deduced from consideration of "large" and "small" droplet sizes, and the convergence or divergence of the air streamlines to the inlet area A_i are qualitatively described from the incompressible form of the airflow continuity equation

$$\rho_o A_o V_o = \rho_i A_i V_i$$

$$\rho_o \approx \rho_i$$

so,

$$\frac{A_o}{A_i} \approx \frac{V_i}{V_o}$$

All symbols are defined in the nomenclature at the end of this report. It is noted that infinitely small droplets exhibiting no inertia would follow these air streamlines, so

$$\left(\dot{m}_{H_2O} \text{ IN } A_o \text{ AT } -\infty\right) = \left(\dot{m}_{H_2O} \text{ IN } A_i \text{ AT INLET}\right) \qquad \text{FOR "SMALL" DROPLETS}$$

From the definition

$$C_t = \frac{\dot{m}_{H_2O} \text{ IN } A_i \text{ AT INLET}}{\dot{m}_{H_2O} \text{ IN } A_i \text{ AT } -\infty}$$

it follows for "small" droplets that

$$C_{t_{\text{"SMALL" DROPLETS}}} = \frac{\dot{m}_{H_2O} \text{ IN } A_i \text{ AT INLET}}{\left(\dot{m}_{H_2O} \text{ IN } A_o \text{ AT } -\infty\right)\left(A_i/A_o\right)} = \frac{A_o}{A_i} = \frac{V_i}{V_o}$$

This equation for "small" droplets is shown as the 45 degree line on the data plot. Contrastingly, "large" droplets exhibiting large inertia enter the inlet by straight paths independent of inlet velocity ratio according to

$$\left(\dot{m}_{H_2O \text{ IN } A_i \text{ AT } -\infty}\right) = \left(\dot{m}_{H_2O \text{ IN } A_i \text{ AT INLET}}\right) \qquad \text{FOR "LARGE" DROPLETS}$$

So,

$$C_{t_{\substack{\text{"LARGE"} \\ \text{DROPLETS}}}} = 1.0$$

This limiting equation for "large" drops is shown as the horizontal dashed line at $C_t = 1.0$ on the data plot of Figure 3-2. The actual data for typical icing cloud droplets, as would be expected, plots between the limiting values. The data for 19.4 micron diameter appears to approach an assymtote value of $C_t \approx 1.3$ at V_i/V_o ratios greater than 2.0.

The total water ingestion rate by the inlet is determined using the C_t and LWC_o (cloud) data in the following equation:

$$\dot{m}_{H_2O_{①}} = (LWC)_o \, V_o \, A_i \, C_t \qquad \text{EQU 3.1}$$

The liquid water content within the inlet is

$$(LWC)_{①} = \frac{\dot{m}_{H_2O\,①}}{\dot{W}_i\left(\frac{1}{\rho_i}\right)} = \frac{(LWC)_o \, V_o \, A_i \, C_t}{V_i \, A_i}$$

So,

$$(LWC)_{①} = (LWC)_o \frac{V_o}{V_i} C_t \qquad \text{EQU 3.2}$$

The following table has been constructed to show the effects of operational modes on inlet parameters for a typical commercial application.

Table 3-I

ENGINE INLET INGESTION PARAMETERS VERSUS OPERATIONAL MODES

Point No.	Engine/Airframe Operational Mode	Vi/Vo	C_t At 20 Microns	LWC_1/LWC_o	Comments
1.	Static ground idle		1 to ∞ $\approx$ (1.3)	undefined $\approx$ (0.48)	Recommended procedure for points 1 & 2a: (a) Assume Vo = 30 mph wind
2a.	80% N_1 run-up, static		1 to ∞ $\approx$ (1.3)	undefined $\approx$ (0.13)	(b) Calculate $V_i = \frac{\dot{W}_i}{\rho_i A_i}$
2b.	Takeoff $M_\infty \approx$ 0.2	2.2	1.3	0.59	(c) Assume C_t = 1.3 based on assymtotic extension of Fig. 3-2 to V_i/V_o for 20 micron drops.
3.	Mid Climb	0.75	0.85	1.13	(d) Solve LWC_1/LWC_o from Equ. 3.2
4.	Cruise	0.64	0.75	1.17	(e) Representative values thus obtained are indicated in parenthesis in the table
5a.	Mid-descent, idle	0.35	0.52	1.49	
5b.	Mid-descent, Powered	0.64	0.75	1.17	
6.	Hold	1.0	1.0	1.0	

3.1.1.2 Liquid Water Content Affected by Nose Cap Blockage

From Region 1 to Region 2 of Figure 3-1, the conservation of mass specifies that the water flow rate at 2 must equal the water flow rate at 1, except for that water which is "caught" on the nose cap surface. However, it is suggested that for this portion of the analysis, it should be considered that no water is "caught" by the nose cap surface because any such water (assuming it is not allowed to turn to ice) is only momentarily delayed by the nose cap and eventually re-enters the air stream at location 2. Furthermore, experience has shown that in actual icing conditions with no anti-icing on the nose cap, only a small fraction (about one percent) of the total water flow at location 1 is turned to ice on the nose cap. Therefore, with possibly slight conservatism, it can be stated that:

$$\dot{m}_{H_2O\,①} = \dot{m}_{H_2O\,②}$$

$$\dot{W}_① = \dot{W}_② \qquad \text{EQU 3.3}$$

and from general observation that $\dot{M}_{H_2O} = (LWC)AV$, it can be further stated that:

$$(LWC)_② = (LWC)_① \frac{A_① V_①}{A_② V_②}$$

Substitution of $AV = \frac{\dot{W}}{\rho}$ yields the final desired result

$$(LWC)_② = (LWC)_① \frac{\rho_②}{\rho_①} \qquad \text{EQU 3.4}$$

In Equation 3.4, the ratio of $\rho_②/\rho_①$ is usually very close to 1.0, upstream of a fan blade, and can be determined from the engine fan compression characteristics if it is desired to know (LWC) behind a fan blade where there is no splitter duct.

3.1.1.3 Water Ingestion and Liquid Water Content Inside the Splitter Duct Behind the Fan

To calculate the water ingestion and resulting liquid water content inside the splitter duct behind the fan, the designer will need engine performance characteristics which specify the engine air flow split of $\dot{W}_e$ and $\dot{W}_f$, where $\dot{W}_i = (\dot{W}_e + \dot{W}_f)$. The designer will also need performance characteristics which specify the air pressures and temperatures across the fan so that he can calculate the density ratio $\rho_③/\rho_①$. These performance characteristics are airflow calculations to be obtained independently, at various engine power settings, for selected points along the Single Operating Line of Figure 2-14. (Recommendations for determining which points to select are discussed in "Flight Cycle Analysis", Section 3.2).

The analysis of the splitter duct ingestion rates is accomplished by referring to Figure 3-3, which shows three posibilities of air streamlines entering the splitter duct. The compression across the fan is already accounted for in the streamline shapes shown. It is assumed that all streamlines at location 1 are parallel and uniformly spaced, and the water droplet velocity is equal to air velocity.

From aerodynamic considerations, it can be deduced that:

$$\text{IF} \quad \frac{\dot{W}_e}{\dot{W}_e + \dot{W}_f} > \frac{A_E}{A_1} \quad \text{THEN STREAMLINE POSSIBILITY I APPLIES,} \quad \frac{A'_{O_I}}{A_1} = \frac{\dot{W}_e}{\dot{W}_e + \dot{W}_f} \qquad \text{EQU 3.5}$$

$$\text{IF} \quad \frac{\dot{W}_e}{\dot{W}_e + \dot{W}_f} = \frac{A_E}{A_1} \quad \text{THEN STREAMLINE POSSIBILITY II APPLIES,} \quad \frac{A'_{O_{II}}}{A_1} = \frac{\dot{W}_e}{\dot{W}_e + \dot{W}_f} \qquad \text{EQU 3.6}$$

$$\text{IF} \quad \frac{\dot{W}_e}{\dot{W}_e + \dot{W}_f} < \frac{A_E}{A_1} \quad \text{THEN STREAMLINE POSSIBILITY III APPLIES,} \quad \frac{A'_{O_{III}}}{A_1} = \frac{\dot{W}_e}{\dot{W}_e + \dot{W}_f} \qquad \text{EQU 3.7}$$

The water catch efficiency for the engine splitter duct is defined as C_{te}, which is similar to the catch efficiency C_t of the basic inlet.

$$C_{te} = \frac{\text{water flow rate actually ingested by the splitter duct } A_E}{\text{water flow rate at location 1 contained within streamlines } A'_{O\text{-}II}}$$

Following a similar line of reasoning as was presented in the basic inlet discussion regarding the tendency of "small" water drops to follow the air streamlines, and the tendency of "large" water drops to travel straight, the following deductions can be made. These deductions ignore the tendency of the fan blades to sling the water outward, but it is conservative to ignore this.

If streamline possibility I applies, then C_{te} is greater than 1.0, and has a lower bound of 1.0, and an upper bound equal to A'_{O_I}/A_E, where A'_{O_I} is determined from Equ. 3.5. If streamline possibility II applies, then C_{te} is equal to 1.0.

If streamline possibility III applies, then C_{te} is less than 1.0, and has an upper bound of 1.0 and a lower bound equal to $A'_{O_{III}}/A_E$, where $A'_{O_{III}}$ is determined from Equ. 3.7.

In the absence of any better data than that shown on Figure 3-2 for locating the actual catch efficiency within its upper and lower bounds, it is recommended that this figure also be used to determine C_{te}. To do this, one simply enters the chart at an abscissa value equal to the appropriate area ratio (A'_{O_I}/A_E, $A'_{O_{II}}/A_E$, $A'_{O_{III}}/A_E$) and reads the value of the ordinate (C_{te} in this case) for the 19.4 micron drop diameter curve.

Letting A'_{O_I}, $A'_{O_{II}}$, or $A'_{O_{III}}$, whichever applies, be denoted by the symbol A'_{O_X}, the following equations can be written for water flow rate and liquid water content inside the splitter duct at location 3 of Figure 3-1 or 3-3.

$$\dot{m}_{H_2O_③} = [\text{PORTION OF } \dot{m}_{H_2O_①} \text{ CONTAINED IN AREA } A'_{O_{II}}] \times C_{te}$$

SO,

$$\dot{m}_{H_2O_③} = \left[\dot{m}_{H_2O_①}\right] \frac{A_E}{A_1} C_{te} \qquad \text{EQU 3.8a}$$

where C_{te} is read from Figure 3-2 at an abscissa of A'_{ox}/A_E

and $$A'_{ox} = A_1 \frac{\dot{W}e}{\dot{W}e + \dot{W}f}$$

Substituting Equ. 3.1 for $\dot{M}_{H_2O_①}$ yields

$$\dot{m}_{H_2O_③} = \left[(LWC)_o V_o A_1 C_t\right] \frac{A_E}{A_1} C_{te} \qquad \text{EQU 3.8b}$$

or substituting Equ. 3.2,

$$\dot{m}_{H_2O_③} = \left[(LWC)_① V_①\right] A_E C_{te} \qquad \text{EQU 3.8c}$$

and transforming the previously used general equation of

$$(LWC)\, A V = \dot{m}_{H_2O}$$

to a more convenient form of $\dot{M}_{H_2O} = (LWC)\frac{\dot{W}}{\rho}$

it can be shown that

$$(LWC)_③ = \frac{\rho_③}{\dot{W}e}\left[(LWC)_① \frac{\dot{W}e + \dot{W}f}{\rho_①}\right] \frac{A_E}{A_1} C_{te} \qquad \text{EQU 3.9}$$

OR

$$(LWC)_③ = \frac{\rho_③}{\rho_①}\left[\frac{\dot{W}e + \dot{W}f}{\dot{W}e}\right] \frac{A_e}{A_1} C_{te} (LWC)_o \frac{V_o}{V_1} C_t \qquad \text{EQU 3.9a}$$

For a typical airplane in a holding-pattern flight condition, typical values of $(LWC)_3$ in the engine are about 1.5 times $(LWC)_o$.

It is noted that the annular area (A_E-A_R) never appears in the above equations, and it is never needed. The only usefulness of (A_E-A_R) would be to compute an axial air flow velocity at location 3 from $(V_{axial})_{③} = \dfrac{\dot{W}_e}{(\rho\ ③)(A_E - A_R)}$

However, because of the swirl imparted by the fan, this axial velocity at location 3 is not of much use for icing calculations.

3.1.2 Water Impingement Rates

The water impingement rate is the time rate at which a portion of the surface area of a solid object is bombarded by the water droplets is a moving air stream. In general, the water impingement rate depends upon the geometry of the bombarded object, and the properties of the approaching air and water droplets. The quantitative determination of impingement rates for a variety of objects in various environments has been the subject of extensive research documented in many references. However, for purposes of engine anti-icing design calculations, the designer need concern himself only with enough of this literature to enable him to correctly use the final working curves and equations which are recommended in this section. Whereas these working curves and equations do not encompass the full extent of detailed information available from a thorough study of the literature, they do enable the designer to make reasonably accurate and conservative estimates of design water impingement rates on engine surfaces, such as airfoils and nose cones.

The basic theory for water impingement requires analysis of droplet trajectory considerations previously discussed for water ingestion rates. In an air flow field (containing water droplets) approaching and going around an airfoil, the water droplets have more inertia than the air and tend to have less curvature around the airfoil than do the air streamlines, which results in considerable droplet bombardment in the leading edge region. On the other hand, the air streamlines flowing around the foil develop considerable potential to blow the water droplets parallel to the surfaces such that no further impingement occurs. These phenomena are shown on Figure 3-4, where the symbols S_u and S_L are arc lengths around the foil surface measured from the leading edge. The distance S_u is the upper surface limit of water impingement, and the distance S_L is the lower surface limit of water impingement. The airfoil surface regions downstream of S_u and S_L receive no water impingement. The definitions of several important water impingement parameters are also shown on Figure 3-4. These are:

- H = projected blockage height of airfoil
- E_M = overall impingement efficiency
- W'' = average water impingement rate per unit wetted area

It is interesting to note that the calculation of the quantity W' is accomplished without a direct need to know the impingement limits S_u and S_L. These limits, however, are needed to calculate the term W'' which is used in later calculations. Working charts for determining the S_u and S_L limits, along with working charts for determining the impingement efficiency E_M will be presented shortly, but first it is of interest to define a few more terms of basic impingement theory.

Because the term E_M is defined as an overall impingement efficiency for the entire object, the resulting value of W" from note 6 on Figure 3-4 will also be an overall average value which does not allow for assessment of local distribution of water impingement. It is sometimes desired (and/or required) that this distribution be assessed, so Figure 3-5 is presented. On Figure 3-5, the leading-edge portion of the Figure 3-4 airfoil is shown enlarged, and some local water stream lines are considered to define a local impingement efficiency β which applies to a differential area. An important feature of this definition:

$$\beta = \frac{\text{Actual water impingement rate of Diff. Area}}{\text{Max. possible water impingement rate of Diff. Area}}$$

is that the maximum possible water impingement rate on the differential area is, by definition, that which would occur when the differential area is normal to the streamlines.

Figure 3-5a is presented to show the concepts of E_M and β as applied to a non-cylindrical body of revolution. These concepts are very similar to the 2-dimensional concepts previously discussed, and Figure 3-5a is considered to be self-explanatory.

In order to determine the impingement efficiencies β and E_M in terms of the known properties of the approaching airstream, the following equations are recommended:

From Reference 1, (and others), define

INERTIA PARAMETER $K = \dfrac{2\left(\frac{d}{2}\right)^2 \rho_{H_2O} V_o}{9 L_c / \mu}$ (DIMENSIONLESS) EQU 3.10

WHERE CHARACTERISTIC LENGTH L_c OF OBJECT IS:

AIRFOILS L_c = CHORD CYLINDERS L_c = RADIUS

SPHERES L_c = RADIUS CONES L_c = BASE RADIUS

APPROACH STREAM REYNOLDS NUMBER FOR WATER DROPLETS $Re_{o,d} = \dfrac{\rho_o V_o d}{\mu_o}$ (DIMENSIONLESS) EQU 3.11

$\dfrac{\text{TRUE DROPLET "RANGE"}}{\text{STOKES' LAW "RANGE"}} = \dfrac{\lambda}{\lambda_s}$ (DIMENSIONLESS) EQU 3.12

MODIFIED INERTIA PARAMETER OR IMPINGEMENT PARAMETER $K_o = K \dfrac{\lambda}{\lambda_s}$ (DIMENSIONLESS) EQU 3.13

The procedure, then, is to first calculate K and $R_{eo,d}$. Then the quantity λ/λ_S, which depends only on $R_{eo,d}$, is determined from Figure 3-6, which shows a graph of λ/λ_S vs. $R_{eo,d}$, suitable for design calculations. The modified inertia parameter K_o is thus directly available from Equ. 3-13.

Working charts showing appropriate value of E_M vs. K_o; β vs. K_o; and impingement limits S/L and S/R vs. K_o are presented on Figures 3-7 thru 3-17. The characteristic object dimensions for K_o on these plots are the same as those specified for K in Equation 3-10. A mean effective droplet diameter of 20 microns is recommended for E_M and β. For impingement limits S_u, S_l and S/R, a droplet diameter of 40 to 50 microns is recommended in accordance with ADS-4 and the FAA Advisory Circular AC 20-73.

In using the impingement working charts of Figures 3-7 thru 3-17, it is helpful to keep in mind that the ultimate goal of evaluating either an E_M value or a β value is to enable the W′ and W″ quantities (cf. Notes 5 and 6 on Figures 3-4 and/or 3-5) to be finally calculated. These W′ and W″ quantities are used in subsequent heat-balance calculations which will be presented in the following section, but in general, it is helpful to thoroughly understand the definitions of W, W′ and W″ now, so that a suitable choice can be made regarding whether one wants to work with E_M or β.

For 2-dimensional finite surfaces of arbitrary dimension Z into the page and characteristic blockage height H,

$$W = (LWC)_o Z V_o H E_M \qquad \left(\frac{\text{MASS}}{\text{TIME}}\right) \qquad \text{EQU 3.14}$$

$$W' = \frac{W}{Z} = (LWC)_o V_o H E_M \qquad \left(\frac{\text{MASS}}{\text{TIME} \times \text{LENGTH}}\right) \qquad \text{EQU 3.15}$$

$$W'' = \frac{W'}{\int_{S_L}^{S_u} dS} = \frac{1}{|S_u - S_L|}(LWC)_o V_o H E_M \qquad \left(\frac{\text{MASS}}{\text{TIME} \times \text{AREA}}\right) \qquad \text{EQU 3.16}$$

Thus, it is clear that if the subsequent heat balance is to be done on the bulk total wetted area, i.e., using E_M, one will also need to evaluate the impingement limits S_u and S_L in order to ultimately obtain the very important quantity W″. Note that it is not correct to obtain W″ by dividing by H. The divisor must be the arc length from S_u to S_L.

If, as is frequently desired, one choses to perform the subsequent heat balance on an elemental strip (ds) of a 2-dimensional surface, the local W terms are given by:

$$W_\ell = (LWC)_o \int V_o \beta \, ds \qquad \left(\frac{MASS}{TIME}\right) \qquad \text{EQU 3.17}$$

$$W'_\ell = \frac{W_\ell}{z} = (LWC)_o V_o \beta \, ds \qquad \left(\frac{MASS}{TIME \times LENGTH}\right) \qquad \text{EQU 3.18}$$

$$W''_\ell = \frac{W'_\ell}{ds} = (LWC)_o V_o \beta \qquad \left(\frac{MASS}{TIME \times AREA}\right) \qquad \text{EQU 3.19}$$

Thus, if one had β charts for 2-dimensional surfaces, the desired quantity W_ℓ'' would be directly available from Equ. 3-19, and exact knowledge of the impingement limits S_u and S_L would not be directly required. The unfortunate fact that no charts for 2-dimensional surfaces are available will be discussed shortly under the heading of "Recommended Procedures for Engine Airfoils," but first it is of interest to show the corresponding form of Equations 3-14 thru 3-19 as applied to axi-symmetric surfaces of revolution.

FOR E_M :

$$W = (LWC)_o V_o \pi R_{BASE}^2 E_M \qquad \text{EQU 3.20}$$

$$W' = W_{\substack{\text{PER LENGTH CIRCUMFERENCE} \\ \text{AT } S_{MAX}}} = \frac{W}{2\pi r_{MAX}} \qquad \text{EQU 3.21 (NOT NORMALLY NEEDED)}$$

$$W'' = \frac{(LWC)_o V_o \pi R_{BASE}^2 E_M}{\int_0^{2\pi} \int_0^{S_{MAX}} r \, d\theta \, ds} = \frac{W}{A_{WET}} \qquad \text{EQU 3.22}$$

The impingement limit S/R required for Equ. 3-22 is obtained from Figure 3-13. Rather than evaluate the surface area integral in Equation 3-22 to get the desired term W'', it is usually sufficiently accurate to estimate the surface area by some other means because the real nose cap shape is seldom amenable to precise mathematical surface integrals.

FOR β:

$$W_\ell = (LWC)_o V_o (r d\theta ds) \beta \qquad \text{EQU 3.23}$$

$$W_\ell' = \frac{W_\ell}{r d\theta} \qquad \text{(NORMALLY NOT NEEDED)} \qquad \text{EQU 3.24}$$

$$W_\ell'' = \frac{W_\ell}{r d\theta ds} = (LWC)_o V_o \beta \qquad \text{EQU 3.25}$$

3.1.2.1 Impingement Efficiency For Engine Airfoils

To calculate the rate of water impingement on engine airfoils, in particular the term W'' of Equation 3-16 it would at first-glance appear that E_M and $|S_u - S_L|$ could be evaluated directly from Figures 3-7 and 3-8 and 3-9. Direct substitution into Equation 3-16 would then produce the desired term W''. However, a correct calculation procedure for engine airfoils is not that simple. Because of the heavy dependence of airfoil E_M values upon the precise behavior of the particle dynamics (air streamlines and water droplet trajectories) around the specific airfoil shape in question, *it is not possible to obtain accurate impingement limits from an airfoil chart unless the airfoil in question has geometry and flow field properties that closely duplicate those of the exact airfoil for which the chart was drawn.* Whereas the complexities of airfoil streamline and water droplet trajectory analysis are not presented in this report, a gross realization of their importance to impingement limits is evident from a cursory inspection of the band-width of S_u and S_L values shown on Figures 3-8 and 3-9. The band-width would get considerably worse if these figures were to include data points for small angles-of-attack. Furthermore, these airfoils are primarily airplane wing shapes which bear little resenblance to engine vane and blade airfoils. Accurate evaluation of the arc length of impingement limits is extremely important to the correct evaluation of the W'' term in Equation 3-16, and the airplane airfoil working charts for evaluating these limits are inherently inaccurate for compressor foils. At the present time, there are no working charts to be found in literature for E_M and S_u, S_L which can be considered valid for engine airfoils.

It is therefore recommended that for engine airfoil water impingement calculations, the airplane-wing E_M and S_u, S_L charts of Figures 3-7 thru 3-9 should be disregarded. Instead, it is recommended that engine airfoil analyses of water impingement be based upon the local impingement parameter β, and Equations 3-17 thru 3-19. The need to know the exact impingement limits is thereby by-passed, and reasonably accurate, conservative assumptions can be made for β. The values of β to be used are calculated (there are no working charts for β on airfoils), and confidence in the accuracy of the calculated values can be justified by the following observations.

Observation 1. It can be deduced from general intuitive knowledge (and perhaps other knowledge) of particle dynamics than an E_M value of 1.0 for, say, a cylinder corresponds to a strong tendency for the approaching water streamlines to remain straight without diverting themselves around the cylinder.

Observation 2. For any differential strip area dS wide, tilted at an angle relative to undeflected approaching streamlines, (Figure 3-18), the local impingement parameter, β, is given by:

$$\beta = \frac{dy_o}{dS} = \cos\theta$$

Hence, the recommended procedure for engine airfoil analysis of water impingement is to: (a) hypothetically replace the airfoil (as shown on Figure 3-19) with a cylinder of diameter equal to airfoil maximum thickness, and calculate the E_M for that cylinder based on Figure 3-10. (b) Observe that this value of E_M is quite close to 1.0, so conclude that the approaching water streamline do not bend appreciably as they approach either the ficticious cylinder or the real airfoil. (c) Return to the real airfoil contour and calculate local β values as shown on Figure 3-18. (d) Use Equation 3-17 to obtain the needed quantity W_β'' for future use in heat-balance considerations.

Step (b) of the above procedure simply shows that, while this method for getting E_M is somewhat conservative, it is not overly so. This is demonstrated with the following numerical example.

Sample Calculation For The Typical Vane of Figure 3-19

(FOR A TYPICAL HOLDING CONDITION)

GIVEN:

$M_{N\infty} = M_{N_i} = 0.3$

$t_\infty = -4\,^\circ F$

$P_\infty = 12.2$ PSIA (ALTITUDE = 5000 FEET)

IGV MAX THICKNESS = 0.3 INCH

DROPLET DIAMETER d = 20 MICRONS

CALCULATION:

SINCE $M_{N\infty} = M_{N_i}$ THEN, $t_i = t_\infty = -4\,^\circ F$ AND $P_i = P_\infty = 12.2$ PSIA

$$\rho_i = \frac{P_i}{RT_i} = \frac{\left(12.2\ \frac{LB_f}{IN^2}\right)\left(144\ \frac{IN^2}{FT^2}\right)}{\left(53.36\ \frac{FT\text{-}LB_f}{LB_m\text{-}^\circ R}\right)(454^\circ R)} = 0.072\ \frac{LB_m}{FT^3}$$

$$V_i = M_{N_i}\sqrt{\gamma R_g T_i} = 0.3\sqrt{1.4\left(53.36\ \frac{FT\text{-}LB_f}{LB_m\text{-}^\circ R}\right)\left(32.2\ \frac{FT\text{-}LB_m}{LB_f\text{-}SEC^2}\right)(454^\circ R)} = 314\ \frac{FT}{SEC}$$

$$\mu = 1.1 \times 10^{-5}\ \frac{LB_m}{FT\text{-}SEC}$$

FROM EQU 3.10:

$$K = \frac{2}{9}\frac{(d/2)^2 \rho_{H_2O} V_i}{L_c \mu} = \frac{2}{9}\frac{\left[\left(\frac{20}{2}\text{ MICRONS}\right)\left(3.281\times10^{-6}\frac{\text{FT}}{\text{MICRON}}\right)\right]^2\left(62.4\frac{\text{LBm}}{\text{FT}^3}\right)\left(314\frac{\text{FT}}{\text{SEC}}\right)}{\left(\frac{0.3}{2}\text{ INCH}\right)\left(\frac{1}{12}\frac{\text{FT}}{\text{INCH}}\right)\left(1.1\times10^{-5}\frac{\text{LBm}}{\text{FT-SEC}}\right)} = 34.1$$

FROM EQU 3.11:

$$Re_{o,d} = \frac{\rho_i V_{id}}{\mu_i} = \frac{\left(0.072\frac{\text{LBm}}{\text{FT}^3}\right)\left(314\frac{\text{FT}}{\text{SEC}}\right)\left(20\text{ MICRONS}\right)\left(3.281\times10^{-6}\frac{\text{FT}}{\text{MICRON}}\right)}{1.1\times10^{-5}\frac{\text{LBm}}{\text{FT-SEC}}} = 1349$$

FROM FIGURE 3-6:

$$\frac{\lambda}{\lambda_s} = 0.32$$

FROM EQU 3.13:

$$K_o = \frac{\lambda}{\lambda_s}K = 0.32\,(34.1) = 10.9$$

FROM FIGURE 3-10:

$$E_M \approx 0.90$$

Based upon such high impingement efficiencies for engine airfoils, it appears justified to be conservative and use a value of E_M = 100% (i.e., straight line trajectories) for analysis. For such straight-line trajectories with uniform droplet size and dispersion, local impingement rates are determined from Figure 3-18. (End of sample calculation).

The impingement limits S_u and S_L associated with the recommended (β) procedure are assumed to occur at the tangency point of the ficticious cylinder, or at the point where Cos θ goes to zero, whichever occurs first. These limits are of secondary importance when β is used, and they serve as a guide for ultimately deciding how much of a vane should be anti-iced. The number $|S_u - S_L|$ never appears in the calculations.

3.1.2.2 Impingement Efficiency for Compressor Blades

Local values of β and W_ℓ on rotating blades could be estimated in the same manner as for stators except that angle of attack and velocities used would be determined by the velocity triangle relative to the rotating airfoil, and the centrifugal effects of rotating would have to be ignored. However, based on the comments made later in this report (under the heading of "Design Considerations") ice accumulation on blades has not been a problem in the past because ice is shed prior to building up intolerable thicknesses. There is at the present time, no specific recommended procedure for water impingement rates for icing analysis of rotating compressor blades.

3.1.2.3 Impingement Efficiency For Engine Nose Caps and Spinners

The method of applying the impingement data for the bodies of revolution on Figures 3-10 thru 3-17 is of less inaccuracy than described for 2-D airfoils. In much of the E_M and β

literature for bodies of revolution, deviations are found in that the characteristics lengths (great care should be taken because references vary) used are often simi-minor axis or the maximum radius of the body. Additionally, the overall impingement efficiency E_M is defined as the frontal area bounded by the starting trajectories far upstream divided by the projected frontal area of the body, as shown in Figure 3-5a.

NACA TN 4092, "Experimental Droplet Impingement on Four Bodies of Revolution," by J. P. Lewis and R. S. Ruggeri, 1957 gives data for some spheres, ellipsoidal forebodies, and a conical forebody. This study concluded that rotation of the bodies had a negligible effect on the impingement characteristics except for having an averaging effect at angle of attack. Selected data giving β and E_M for these bodies have been lifted from this reference and are included here as Figures 3-10 through 3-17.

Use of this data is recommended for design calculations, but usually involves a great deal of judgement because the particular body in question may not match the geometric shape of bodies for which the data is available. Therefore, it is necessary to match contours and/or match pressure distributions for the body in question against the same information for bodies of known impingement characteristics. This process can be very tedious.

It is therefore recommended that for water impingement calculations on nose cones and spinners, the design should:

(a) Decide whether the nose-cone or spinner in question looks like it would be best approximated by a cone, a sphere, or an ellipsoid.

(b) Determine impingement parameters either β or E_M by logical conservative interpolation among the various values plotted on Figures 3-10 thru 3-17.

(c) Use Equations 3-22 or 3-25 to calculate the value of W'' for future use in heat-balance equations.

3.1.3 Effective Wet-Bulb Temperature

Estimation of the temperatures of unheated surfaces under conditions of icing is an intermediate step in calculating possible ice accumulation and in determining whether anti-icing protection might be required. Two methods of estimating such temperatures are employed. Each differs in degree of analytical exactness, difficulty with which it is applied, and amount of information contained in the result. Prior to showing these methods, it is first necessary to present the heat-mass transfer relationships applicable to wet surfaces.

3.1.3.1 Analytic Solution For Heat Transfer Coefficients

Standard text book type correlations for heat transfer coefficients are presented herein. Any deviation from such which might be necessary to account for unique situations (turbulence level, surface roughness, or entrance effects) is beyond the scope of this report. Pertinent literature sources should be investigated if the more detailed information is deemed necessary for any specific analysis.

The external heat transfer coefficients may be estimated by the following equations:

A. Leading edge region of an airfoil is approximated by the correlation for a long cylinder

$$N_{NU,D} = \frac{h_o D}{k} = 1.14 \left(N_{Re,D}\right)^{0.5} \left(N_{Pr}\right)^{0.4} \left[1 - \left(\frac{\theta}{90}\right)^3\right] \qquad \text{EQU 3.26}$$

WHERE

D = 2 x (AIRFOIL LEADING EDGE RADIUS)

θ = ANGLE FROM STAGNATION POINT (0° TO 80°)

$$N_{Re,D} = \frac{\rho_o V_o D}{\mu_o}$$

N_{Pr} = PRANDTL NUMBER OF AIR

B. Stagnation point on a nose cone or spinner is approximated by an equivalent form of the equation in (A) except the constant is determined from "The Problem of Aerodynamic Heating", by E. R. Van Driest, North American Aviation, Inc., 1956.

$$N_{NU,D} = \frac{hD}{k} = 1.32 \left(N_{Re,D}\right)^{0.5} \left(N_{Pr}\right)^{0.4} \qquad \text{EQU 3.27}$$

WHERE

$$N_{Re,D} = \frac{\rho_o V_o D}{\mu_o}$$

and D is the diameter of an equivalent sphere of the foremost section of the body.

C. Side panel regions of airfoils and the surfaces of nose cones and spinners aft of the stagnation point may be approximated by flat plate correlations using the local velocity distributions along the outer layer of the boundary layer and surface contour distance S from the stagnation point

$$N_{NU,S} = \frac{hS}{k} = 0.322 \left(N_{Re,S}\right)^{0.5} \left(N_{Pr}\right)^{0.33} \quad \text{LAMINAR FLOW} \qquad \text{EQU 3.28}$$

$$N_{NU,S} = \frac{hS}{k} = 0.0296 \left(N_{Re,S}\right)^{0.8} \left(N_{Pr}\right)^{0.33} \quad \text{TURBULENT FLOW} \qquad \text{EQU 3.29}$$

WHERE

$$N_{Re,S} = \frac{\rho_l V_l S}{\mu_l}$$

Determination of the position of the boundary layer from laminar to turbulent is difficult. Sogin in WADC TR 54-313 recommends that preliminary calculations can be made assuming the entire boundary layer is turbulent (conservative because this gives higher heat loads). (Local velocities on a rotating spinner may be approximated by vectorily adding the longitudinal flow component to the surface rotational component.)

Heat transfer coefficients within internal anti-icing bleed air passages may be approximated using the correlation for fully developed turbulent flow in ducts.

$$N_{Nu,De} = \frac{h D_e}{k} = 0.023 \left(N_{Re,De}\right)^{0.8} \left(N_{Pr}\right)^{0.4} \quad \text{TURBULENT FLOW} \quad \text{EQU 3.30}$$

WHERE

$$N_{Re,De} = \frac{\rho V D_e}{\mu} > 10{,}000$$

$$D_e = \frac{4 \times (\text{CROSS-SECTIONAL FLOW AREA})}{\text{INSIDE WETTED PERIMETER}}$$

It is generally not good heat-exchanger design practice to allow laminar flow in the passages, so no equation is given.

It may be necessary to assess entrance effects or aspect ratio of rectangular passages for unique situations.

3.1.3.2 General Energy Balance of the Heat/Mass Transfer for a Wet Surface Above Freezing

The equation for energy transfer from a wetted surface above 32°F is presented now, but is expanded later in this report, when dealing with Ice Accumulation Calculations, to cover the situation of freezing and the associated heat of fusion. Dr. Harold Sogin in report WADC TR 54-313, "A Design Manual for Thermal Anti-Icing Systems," 1954 gives a detailed derivation of the heat/mass transfer equation for an airfoil traversing a cloud. Figure 3-20, taken from that reference shows the various heat balance terms on an elemental section of a wet airfoil of unit depth and Δs length (the i terms designate enthalpy values of the mass transfer components). The assumption has been made that the temperature gradient across the combined metal skin and water film thickness is negligible. After summing all the terms, and evaluating the various enthalpies, the general equations for true equilibrium heat transfer becomes:

$$q''_{A/I} = \left[h\left(t - t_\ell - \frac{\eta_r V_\ell^2}{2 g_c J C_p}\right) + m'' \epsilon L_s + W'' C_{p,w}(t - t_o) \right.$$

CONVECTION HEAT; EVAPORATION HEAT; SENSIBLE HEAT

$$\left. - W'' \frac{V_o^2}{2 g_c J} + C_{p,w} w' \frac{dt}{dS} - k_{SK} y_{SK} \frac{d^2 t}{dS^2} \right]$$

DROPLET KINETIC ENERGY; HEAT CARRIED OFF BY WATER FILM TO NEXT dS STRIP; HEAT CONDUCTED IN METAL TO NEXT dS STRIP

EQU 3.31

where h dry air heat transfer coefficient

t surface temperature

t_ℓ local outer edge boundary layer temp

η_r recovery factor (0.89 turbulent, 0.84 laminar)

V_ℓ local air velocity @ outer b.l.

m'' mass evaporation rate

ϵ surface wetness fraction = 1.0 when fully wet

L_s latent heat of vaporization = 1093 – 0.55°F btu/lb

w' local water film flow per unit length of the invarient dimension

W'' local water impingement rate per unit area

t_o droplet temperature in free-stream

V_o free-stream droplet velocity

$q''_{A/I}$ anti-icing heat (btu/ft^{2}hr) supplied at dry side of surface

Usually, for hand calculations or preliminary design work the last two terms are also assumed negligible. Sogin also evaluates the mass evaporation rate as

$$m'' = \frac{hI}{C_p} \frac{M_v}{M_a} \left[\frac{P_{v,s} - P_{v,\ell}}{P_\ell - P_{v,s}} \right]$$

EQU 3.32

WHERE

$$I = \frac{(N_{St})_{MODIFIED}}{N_{St}} = \begin{matrix} 1.1 & \text{LAMINAR FLOW} \\ 1.0 & \text{TURBULENT FLOW} \end{matrix}$$

$M_v = 18.016$
$M_a = 28.996$ } molecular weights vapor, air

$P_{v,s}$ = vapor pressure (saturated) evaluated at surface temp.

$P_{v,\ell}$ = local vapor pressure at outer edge of boundary layer, at the relative humidity of the local flow stream

Note: $P_{v,\ell}$ is evaluated by applying Dalton's Law of partial pressures from the saturated cloud environment to the engine surface in question. Thus, according to Ref. 13:

$$P_{v,\ell} = \left[P_{v,\infty\,(SAT)}\right] \frac{P_\ell}{P_\infty}$$

P_ℓ = local static air pressure at outer edge of boundary layer.

The true equilibrium heat transfer equation now becomes

$$q''_{A/I} = \left[h\left(t - t_\ell - \frac{r_r V_\ell^2}{2g_c J C_p}\right) + \frac{0.622 h I \epsilon L_s}{C_p}\left(\frac{P_{v,s} - P_{v,\ell}}{P_\ell - P_{v,s}}\right) \right.$$

CONVECTION — EVAPORATION

$$\left. + W'' C_{p,w}(t - t_o) - W'' \frac{V_o^2}{2g_c J} \right] \qquad \text{EQU 3.33}$$

SENSIBLE — KINETIC ENERGY

WHERE

$$P_{v,\ell} = \left[P_{v,\infty\,(SAT)}\right] \frac{P_\ell}{P_\infty}$$

and, it is usually true that $(P_\ell - P_{v,s}) \approx P_\ell$, so this can be used during the early stages of iterative solutions.

The true equilibrium temperature of an unheated wet surface may be calculated using the previous equation by setting $q''_{A/I} = 0$. All of the heat/mass transfer boundary conditions and the local water impingement rate are known. Solution of the equation for surface temperature t yields the "effective wet-bulb temperature," for wet surfaces. The solution involves an iterative calculation between t, and $P_{v,s}$, until q" net is zero (guess t, evaluate $P_{v,s}$ at t from Steam Tables, calc q" net). The use of t_o in the sensible heat term implies that one has assumed that the droplet temperature is still at its ambient atmospheric cloud value when it arrives at the engine surface, in spite of ram air temperature increases and fan temperature rises of the air. This assumption is recommended by Sogin in Reference 13, and is discussed further in Section 6.1.2.2.

It is noted that both Sogin in his document and Vernon Gray in NACA TN 2799 have developed graphical solutions of this equation for specific conditions (particularly for when t droplet = t air$_\ell$). Such graphs are not of much use inside engines because they violate the recommended assumption that droplet temperature should be held at its ambient cloud value until it contacts an engine surface.

3.1.3.3 "Datum" Temperature

An approximate method of estimating the temperature of a surface in icing was developed by J. K. Hardy in "Kinetic Temperature of Wet Surfaces, A Method of Calculating the Amount of Alcohol Required to Prevent Ice, and the Derivation of the Psychrometric Equation," NACA ARR No. 5G13, 1945 (Reference 15). The recommended form of this "datum" temperature is shown on Figure 3-21, and is Equ. 3-34. The equation form shown on Figure 3-21 can be derived from Equation 3-33 as follows.

If equation 3-33 is modified by:

1. dropping the sensible heat term (i.e. impinging water temperature assumed equal to final surface temp.)
2. dropping the kinetic energy term
3. ignoring $P_{v,s}$ in the denominator of evaporation term because $P_{v,s} \ll P_\ell$
4. letting $I=1, \in = 1$
5. setting $q'' A/I = 0$

then,

$$0 = h\left(t - t_\ell - \frac{\eta_r V_\ell^2}{2 g_c J C_p}\right) + \frac{0.622 h L_s}{C_p}\left(\frac{P_{v,s} - P_{v,\ell}}{P_\ell}\right)$$

Solving for surface temperature t datum,

$$t_{DATUM} = t_\ell + \frac{\eta_r V_\ell^2}{2 g_c J C_p} - \frac{0.622 L_s}{C_p}\left(\frac{P_{v,s} - P_{v,\ell}}{P_\ell}\right) \qquad \text{EQU } 3.34$$

which is essentially Hardy's "datum" temperature. As Messinger (Ref. 16) points out, this represents the temperature in clear air (no LWC) of a surface that is wetted by water (possibly from within the surface) supplied at the temperature of the surface itself. One can rapidly apply this equation because impingement rate W'', heat transfer coefficient h, and droplet temperature prior to impingement are not used.

It is noted that for surfaces above freezing the "datum" temperature predicts high, and predicts low for surfaces below freezing.

3.1.3.4 Energy Balances With Freezing

Ice will build up on a surface when its equilibrium temperature is less than or equal to 32°F under icing conditions. The rate of accumulation is a function of the atmospheric conditions and engine/airframe operational conditions as they affect water ingestion rate by the engine inlet, water impingement rate upon the surface, and heat/mass transfer from the surface. Two methods of calculating ice accumulation are used. The first is involved in that it uses the concept of a "freezing fraction" and the associated latent heat of fusion when t = 32°F; the second assumes that when the surface is 32°F or lower, all droplets that impinge upon the surface freeze.

Messinger (in Reference 16) has introduced the concept of freezing fraction n as that portion of the impinging liquid W″ that freezes at 32°F. When water freezes at 32°F the latent heat of fusion released is L_f = 144 BTU/lbm. Accounting for the fraction of impinging water that freezes and letting t = 32°F, the general heat transfer equation (i.e. Equ 3.33) becomes:

$$q''_{A/I} = \left[h\left(32 - t_\ell - \frac{\eta_r V_\ell^2}{2g_c J C_p}\right) + \frac{0.622 I \epsilon L_s h}{C_p}\left(\frac{P_{v,s} - P_{v,\ell}}{P_\ell - P_{v,s}}\right) \right.$$

$$\left. + W'' C_{p,w}(32 - t_o) - W'' n(144) - W'' \frac{V_o^2}{2g_c J} \right] \qquad \text{EQU 3.35}$$

WHERE

n = FREEZING FRACTION (PORTION OF W'' THAT FREEZES)

NOTE: AT 32°F,

$$P_{v,s} = 0.1802 \text{ "Hg}$$

$$L_s = \left[1093 - 0.55(32)\right] = 1075.4 \ \frac{BTU}{LBm}$$

$$C_{p,w} = 1.0 \ \frac{BTU}{LBm - °F}$$

WHEN

$t > 32°F$, $n = 0$

$t < 32°F$, $n = 1.0$

When the surface temperature is 32°F (t = 32), the freezing fraction n can be determined for a non anti-iced surface by setting q'' A/I = 0 in Equation 3-35. For an anti-iced surface, the numerical value of q'' A/I has to be known input (independently determined), and the freezing fraction n is then directly obtainable from Equation 3-35. In Equation 3-35, the surface temperature of 32°F is the "effective wet-bulb temperature" for partially icing surfaces.

When the surface temperature is less than 32°F, the true equilibrium general heat transfer equation (i.e. Equation 3-33) becomes:

$$q''_{A/I} = \left[h\left(t - t_l - \frac{r_r V_l^2}{2 g_c J C_p}\right) + \frac{0.622 h I \epsilon L_s}{C_p}\left(\frac{P_{v,s} - P_{v,l}}{P_l - P_{v,s}}\right) - W'' C_{p,ice}(32 - t) - W''(144) + W'' C_{p,w}(32 - t_o) - W'' \frac{V_o^2}{2 g_c J} \right]$$

EQU 3.36

Solution of Eq. 3-36 with q'' A/I = 0 yields the "effective wet bulb temperature" for fully iced surfaces below 32°F.

All of the important true equilibrium energy balances of Equations 3-33, 3-35, and 3-36 are similar and differ only in the terms containing W''. The term W'' ($V_o^2/2g_c$ J) is the same in all equations because it represents the difference from total enthalpy to static enthalpy of the approaching droplets. All the other W'' terms represent the change of water enthalpy as the droplet temperature changes from freestream temperature to surface temperature. The various sub-equations for this enthalpy change can be visualized from Figure 3-22, which shows the general enthalpy - temperature graph of the water droplet surface process.

3.2 ICE ACCUMULATION CALCULATIONS

Even though the freezing fraction is calculable, a simplifying assumption that all impinging water freezes is generally applied when accuracy is not as important as conservatism. Also because of difficulties in solving Equ. 3-35 when q'' A/I is not zero, this assumption is usually used for calculating ice accumulation during transients on an inadequately anti-iced surface. However, the freezing fraction calculation can be used if more accuracy is required, and can sometimes show significant savings in ice accumulation thickness.

3.2.1 Assuming All Impinging Water Freezes

When the assumption is made that all impinging water freezes:

$$\text{Ice Thickness} = \frac{W'' (\Delta \text{ TIME})}{\rho_{ice}} \qquad \text{Equ. 3.37}$$

3.2.2 Using the Freezing Fraction

If the freezing fraction is calculated, then W'' in Equ. 3-37 is replaced by (n W'') to yield:

$$\text{Ice Thickness} = \frac{n\, W'' (\Delta \text{ TIME})}{\rho_{ice}} \qquad \text{Equ. 3.38}$$

3.3 ICE ACCUMULATION LIMITS

In general, it is not possible to define a numerical thickness of allowable ice accumulation to any given region of an engine, because the allowable limits are likely to be significantly different for various engines. The following general trends, however, can be discussed.

3.3.1 Spinners

For a rotating nose-cap spinner, significant ice accumulation can be tolerated, provided that it can be safely ingested by the engine if it sheds, and provided that it does not induce untenable rotor vibration if it does not shed. The recommended limits are stated in Recommendation 23 of Chapter I.

3.3.2 Blades

For fan blades and other compressor blades, the above comments are applicable. Fan blades and other compressor blades have generally demonstrated, over many years of flight experience, that their ice shedding characteristics are compatible with engine tolerances to ingestion.

3.3.3 Non-Rotating Nose Caps

For non-rotating nose caps, significant ice accumulation may be tolerable, provided that it can be safely ingested by the engine if it sheds. Shedding from a non-rotating nose cap is not as apt to happen as from a rotating spinner, so the ice thicknesses could easily become intolerably large if non-rotating nose caps were not actively anti-iced. The recommended limits are stated in Recommendation 25 of Chapter I.

3.3.4 Stator Vanes

Stator vane ice accumulation can reach intolerable amounts if either of two considerations is violated. The first is similar to ice ingestion consideration of nose caps, but should be modified to account for the possibility that several stator vanes might shed simultaneously. Hence, the maximum allowable ice accumulation on any one stator vane tends to be significantly less than on a single nose cap.

The second consideration for stator vane ice accumulation limits pertains to the vane ice thicknesses which will unduly degrade the aerodynamic performance of the compressor. This allowable thickness varies considerably for the various vane stages in various engines, and is dependent upon the vane aerodynamics and the physical distance circumferentially between the vanes in any one stage. The engine anti-icing designer generally has to consult a compressor aerodynamicist to obtain this limit. A first estimate can be assumed to be that ice thickness which will significantly reduce the air flow in a vane stage.

Recommended limits for stator vane ice accumulation are stated in Recommendations 26 and 27 of Chapter I.

3.3.5 Probes

For engine probes on which icing could affect flight safety:

(a) Ice accumulation on the sensing element of an engine probe or static pressure tap should be in general limited to zero accumulation, unless the probe is equipped with a de-icing system to completely remove ice in the event of sensor malfunction.

(b) Furthermore, the sensing element of temperature probes should generally be protected from liquid water impingement if the probe is of such a design that evaporation from a wetted sensor might induce intolerable errors in the air temperature readings.

Ice accumulation limits for the supporting structure and/or housing of a probe are considered to be essentially the same as for stators.

The above limits are also stated as Recommendation 28 of Chapter I.

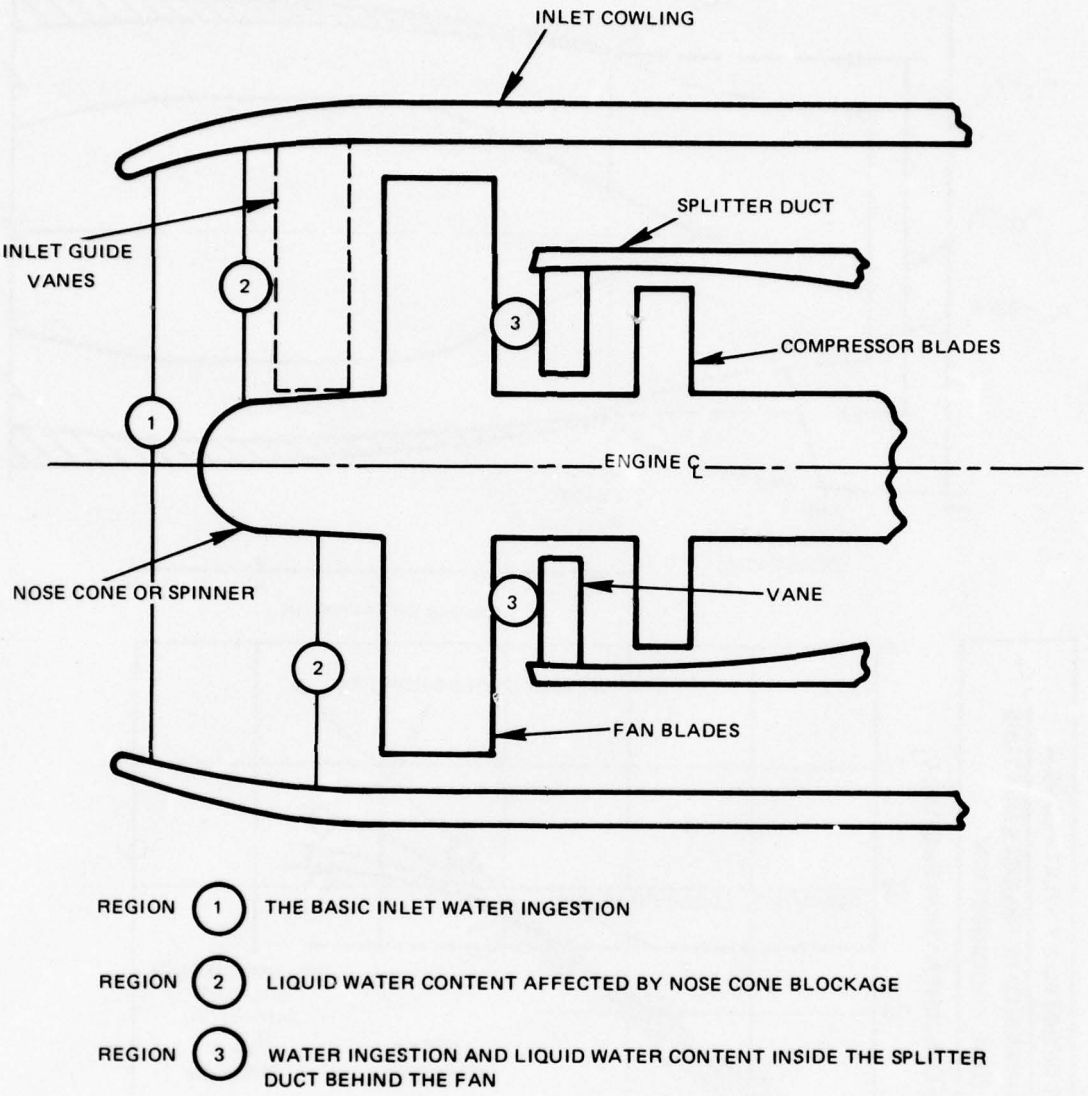

Figure 3-1 Typical Inlet Configuration for a Fan Engine, Three Regions of Concern for Water Ingestion

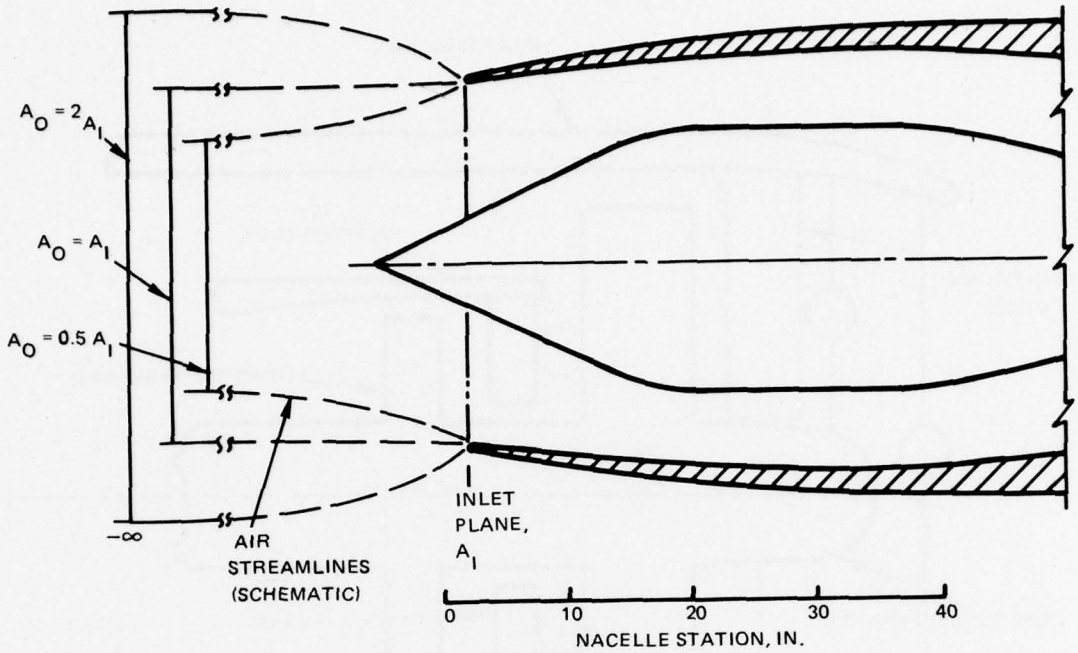

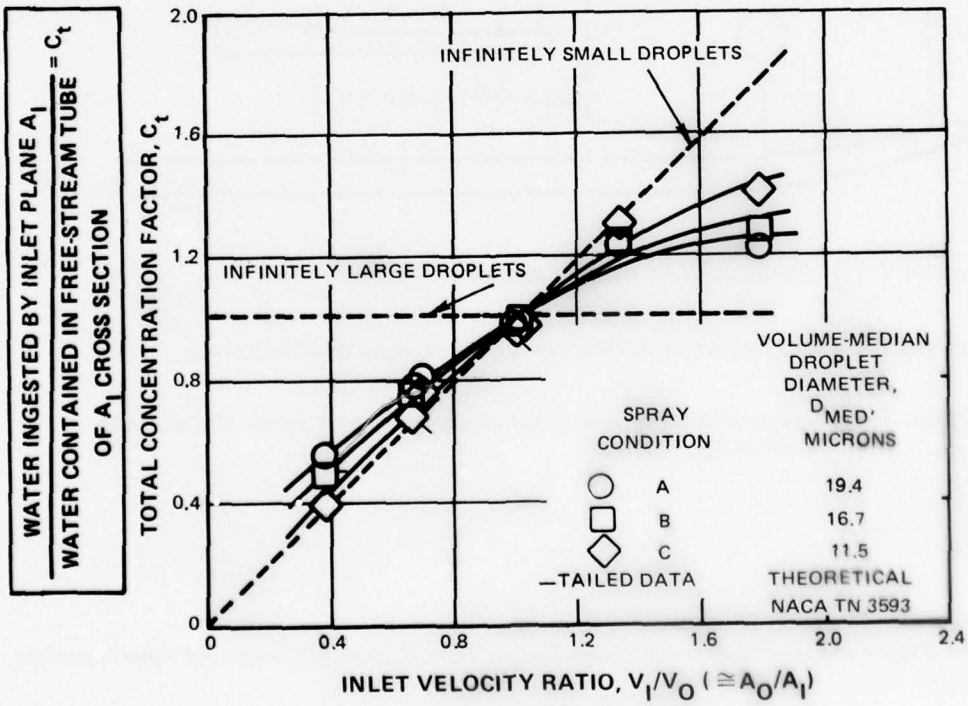

(COPIED FROM NACA TN 4268)

FOR 0° ANGLE OF ATTACK

Figure 3-2 Inlet Catch Efficiency

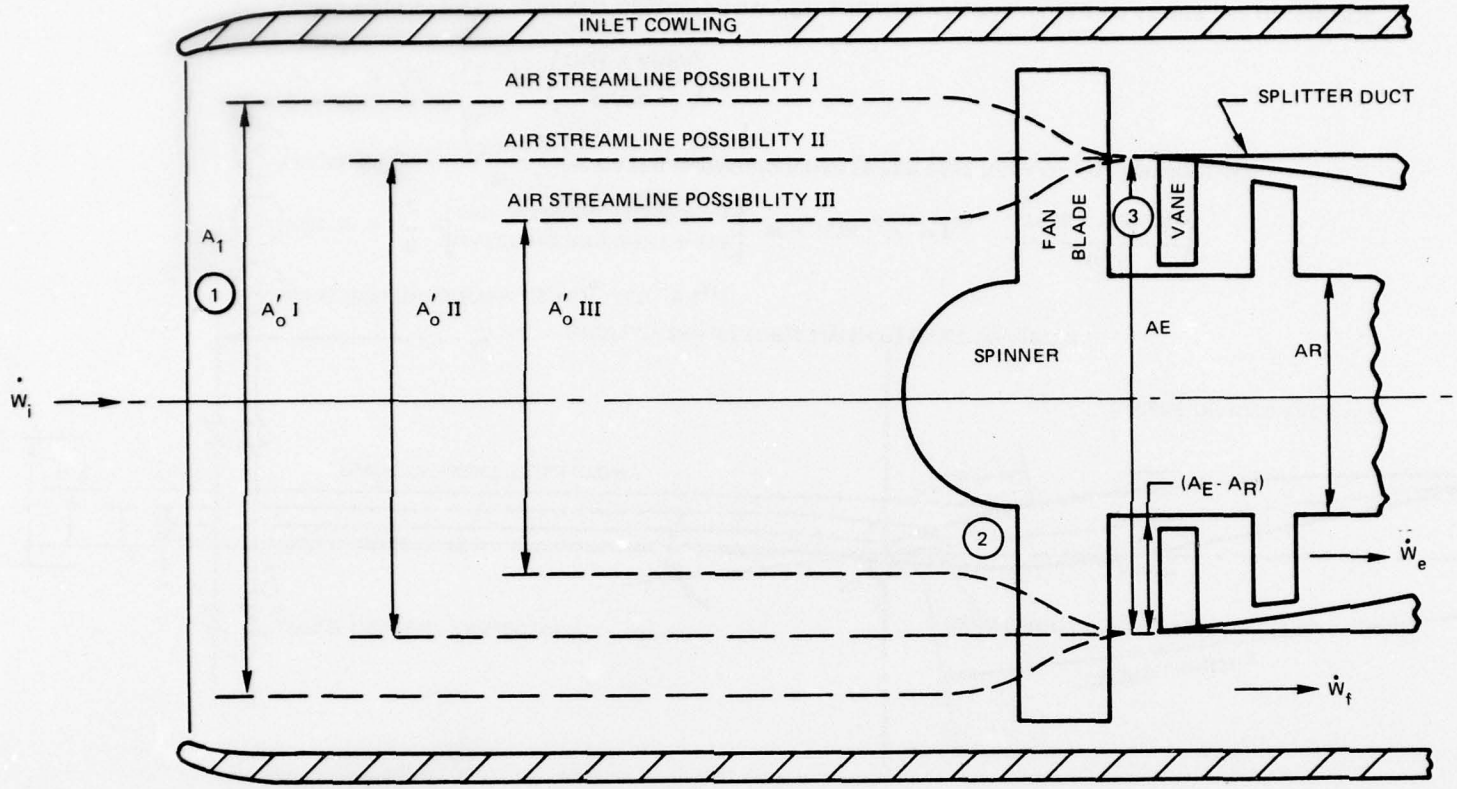

Figure 3-3 Inlet Streamline Possibilities for Splitter Duct Behind a Fan

(1) MAX. POSSIBLE WATER IMPINGEMENT RATE, $\frac{\text{MASS}}{\text{TIME}} = \dot{M}_{H_2O}$ IN BLOCKAGE HEIGHT H

$= [(LWC)_o (zH) V_o]$

(2) LET W = ACTUAL TOTAL WATER IMPINGEMENT RATE, $\frac{\text{MASS}}{\text{TIME}} = \dot{M}_{H_2O}$ IN $\left| y_{o\ell} - y_{o_u} \right|$

$W = [(LWC)_o (Z) (y_{o\ell} - y_{ou}) V_o]$

(3) DEFINE $E_M = \frac{(2)}{(1)} \frac{\left| y_{c\ell} - y_{ou} \right|}{H}$ = IMPINGEMENT EFFICIENCY

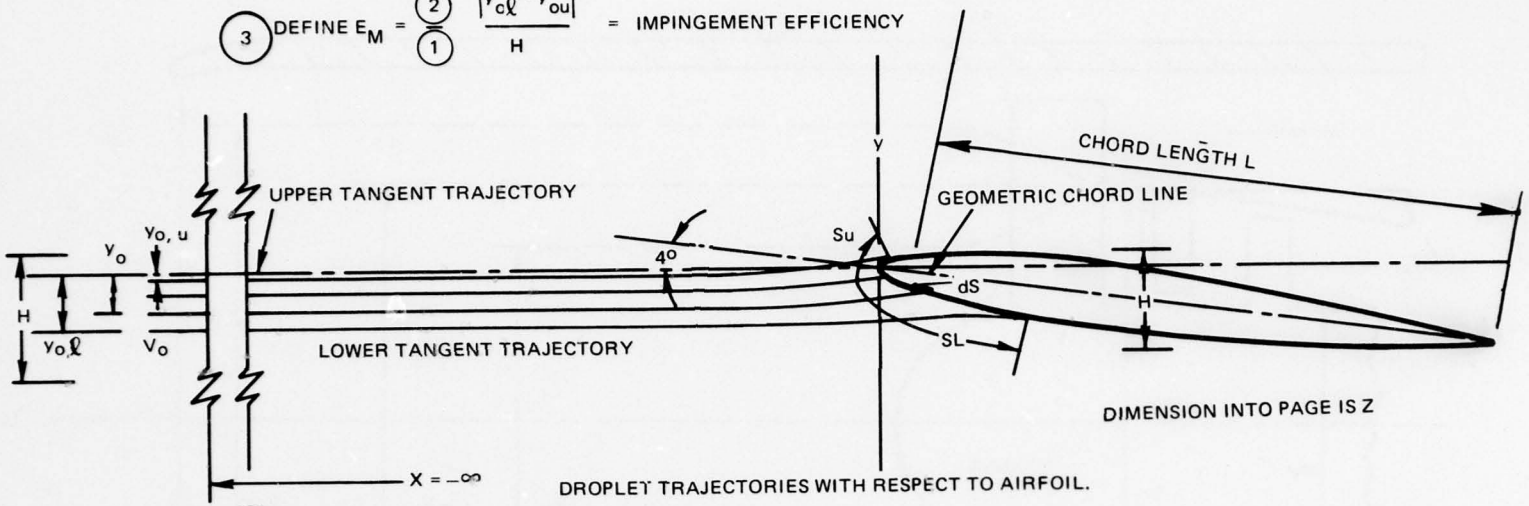

(4) BY SUBSTITUTION, $W = [(LWC)_o (Z) V_o H E_M]$

(5) AND $W' = \frac{W}{Z} = \left[\begin{matrix}\text{WATER IMPINGEMENT RATE,} \\ \text{PER UNIT LENGTH OF SPAN}\end{matrix}\right]$ $W' = (LWC)_o V_o H E_M \quad \left(\frac{\text{MASS}}{\text{TIME X LENGTH}}\right)$

(6) ALSO, $W'' = \frac{W'}{\int_{SL}^{SU} dS}$ = WATER IMPINGEMENT RATE PER UNIT AREA OF WETTED SURFACE

$W'' = W' / |S_u - S_L| \quad \left(\frac{\text{MASS}}{\text{TIME X AREA}}\right)$

(7) NOTE THAT S_u AND S_L ARE NOT NEEDED FOR W', THESE LIMITS ARE ONLY USED TO ASSESS THE GEOMETRIC CHORDWISE EXTENT OF IMPINGEMENT, AND TO OBTAIN THE VALUE OF W''.

Figure 3-4 Total Impingement Efficiency E_m

① MAX POSSIBLE WATER IMPINGEMENT RATE ON dS, $\frac{\text{MASS}}{\text{TIME}} = \dot{M}_{H_2O}$ WITHIN y_o STREAMLINES WHICH ARE INITIALLY dS APART

$= [(LWC)_o (zdS) V_o]$

② LET W_ℓ = ACTUAL LOCAL WATER IMPINGEMENT RATE ON dS, $\frac{\text{MASS}}{\text{TIME}} = \dot{M}_{H_2O}$ IN dy_o $\quad W_\ell = [(LWC)_o z\, dy_o V_o]$

③ DEFINE $\beta = \frac{②}{①} = \frac{dy_o}{dS}$ = LOCAL IMPINGEMENT EFFICIENCY

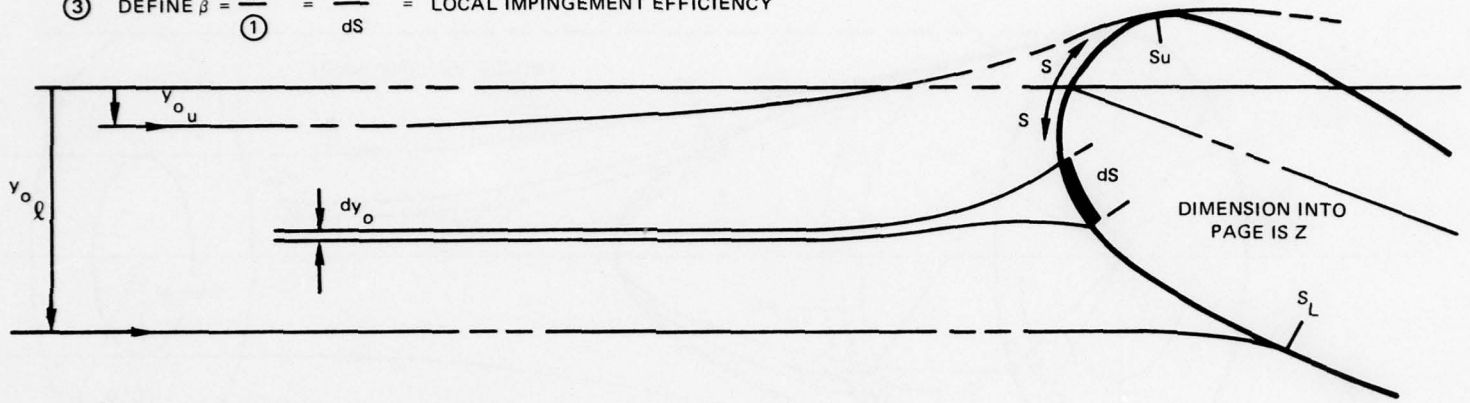

④ BY SUBSTITUTION, $W_\ell = [(LWC)_o (Z) V_o \beta\, dS]$

⑤ AND $W'_\ell = \frac{W_\ell}{Z}$ = LOCAL WATER IMPINGEMENT RATE UNIT LENGTH OF SPAN $\quad W'_\ell = (LWC)_o V_o \beta\, dS \quad \frac{\text{MASS}}{\text{TIME X LENGTH}}$

⑥ IT IS SOMETIMES USEFUL TO DEFINE $W''_\ell = \frac{W_\ell}{zdS}$ = LOCAL WATER IMPINGEMENT RATE, PER UNIT AREA

$W''_\ell = (LWC)_o V_o \beta \quad \frac{\text{MASS}}{\text{TIME X AREA}}$

⑦ COMPARISON OF EQU ⑤ ON THIS FIGURE, WITH EQU ⑤ OF THE PREVIOUS FIGURE, YIELDS THE RELATIONSHIP BETWEEN β AND E_M:

$$\left[\int_{S_L}^{Su} W'_\ell\right] = W' \quad \text{so} \quad H E_M = \int_{S_L}^{Su} \beta\, dS$$

Figure 3-5 Local Impingement Efficiency, β

$$E_M = \frac{\text{ACTUAL WATER IMPINGEMENT ON WETTED SURFACE FROM S = 0 to S = } S_{MAX}}{\text{MAX POSSIBLE IMPINGEMENT ON PROJECTED } A_{BASE}} = \frac{\dot{M}_{H_2O} \text{ IN } \pi \, (r_{o,\,MAX})^2}{\dot{M}_{H_2O} \text{ IN } \pi (R_{BASE})^2}$$

$$\beta = \frac{\text{ACTUAL WATER IMPINGEMENT ON dA}}{\text{MAX POSSIBLE WATER IMPINGEMENT ON dA}} = \frac{da_o}{dA}$$

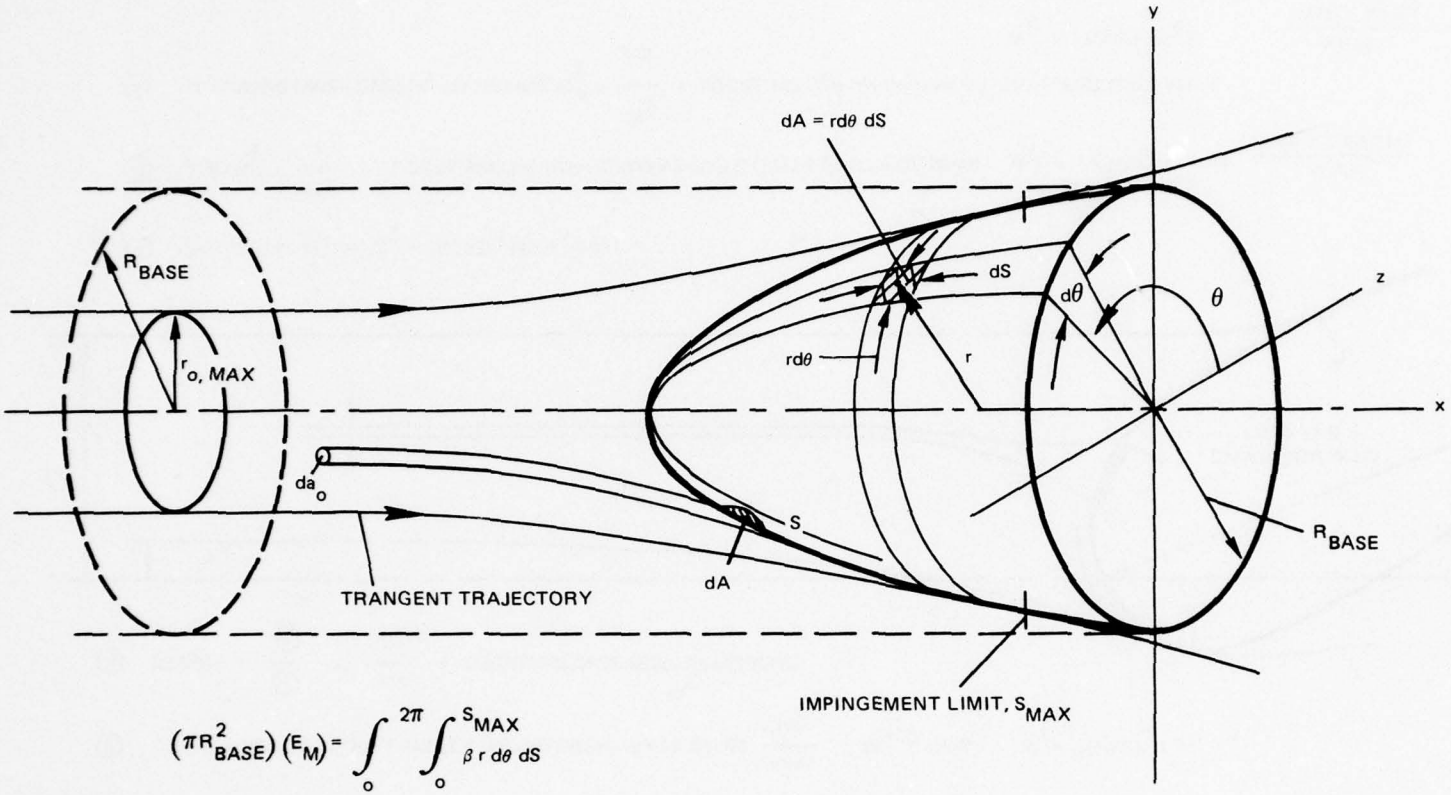

$$(\pi R_{BASE}^2)(E_M) = \int_0^{2\pi} \int_0^{S_{MAX}} \beta \, r \, d\theta \, dS$$

Figure 3-5a Axi-Symmetric Surface of Revolution, Droplet Impingement at Zero Angle of Attack

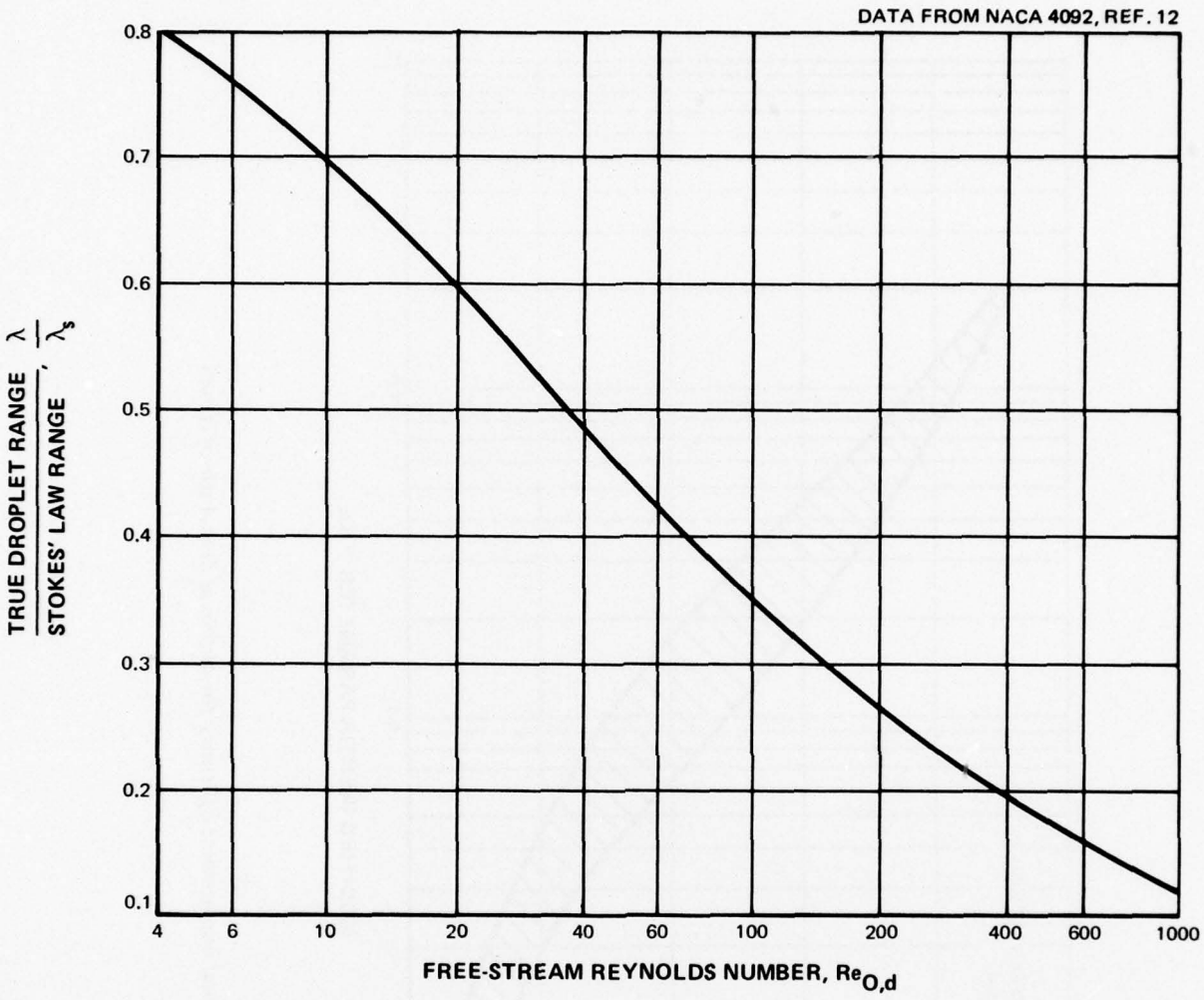

Figure 3-6 Droplet Range Ratio λ / λ_s

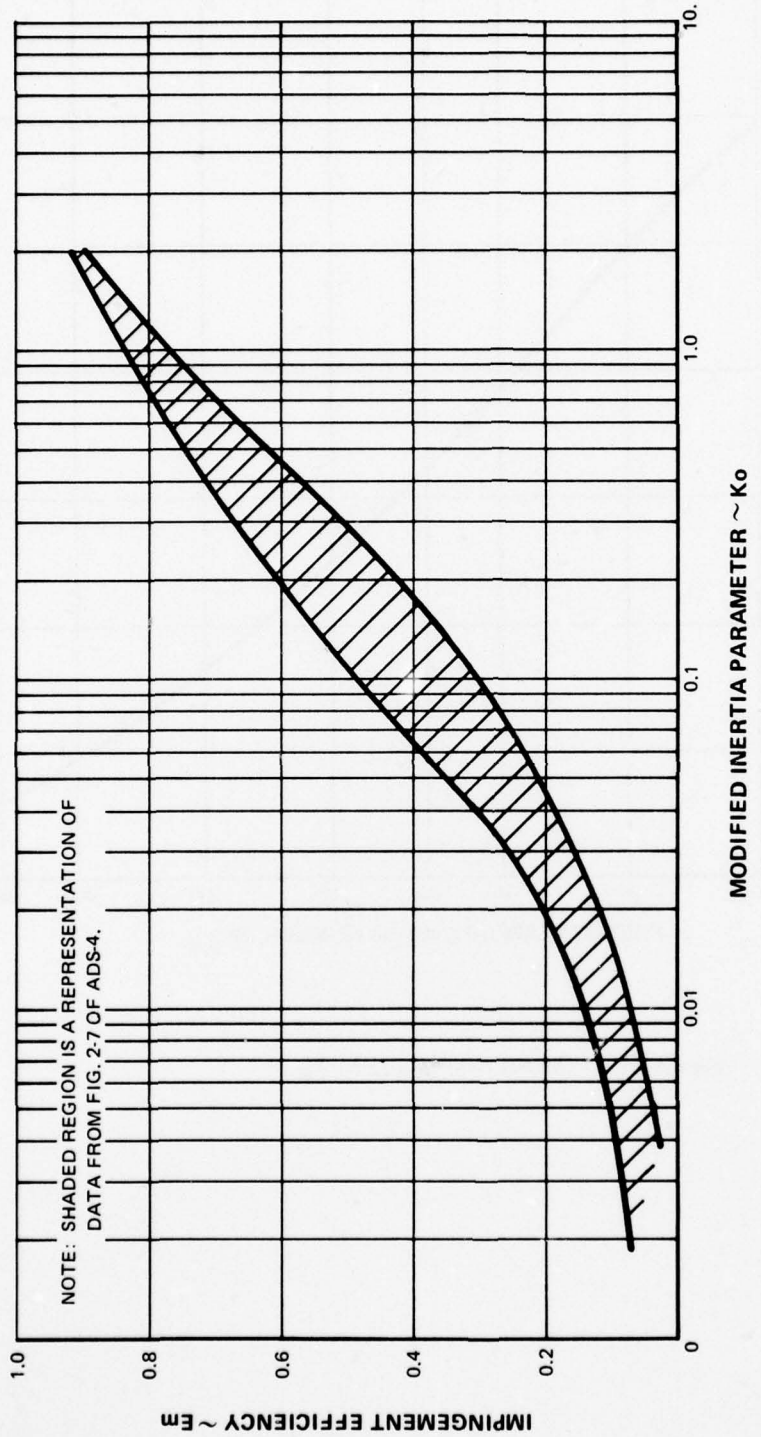

Figure 3-7 Total Impingement Efficiency for Airfoils at Zero Angle of Attack

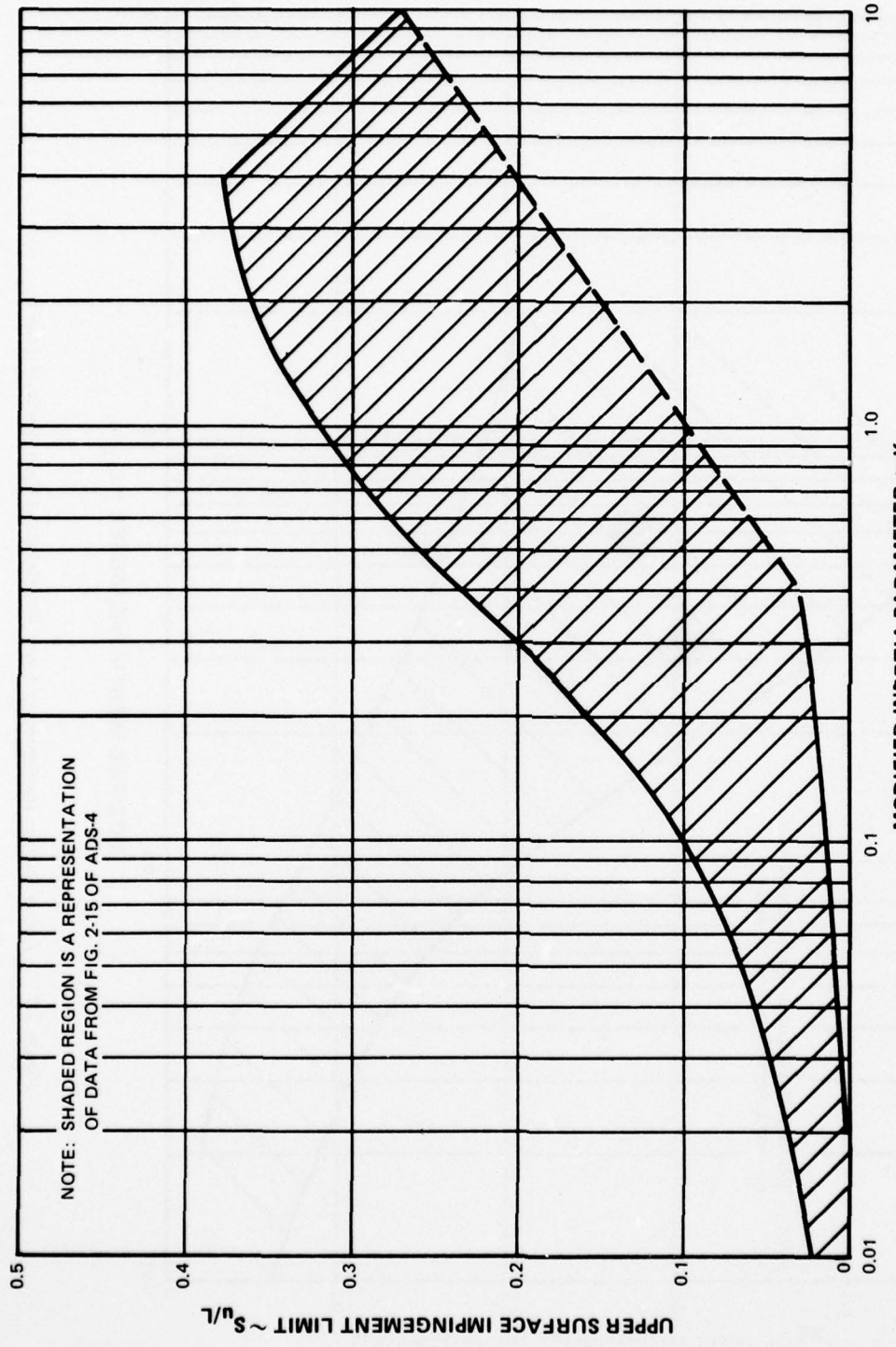

Figure 3-8 Upper Surface Impingement Limit for Airfoils at Zero Angle of Attack

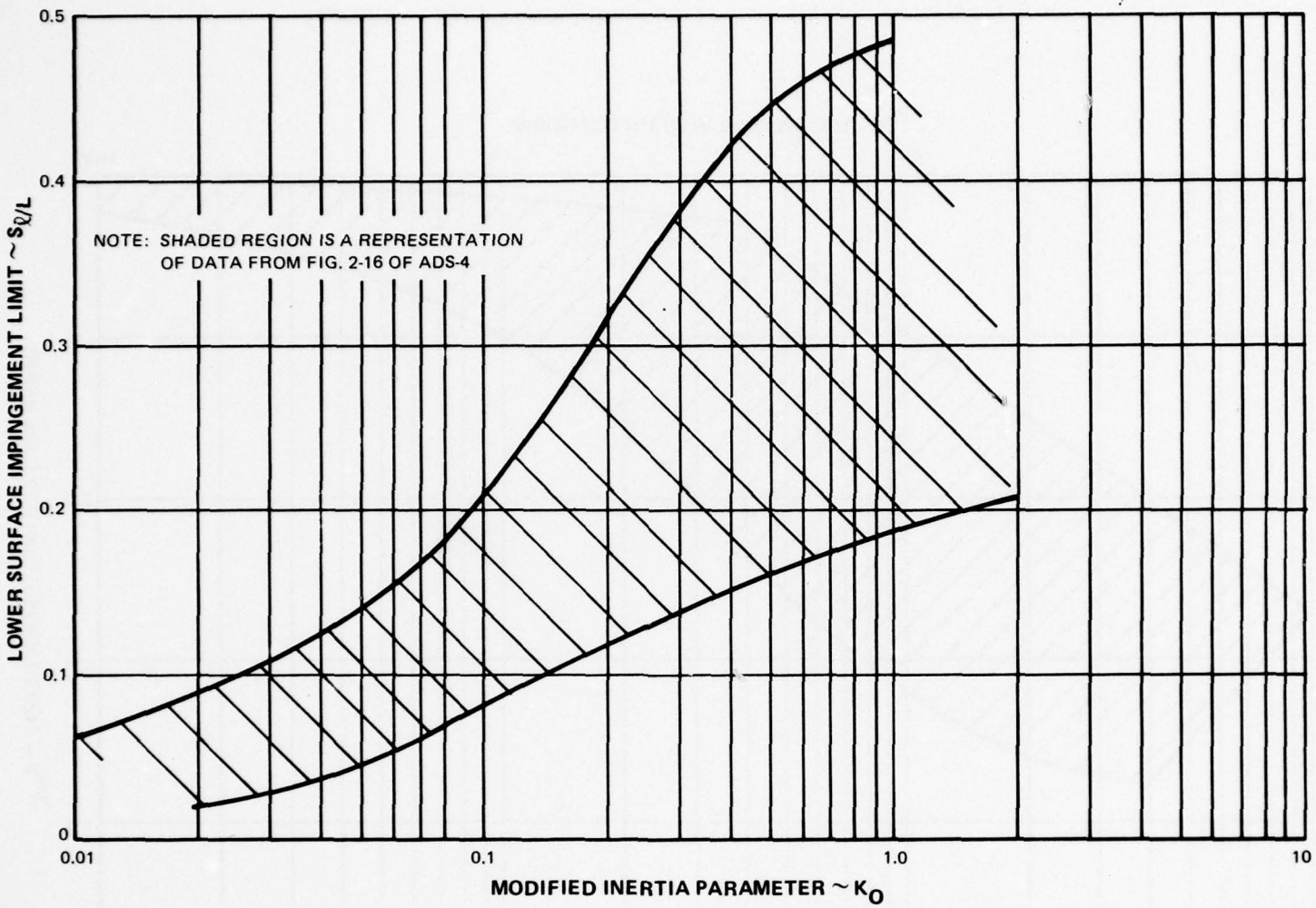

Figure 3-9 Lower Surface Impingement Limit for Airfoils at Zero Angle of Attack

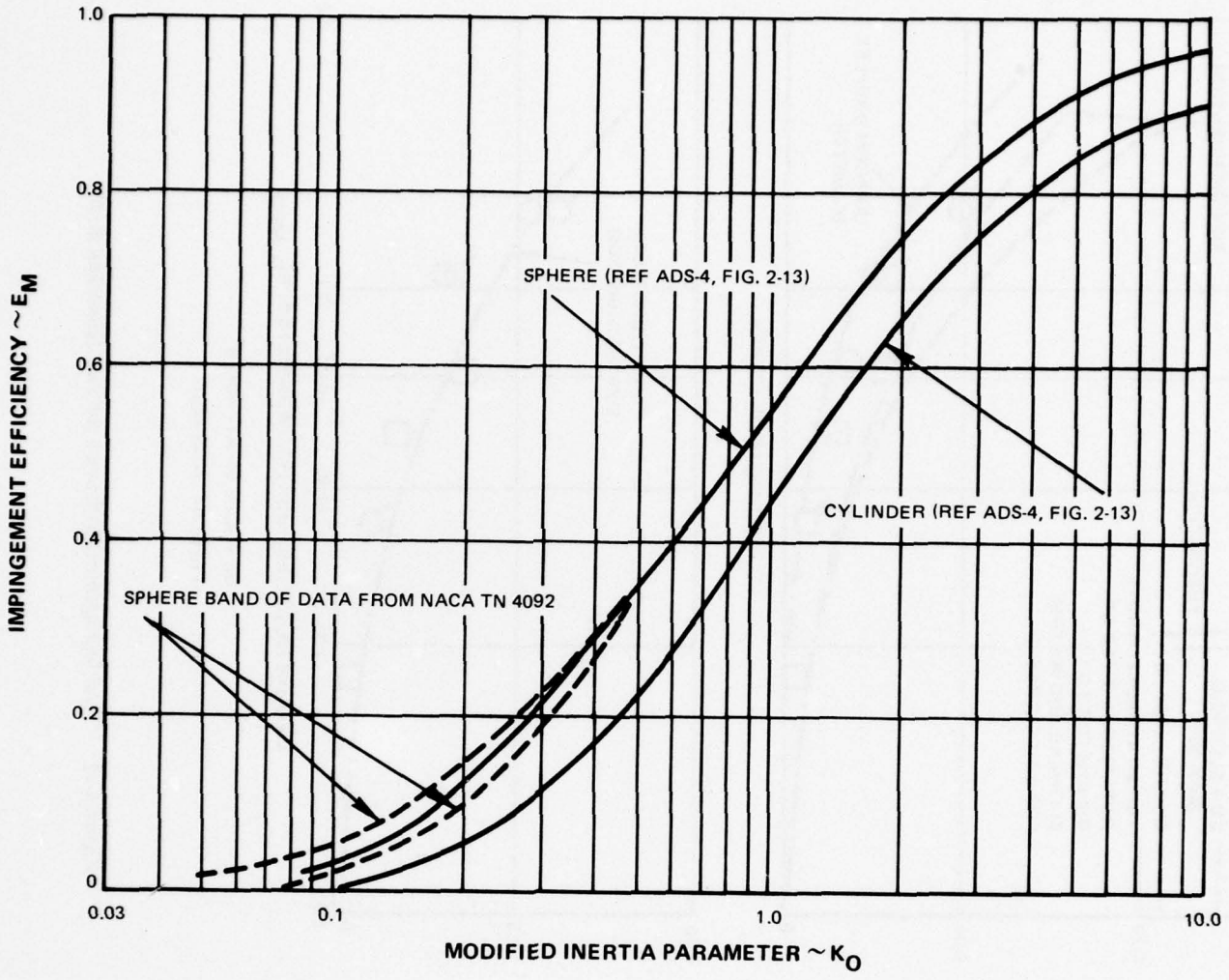

Figure 3-10 Total Impingement Efficiency for Spheres and Cylinders

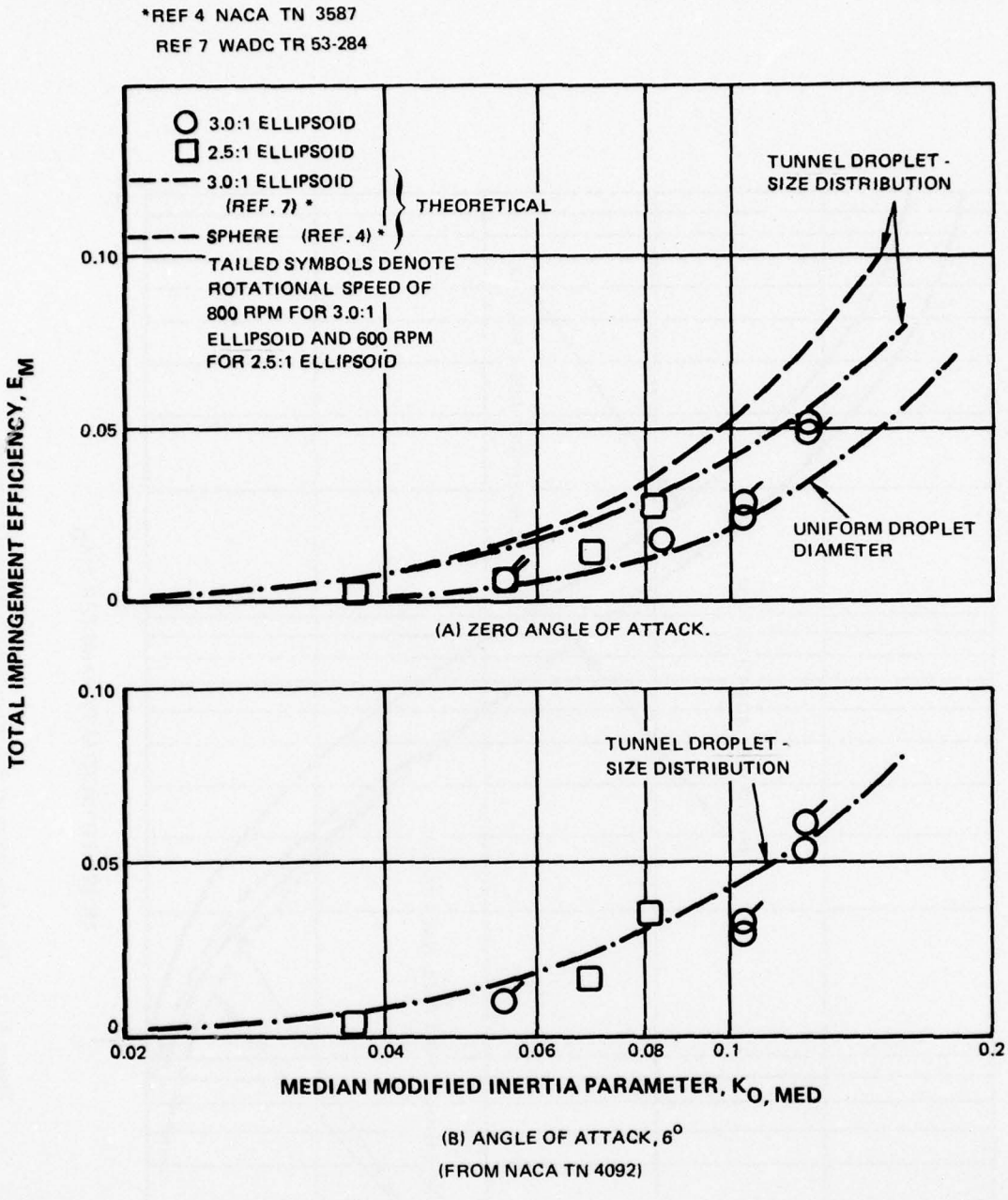

Figure 3-11 Total Impingement Efficiency for Two Ellipsoidal Bodies

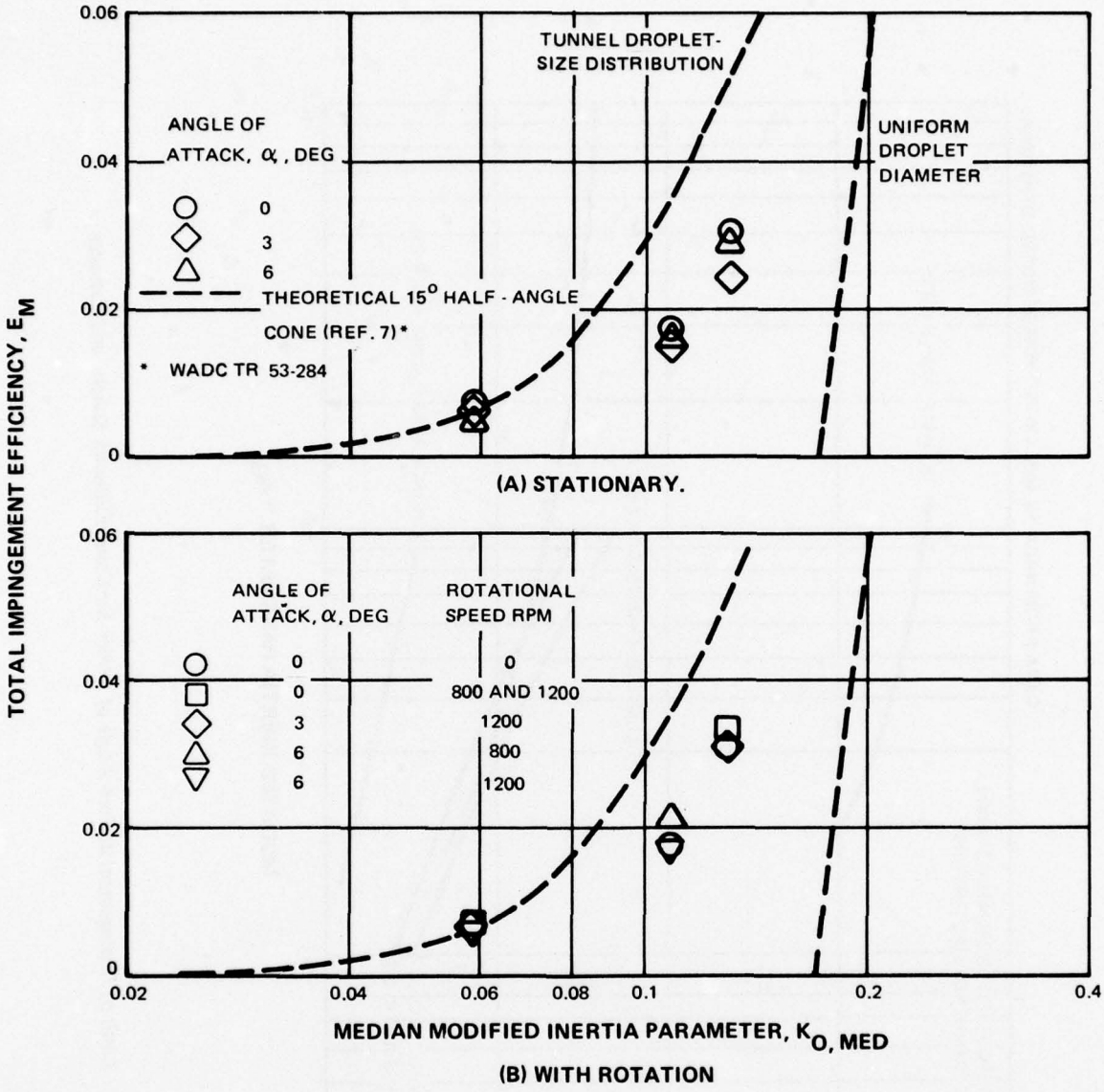

Figure 3-12 Total Impingement Efficiency on a Conical Forebody

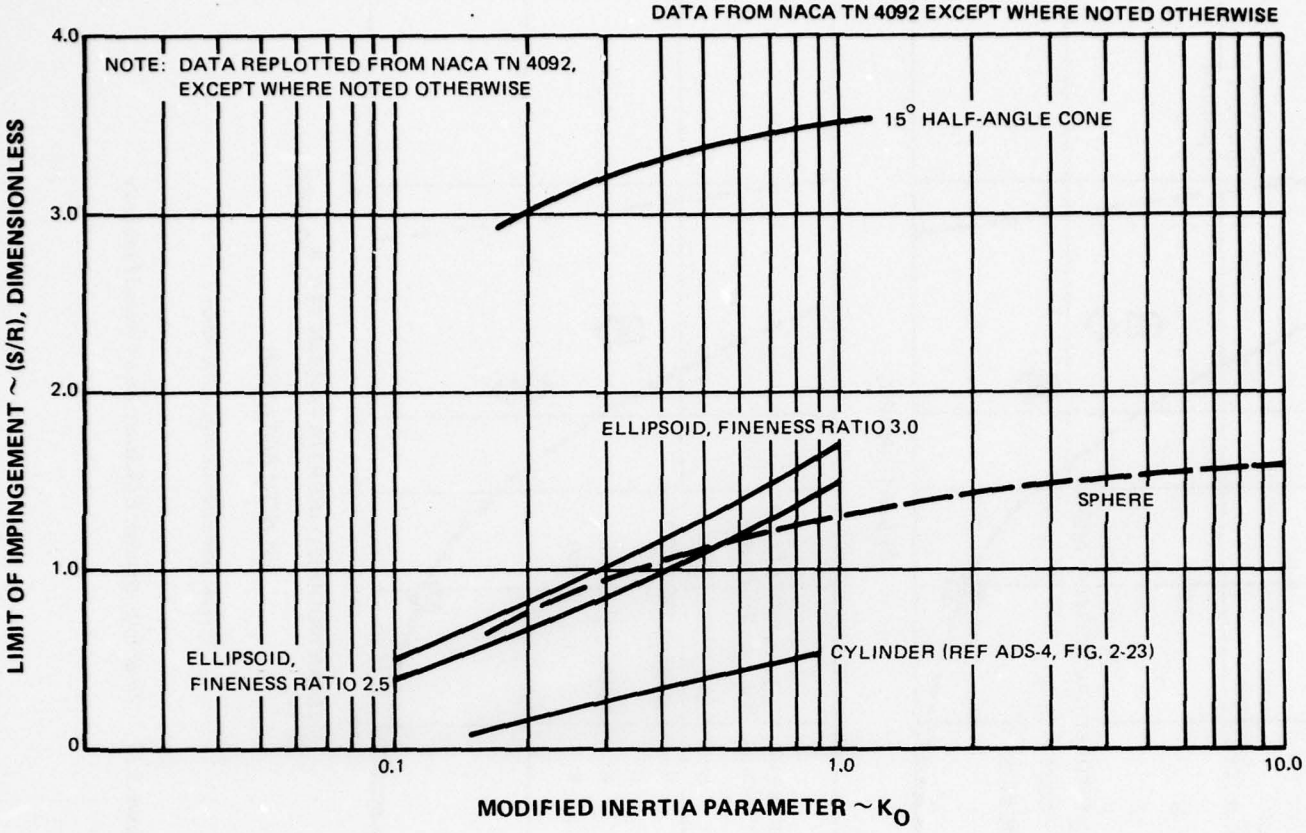

Figure 3-13 Limit of Impingement at Zero Angle of Attack for Cone, Ellipsoid, Sphere, and Cylinder

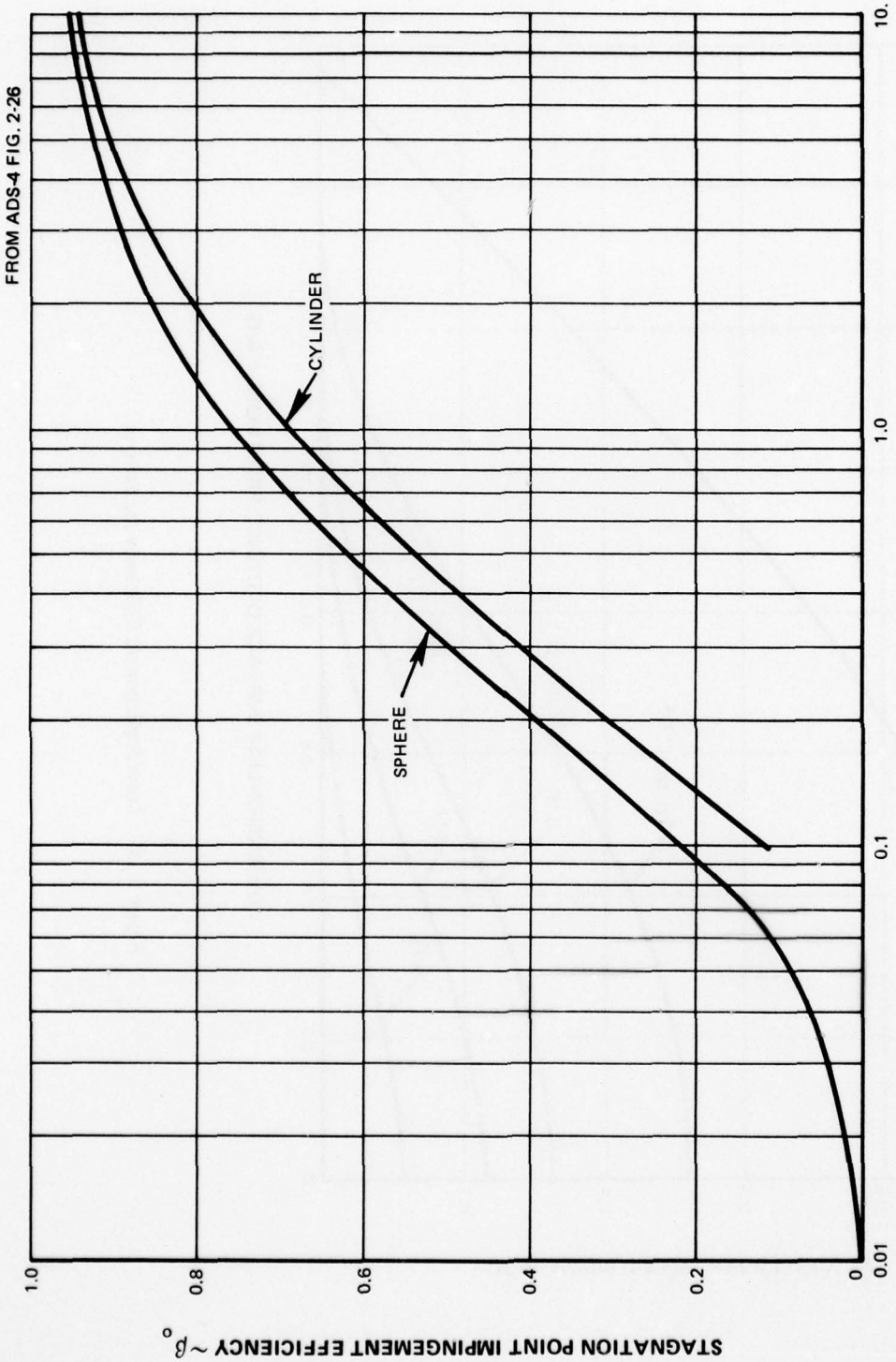

Figure 3-14 Stagnation Point Impingement Efficiency for Spheres and Cylinders

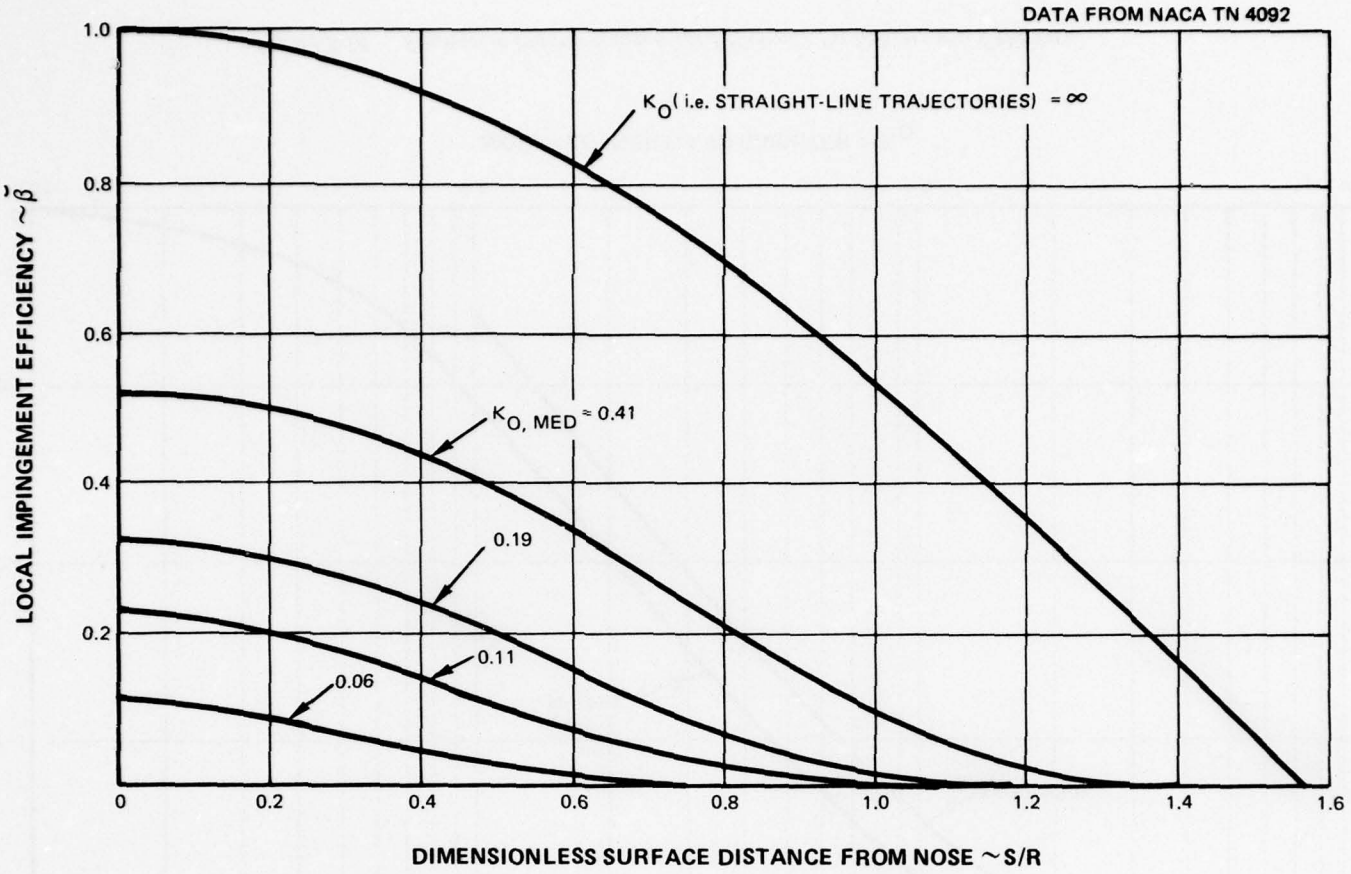

Figure 3-15 Local Impingement Efficiency for Spheres

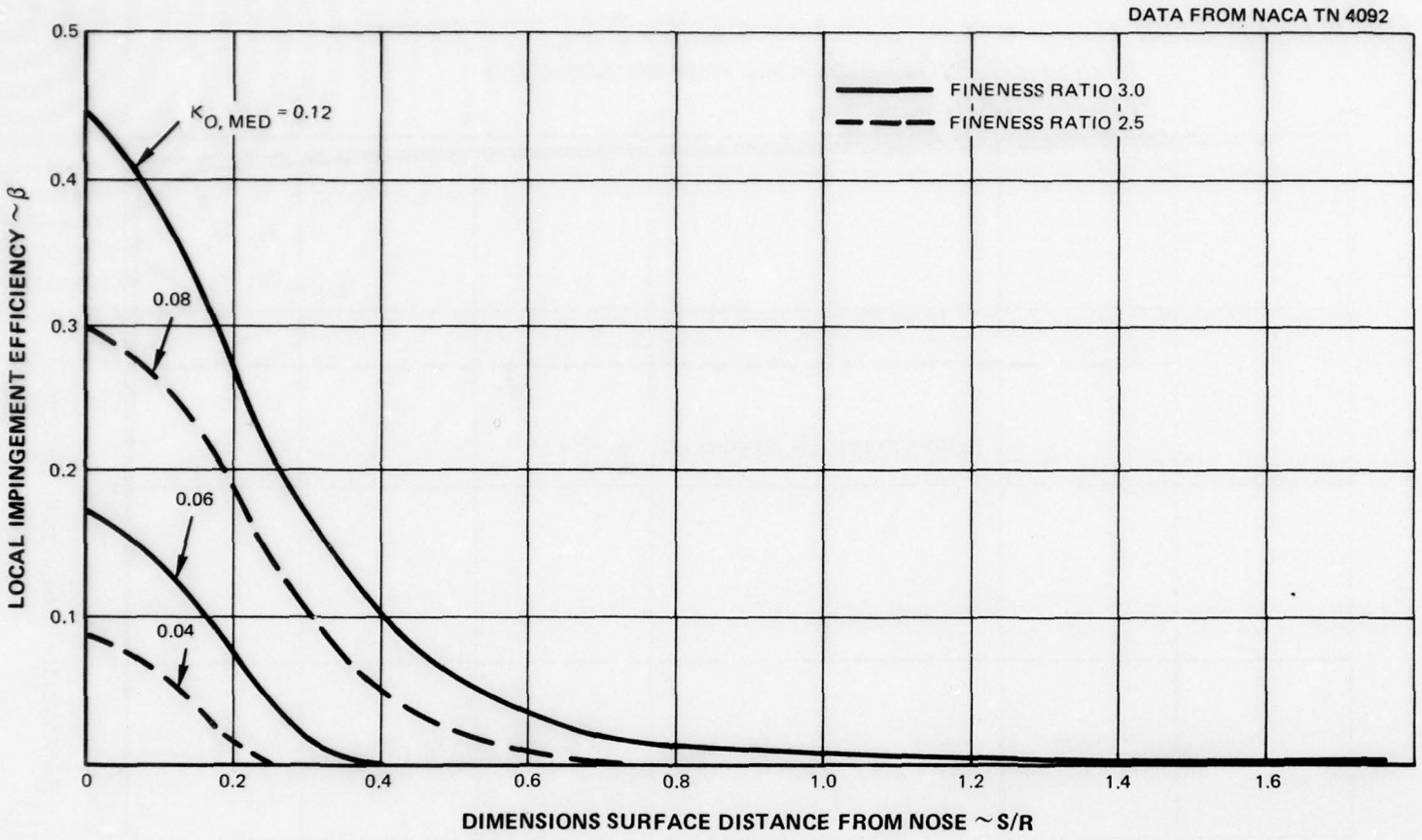

Figure 3-16 Local Impingement Efficiency for Two Ellipsoids

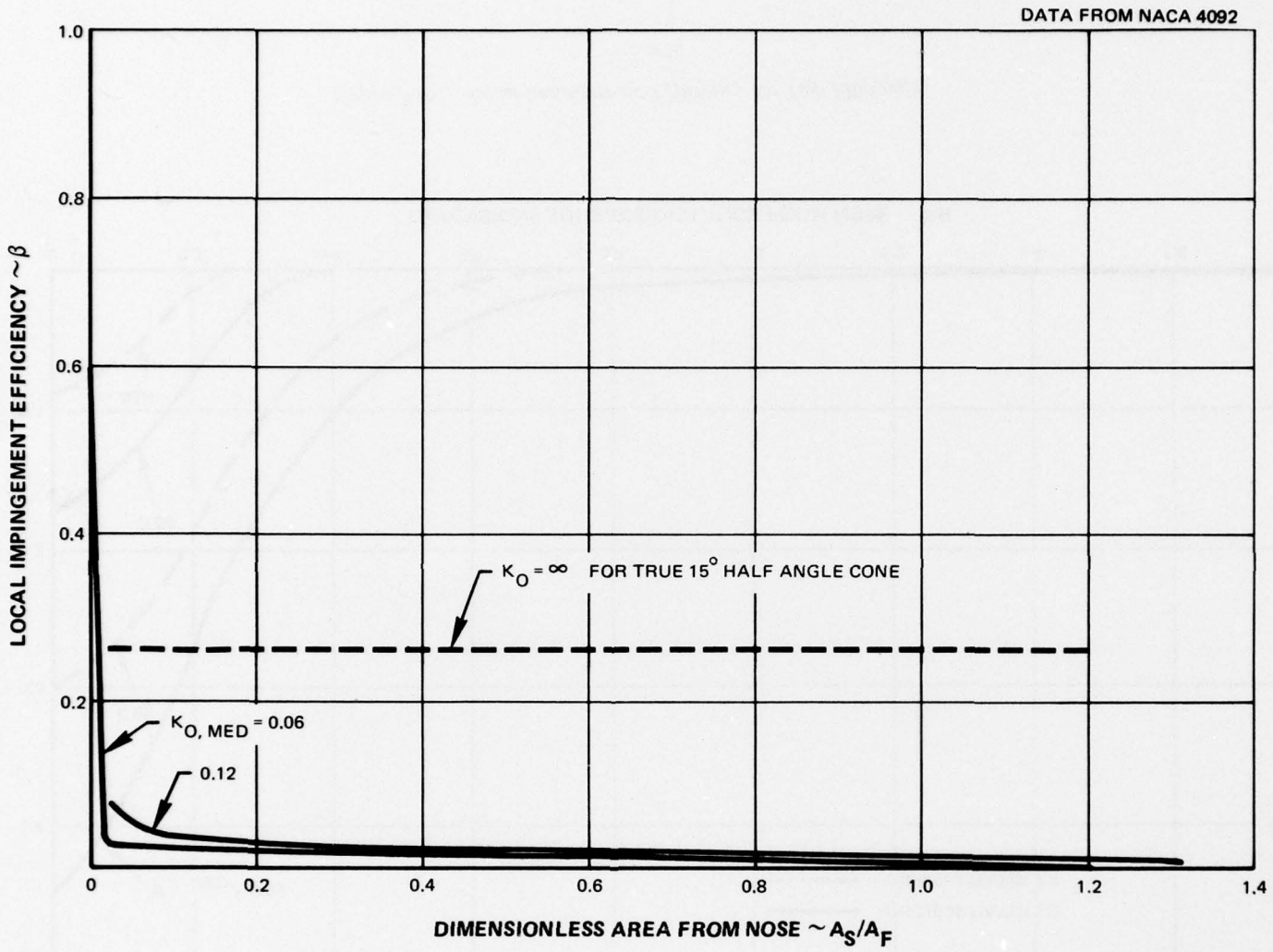

Figure 3-17 Local Impingement Efficiency for a Conical Forebody of About 15° Half- Angle

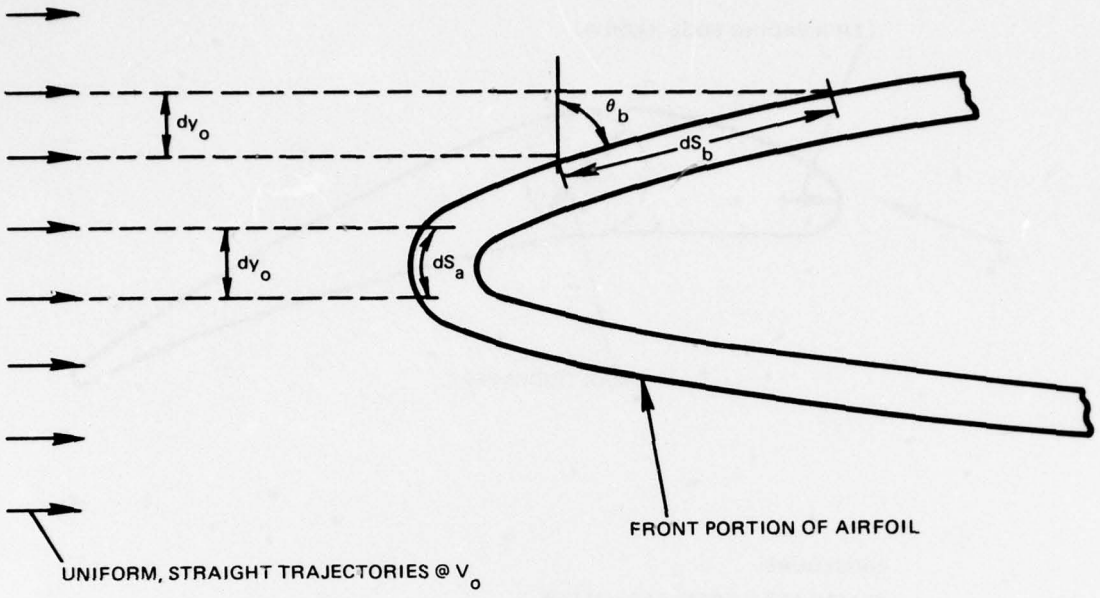

(1) AT STAGNATION REGION

$$\beta_a = \frac{dy_o}{dS_b} \approx 1.0$$

$$W''_a = (LWC_o)\, V_o\, \beta_a \qquad \frac{\text{MASS WATER}}{\text{UNIT AREA – UNIT TIME}}$$

(2) AFT OF STAGNATION REGION

$$\beta_b = \frac{dy_o}{dS_b} \cong \cos\theta_b$$

$$W''_b = (LWC_o)\, V_o \cos\theta_b \qquad \frac{\text{MASS WATER}}{\text{UNIT AREA – UNIT TIME}}$$

Figure 3-18 Local Impingement Rates on Compressor Airfoils When E_m is Approximately 1.0

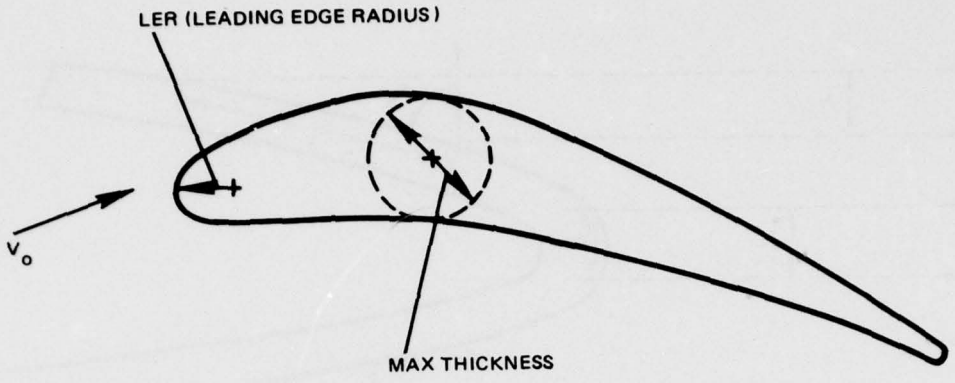

PROCEDURE:

CALCULATE INERTIA PARAMETER

$$K = \frac{\frac{2}{9}(d/_2)^2 \rho_{H_2O} V_{o\,AIR}}{L_C \mu_{AIR}}$$

$$\text{WHERE } L_C = \frac{\text{MAX THICKNESS OF FOIL}}{2} = \text{CYLINDER RADIUS}$$

Figure 3-19 Equivalent Cylinder Method for Compressor Airfoils

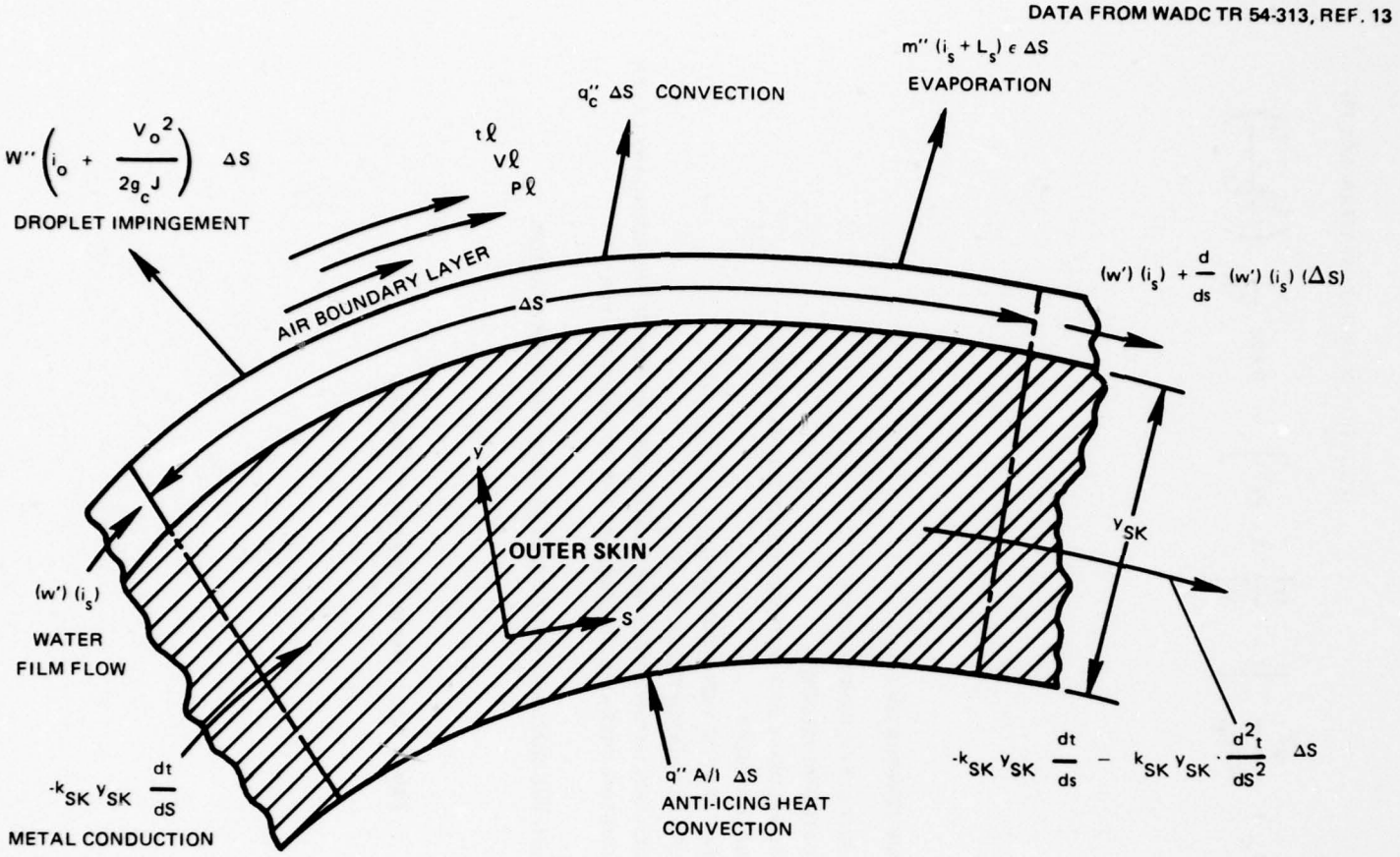

Figure 3-20 Heat Balance on an Elemental Section of a Wet Airfoil

(EQUATION COPIED FROM REFERENCE 16)

$$t_{o_k} = t_o + \frac{V^2}{2g\,J\,C_p}\left[1 - \frac{U^2}{V^2}\left(1 - Pr^{1/2}\right)\right] - 0.622\,\frac{L_s}{C_p}\left(\frac{e_{o_k} - e_i}{P_1}\right)$$

WHERE

t_{o_K} = DATUM TEMPERATURE

t_o = AMBIENT STATIC TEMPERATURE

V = FREE-STREAM VELOCITY

U = LOCAL VELOCITY JUST OUTSIDE THE BOUNDARY LAYER

Pr = PRANDTL NUMBER

L_s = LATENT HEAT OF VAPORIZATION (L_e)

e_{o_K} = SATURATION VAPOR PRESSURE AT t_{o_K}

e_1 = SATURATION VAPOR PRESSURE OF WATER JUST OUTSIDE OF THE BOUNDARY LAYER

P_1 = BAROMETRIC PRESSURE JUST OUTSIDE THE BOUNDARY LAYER

THE TERM WITHIN THE BRACKET REPRESENTS THE LOCAL RECOVERY FACTOR.

Figure 3-21 Datum Temperature Equation

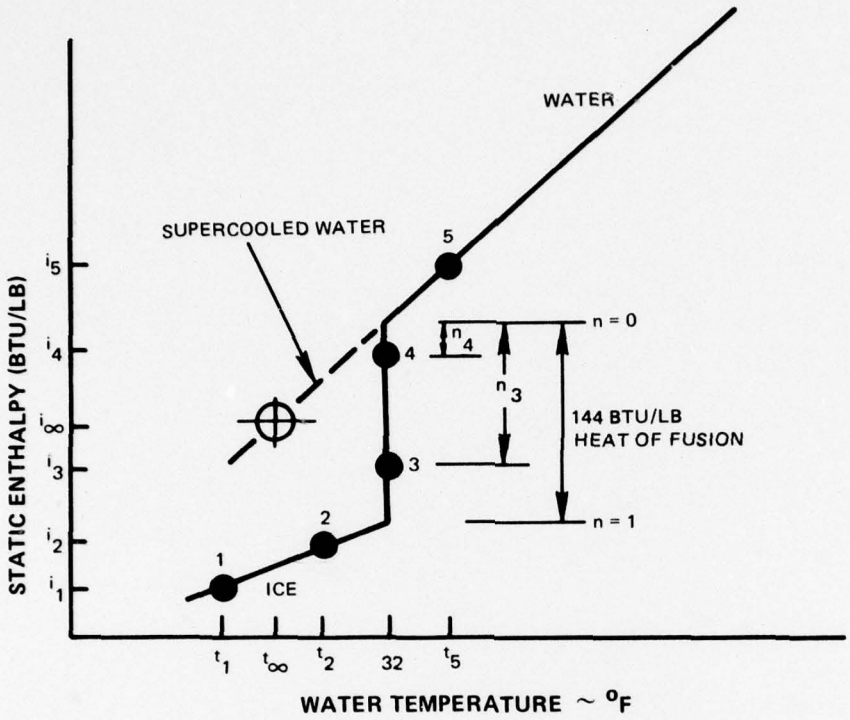

A supercooled water droplet, initially at (i_∞, t_∞) can change to any of points 1, 2, 3, 4, or 5, upon impingement. The various equations for enthalpy change are:

1. $i_\infty - i_1 = C_{pice}\,(32 - t_1) + 144 - C_{pw}\,(32 - t_\infty)$

2. $i_\infty - i_2 = C_{pice}\,(32 - t_2) + 144 - C_{pw}\,(32 - t_\infty)$

3. $i_\infty - i_3 = n_3\,(144) - C_{pw}\,(32 - t_\infty)$

4. $i_\infty - i_4 = n_4\,(144) - C_{pw}\,(32 - t_\infty)$

5. $i_\infty - i_5 = C_{pw}\,(t_\infty - t_5)$

of which 1 and 2 are identical equations for full freezing
3 and 4 are identical equations for partial freezing

Figure 3-22 Water Droplet Static Enthalpy Change From Supercooled State to Surface Temperature

CHAPTER IV FLIGHT CYCLE ANALYSIS

The purpose of flight cycle analysis of engine icing and/or anti-icing is:

(a) to determine specific candidate surfaces of the engine which are likely to require active anti-icing protection,

(b) to establish the point or points in the flight cycle which represent the most difficult anti-icing requirement for each of the candidate surfaces (i.e., establish the flight cycle anti-icing design points), and

(c) to analytically verify that any and all anti-iced surfaces, designed for the isolated conditions of (b), are indeed adequately protected over the full spectrum of flight-cycle conditions.

To accomplish the required flight cycle analyses, the designer will need the input information listed in Table 4-I.

TABLE 4-I

FLIGHT CYCLE ICING ANALYSIS INPUT INFORMATION REQUIRED

	Input Item	Suggested Source of Information
1.	Altitude and Free-Stream Mach number time graphs for the flight cycle. (Typical graphs are shown on Figure 4-1)	Supplied by airframe manufacturer.
2.	Engine Power Setting vs. time, corresponding to the cycle of Item 1. (A typical graph is shown on Figure 4-1)	Engine performance tables which include operating at the "icing day" conditions defined by the Single Operating Line of Figure 2-14, and which include powered descent and intermittent engine rev-up during ground idle.
3.	Design charts of atmospheric icing conditions, showing the Single Operating Line and recommended droplet diameters.	Figures 2-14 thru 2-17 of this report
4.	Drawings of the actual engine compressor (A typical sketch is shown on Figure 4-2)	Design drawings
5.	Sufficient equations and graphs to calculate water ingestion rates in the engine inlet.	As in Section 3.1.1 of this report

Table 4-1 (Cont'd)

Input Items	Suggested Source of Information
6. Sufficient equations and graphs to calculate water impingement rates on various engine parts.	As in Section 3.1.2 of this report
7. Sufficient equations to calculate datum temperatures, effective wet-bulb temperatures, and surface heat balances.	As in Section 3.1.3 of this report
8. Sufficient equations to calculate ice accumulation	As in Section 3.2 of this report

The complete flight cycle analysis is done in three major steps:

Step I: A preliminary Flight Cycle analysis is performed to expose those engine surfaces in the inlet and first few stages of the compressor which definitely do (and/or definitely do not) require active anti-icing and to establish which surfaces are marginal candidates for further analysis. The preliminary flight cycle analysis is also useful to expose those regions of the flight cycle which appear to be troublesome icing regions for the engine.

Step II: Detailed surface heat balance analyses are performed for all troublesome flight cycle regions to establish which of the candidate surfaces:

- definitely do not require active anti-icing
- definitely do require active anti-icing
- are marginal in that icing only occurs during brief transients (like descent) and resulting ice accumulations may be within tolerable limits.
- are marginal in that the accuracy of the analysis is insufficient to make a definite conclusion as to whether icing will occur in a tolerable or intolerable manner.

These detailed surface heat-balance flight cycle analyses are also applied to those surfaces which will be anti-iced, so as to determine the most severe anti-icing heating requirement in the flight cycle as influenced by engine performance. This establishes a "worst" design point upon which to base detail designs of active anti-icing systems.

Step III: Detailed heated-surface heat-balance analyses are performed over the flight cycle to assure that the anti-icing heat available is indeed always greater than the heat required.

The design procedure of these steps for flight cycle analysis is illustrated by the following analysis of the schematic engine of Figure 4-2.

4.1 PRELIMINARY FLIGHT CYCLE ANALYSIS

For the preliminary flight cycle analysis, each of the level altitudes of Figure 4-1, and several altitudes along each of the sloping lines, are assigned an atmospheric temperature as determined from the Single Operating Line of Figure 2-14. The corresponding flight Mach numbers of Figure 4-1 for each selected altitudes are also noted, and the inlet ram temperatures at each flight-cycle point is calculated from

$$T_{RAM} = T_{\infty}\left[1 + \frac{\gamma-1}{2}(M_{N\infty})^2 \eta_r\right]$$

Typical values of the ram recovery factor (ηr) are usually between 0.85 and 1.0, and can be more accurately determined by consulting the engine performance tables.

Using a standard-day definition of atmospheric pressure, the ram total pressure at each point on the flight cycle can be determined from

$$P_{RAM} = P_{\infty}\left[1 + \frac{\gamma-1}{2}(M_{N\infty})^2\right]^{\frac{\gamma}{\gamma-1}}$$

One can obtain values of [illegible] and temperature for each of the first few compressor stages at each of the selected flight-cycle points. The corresponding "datum temperature" for a stagnation point at each of these locations is then calculated at each selected point on the flight cycle from the Datum Temperature Equation shown on Figure 3-21, or from Equation 3-34.

4.1.1 Datum Temperature

As applied to engine surface stagnation points, this equation is:

$$t_{ok} = t_T - 0.622\,\frac{L_s}{c_p}\left(\frac{e_{ok} - e_l}{P_T}\right)$$

where
- e_{ok} = saturation vapor press. of water at t_{OK}
- e_l = $Pv_{\infty}\ (P_T/P_{\infty})$ = local vapor pressure
- L_s = $(1093 - 0.55\ t_{OK})$ = latent heat of vaporization, Btu/lb
- c_p = const. press. specific heat of air = 0.241 Btu/lb °F

An implicit solution for t_{OK} at each of the first few compressor locations, and at each of the selected flight cycle points, then allows a graphical display of the various flight cycle datum temperatures to be drawn. The schematic for a typical engine used for this example is shown on Figure 4-2, and a plot of datum temperatures is shown on Figure 4-3.

Also shown on Figure 4-3 is a corresponding plot of the cloud liquid water content values for the flight cycle, obtained from Figure 2-16.

4.1.2 Deductions

Figure 4-3 demonstrates the benefits of the preliminary flight cycle analysis. First, the graph can be easily generated since the preliminary "datum" temperatures do not require any knowledge of engine inlet water ingestion parameters or water impingement parameters. The "datum" temperature equation gives only two possible answers for a given airflow condition: a "wet" answer good for any finite water content, and a "dry" answer for zero water content. Even though the "wet" answer is an incorrect value when it comes out less than 32°F, it is qualitatively correct in that the true temperature is somewhere between the calculated value and the freezing point, i.e., definitely icing. Secondly, by comparing the datum temperatures of Figure 4-3 with the values of cloud liquid water content (it can be assumed here that when the cloud liquid water content is significant, the liquid water content in the engine will also be significant), several important conclusions can be deduced regarding requirements for additional analytical efforts.

It can be safely assumed that all of the static structure downstream of the second fan blade will be warmer than the first stator by an amount roughly equal to the datum temperature difference shown between the first stator and the inlet structure. Thus for all flight cycle times at which there is a finite amount of cloud liquid water content, all this downstream structure is well above the freezing point. One possible exception might occur transiently at about mid-descent, but the graph is conservatively drawn for an idle descent rather than for the more realistic situation of a powered descent, so this one short time-duration point is disregarded. It is therefore concluded from Figure 4-3 that all surfaces of the Figure 4-2 engine downstream of the second fan blade are not candidate icing surfaces. A similar line of reasoning leads to the conclusion that the inlet structure is definitely an icing surface. Because the first stator appears somewhat marginal, it is retained, for the moment, as a candidate icing surface for additional analyses.

It can be deduced from Figure 4-3 which portions of the flight cycle should be concentrated upon for further analysis. It appears that the inlet structure would have ice everywhere except at cruise, while the first stator appears to have its worst problem during descent and possibly lesser problems at ground idle and holding. It is therefore concluded that further analyses should cover the entire flight cycle, with additional points added for ground idle intermittent power rev-up, some additional points for powered descents, and some additional points for increased holding power.

4.2 DETAILED HEAT BALANCE ANALYSES IN TROUBLESOME FLIGHT CYCLE REGIONS

To perform detailed surface heat balance analyses, the designer will first need to obtain detailed engine aerodynamic performance tables for all the troublesome flight cycle regions. These performance tables must apply specifically to the "icing" day Single Operating Line of Figure 2-14. A Standard Day atmospheric pressure vs. altitude curve may be assumed, and values are given along the abscissa of Figure 2-14. The designer now has sufficient information for the surface heat-balances of Equation 3-33, 3-35, and 3-36 to determine the heating requirements of the anti-iced surfaces, and to determine more accurate unheated wetted temperatures of the marginal candidate surfaces. These calculations require, first, the solution of the inlet water ingestion equations (presented in Section 3.1 1) at each flight cycle point. Figures 4-4 and 4-5 show the pertinent performance points and the resulting inlet water ingestion rates over the flight cycle. Secondly, the water impingement calculations of Section 3.1.2 must be performed for each surface over each of the troublesome flight cycle regions and at each of the reved-up power levels in the ground "idle" and descent modes. It is usually adequate to perform these calculations, for the moment, only for the stagnation regions of the various surfaces. The rest of the terms in the heat balance equations 3-33, 3-35 or 3-36 of Section 3.1.3, such as the heat transfer coefficients and latent heat term, must also be evaluated at each of the performance points and these may also be limited to only stagnation point areas.

4.2.1 Effective Wet Bulb Temperatures on Unheated Surfaces

An implicit solution of Equations 3-33, 3-35, or 3-36 on each of the marginal candidate surfaces at each of the performance points is required to obtain the effective wet-bulb temperatures. Display of the results as shown on Figure 4-6 leads to valuable conclusions regarding the previously marginal candidate surface of the first stator (Figure 4-2). Before presenting the conclusions, however, it is of interest to first make a few observations regarding the accuracy of the "effective wet-bulb temperature".

The first-stator effective wet-bulb temperatures shown on Figure 4-6 were calculated from the true heat-balance Equations 3-33, 3-35, or 3-36, and include an accounting of the freezing fraction for values at 32°F. Hence the temperatures shown are analytically correct at and below freezing. The surrounding air temperature is shown for reference. Water droplet temperature, which is conservatively assumed to retain its atmospheric value in spite of the tendency to be increased by both ram air and fan compression air temperature increases, is also shown for reference. It is interesting to observe that during an idle descent, the stator surface temperature is slightly warmer than the surrounding air temperature. This happens because the heat of fusion which is absorbed by the freezing fraction creates an unbalance to the normal surface heat balance of (Qin - Qout) = 0. With complete freezing occurring, the surface heat balance is (Qin + Qgen − Qout) = 0. The freezing appears as a heat-generated term because, when a supercooled liquid water droplet flashes to ice, it must give up entalpy (as shown in Figure 3-22). Hence enthalpy is generated on the surface as ice forms, and it is not unreasonable to see a surface which starts generating heat get warmer than the temperature of what was previously its sole heat source.

Another point of interest worth mentioning is shown on Figure 4-7, which presents a direct comparison between the effective wet-bulb temperature of Equ. 3-33, 3-35, or 3-36 and previously used "datum" temperature of Equ. 3-34. On this graph, it is observed that the datum temperature is consistently lower than the true temperature when below freezing, and this is consistent with a previous comment the datum temperature equation is expected to yield too low a value below freezing. However, the fact that the datum temperature is consistently higher than true temperature when above freezing demonstrates that, in general when the datum temperature predicts a surface to be only slightly above freezing, it is not permissible to immediately conclude that no icing occurs. Such marginal surfaces must be considered as candidate surfaces in further analysis.

Referring now, back to Figure 4-6, the following information can be deduced from the true effective wet-bulb flight cycle temperatures shown for the first stator. Under standard operational procedures of intermittent engine rev-up during ground idle operation, it is concluded that the first stator will not have an icing problem during ground operation. Similarly, under standard operational procedures of powered descents, it concluded that the first stator will not experience descent icing, except possibly at mid-descent altitudes where the stator temperature shows below freezing in a non-zero liquid water content zone. After checking to verify that the higher-than-"descent" power levels for cruising at these altitudes are sufficient to provide steady-state stator temperatures above freezing, one concludes that ice accumulation on the stator during the 1½ minute descent icing transient will be tolerable, especially when this period is immediately followed by warmer-than-freezing temperatures during the hold portion of the flight-cycle. Therefore the first stator will not require an active anti-icing system. Whereas this conclusion is made intuitively in this example for the sake of brevity, the recommended procedure is for the designer to actually calculate the *expected maximum ice accumulation to prove that it is within tolerable limits.* In the calculation of the maximum ice accumulation during short time periods such as this example, it is recommended that the designer should consider the possibility that some portion of the time period could correspond to flight through clouds of short horizontal extent and increased liquid water content as defined in the FAR Part 25 Regulations, Figure A-6. Appropriate multiplying factors to liquid water content should be applied, and the solution to Equ. 3-33, 3-35, or 3-36 should be updated. Ice accumulation can be calculated by either Equation 3-36 or Equation 3-37, depending on the degree of accuracy required to prove the point.

4.2.2 Detailed Heat Requirements of Anti-Iced Surfaces

One of the results from the Preliminary Flight Cycle analysis of Section 4.1 was that the inlet structure of the example engine would definitely require active anti-icing. The required follow-on analysis will be discussed herein. The intent of the follow-on flight cycle analyses for surfaces which will be actively anti-iced is to determine the region of the flight-cycle where the anti-icing heating requirements are the most difficult to provide. Such a flight-cycle region -- which will then be used as the design point for the detailed design of the final anti-icing system -- can be expected to occur when the heat required for anti-icing is relatively high, and the compressor bleed's ability to supply hot air flow is relatively low. Focusing attention first on calculating the heat required, the analysis proceeds as follows.

It is recommended that all anti-icing systems be designed to maintain a wetted surface temperature of at least 35°F, as discussed under "Design Considerations".

By assuming that the anti-iced surfaces will be, somehow, always actively heated to a minimum surface temperature of 35°F, the designer can apply all of the liquid-water content, impingement rates, heat transfer coefficient, etc. results (previously obtained as described in the first few paragraphs of Section 4.2) directly to Equation 3-33 to solve for surface heat flows at each of the pertinent performance conditions over the full flight cycle. The surface heat flows thus calculated are the required anti-icing heat flows. For the stagnation point of the inlet guide vane of the example engine, resulting heat flows for each of the individual terms of Equ. 3-33 are shown for completeness on Figure 4-8, and net algebraic summation of these – i.e., the required anti-icing heat flow at each point along the flight cycle – are shown on Figure 4-9.

The following observations are deduced from Figure 4-9. In the ground-"idle" portion of the flight cycle, the heat requirement is relatively low, and the two discreet jumps in heat load shown here correspond to intermittent engine rev-ups which induce increased evaporation and convection in the inlet, thereby creating temporary increases in the heat required. The experienced designer will realize that these jumps in heat required are generally more-than-adequately compensated for by much larger jumps in the heat actually supplied to the anti-ice vane during such rev-ups, so ground idle is not considered to be a crucial design-point portion of the flight cycle. The largest heat requirements appear to occur during the climb and powered-descent portions of the flight cycle. The powered-descent heating requirements are greater than the idle-descent heating required because of increased levels of liquid water content, convection, and evaporation. Both of the descent heating requirements are somewhat less than those during climb because the higher engine power level during climb creates somewhat greater liquid water content, evaporation, and convection in the engine inlet. However, the slightly higher heating requirements during climb will be more-than-compensated for by even greater increases in the heat actually supplied for anti-icing during climb because this flight cycle region corresponds to maximum engine power levels. It is therefore concluded that descent is a more severe anti-icing condition than climb. It is to be noted that this conclusion is true for hot-air anti-icing systems which use a compressor bleed hot-air source, but is not necessarily true for other types of anti-icing systems. For an electrical anti-icing system, for example, the generated voltage would probably be regulated to a constant value at all regions of the flight-cycle, and the maximum ampere demand would occur during climb. That system would have to be sized to meet the climb demand for amperes, and might require additional examination of the generator's ability to produce the rated voltage at lesser engine power settings.

To complete the discussion of pertinent observations from Figure 4-9 for the compressor-bleed hot air anti-icing system on the example engine, the experienced designer will realize that idle descent will be a more severe anti-icing condition than powered descent, but idle descents are generally forbidden by various specifications in the "Operational Procedures" manuals for either the engine or the airplane.

Hence the designer can conclude from Figure 4-9 that descent -- specifically, a powered descent – represents the most severe flight-cycle anti-icing condition.

Whereas the powered descent appears to be the proper design point upon which to base the detailed design of the anti-icing system, it must be kept in mind that this conclusion has been derived purely from technical considerations, and other considerations of realistic design features must also be taken into account. The first of these other considerations is that engine weight, vane-size, performance losses, mechanical design complexity, and cost all tend to increase drastically as the anti-icing heat supply capability increases. Hence, the designer will not want to over-design the system. The relatively short time-duration icing condition at descent may be tolerable with insignificant ice accumulation on an anti-iced vane whose heat-output was designed to fully satisfy the lesser intensity but longer time-duration (essentially steady-state) flight cycle condition of "holding". Secondly, it will be desirable to incorporate some sort of safety factor into the final design heating capability, and such safety factors will probably satisfy the maximum transient requirement. Therefore, it appears from a realistic point of view that the designer should, as a first pass, size the heating capability of the anti-ice system to an as yet undefined "worst icing holding" steady-state condition, and check to see that the safety factors thus incorporated prove to be adequate for the technically worst condition of descent. The specification of this "worst icing" holding design point is a matter of engineering judgement. As a guide, the Regulatory Agency certification test specifications previously shown on Figure 2-15 can be used to advantage. It is observed on that figure that, for United States military and FAA specs, the maximum cloud liquid water content specified is two gms/meter^3, and the minimum ambient temperature specified is $-4°$F. Hence a minimum-power-holding design point with liquid water content of two gm/m^3, but with a conservative ambient temperature of only $-4°$F, appears to be conservatively-safe selection for a steady-state holding design point upon which to base the detail design of the anti-icing system.

At this single, conservatively selected design point, it is necessary to obtain new aerodynamic engine performance tables (for the $-4°$F ambient temperature) and re-evaluate Equation 3-33 for the design point surface heat flows for a 35°F surface. In this example problem, the stagnation point heat flow for this conservative holding condition is essentially equal to the maximum heat flow during descent, as shown on Figure 4-9. This calculation, performed at only one performance point, should then be repeated at enough points along the vane surface to establish a distribution of heat load between the wetted impingements limits of the vane. This information will be useful for the final detail design. The detail design itself is discussed later under "Design Considerations".

4.3 FINAL FLIGHT CYCLE COMPARISON OF HEAT REQUIRED TO HEAT AVAILABLE

As soon as the detail design of the anti-icing system is reasonably complete (see Chapter V for discussion of detail design considerations and procedures), the flight cycle analysis of anti-icing heat available should be compared to the heat requirements of Figure 4-9 to assure that the final system is indeed adequate over the full flight cycle.

The anti-icing system heat available at any point on the flight cycle is defined as the heat flux (Btu/ft^2 hr) which flows from the interior of an anti-iced vane to the wetted surface, when the wetted surface is 35°F. Thus when the heat available is greater than the heat required, the system is deemed adequate.

To calculate the heat available at each flight cycle point, the designer will need as input, all of the aerodynamic performance tables pertinent to the flight-cycle, and the compressor stage bleed source temperature and pressure selected for the final system design. From this much information, the heat available to the stagnation region of the anti-iced surface can be scaled over the full flight cycle (from the known single detailed design point) with reasonable accuracy as follows, based on one-dimensional heat transfer to a 35°F stagnation region.

4.3.1 Calculation of Heat Available

Step 1. The bleed source pressure and temperature at any flight cycle point can be approximated from the relationships:

$$\frac{P_{BLEED\ F.C.} - P_{COMP\ IN\ F.C.}}{P_{COMP\ OUT\ F.C.} - P_{COMP\ IN\ F.C.}} = \frac{P_{BLEED\ D.P.} - P_{COMP\ IN\ D.P.}}{P_{COMP\ OUT\ D.P.} - P_{COMP\ IN\ D.P.}} \qquad \text{EQU 4-1}$$

$$\frac{T_{BLEED\ F.C.} - T_{COMP\ IN\ F.C.}}{T_{COMP\ OUT\ F.C.} - T_{COMP\ IN\ F.C.}} = \frac{T_{BLEED\ D.P.} - T_{COMP\ IN\ D.P.}}{T_{COMP\ OUT\ D.P.} - T_{COMP\ IN\ D.P.}} \qquad \text{EQU 4-2}$$

In Equations 4-1 and 4-2 all the design-point values are known, and the flight-cycle point values of compressor inlet and outlet values are directly available from the performance tables. Solve for the bleed source values of P and T at each point along the flight cycle. If the anti-icing air flow discharge (sink) is not located at the compressor inlet, then Equations 4-1 and 4-2 should be repeated with ($P_{sink\ F.C.}$) and ($T_{sink\ F.C.}$) as the unknowns. For the flight cycle of the example anti-iced vane, the source and sink values are plotted on Figure 4-10.

Step 2. A single discharge coefficient, C_D, is assigned to the entire anti-icing flow path from source to sink, as defined on Figure 4-11. This discharge coefficient is assumed to be constant at all pressure ratios. Hence at any flight-cycle point:

$$\frac{[\dot{W}_{A/I}]_{F.C.}\sqrt{T_{BLEED\ F.C.}}}{P_{BLEED\ F.C.}} = (C_D A_{FLOW})\left[(FP)_{ISEN}\right]_{F.C.}$$

Taking the ratio of this equation to the similar equation for the design point shown on Figure 4-11 yields

$$\frac{[\dot{W}_{A/I}]_{F.C.}}{[\dot{W}_{A/I}]_{D.P.}} = \frac{[(FP)_{ISEN}]_{F.C.}}{[(FP)_{ISEN}]_{D.P.}}\left[\frac{P_{BLEED\ F.C.}}{P_{BLEED\ D.P.}}\right]\sqrt{\frac{T_{BLEED\ D.P.}}{T_{BLEED\ F.C.}}} \qquad \text{EQU 4-3}$$

Thus to obtain the anti-icing systems flow rate at any flight cycle point in terms of the system flow rate at the design point, the actual value of C_D is not required. All that is needed is to assume that it is a constant.

Step 3. The heat transfer coefficient of the anti-icing air within the vane may be assumed to be proportional to the air properties:

$$h_{A/I} \overset{\Delta}{\approx} k \left(\frac{\dot{W}_{A/I}}{\mu}\right)^{0.8} (N_{Pr})^{0.4}$$

Hence the anti-icing heat transfer coefficient at any point in the flight cycle can be ratioed to the design point value by:

$$\frac{h_{A/I\ F.C.}}{h_{A/I\ D.P.}} = \frac{k_{F.C.}}{k_{D.P.}} \left[\frac{\mu_{D.P.} (\dot{W}_{A/I})_{F.C.}}{\mu_{F.C.} (\dot{W}_{A/I})_{D.P.}}\right]^{0.8} \qquad \text{EQU 4-4}$$

The Prandl number ratio is very close to unity, so it has been cancelled.

Step 4. The available heat flow, from the anti-icing air to the wetted 35°F surface of the anti-iced part, can be approximated by the following equation, which ignores metal wall heat conduction.

$$q''_{AVAIL} = h_{A/I}(t_{A/I} - 35)$$

And the heat available at any point in the flight cycle, ratioed to the heat available at the design point, is given by

$$\frac{q''_{AVAIL\ F.C.}}{q''_{AVAIL\ D.P.}} = \frac{h_{A/I\ F.C.}}{h_{A/I\ D.P.}} \left(\frac{t_{A/I\ F.C.} - 35}{t_{A/I\ D.P.} - 35}\right) \qquad \text{EQU 4-5}$$

It is further assumed that very little temperature drop of the anti-icing air occurs between the bleed source and the vane, and the temperature-drop characteristics within the vane are assumed to be similar at all flight conditions, so the following equation is assumed.

$$\frac{t_{A/I\ F.C.} - 35}{t_{A/I\ D.P.} - 35} = \frac{t_{BLEED\ F.C.} - 35}{t_{BLEED\ D.P.} - 35} \qquad \text{EQU 4-6}$$

Step 5. Substitution of Equations 4-3, –4, and –6 into Equation 4-5 yields the final desired result:

$$\frac{\left[q''_{AVAIL}\right]_{F.C.}}{\left[q''_{AVAIL}\right]_{D.P.}} = \frac{k_{F.C.}}{k_{D.P.}}\left[\frac{\mu_{D.P.}}{\mu_{F.C.}}\frac{\left[(FP)_{ISEN}\right]_{F.C.}}{\left[(FP)_{ISEN}\right]_{D.P.}}\frac{P_{BLEED\ F.C.}}{P_{BLEED\ D.P.}}\sqrt{\frac{T_{BLEED\ D.P.}}{T_{BLEED\ F.C.}}}\right]^{0.8}\frac{t_{BLEED\ F.C.}-35}{t_{BLEED\ D.P.}-35} \qquad \text{EQU 4-7}$$

At the design point, the heat available is exactly equal to the heat required, and their numerical value (Btu/ft^2 hr) is known.

Hence a numerical solution of Equation 4-7 at each point on the flight cycle is readily accomplished to determine all flight cycle numerical values of (q" AVAIL F. C.) in terms of (Btu/ft^2 hr) as each point. These heat-available values are then plotted, as shown on Figure 4-12, for direct comparison to the heat-required values of Figure 4-9 obtained previously.

4.3.2 Deductions

Inspection of the heat-available versus heat-required graph of Figure 4-12 shows that, as expected, the anti-icing system provides substantially more heat-available then is required at ground-idle rev-up, take-off, and climb. At holding, there is also ample margin because the actual design point selected was a conservative ficticious holding condition. For a brief time period just prior to mid-descent the heat available appears to equal that heat required. This means that the surface temperature will be exactly 35°F here, so there appears to be no icing problem. However, it should be noted that the comparison shown on Figure 4-12 is based on an approximation of the heat available. Hence marginal points should be examined in more detail for both steady-state cruise and transient performance. If only transient icing appears likely, it is recommended that the designer should consider the possibility that some portion of the time period could correspond to flight through clouds of short horizontal extent and increased liquid water content as defined in the FAR Part 25 Regulations, (Figure A-6). Appropriate multiplying factors to liquid water content should be applied, and the heat-required over the brief transient time-period should be updated before a final decision is made regarding whether or not any resulting short-term ice accumulation is tolerable. If not tolerable, then the detail anti-icing design system must be redesigned to accommodate the new requirements.

As a final comment in this Flight Cycle Analysis section, it is noted that two of the "worst icing" points indicated on the graphs for mid-descent of an unheated stator (Figure 4-6) and for mid-descent of an anti-iced inlet guide vane (Figure 4-12) were checked against similar calculations for a Standard Day rather than for the Single Operating Line "Icing Day". In all cases checked, the icing for the Single Operating Line "Icing Day" was more severe, and more difficult to anti-ice. Whereas this limited number of comparative calculations do not constitute an absolute proof, it would certainly appear that the NACA 2569 "Most Probable

Icing" line previously presented on Figure 2-13, which roughly corresponds to a Standard Day atmosphere, does not represent the most severe icing – only the most probable. It is further noted that the British regulatory test specifications of Reference 11 call for test points only along a temperature-versus-altitude line that corresponds to the sloping right-hand boundary of the cumuliform icing envelope of Figure 2-13.

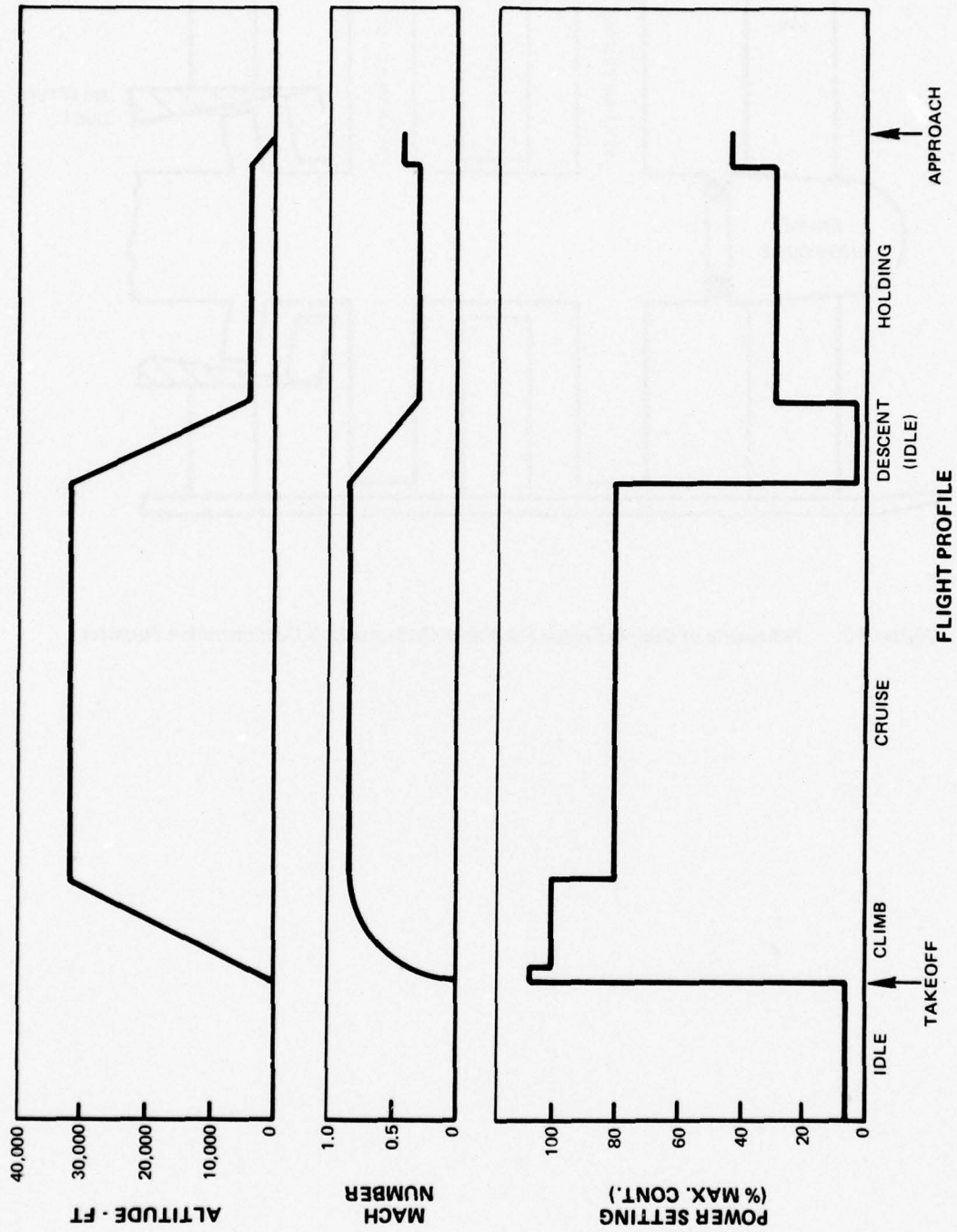

Figure 4-1 Typical Flight Cycle (Altitude, Mach Number and Power)

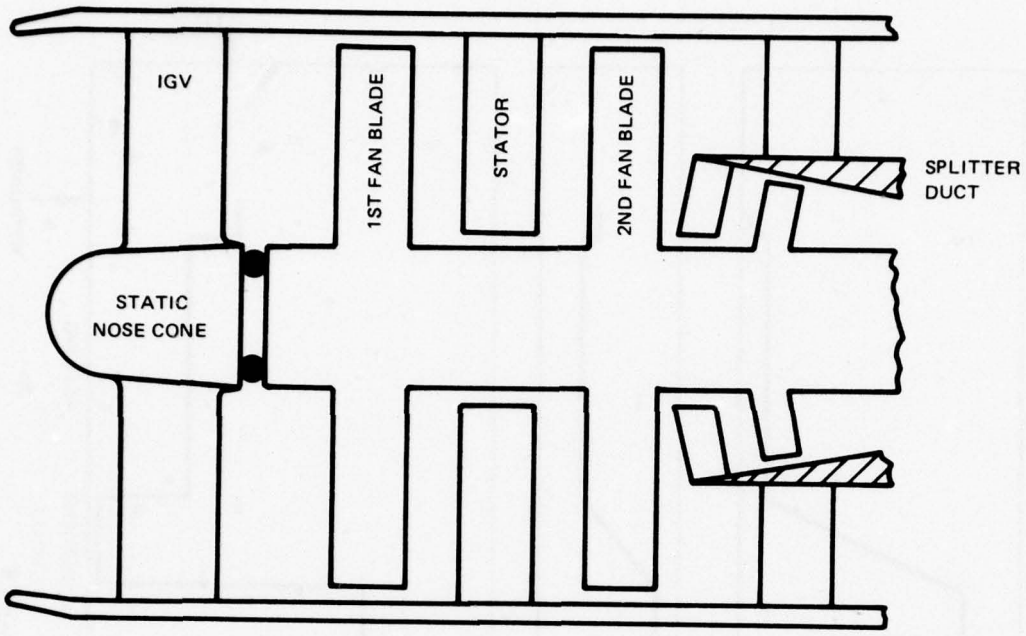

Figure 4-2 Schematic of Sample Engine For Flight-Cycle Analysis Demonstration Purposes

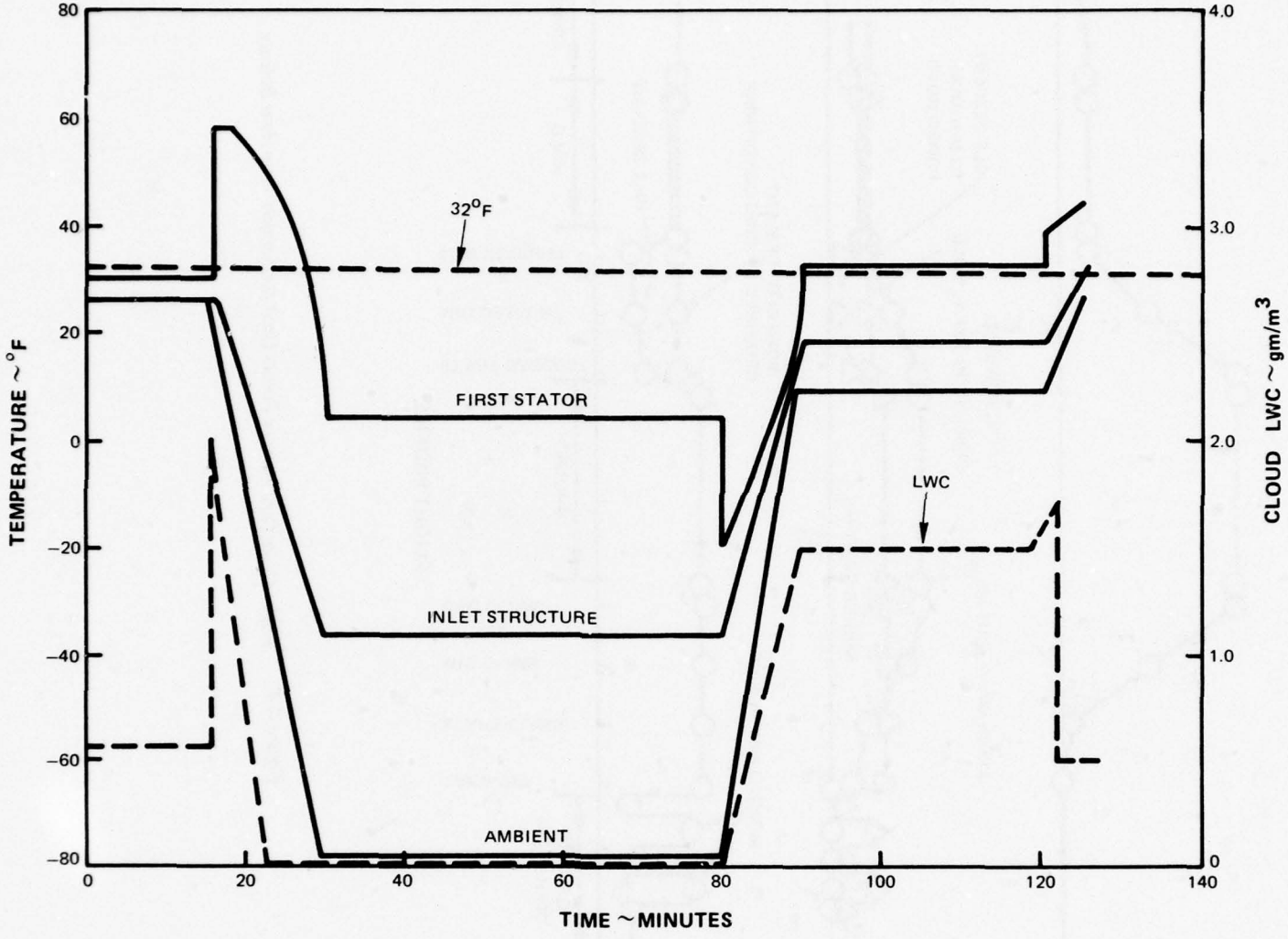

Figure 4-3 Preliminary Flight Cycle Analysis, "Datum Temperature" Results

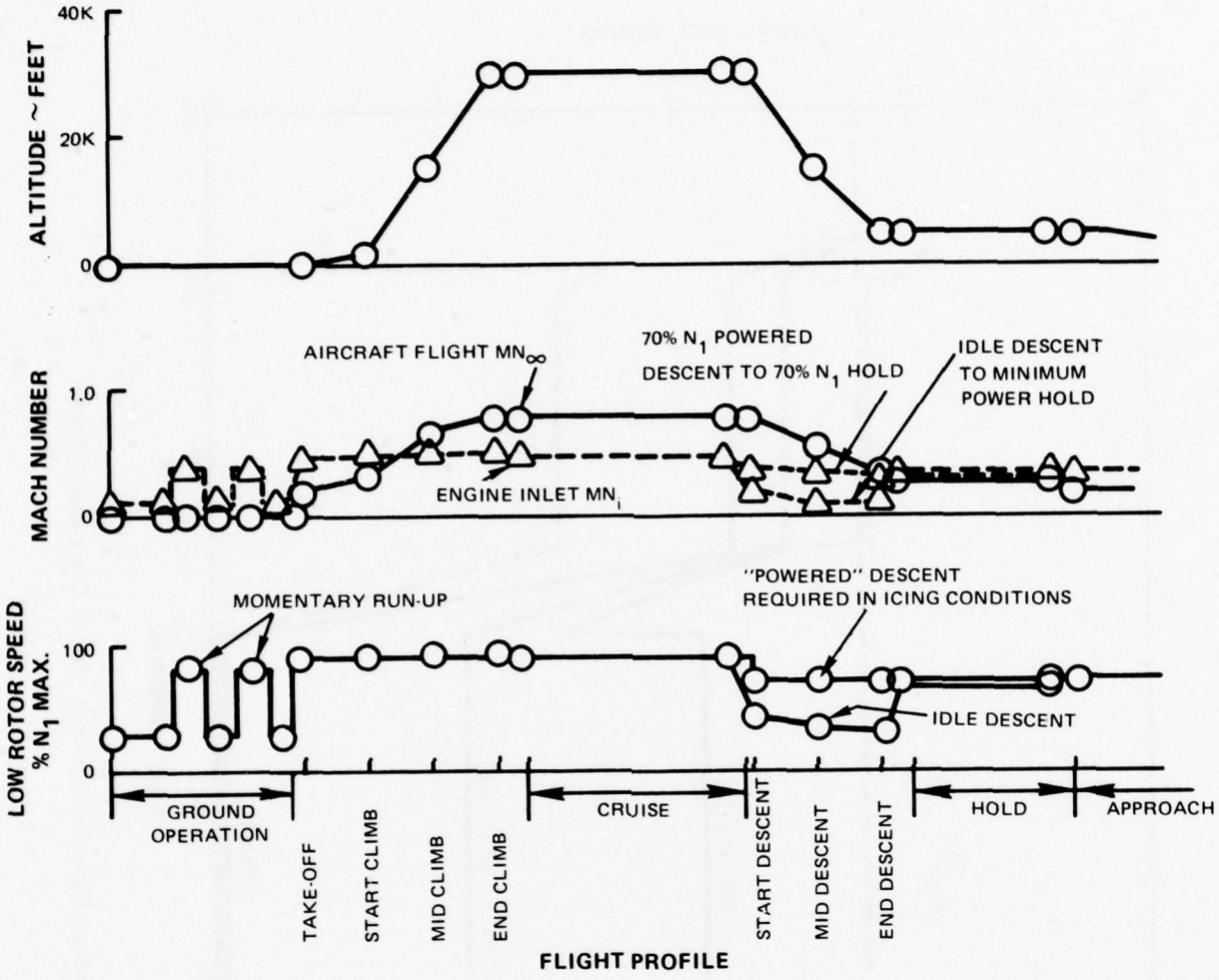

Figure 4-4 *Flight Cycle Performance Points Used for Sample True Heat Balance*

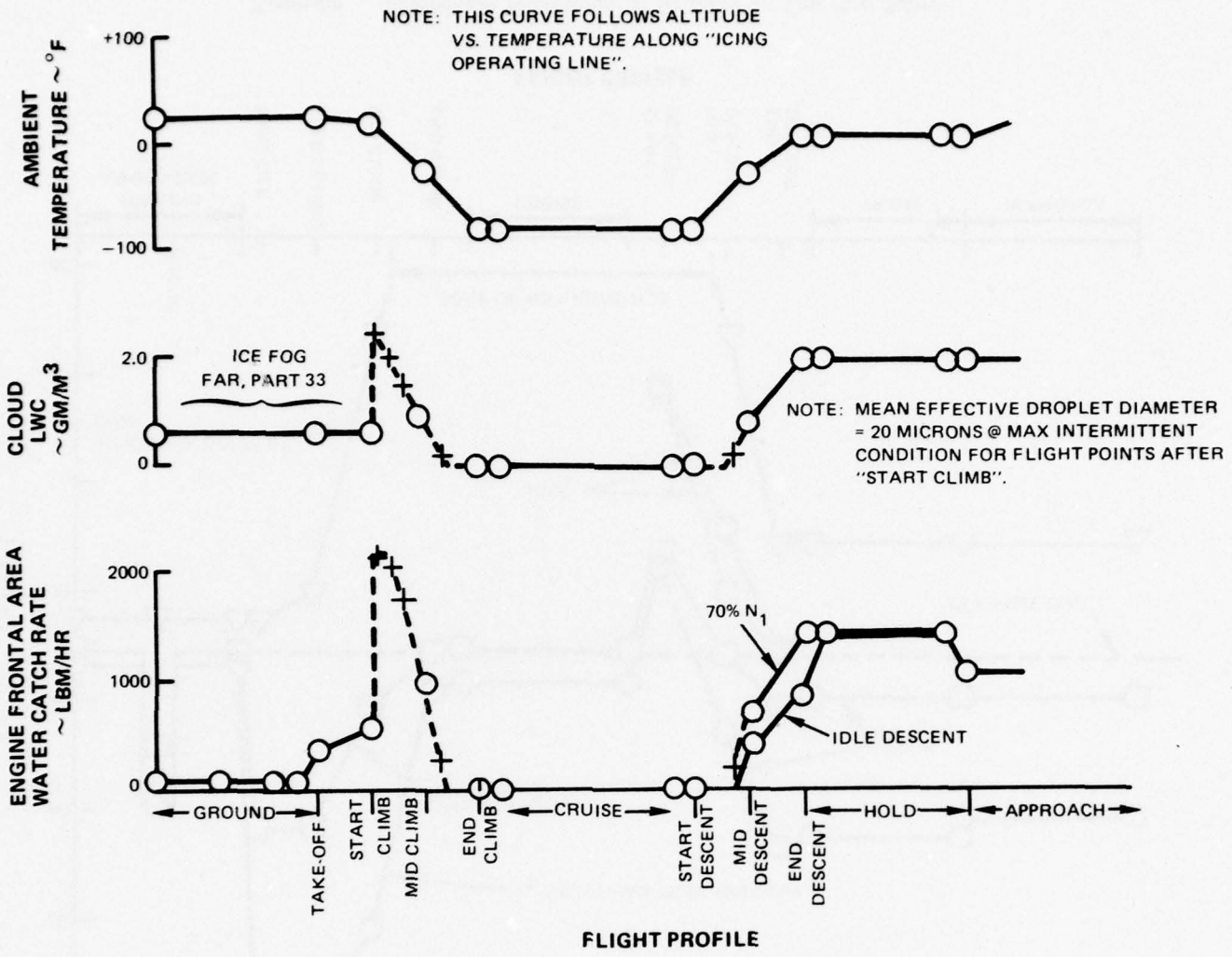

Figure 4-5 Engine Water Catch Rate for True Heat Balance

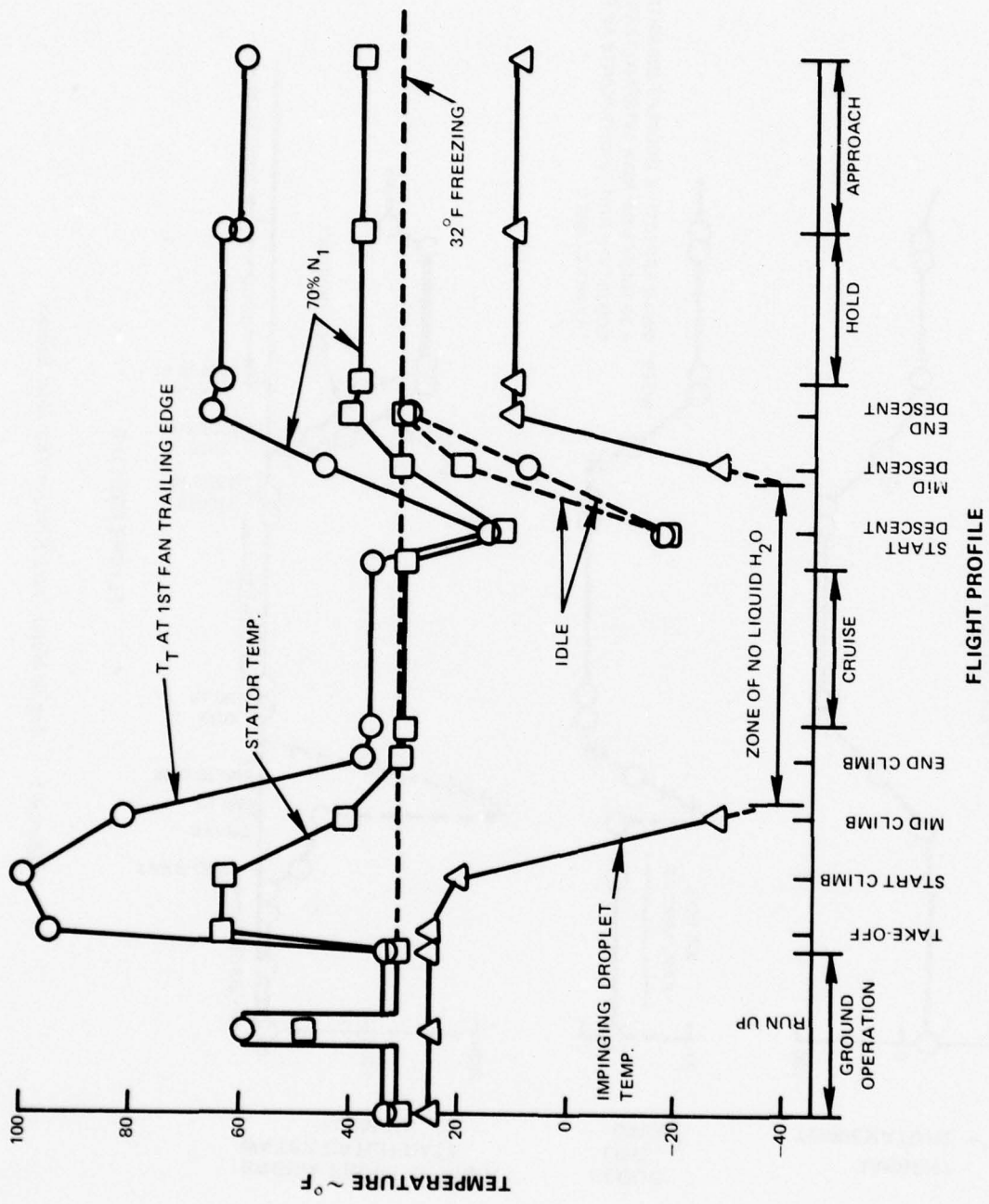

Figure 4-6 Equilibrium Temperature of 1st Stator for True Heat Balance

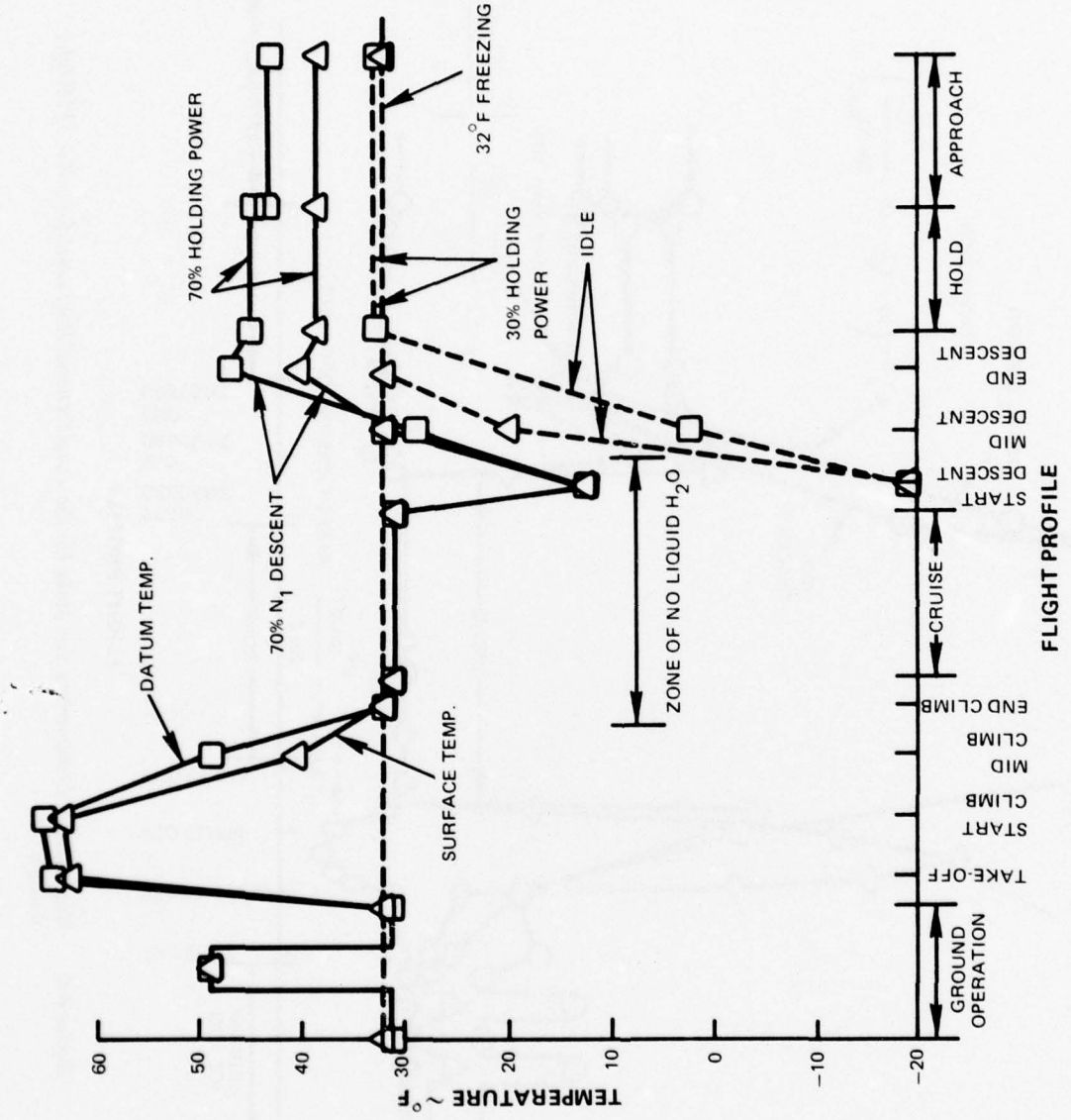

Figure 4-7 Comparison of True Heat Balance Surface Temperature and "Datum Temperature", for 1st Stator

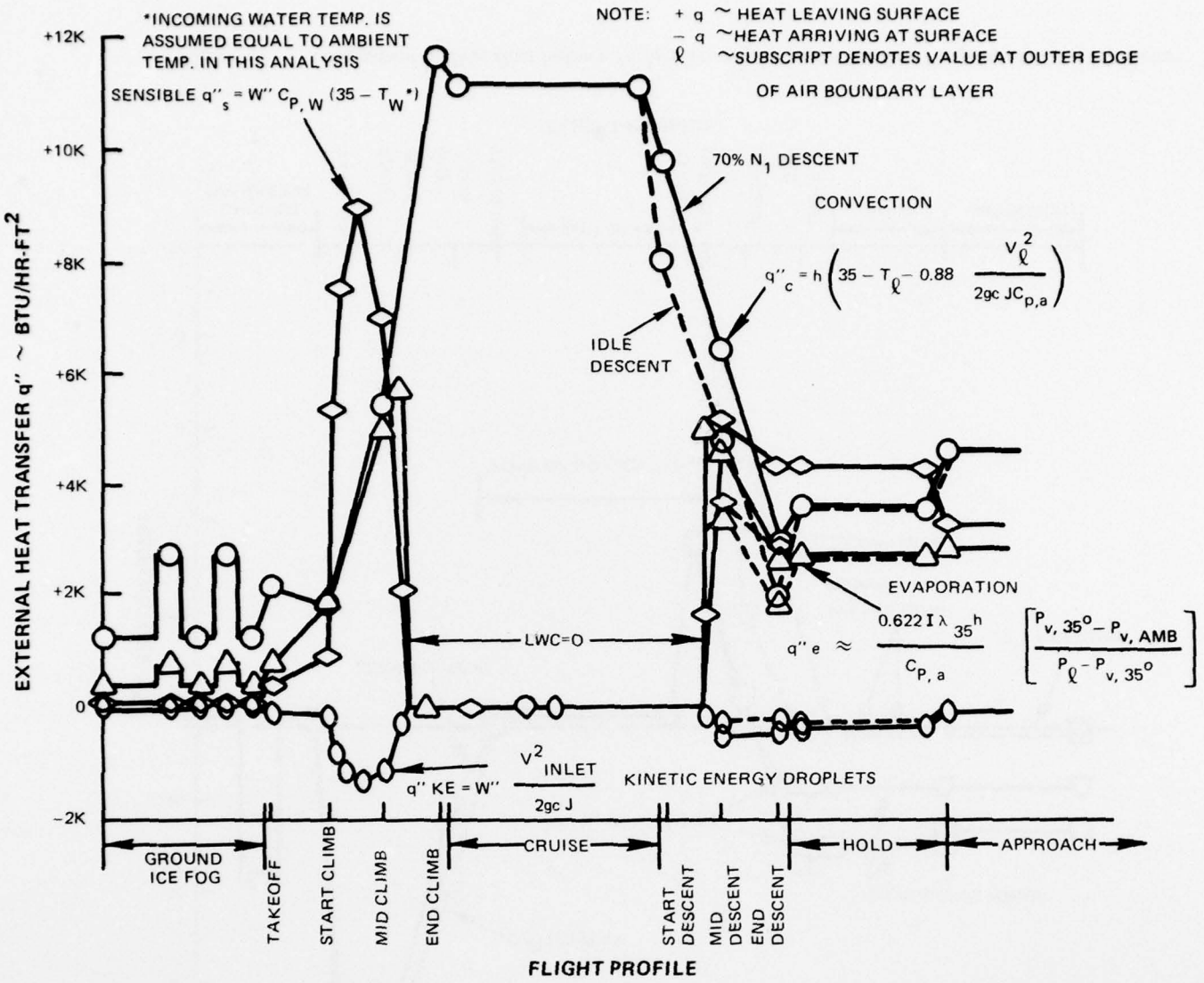

Figure 4-8 *Magnitude of Components that Make Up the Total External Heat Load for a Wet 35°F Inlet Guide Vane*

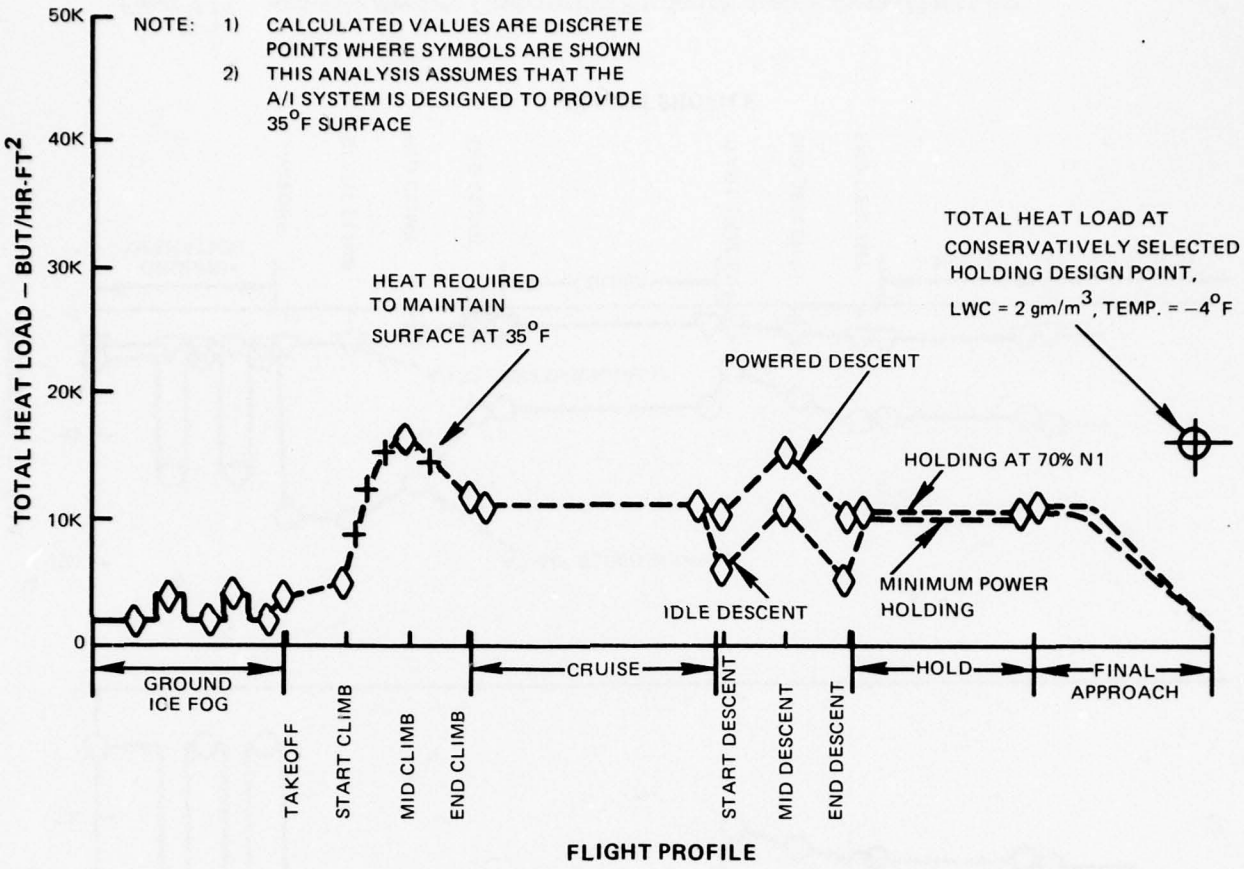

Figure 4-9 Total External Heat Load for a Wet 35°F Inlet Guide Vane

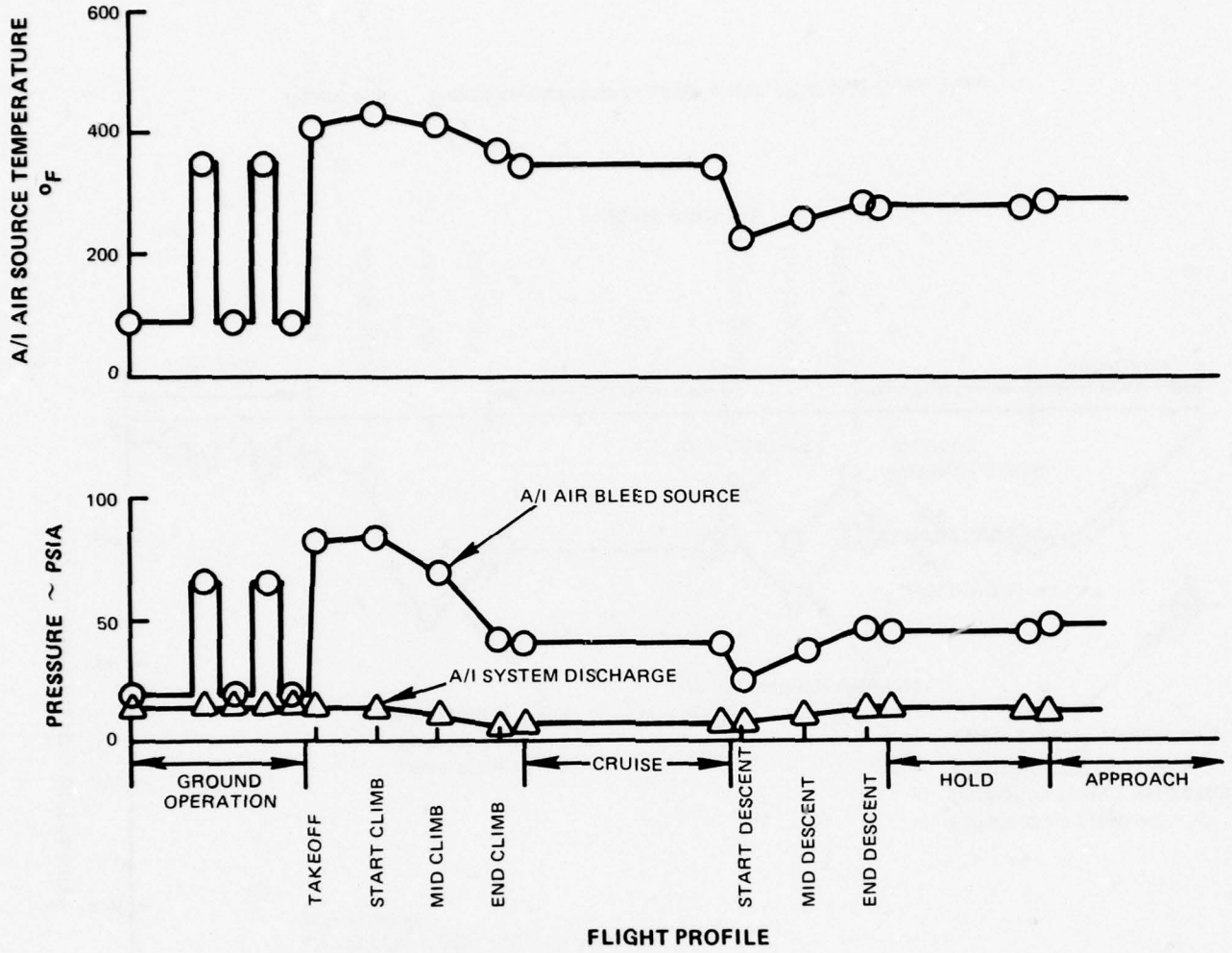

Figure 4-10 Anti-Icing Bleed Air Characteristics For Sample Analysis During Flight Cycle

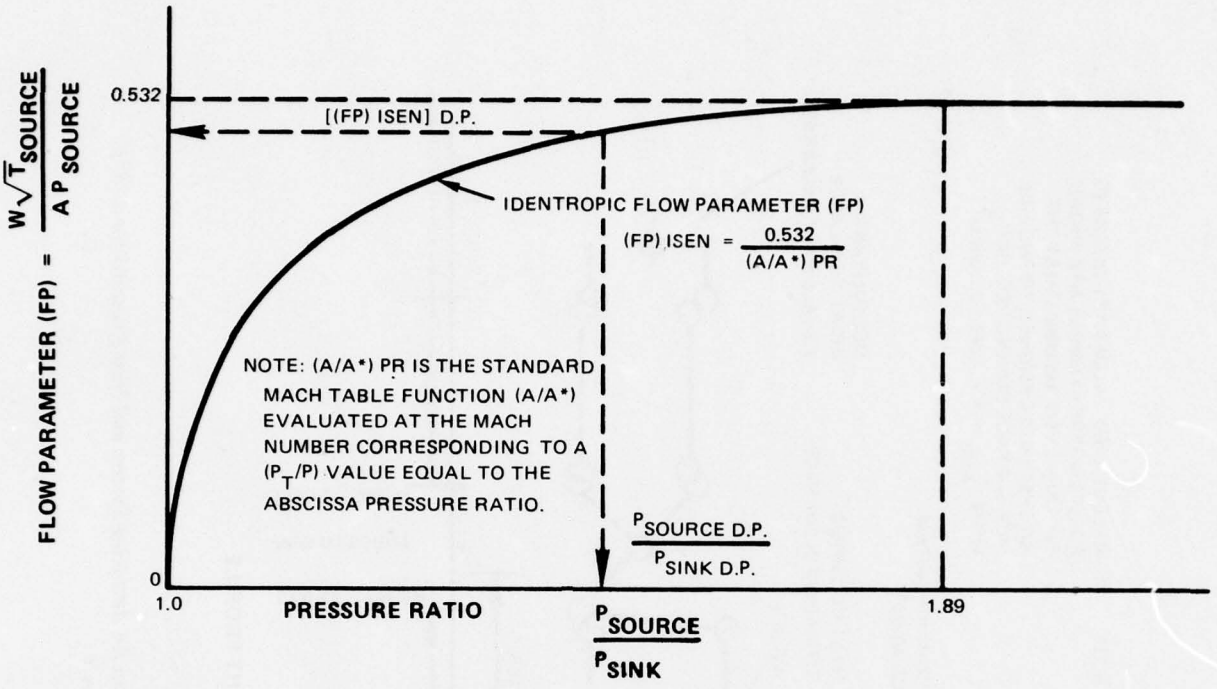

Figure 4-11 Flow Parameter and Discharge Coefficient for Anti-Icing System

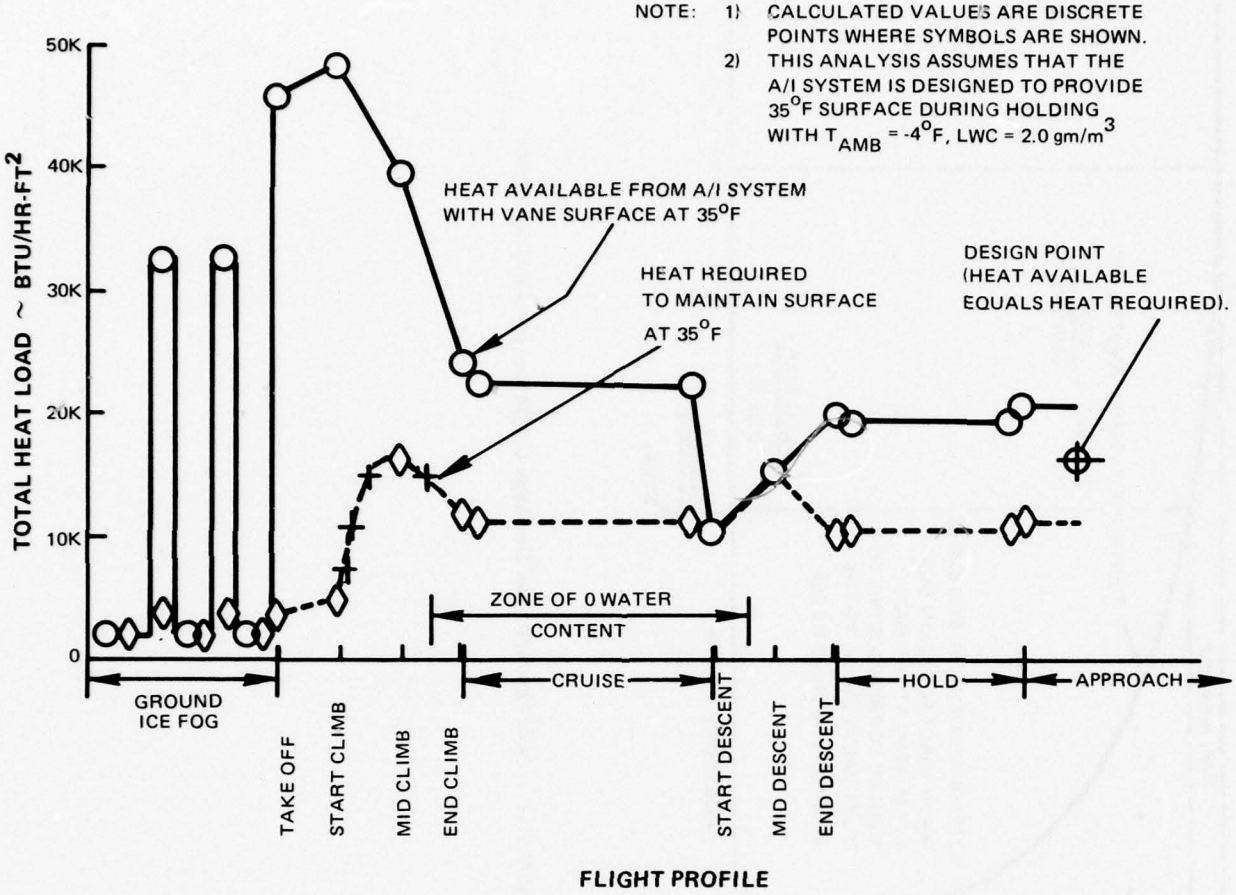

Figure 4-12 Comparison of Heat Available From An Anti-Icing System and Heat Required for a 35°F Inlet Guide Vane During Flight Cycle

CHAPTER V DESIGN CONSIDERATIONS

The design engineer who is faced with configuring an engine anti-icing system must be aware of the various types of systems from which to choose, their effectiveness, relative complexity and reliability, and other practical limitations. Typical systems for consideration are electrical, ice-phobic coatings, compressor hot air bleed, and naturally inherent anti-icing. Thermal systems may vary in the level of protection they provide, ranging from complete evaporation of all water that impinges, to allowing the body surface to run wet (with water runback) at a preselected temperature, say 35°F, above freezing. Furthermore, a periodic de-icing system is also a possibility. A system that achieves a high degree of evaporation on engine components is one that requires an uneconomically high heat input; therefore, the design philosophy herein is to provide a running wet surface in icing conditions. The detailed procedures below for configuring an anti-icing system are primarily geared to the hot air compressor bleed type.

5.1 TYPES OF SYSTEMS

5.1.1 Electrical Systems

A typical electrical anti-icing system which embeds resistance heaters within the component to be protected would probably obtain its energy from the airframe supplied generator. Such a system would not be an integral part of the powerplant and sizing of the generator would be affected by the engine anti-icing requirements. Electrical heating of rotating components, such as a spinner, would require the incorporation of a slip ring arrangement which would probably present a reliability problem. A particular merit of an electrical system would be the ability to embed the heat source close to the leading edge of a very thin stator where routing of the hot air to achieve adequate effectiveness would be difficult. All aspects considered, it appears at the present time, that electrical anti-icing systems for turbine engines are not in general acceptance by the Industry.

5.1.2 Ice-Phobic Coatings

Coatings which show a decrease in adhesion for ice under static conditions do not seem to do so under high speed impingement tests, according to E. E. Striebel in "Ice Protection for Turbine Engines," 1969. Additionally, engine inlet surfaces are subject to abrasion from foreign particles entrained in the airstream, and deterioration of any such coatings used would increase maintenance efforts. Consequently, ice-phobic coatings are not relied upon as a sole anti-icing system.

5.1.3 Hot Air Systems

The typical hot air system bleeds off a portion of the relatively high temperature and high pressure air in the compressor gas path and uses that air to heat the component in question. The A/I heat available is dependent upon bleed location, ambient temperature and pressure, flight Mach number, and engine power level. The necessary elements of such a system are a bleed port at the proper compressor stage, piping or passages to transport the air between bleed port and the component, convective heat transfer passages within the component, and

a location to expel the air once it has done the job of anti-icing (usually back into a low pressure region of the compressor gas path). A flow metering restriction should also be provided, whether it be an orifice or the anti-iced component itself. Such a system is an integral part of the powerplant.

Non-rotating parts such as inlet guide vanes and stators usually incorporate an "O.D." bleed system, in most instances with external piping. The airfoil may be of single pass or multiple pass internal flow configuration, as shown in Figures 5-1 and 5-2. Stiffening strips and vibration damping materials are fairly common within inlet guide vanes. An on-off valve is a standard feature so that when anti-icing protection is not needed the bleed airflow can be turned off.

Anti-icing of a rotating spinner would require that the bleed air must get "on board" rotating parts internal to the engine. The most practical way to route bleed air is from I.D. gas path through the shaft which drives the fan and spinner. The convective passages for the spinner may be double wall configuration with a narrow passage height. Such a system is usually "always on" because of the obvious difficulty with incorporating a valve in the rotating hardware.

The rotating blades on fans and compressors of gas turbine engines are not anti-iced per se, but ice protection is provided by the inherent centrifugal forces and vibration as discussed next.

Typical O.D. and I.D. bleed anti-icing flow routing paths are shown in Figure 5-3, reprinted from Reference 20.

5.1.4 Naturally Inherent Systems

There is naturally inherent ice protection present in several areas of the compressor. This is due to rotation or the compression process itself.

Blades and spinners may self-shed ice due to the centrifugal and vibrational forces set up by rotor spinning. The shedding characteristics are highly dependent upon engine rotor speed and frequency of intermittent run-ups. Engine tolerance to ingestion of ice chunks must be considered.

5.1.4.1 Ground Idle Rev-Ups For Stators

One flight-cycle region where naturally inherent systems are frequently depended upon is the ground idle freezing rain intermittent rev-up regime. Because the atmospheric conditions of ground level freezing rain are not well defined (as was noted in Chapter II), it is difficult to use this region as a detailed design point, and engine rev-ups in freezing rain are sometimes required to shed ice accumulated while taxiing about on the runway. Ice shedding from anti-iced stators and non-anti-iced blades has been effectively accomplished by engine rev-up in many instances of severe ground level freezing rain. Figure 5-4 shows typical N_1 rev-up speeds required to develop sufficient anti-icing air temperature and fan temperature rise, as a function of ambient air temperature, to de-ice inlet guide vanes and first stators. The

graph was calculated by assuming an environment liquid water content of 0.15 grams per cubic meter in accordance with the NACA freezing rain atmosphere of Table 2-IV in Chapter II, and shows that at an ambient temperature of 27°F, the required rev-up speed is nominal, and should be able to be accomplished without skidding the aircraft.

5.1.4.2 Rev-Ups For Blades

Figure 5-5 is a similar plot that shows the required N_1 to shed various ice thicknesses from the root section of fan blades. The curves are based on the average ice removal force for titanium, as shown on Figure 5-6, taken from Reference 19. Other references indicate substantial disagreement with these data, depending upon the surface cleanliness and other nebulous factors.

The flight ram and fan compression work imparts energy to the engine airflow. The resultant total temperature of that airstream may provide sufficient heat to protect the stators behond the fan. The airstream total temperature is dependent upon ambient temperature and pressure, flight Mach number, and engine power level.

Some ice build-up is tolerable on stators, particularly during short time transient conditons like descent. The tolerable level of ice accumulation is highly dependent upon the specific engine design in terms of airfoil geometry, blockage of the engine airflow annulus (spacing of stators) and ability of the engine to ingest shedding ice without damage. This is also discussed in Section 3.3.4.

5.2 SYSTEM DESIGN (COMPRESSOR BLEED)

Once it has been established that a given engine component requires anti-icing protection, the recommended design philosophy is to provide enough heating to maintain a running wet surface of 35°F, or greater, at a single "worst" design point as determined in the Flight Cycle Analysis. The recommendation of 35°F, as opposed to 32°F, is made to provide a safety margin to the design. This safety margin is useful for establishing confidence that the final design will automatically incorporate an ability to:

(a) De-ice a surface which has, for some reason, been exposed to a short time duration transient icing condition of greater than design intensity.

(b) Provide sufficient leakage heat and enthalpy in the running wet surface water so that refreezing of the run-back water does not occur.

The general procedure for the final design of a hot-air anti-icing system involves: (1) using the design point heat loads to estimate the bleed flow/temperature required to achieve a 35°F surface, (2) using the resultant bleed flow/temperature to select the required compressor bleed stage location, (3) size the pipes and bleed ports to get the required bleed flow for the selected temperature and bleed stage, and (4) thermal design of anti-iced part. Preliminary hand calculations based upon one-dimensional heat transfer at the stagnation point of an inlet guide vane may be used, initially, to get a rough idea of bleed flow and temperature required. The final detailed heat transfer analysis can be accomplished via a three-dimensional finite element heat transfer computer analysis, with the preliminary bleed flow

estimate used as a starting point for internal boundary conditions. Fine adjustments to bleed flow can then be made, based upon the initial computer results.

5.2.1 Selection of Compressor Bleed Stage

The following is a step-by-step procedure for preliminary calculations to determine the optimum compressor bleed location. A typical inlet guide vane nose section scheme is used for discussion purposes. (See Figure 5-7).

a) The heat required for a 35°F leading edge (stagnation point), from the Flight Cycle Analysis concluding calculations, is known.

b) The internal (hot side) heat transfer coefficient is a function of the bleed flow through the nose passage and the passage geometry. It is assumed that if the airfoil outer contour is known, that the nose passage geometry (A_{flow}, D_e, S, b) has been roughed in. It is also noted that for the cross-flow scheme shown in Figure 5-7, the I.D. span (after cool-down has taken place) is the region of coldest surface temperature.

$$h_{A/I} = \frac{k_{A/I}}{D_e}(0.023)\left(N_{Re,De}\right)^{0.8}\left(N_{Pr}\right)^{0.4}$$

WHERE

$$D_e = \frac{4 \times A_{FLOW}}{S+b} \qquad \text{(HYDRAULIC DIAMETER)}$$

$$N_{Re,De} = \frac{\dot{w}_{A/I}\, D_e}{A_{FLOW}\, \mu_{A/I}}$$

$$\mu_{A/I} \approx 1.6 \times 10^{-5} \frac{LB_m}{FT\text{-}SEC}$$

(TYPICAL $t_{A/I} \approx 300°F$ AT HOLDING D.P.)

$$N_{Pr} = 0.72$$

The procedure is to assume a value of $\dot{\omega}_{A/I}$, then calculate $h_{A/I}$.

c) The required bleed air temperature $t_{A/I\ out}$, associated with the assumed flow, at I.D. span is estimated using 1-D analysis of the stagnation region (neglecting conduction) is obtained from the equation

$$q''_{\substack{REQ'D \\ 35°}} = h_{A/I}\left(t_{\substack{A/I \\ OUT}} - 35\right)$$

WHERE

$q''_{\substack{REQ'D \\ 35°}} \longrightarrow$ FROM (a)

$h_{A/I} \longrightarrow$ FROM (b)

The procedure is to solve for $t_{A/I_{out}}$.

d) The cool-down, and required $t_{A/I_{in}}$ of the bleed air is now estimated assuming the entire nose-section is at 35°F for full span:

$$\frac{t_{\substack{A/I \\ OUT}} - 35}{t_{\substack{A/I \\ IN}} - 35} = e^{-\left(h_{A/I} A_{\substack{SURF \\ NOSE}}\right)/\left(\dot{W}_{A/I} C_p\right)}$$

WHERE

$A_{\substack{SURF \\ NOSE}} = \pi S$

$t_{\substack{A/I \\ OUT}} \longrightarrow$ FROM (c)

$C_p = 0.24 \ \frac{BTU}{LB_m - °F}$

The procedure is to solve for $t_{A/I_{in}}$.

e) Steps (a) through (d) can be repeated for several assumed values of $\dot{\omega}_{A/I}$, and the curve shown schematically in Figure 5-8 can be plotted. Practical limits on temperature availability are noted; 35°F (requires $\dot{\omega}_{A/I} = \infty$) at the low end, and high compressor discharge temperature at the high end.

f) From experience it is generally found that the bleed flow system is choked, (i.e., system source pressure at the compressor bleed is more than 1.9 times the system discharge pressure). If most all the pressure drop available is allotted across the IGV, (piping losses should be small) then

$$P_{SOURCE\ REQ'D} \approx \frac{\dot{W}_{A/I}\sqrt{T_{A/I}}}{(C_D A_{FLOW})(0.532)}$$

where C_D is the flow system discharge coefficient.

A_{flow} is the smallest flow area expected for the anti-icing air as it flows through the vane. A recommended first choice is $C_D = 0.6$.

It is noted that the farther forward in the compressor the bleed location is selected, $t_{A/I_{in}}$ decreases, $\dot{W}_{A/I_{req'd}}$ increases, and P_{source} decreases while P_{source} req'd increases. A point will be reached where stage pressure becomes less than that required to supply enough flow for the stage air temperature.

In order to properly assess the above information as plotted in Figure 5-8, the designer will need to obtain the values of bleed temperature and pressure at each stage of the compressor as additional input information.

The above steps serve to set the fore and aft limits, based upon heat transfer and flow, within the compressor from which the bleed stage may be selected.

Other practical considerations usually are involved in selecting the bleed location. In addition to heat transfer requirements, a hot air system must be configured around structural integrity, engine performance, cost, compressor aerodynamics and airframe bleed requirements. Selection of the bleed port location is usually secondary to the determination of the other bleeds required for compressor aerodynamics, airframe requirements, and turbine cooling. One of these priority locations is usually selected as a simultaneous A/I source.

The inlet case structure should be designed to survive highest temperatures and pressures produced by the bleed, such as would occur during maximum power, hot day conditions with the A/I valve open (precludes a valve failure). Current practice for inlet case and A/I hardware is to design them for low weight and cost effectiveness. As such, they are usually constructed of titanium with vibration damping materials of moderate temperature capability incorporated in the inlet guide vanes. Modern engines produce compressor discharge temperatures in excess of 1000°F, and because this is too severe for the aforementioned structure, the A/I bleed is usually located at a mid-stage of the compressor.

Once the bleed location has been selected and the required bleed flow determined, bleed ports and the piping must be sized such that the available system pressure drop delivers the needed flow. The pipes should not be larger than absolutely necessary because weight is a

prime concern in engine design. Since the stators of a compressor act as a diffuser, the static pressure of the gas path is higher downstream of the stator than it is behind the rotor of the same stage. It is because of this that the bleed is usually located aft of the stator.

5.2.2 Detailed Design of Anti-Iced IGV (Computer Analysis)

Fine tuning of the heat transfer analysis via computer modeling techniques allows one to optimize surface temperature distributions and the bleed flow rate. If the final and preliminary bleed flows differ greatly, it may be necessary to select another stage source.

The approach is based on the use of a finite-difference heat transfer computer program capable of handling a three-dimensional nodal breakup of the anti-iced component.

Figure 5-9 depicts the leading edge of an IGV as being "broken" into nodal elements. A computer program, specially written for accomplishing the breakup process, calculates all the elemental information required by the heat transfer program. Such information includes element volumes, conduction areas, sequential numbering of elements/surfaces with associated conduction paths made for adjoining elements.

Input for the heat transfer program consists of combining the nodal elemental information with the heat transfer boundary conditions for the particular analysis. The typical existing program probably can not handle exactly the heat load terms for a "running wet" surface. If such is the case, the following methods prove to be quite useful.

Figure 5-10 shows the boundary condition heat load terms for anti-iced wet surface above 32°F. The water film mass balance is ignored by the program, but once a computer run has been made the results can be used in hand calculations to estimate the mass balance along a chord-wise direction. Generally, the droplet kinetic energy term (energy input to surface for heating) is small compared to the others and is ignored. The external and internal convection terms are handled in the normal manner by the heat transfer program. The sensible heat and evaporation heat terms are most easily handled by expressing them as negative heat generation, at the element external surface, as a function of the surface temperature. The hot anti-icing air is treated as flowing fluid nodes with heat loss to the colder channel surface.

The heat transfer program starts its calculation procedure by assigning an initial temperature to all elements and surfaces, that temperature being an arithmetic average of the boundary condition temperatures. All pertinent elemental heat loads are calculated based on this initial temperature and heat balance comparisons are then made. If the heat flows don't balance, systematic adjustment of element and surface temperatures are made and a new heat flow comparison is made. This iterative procedure continues until the heat flow balance converges, at which time the program prints out the final temperature/element relationships.

To insure structural integrity, it is recommended that a detailed heat transfer and stress analysis be made on the anti-iced structure for maximum power hot day take-off conditions with the anti-icing system operating. The resultant temperature levels and gradients will be vastly different for this operation condition than for icing conditions.

5.2.3 Probes

As part of the overall design considerations of engine ice protection systems, the potential icing of various engine instrumentation probes should be examined. The general family of instrument probes normally associated with the general area of the engine inlet includes items such as ice-detector probes, total pressure and temperature probes, static pressure taps, etc. Some of these probes are associated with the inlet duct itself, and are therefore the responsibility of the airframe manufacturer. This report addresses only those probes that are a part of the engine, which normally includes only a non-readable total temperature inlet probe sensor for the fuel control, an inlet total pressure probe for pressure ratio bleed control (sometimes called the PRBC probe), and perhaps an inlet pressure sensor for fuel control signals, and occassionally a Mach number probe at an intermediate compressor location.

The engine designer should consider the ice protection of engine probes with a design philosophy similar to that discussed in ADS-4 for airframe probes.

1. Will ice accumulate on the object in question and in what amount?

2. Will ice accumulation adversely affect the component's function?

3. If the component function is affected, will it have an effect on safe flight of the aircraft?

4. Will ice shedding affect engine operation?

Questions 1 and 4 above can be answered by using the analytical design techniques of this report, as applied specifically to a probe. Most probes can be geometrically approximated by cylinders or spheres, so it is considered that the water impingment and heat transfer calculation procedures already presented are adequate for probes.

Questions 2 and 3 above, which may have different answers for various probes in various engines, should be addressed for each specific probe in each specific engine. The designer should also consider possible adverse affects of water impingement on temperature sensors. The resulting evaporation could induce erroneous readings.

If it is determined that probe anti-icing, or de-icing, is necessary, the design considerations for selecting the type of heating system should take appropriate advantage of the small physical size of the probe itself. Thus, in addition to hot-air anti-icing systems, electrical systems and liquid fluid systems are considered viable candidate selections to provide either anti-icing or de-icing protection of a probe.

In general, PRBC probes are anti-iced, and fuel-control total temperature probes are not. In any temperature probe, it is very difficult to incorporate anti-icing because errors induced by the probe heating tend to be just as undesirable as errors induced by icing, or even simple water evaporation. As a general rule, it is usually true that the fuel control unit is tolerant to evaporation errors and icing errors in its ram temperature signal, so anti-icing or de-icing of these probes is not usually required.

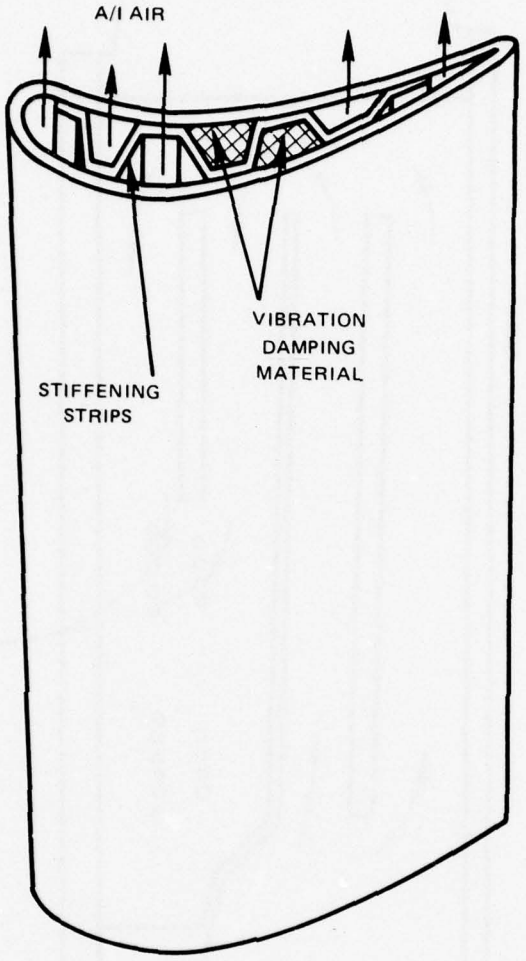

Figure 5-1 Typical Inlet Guide Vane for Single-Pass Internal Flow Scheme

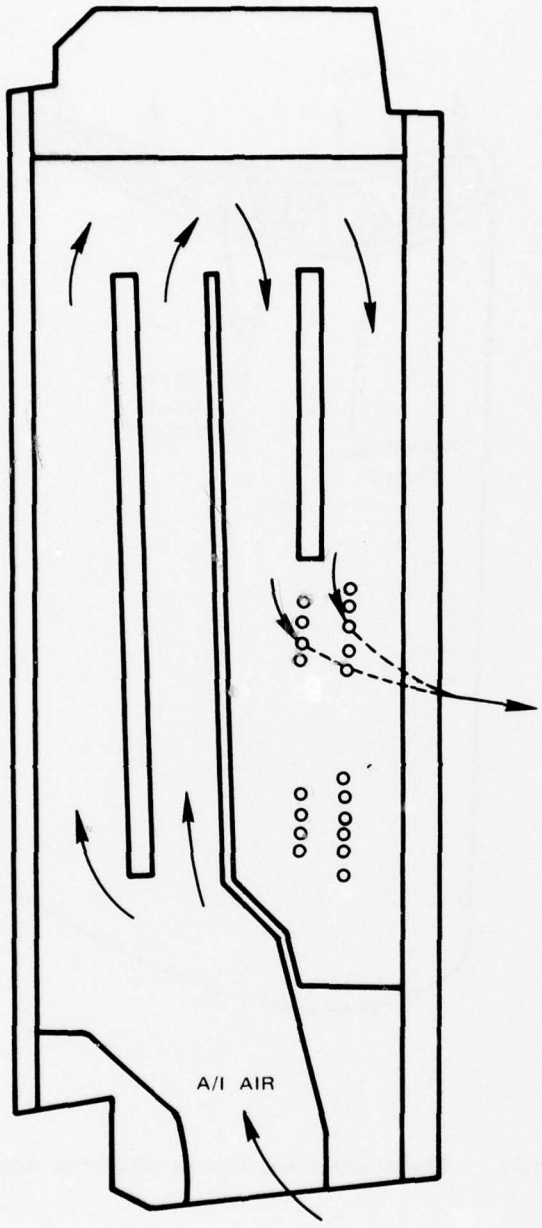

Figure 5-2 Multipass A/I Internal Flow Scheme for a Stator

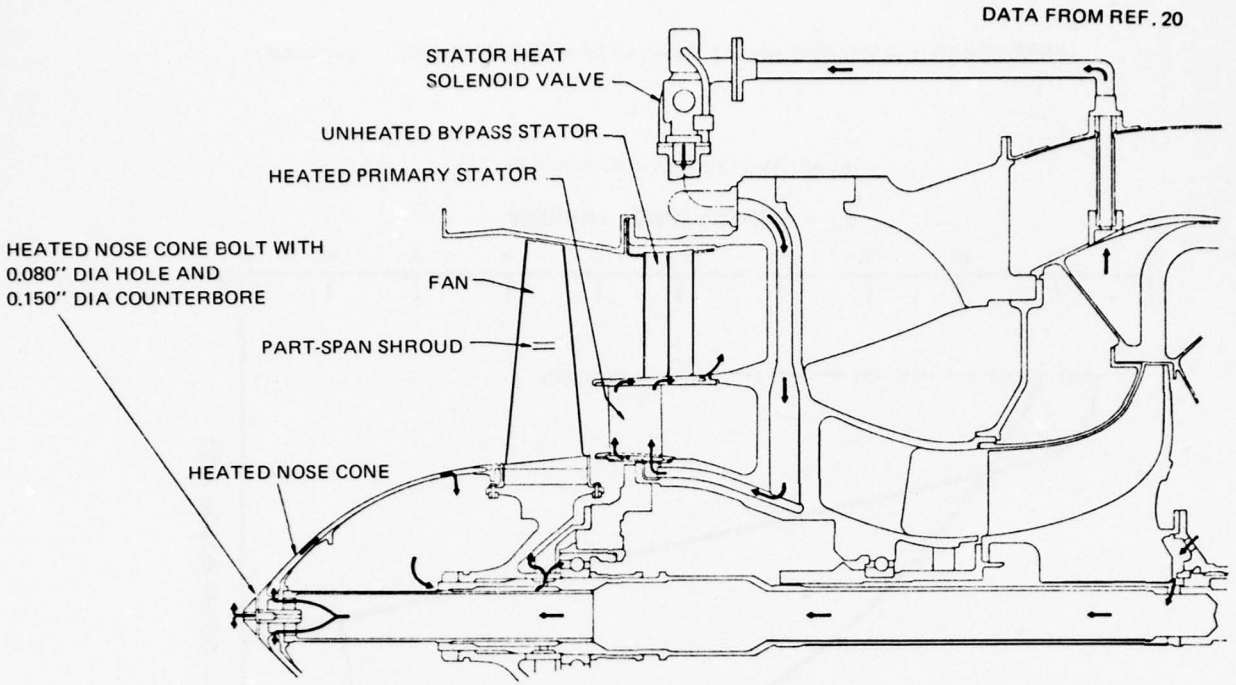

Figure 5-3 Typical Routing of Anti-Icing Air

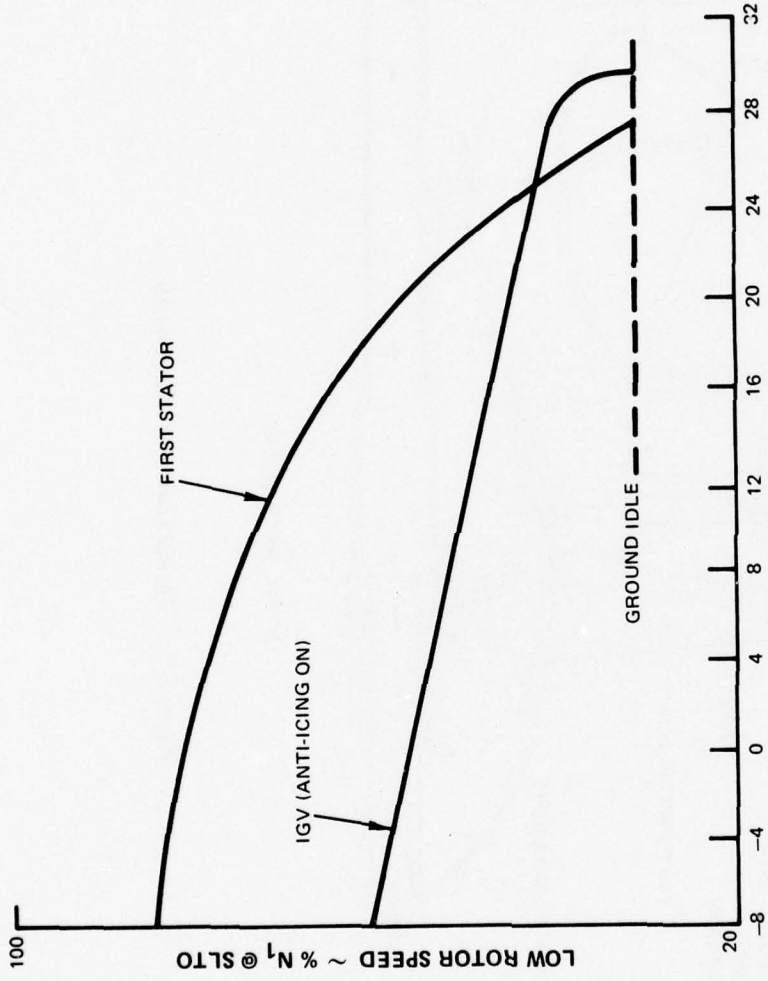

Figure 5-4 Percent N_1 Required to De-Ice Typical Inlet Guide Vane and Stator

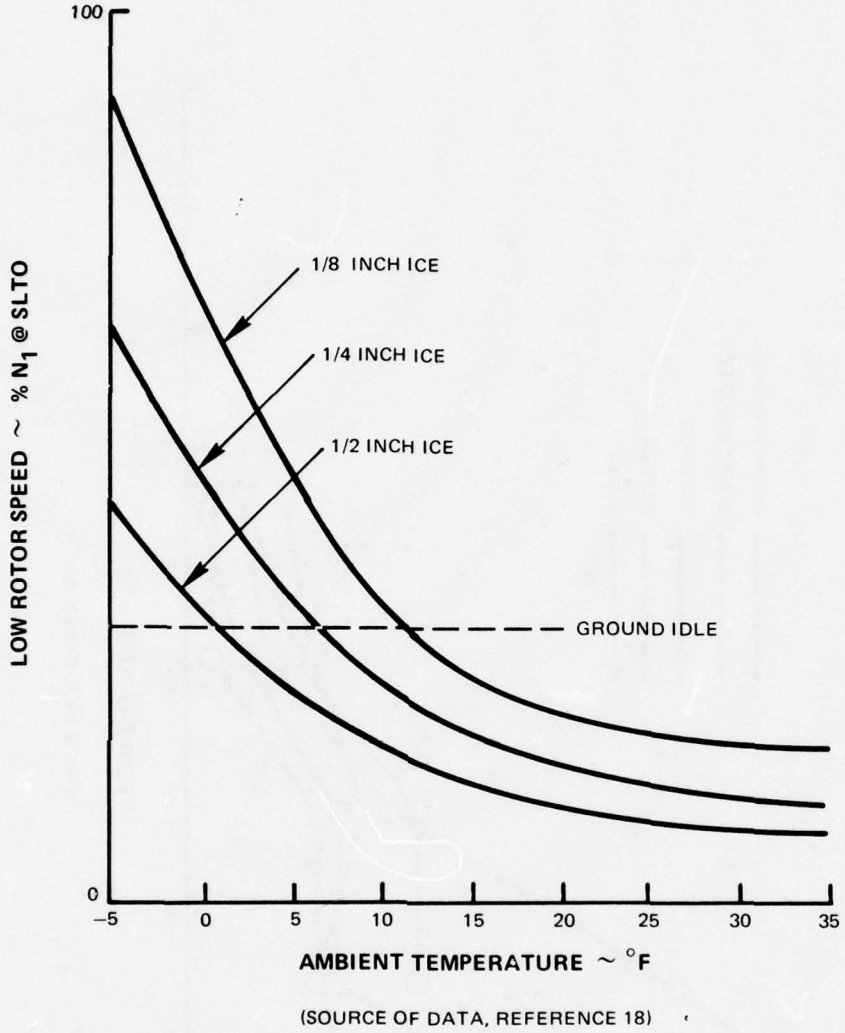

Figure 5-5 Percent N_1 Required to Shed Ice From Root of Typical Fan Blade

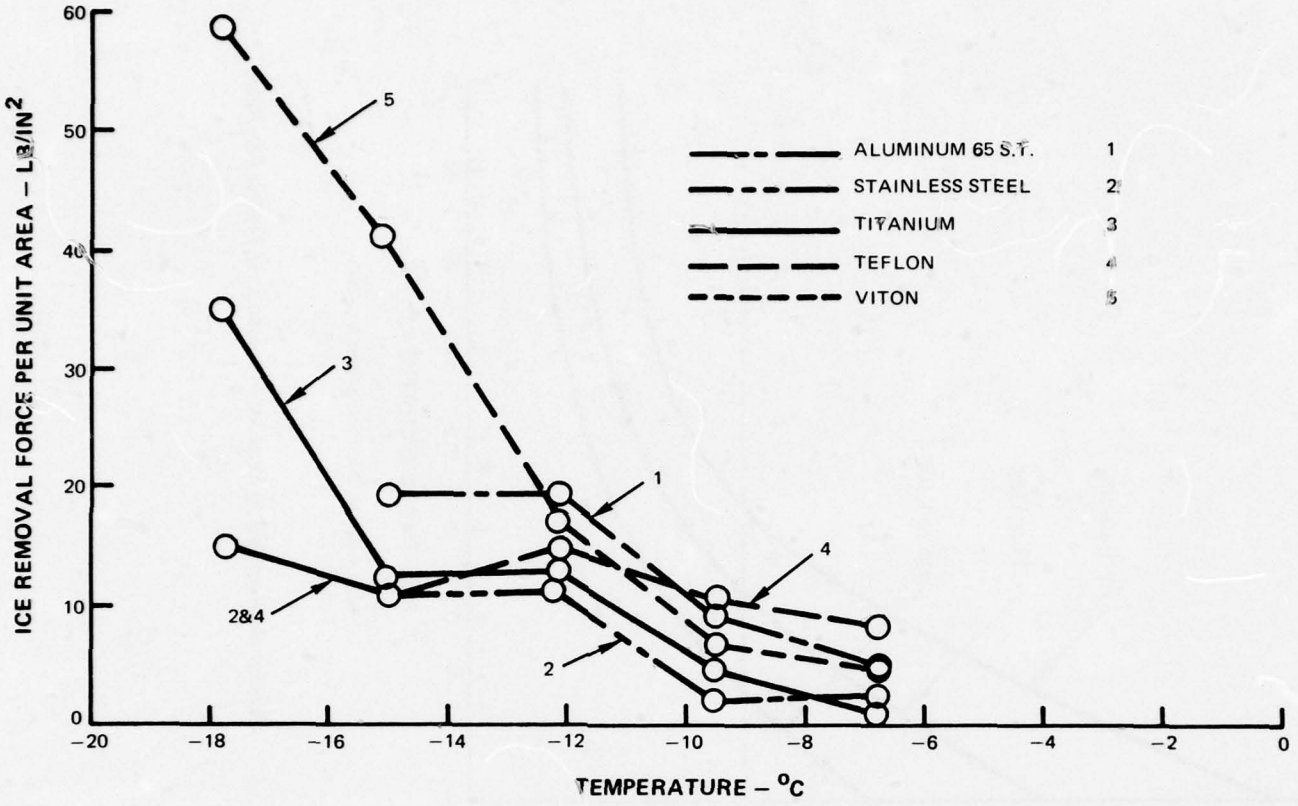

(FROM REFERENCE 19)

Figure 5-6 Ice Removal Force for Various Materials

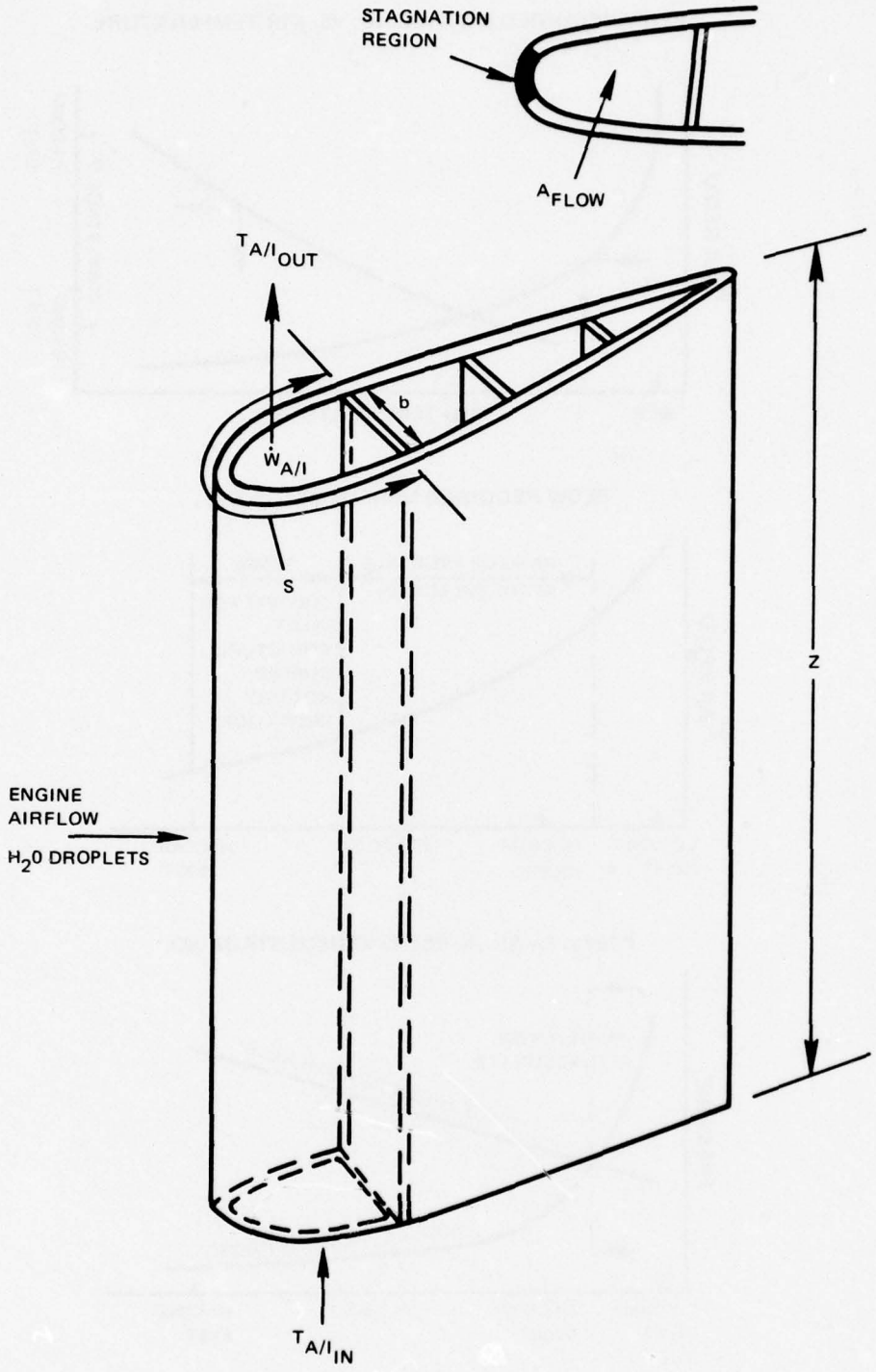

Figure 5-7 Nose Section of an Inlet Guide Vane

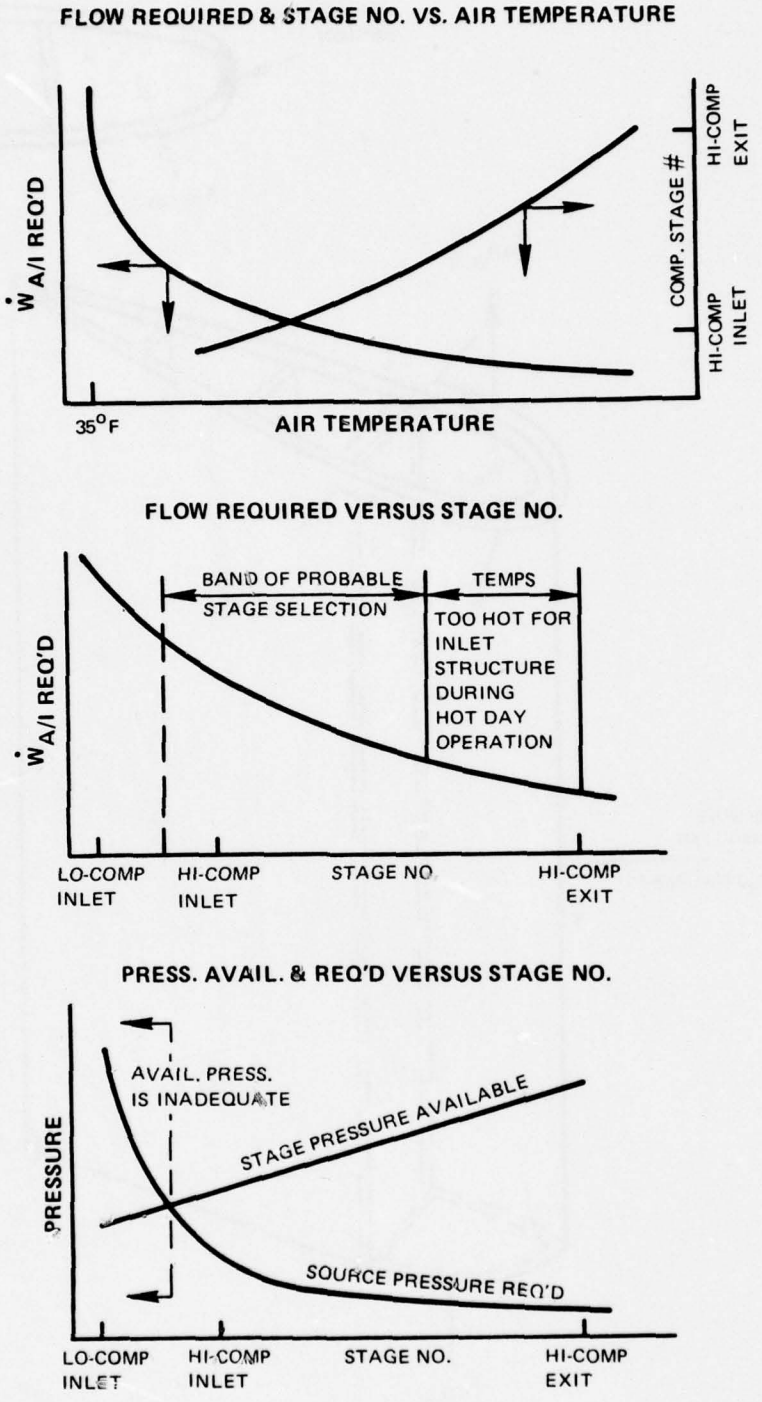

Figure 5-8 Bleed Stage Selection Limitations

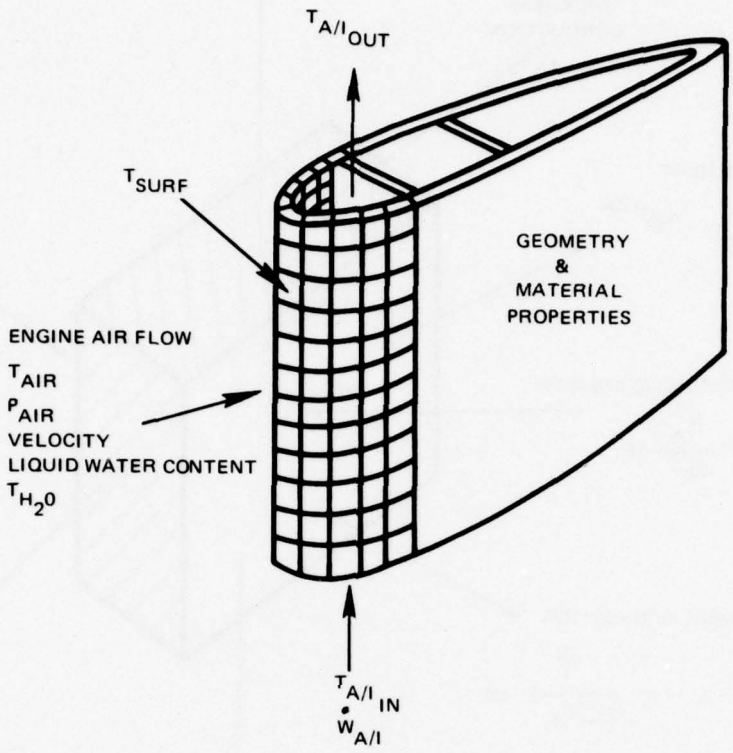

Figure 5-9 Computer Program Input/Ouptut Quantities

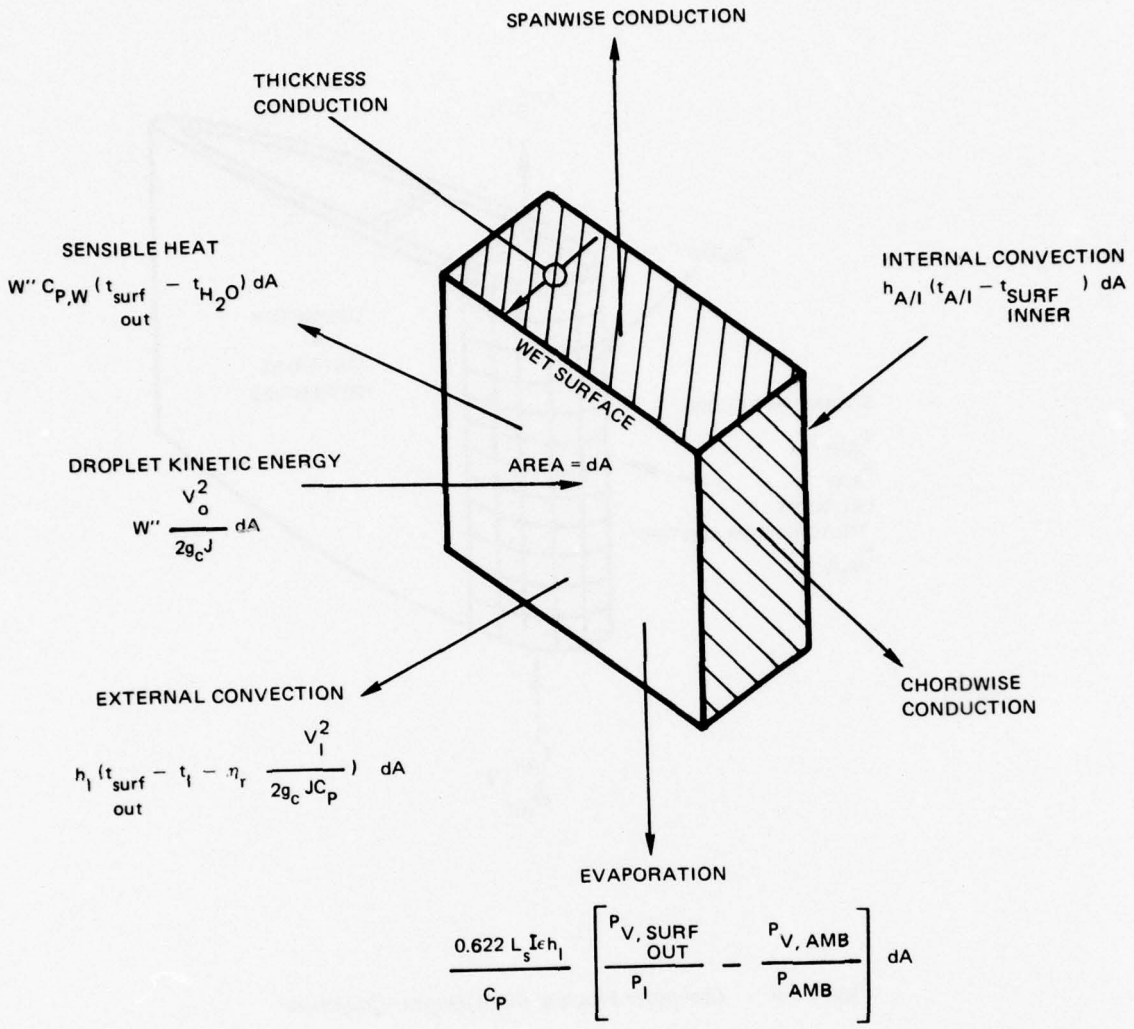

Figure 5-10 Boundary Condition Heat Loads for a Nodal Element

CHAPTER VI SYSTEM VERIFICATION

In general, test verification of engine ice protection and active anti-icing systems in icing conditions can be accomplished in a number of ways:

a) flying the engine through natural clouds,

b) flying the engine at altitude behind a tanker aircraft which creates a simulated cloud with spraying of droplets,

c) ground test the engine in a sea-level facility with spraying of droplets,

d) ground test the engine in a facility capable of simulating altitude conditions with spraying of droplets.

The Military have been very active in the development and use of tankers apparatus for testing aircraft engines and anti-icing systems. The commercial airframe manufacturers are required to test the adequacy of airframe ice protection systems in natural icing clouds as part of the certification requirements by the FAA. Commercial engine manufacturers generally demonstrate compliance with FAA regulations by use of method (d). Schematics of two basic types of engine test facilities are shown on Figure 6-1. A facility of the by-passing type is inherently a larger and more expensive installation than the direct-connect type. For testing of large engines, a facility of the direct-connect type is frequently preferred.

In addition to full scale engine tests, smaller scale and less expensive rig (cascade or component) tests have been used successfully for development work. The results of such rig tests have, in some cases, been accepted by the FAA as a demonstration that retrofit change hardware was at least as good as original certified hardware, thereby eliminating the expense of redoing a full scale engine icing certification test on the new hardware.

The discussions which follow on icing tests of engines are primarily aimed at method (d), i.e., ground tests in a facility capable of simulating altitude conditions, similar to those shown on Figure 6-1. Test procedures for varying temperature, liquid water content, and droplet size are discussed. Various rig tests that have been used for development will also be presented.

6.1 TEST PROCEDURES

For any of the typical test facilities shown on Figure 6-1, the creation of icing test conditions involves drawing the required amount of ambient air into the facility, passing that air through a refrigeration heat exchanger to obtain the desired cold air temperature, and then spraying water droplets of the correct size and distribution into the cold air stream so as to create supercooled water droplets of the desired concentration level. Correct supercooled simulation requires that the droplets be of proper quantity, size and temperature just upstream of the engine face, and there are several important considerations to be commented upon.

6.1.1 Water Droplet Generation

The desired droplet flow rate, size, and distribution is usually obtained by injecting a water spray of properly sized droplets into the cold airstream some distance upstream of the engine inlet. Air-atomizing water nozzles are typically required, such as shown schematically in Figure 6-2 which was taken from report AEDC-TR-71-94.

6.1.1.1 Flow Rate and Droplet Size

The primary passage of the nozzle of Figure 6-2 delivers water at the required flow rate, and the rate can be adjusted by varying the water supply pressure. The water flow rate is measured and that value is used to calculate the LWC of the test air stream. The secondary passage supplies the atomizing air which controls the spray droplet size as a function of the air supply pressure. Both the water and air are typically heated to about 100°F to 200°F so as to preclude freezing within and on the nozzle apparatus itself which sits in the cold airstream. Additionally, the heated atomizing air serves to prevent freeze-out of the droplets. B. D. Lazelle, in "Conditions to Prevent Freeze-Out During Atomization of Water Sprays for Icing Cloud Simulation," reference DEV/TN/262/778, D. Napier and Son Limited, August 1958, gives a rule-of-thumb recommendation for air temperature; the atomizing air temperature in degrees centigrade should be at least twice the numerical value of the air pressure in psig. Figure 6-3 taken from this reference shows data points for incipient freeze-out, along with the recommended correlation.

6.1.1.2 Droplet Size Distribution

Determination of droplet sizes and the distribution of such, for a given cloud or spray sample, have classically been made by capturing droplets on a greased plate or oiled slide which has been exposed momentarily to the flow stream. The sample droplets are quickly photographed and then studied under high magnification to measure the size and distribution. The oiled slide method has many inherent disadvantages and as a result the Arnold Engineering Development Center has recently developed a state-of-the-art droplet size measurement system in conjunction with their J-1 test cell development program. E. S. Gall and F. X. Floyd, in report AEDC-TR-71-94 describe a holography measuring system which can obtain size data on droplets contained within a 2 inch diameter and 3 foot long volume without disturbing the airstream. Figure 6-4, taken from that report, compares droplet mean volume diameter data obtained by both oiled slide and the holography system. As shown, the oiled slide data is on the order of 50% greater than the holographic data. The oiled slide method has been judged inaccurate by the AEDC because the airstream is disturbed, droplets spatter or impinge upon each other, and the droplets flatten upon impact. However, for general icing tests conducted specifically to meet FAA requirements, it is considered in this report that the greased slide method of size determination is adequate, because this method has been, historically, acceptable for many years.

A sample greased-slide water droplet photograph of relatively large droplet diameters is shown on Figure 6-5, and Figure 6-6 shows typical droplets in a relatively small droplet diameter pattern. From similar data, an arithmetic medium droplet diameter for a sample was 25 microns, and the mean effective droplet diameter (as defined in FAA Advisory Circular AC No. 20-73) was 69 microns. The corresponding distribution of droplet water-contents from a greased slide are plotted on Figure 6-7, along with typical water droplet distributions in atmospheric clouds as obtained from Reference 23. Inspection of this figure shows that the sample distribution of droplets and mean effective droplet diameter show general similarities to real clouds, but do not exactly match the desired distribution and mean effective diameter. Any test errors incurred as a result of such mismatches are very difficult, if not impossible, to assess. As long as the droplet water total flow rate and temperature are correct, the icing effects of droplet diameter variations alone cannot be assessed at the present time, and are believed to be of secondary importance. This opinion appears to be confirmed by various comments and information obtained from AEDC-TR-73-144, Reference 23.

6.1.2 Droplet Temperature Simulation

Because the temperature of atmospheric cloud supercooled water droplets is known to equal the static temperature of the ambient air, it is desirable to achieve this condition for the test water droplets in facilities of the "bypassing" type shown on Figure 6-1. For the "direct-connect" type of facility, it will be subsequently shown in Section 6.1.2.2 that the desired water droplet temperature is somewhat different, but both types of facilities require that the supercooled water droplet temperature should be equal to the test air temperature by the time the engine inlet is reached. It is noted that the droplet velocity should also be equal to air velocity. The small droplet sizes generated from the spray nozzles quickly approach air velocities as is pointed out in AEDC-TR-75-144 (Reference 23), and needs no further comment.

6.1.2.1 The Cool-Down Approach Length

Since all test water droplets are necessarily initially injected at warm temperatures, the test facility configuration should provide a suitable flow distance from the water spray nozzles to the engine inlet so that adequate cool-down of the droplets can physically occur. The optimum distance for this purpose is a subject of continuing research, and cannot be definitely established at the present time. The referenced publication on this subject, AEDC-TR-144 (Reference 23) presents some preliminary data which indicates that the optimum cool-down length depends upon - - among other things - - droplet size and relative injection velocity. Figures 6-8 and 6-9, both taken directly from Reference 23, are presented to show that preliminary data indicates that for small droplets of the 20 micron size, an adequate cool-down length appears to be quite short - - less than two feet. Larger diameter droplets appear to require longer cool-down lengths, and the relative velocity of the initial water spray can significantly affect the required cool-down length of small droplets. It is recommended that these factors should be considered in selecting an appropriate cool-down approach length for testing, so that adequate droplet cool-down is achieved.

6.1.2.2 Inlet vs. Free Stream Temperature Considerations

Another aspect of droplet temperature simulation which should be addressed concerns the modeling of droplet temperature within the engine inlet. It is well-known from aerodynamic considerations that the air temperature within a flying engine inlet is generally somewhat different from the environment static air temperature. When the engine inlet Mach number is greater than the flight Mach number, the air static temperature within the inlet is less than the ambient atmosphere static temperature. Conversely, when the engine inlet Mach number is less than the flight Mach number, the air static temperature within the inlet is greater than the ambient atmosphere static temperature. These aerodynamic considerations, however, do not necessarily apply to water droplet temperatures. The tendency of the water droplet temperature to change with engine inlet ram air temperature is not clearly established. A literature search on this subject was conducted during the preparation of this report, but no firm conclusions could be found. In NASA TN 3024 (Reference 24), it is commented that a droplet, as it approaches a solid obstacle, experiences a heat input from its surrounding ram air and a heat output of evaporation, with a net result that the droplet usually increases about two thirds of the air temperature rise. A later document, WADC Technical Report 54-313 (Reference 13), which lists the NASA TN 3024 report as a reference, recommends that the water droplet temperature should be simply held constant at its initial ambient temperature value regardless of ram air temperature changes. These two references were the only two documents found in which this subject was mentioned with enough clarity to warrant citing their recommendations, but even these two references are somewhat incomplete in their treatment of the subject. As a result, no firm conclusion can be recommended in this report regarding the true behavior of water droplet temperature upon entering an engine inlet. In the design analytical presentation of Section 3.1.3.2, it was simply recommended to follow the advice of Reference 13 and hold the water droplet constant at its ambient value, primarily because the heat balance equations presented in that section are taken from that same reference. However, for experimental test procedures, more research on the subject is required before a definite recommendation for proper test simulation can be made.

The foregoing problem of droplet temperature test simulation in engine inlets is of concern only if the test facility is of the "direct-connect" type shown on Figure 6-1. If the test facility is of the "bypassing" type, then the droplets will change temperature, or not change temperature, in the test inlet exactly as would occur in flight, and one is assured that the test modeling is proper. If the test facility is of the "direct connect" type, then one should establish the approaching air and water-droplet temperatures to be equal to the air temperature level ultimately desired within the engine inlet. Such a procedure is substantially correct or slightly conservative for modeling flight modes such as ground idle, climb, and holding where the engine inlet Mach number is close to or slightly greater than the flight Mach number; but tends to be somewhat anti-conservative for modeling descent flight modes. However, this anti-conservative tendency for descent simulation could be of insignificant magnitude if the aforementioned comments of NASA TN 3024 are correct as regards the true behavior of water droplet temperature in inlets. Until future research can resolve the water droplet temperature behavior problem, it is considered acceptable test procedure to model descent flight modes with a "direct-connect" facility operating at conservative higher-than-normal liquid water contents. For example, if one wanted to model a descent point at a flight Mach number of 0.5 in an atmospheric static temperature of, say, -1°F, with a corresponding inlet

Mach number of 0.15 and ram air temperature of about 20°F with an inlet total water catch factor $[(C_t)\, V_\infty / V_i]$ of 1.35, one would select a test liquid water content of:

$$LWC_{TEST} = 1.35\,(2.4\ g/m^3) = 3.25\ g/m^3$$

where the value of 2.4 g/m^3 is read from Figure 2-26 at the inlet temperature of 20°F. The real atmospheric LWC for this example would be read from Figure 2-16 at −1°F, and would be only about 1.6 g/m^3. Hence the test engine liquid water content is conservatively set at a level 50% greater than would be predicted in actual flight.

6.2 DEVELOPMENT TESTING

Development work on anti-icing hardware encompasses a varied field of test techniques, including both icing simulations and dry air methods, applied to component rigs as well as full scale engines. Engine icing testing are expensive to carry out; thus, there is a cost saving incentive to utilize relatively inexpensive rig tests or dry air engine tests, where appropriate, to obtain the engineering data required to assess the performance of an anti-iced component.

6.2.1 Vane Cascade Test Rig

Small scale vane cascade tunnels (as on Figure 6-10) can be modified for useful icing tests. As pointed out by E. E. Striebel in "Ice Protection for Turbine Engines", (Ref. 18), a small scale vane cascade test rig was used to study icing characteristics on anti-iced stators of thin cross-section in which metal conduction resistance at the leading edge impaired internal hot air thermal efficiency. Various hot air schemes were evaluated on the rig for anti-icing a very thin airfoil. The air passage through the vane was initially located 0.70 inch from the leading and trailing edges of the vane. Testing indicated that this design was unsatisfactory and the leading edges of the vanes were then reoperated, compromising to some degree the vane aerodynamics, in order to position the hot iar passage within 0.20 inch of the leading edge. Figure 6-11 indicates the predicted mid-span temperature distribution for the stator subjected to 2.5 GM/M^3 liquid water content at 20°F inlet air temperature. Temperature distributions are shown for the unheated vane and both heated vane configurations. It can be seen that both the leading and trailing edges of the heated vane are below 32°F. However, by relocating the hot air passage, the amount of unprotected leading edge surface is reduced from 0.5 inch to less than 0.10 inch.

Figure 6-12 shows photographs of the unheated vane, and both heated vane configurations after 100 seconds exposure to the stated icing conditions in the vane cascade rig. The first picture shows the unheated vane cascade with ice over much of the vane surface. The second picute shows the heated vane with the hot air passages 0.7 inch for the leading and trailing edges. Ice can be seen on both the leading and trailing edges but the mid-chord section is clear of any accumulation. The last picture is the heated vane with the hot air passage 0.2 inch from the leading edge. A slight ice build up can be seen on the leading edge and some on the trailing edge. Experience with the latter configuration, however, indicated that

any ice that was formed would rapidly shed thereby preventing any significant accumulation.

6.2.2 Retrofit Vane Tests

Occasionally, experience in the manufacturing process or from field operation points to the desirability to incorporate modifications in anti-iced parts that are already certified and flying. A case in particular concerned an anti-iced first stator vane. The originally certificated stator was initially fabricated with weldment construction (including the internal flow passage baffles), which resulted in non-uniformities of leading and trailing edge thicknesses as well as in the anti-icing air flow passage areas. The airfoil and baffle construction was later changed from a weldment to a brazed construction using a pre-selected amount of braze wire for reasonable control of leading and trailing edge thicknesses as well as the internal flow passage areas. In light of the modifications, it was felt necessary to prove that the new stator exhibited anti-icing capability equalling or exceeding that of the original stator. This was accomplished by a series of engine and rig tests described next, without resorting to redoing a full engine icing certification test.

a) Airflow calibration bench tests on a series of both stator configurations demonstrated that the new stators had a 5% higher flow parameter than the original stators. A sketch of the vane anti-icing flow path is shown on Figure 6-13, and a schematic of the flow calibration bench-test set-up is shown in Figure 6-14.

b) Stators of both types were instrumented with thermocouples and then subjected to dry air, full scale engine tests to measure the anti-icing system heating effectiveness. The resultant data, a sample of which is summarized in Figure 6-15, showed that the new fixed-brazed stator had an average anti-icing effectiveness about 2% greater than the original stator.

Anti-icing effectiveness was defined as follows:

$$\eta_{A/I} = \frac{T_{\text{vane metal surface}} - T_{\text{local surrounding air}}}{T_{\text{anti-icing air}} - T_{\text{local surrounding air}}} \times 100\%$$

where $\eta_{A/I} = 0$ means $T_{\text{vane metal surface}} = T_{\text{local surrounding air}}$

$\eta_{A/I} = 100\%$ means $T_{\text{vane metal surface}} = T_{\text{anti-icing air}}$

c) Additional temperature distribution investigations were performed in a dry air heat flux rig on both types of stators using a temperature sensitive liquid crystal coating which exhibits color changes at different temperature levels. Stators coated with liquid crystal on the outer airfoil surface, and instrumented with thermocouples, were installed in a small scale plexiglass wind tunnel, as shown schematically on Figure 6-16, and in the photograph of Figure 6-17. Temperature gradient patterns within the metal of each type of vane were induced by blowing

hot air over the outer surfaces, while chilled air was supplied to the internal passages. Photographic records were made of the resulting coating color patterns, a sample of which is indicated by the black and white isotherm zones shown in Figure 6-18. Visual comparison of these photographs, along with the improved thermal efficiency of the new stator, resulted in sufficient evidence to conclude that no additional anti-icing certification tests were required.

6.2.3 Development Testing of a Complete Engine

It is sometimes desirable that development testing be performed on a complete engine to thoroughly evaluate the potential icing problems, particularly when the engine size is relatively small. A test program of this nature was carried out in 1967 - 1969 by the United Technologies Canada Division (formerly United Aircraft Canada) on their JT15D turbofan engine, and is completely reported upon in Reference 20. Excerpts from this reference are presented in Appendix B, to demonstrate the various problems encountered and subsequently solved. Appendix B shows a schematic view of their test facility. It is basically a "direct-connect" type of facility.

6.2.4 Rotary Wing Aircraft Engines

In general, ice protection systems on engines intended for installation in helicopters are designed and tested by the same standards as for fixed wing aircraft engines. Any effects of a rotary-wing installation, as opposed to a fixed-wing installation, are considered to be of only secondary importance to the engine ice protection design, so all of the design and test considerations discussed in this report are directly applicable to helicopter engines. Icing certification tests for rotary-wing engines are usually performed on the engine alone, without regard to the planned installation aircraft.

There are, however, some interesting helicopter icing phenomena which apply in a secondary manner to the engine. Such phenomena regard engine ice ingestion, and are described in various icing reports of helicopter demonstration tests with the engine installed. These tests are frequently performed by flying the helicopter behind an ice-cloud-generating tanker plane, in a large climatic hanger equipped with an overhead water spray, or in real icing conditions of the natural atmosphere. The major objective of these tests is to demonstrate the ice protection capability of the helicopter itself, not the engine. Occasionally the helicopter will shed large ice chunks, from the rotor hub or engine inlet cowling for example, into the engine with resulting significant engine damage. Such occurrences, however, are usually considered by the airframe manufacturer to be an airframe problem, not an engine problem, and they assume the responsibility for corrective action. A popular corrective action appears to be the airframe incorporation of an ice-chunk metal deflector plate installed in front of the engine inlet cowling in a manner which does not inhibit air flow, but adequately deflects ice.

In Sikorsky Aircraft report SER-61523, (Reference 25), some engine damage is reported to have occurred during climatic hanger icing tests on a HSS-2 helicopter. Ice chunks believed to be roughly 4x2x3/8 inches were ingested, probably from engine air intake duct shedding. Corrective action was to increase the heating capacity of the intake duct anti-icing system.

In Air Force technical report ASD-TR-64-92, (Reference 26), engine damage is reported to have occurred on a CH-3C helicopter during natural icing tests, and during icing tests behind a tanker plane, presumably due to ingestion from rotor blade shedding. Corrective action was to install an ice deflector plate to prevent engine ice ingestion.

Another Air Force technical report, ASD-TR-70-51, (Reference 27), reports successful engine ice ingestion with no damage during natural icing tests of a HH-53C helicopter. Upon landing, an ice chunk 3x4x2 inches was found lying in the left engine inlet. Postflight examination of the engine did not reveal any damage incurred by ice ingestion. No corrective action was necessary.

6.3 ENGINE CERTIFICATION TESTING

In order to become certificated for flight by the FAA, gas turbine aircraft engines must demonstrate, via testing, that they are capable of operating successfully in icing conditions. They must also be subjected to ice ingestion tests. Definitions of such tests are given in the Federal Aviation Regulations FAR Part 33 and Part 25, 25.1093, and Appendix C. The FAR Part 25 Appendix C was previously presented in Chapter II as Appendix A. The requirements of FAR Part 33 are presented as follows. It should be noted by the engine designer that the Specs which follow are presented for his convenience only, and they pertain only to current icing test regulations. It is the designer's responsibility to keep up with any future revisions from the FAA, and to make himself aware of structural design specs that may apply to an anti-iced system, but are not cited here-in.

6.3.1 FAR Part 25 and Part 33

6.3.1.1 FAR Part 25.1093 and 33.67

FAR Part 25.1093 and FAR Part 33.67 are reproduced in Appendix C. Part 33.67 was in effect from 1965 to 1974, when it was up-dated and superseded by FAR Part 33.68. (In 1974, FAR Part 33.67 became a fuel system spec).

6.3.1.2 FAR Part 33.68

The FAR Part 33.68 requirements for the icing environmental required tests are reproduced in Appendix D. These tests are split into two categories. Part (a) addresses flight operation through cumulus and stratiform icing clouds. In essence it says that the engine must operate without serious loss of thrust throughout its flight power range in the conditions spelled out in FAR Part 25, Appendix C (Appendix A of this report). Part (b) is a ground idle test requirement that was added to the Regulations in 1974. It is specific in that ambient temperature, liquid water content, mean effective droplet diameter, and time duration are all given.

The imprecise nature of Part (a) allows each engine manufacturer to work out a set of mutually agreeable compliance tests with the FAA pertaining to his specific engine in his specific test facility.

6.3.1.3 FAA Advisory Circulars

The FAA Advisory Circular AC #20-73, dated April 1971, attempted to clarify FAA views on what specific tests are acceptable in demonstrating compliance with the Regulations. That document, though not mandatory or regulatory in nature, considered the following conditions to be acceptable in conjunction with the specified duration and engine power:

	Condition 1	Condition 2	Condition 3 (Currently Obsolete)
LWC gm/M^3	2.0	1.0	2
Atmospheric Temp. °F	23	–4	29
d_m Microns	25	15	40 minimum

> "Operate the engine steadily under icing conditions 1 and 2 for at least 10 minutes each at takeoff setting, 75% and 50% MC and at flight idle setting, then accelerate from flight idle to takeoff. If ice is still building up at the end of 10 minutes, continue running until the ice begins to shed or until the engine will no longer operate satisfactorily."

Conditions (1) and (2) above are identical to those of the now obsolete Military specifications MIL-E-5007C. The current Military Test Specifications MIL-E-5007D are given in Table 6-I for comparison and reference.

Condition (3) was abandoned for ground idle simulation, and was replaced in 1974 by the FAR Part 33.68 (b) spec previously presented.

6.3.2 Ice Ingestion Tests: FAR Part 33.77

Both the FAA and the Military require tests of engine ice ingestion capability. FAR Part 33.77 reproduced in Appendix E, specifies that ingestion of water ice, or hail under the conditions set forth in this spec may not cause a sustained power or thrust loss or require the engine to be shut down.

For comparison, the MIL-E-5007D ice ingestion test specs are given in Appendix F.

6.3.3 The Proprietary Nature of Actual Certification Test Results

There are many reports regarding the actual test results of icing certification tests run to show compliance with the FAA regulations. However, such reports are proprietary in nature for various engine manufacturers and cannot be reproduced in whole or in part in this report.

TABLE 6-I

SEA LEVEL ANTI-ICING CONDITIONS
MIL-E-5007D ICING SPEC.
(Ref. 10, Table XIII)

	Part 1 (See Note a)			Part 2 (See Note b)
Engine Inlet Total Temperature	-4°F(-20°C) ±1°	+15°F(-10°C)±1°(1)	+23°F(-5°C)±1°	23°F(-5°C)±1°
Velocity	0 to 60 knots	0 to 60 knots	0 to 60 knots	0 to 60 knots
Altitude	0 to 500 ft.	0 to 500 ft.	0 to 500 ft.	0 to 500 ft.
Mean Effective Drop Diameter	20 microns	20 microns	20 microns	30 microns
Liquid Water Content (Continuous)	1 gm/m^3 ±0.25 gm/m^3	2 gm/m^3 ±0.25 gm/m^3	2 gm/m^3 ±0.25 gm/m^3	0.4 gm/m^3 ±0.1 gm/m^3

(1) This condition is deleted for non-fan engines.

a. This part shall consist of two runs at each of several engine power settings under each of the conditions in part 1 of Table XIII. The engine power settings shall include idle; 25 percent, 50 percent, 75 percent of Maximum Continuous; Maximum Continuous and Intermediate Power. At each icing condition and at each power setting, the engine shall be operated for a period of not less than 10 minutes. During each period, at intervals after ice buildup, the engine shall be rapidly accelerated to intermediate power to demonstrate acceleration response.

b. This part shall consist of a 1 hour run at idle with no throttle movement, followed by an acceleration to maximum thrust at the end of the period. During this run the engine shall be operated under the conditions listed in part 2 of Table XIII.

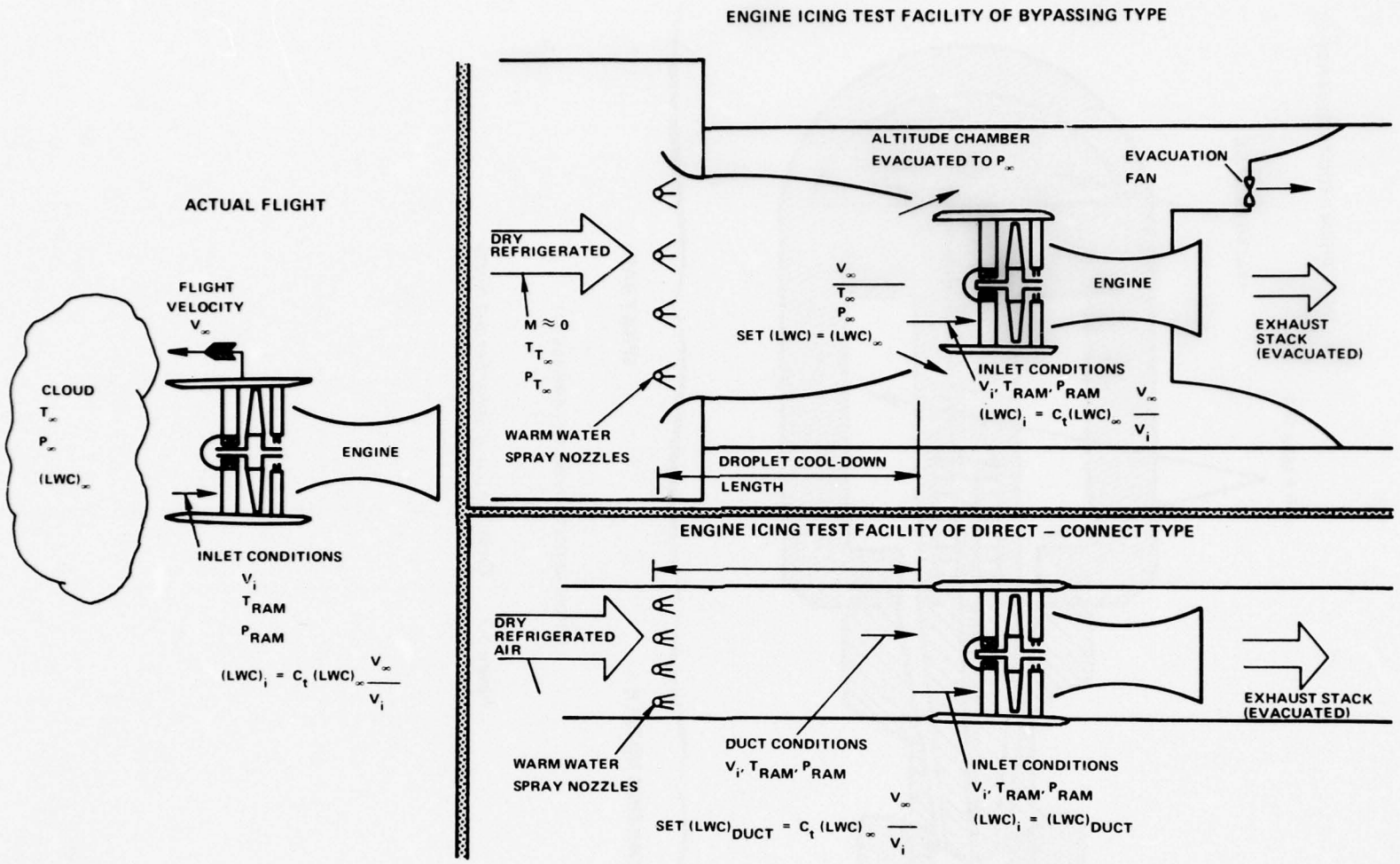

Figure 6-1 Engine Icing Test Simulation

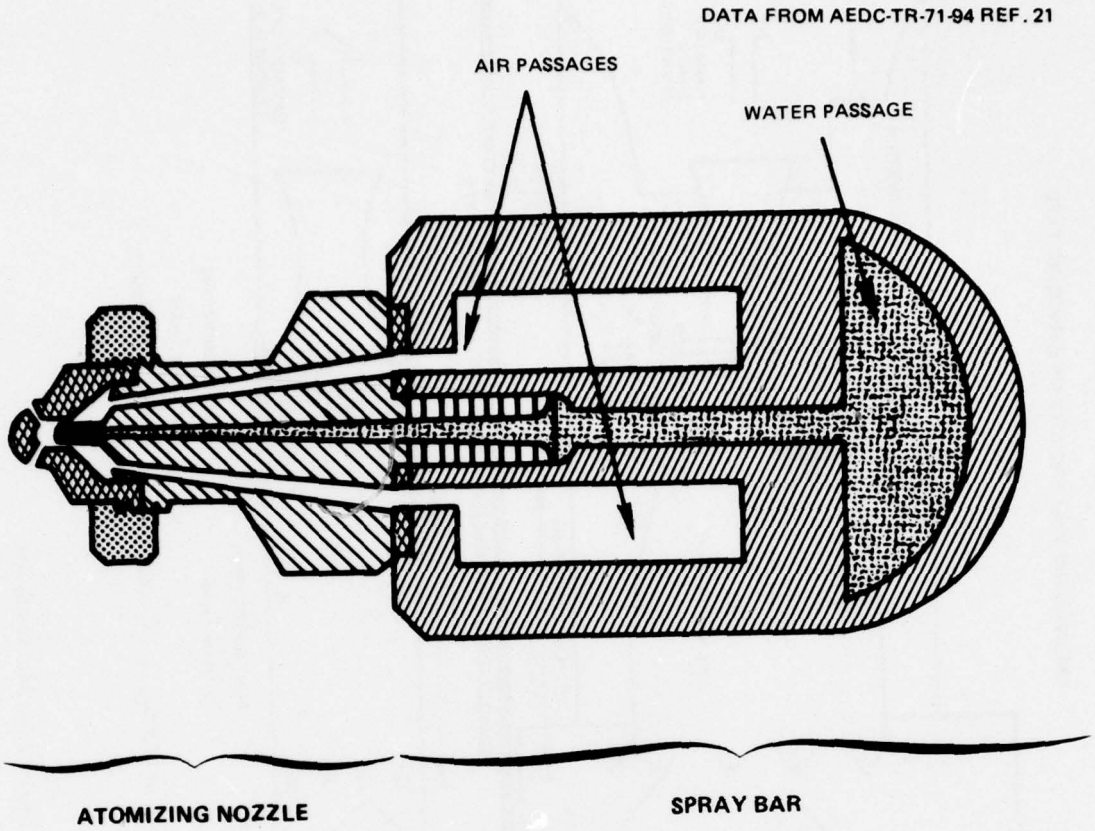

Figure 6-2 Cross Section of Spray Bar and Nozzle

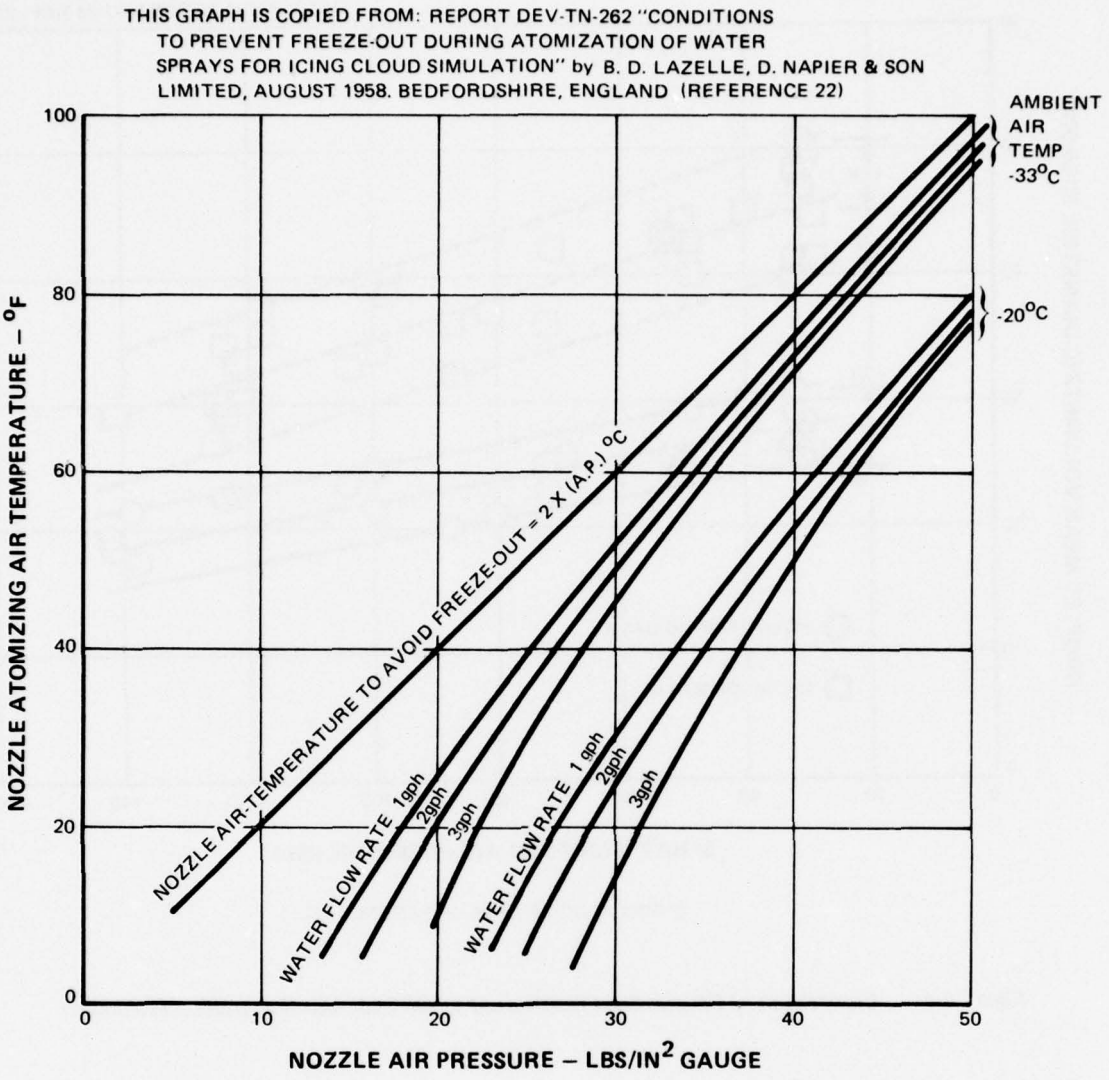

Figure 6-3 Nozzle Atomizing Air Temperatures to Avoid Freeze-Out

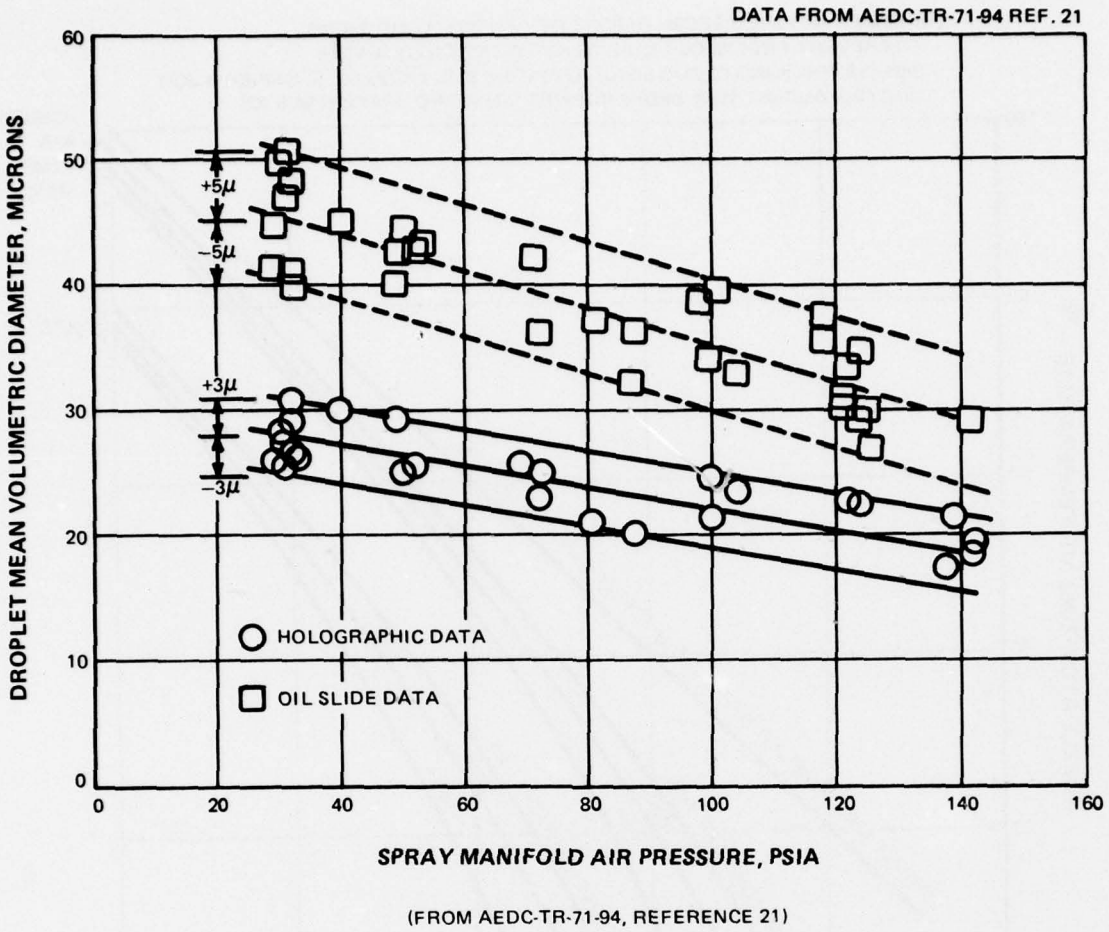

Figure 6-4 Comparison of Droplet Sizes Determined by Oil Slide and Holographic Techniques

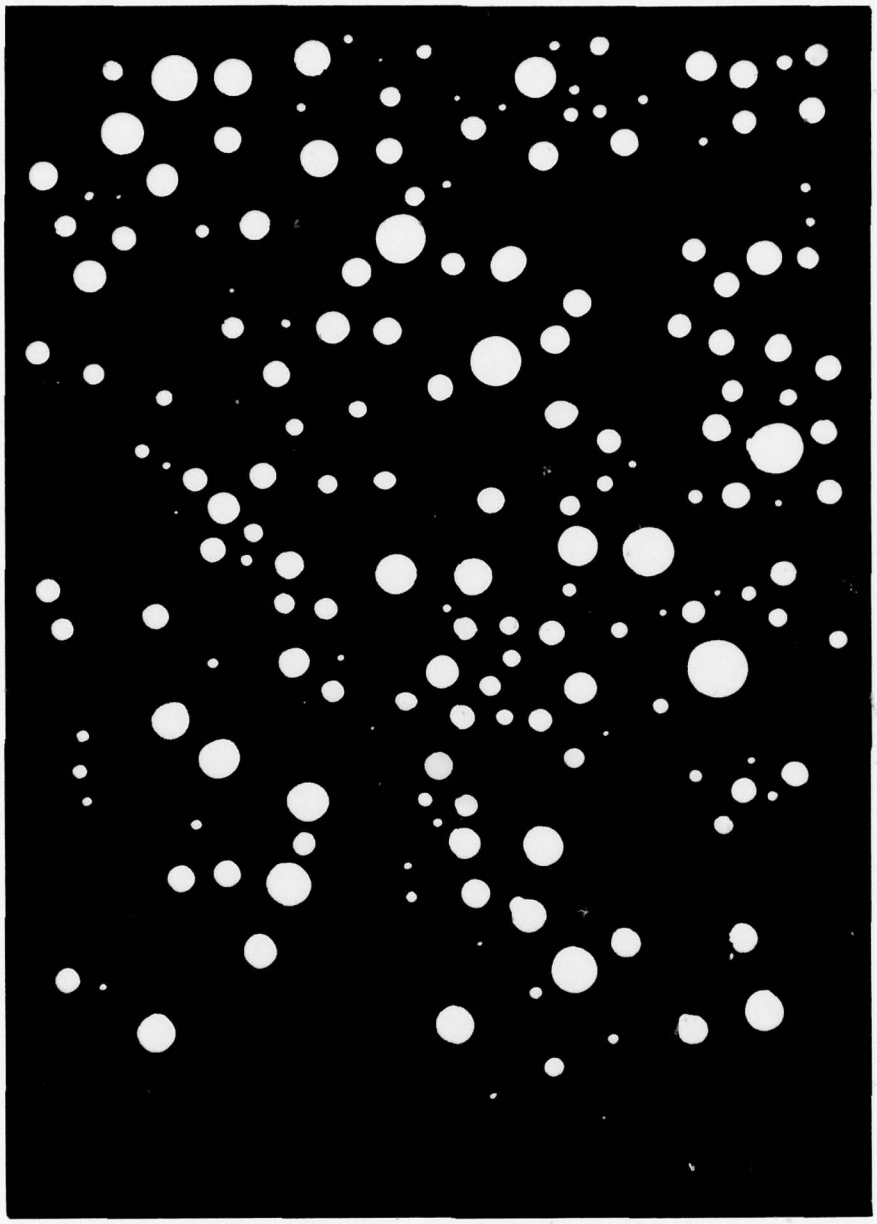

Figure 6-5 *Typical Magnified Photograph of Water Droplets on Greased-Slide (Relatively Large Diameters)*

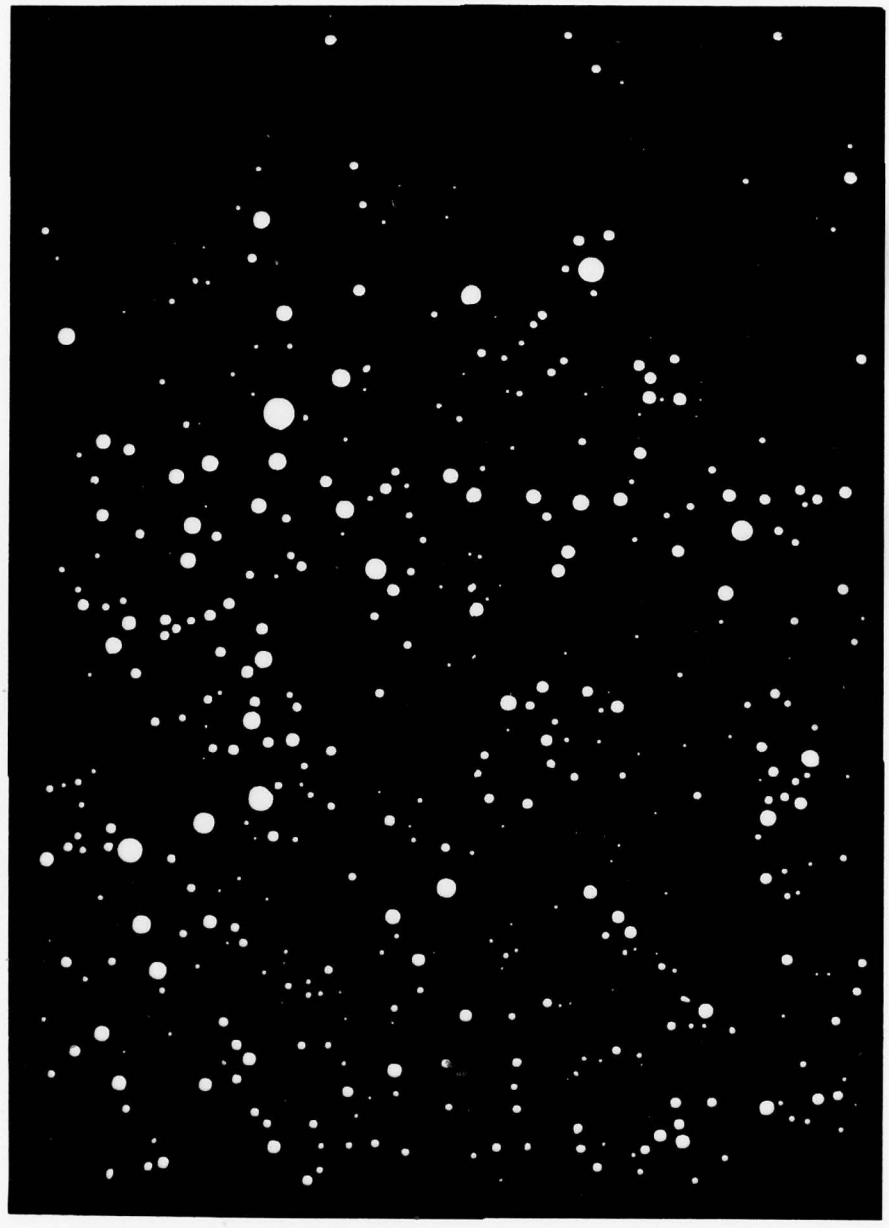

Figure 6-6 *Typical Magnified Photograph of Water Droplets on Greased-Slide (Relatively Small Diameters)*

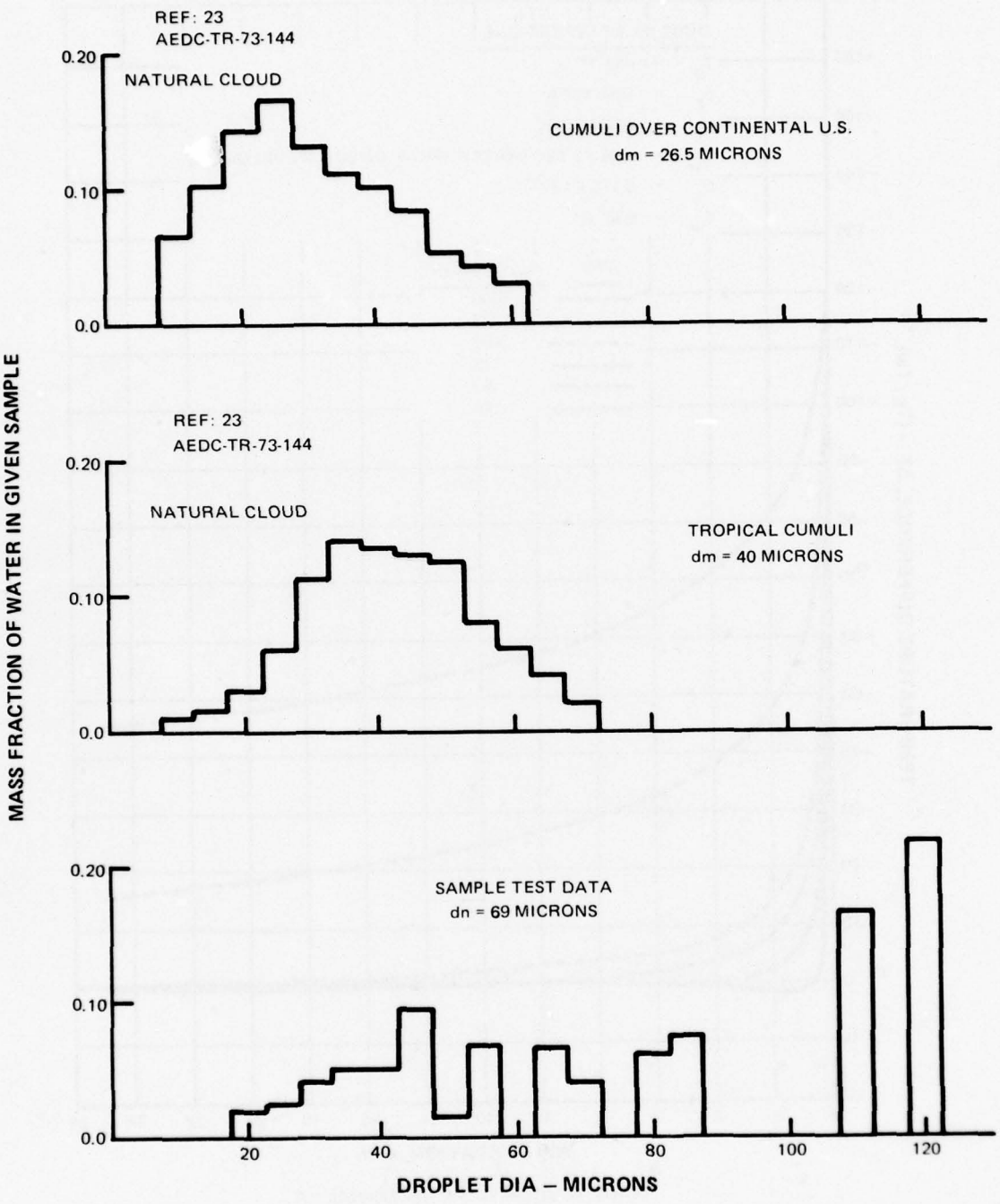

Figure 6-7 Droplet Distribution Comparison of Natural Clouds and a Sample Spray

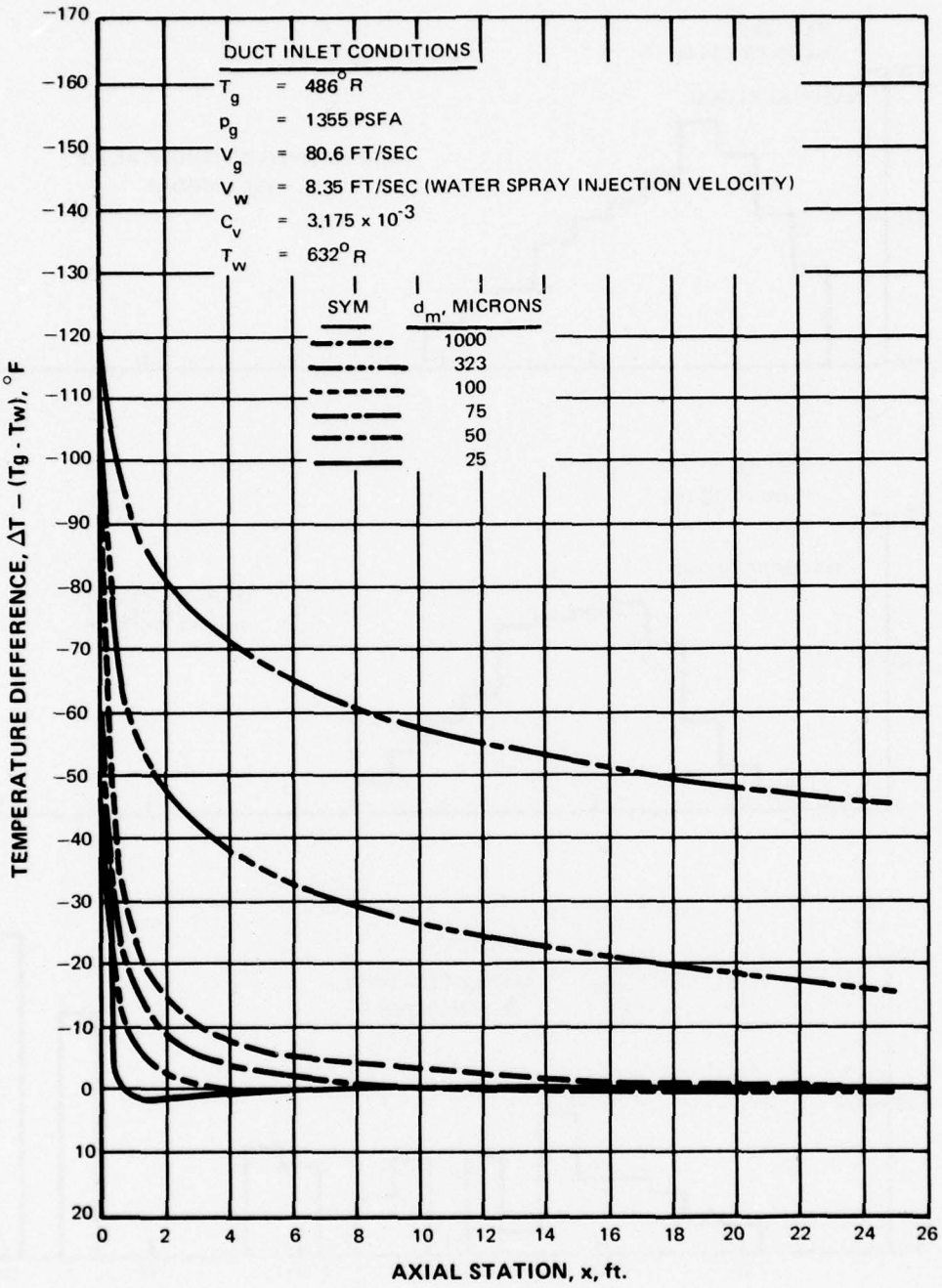

(FROM AEDC-TR-73-144, REFERENCE 23)

Figure 6-8 *Temperature Difference Between Gas and Water Droplets Versus Axial Location in a Ducted Simulation: Effect of Droplet Size*

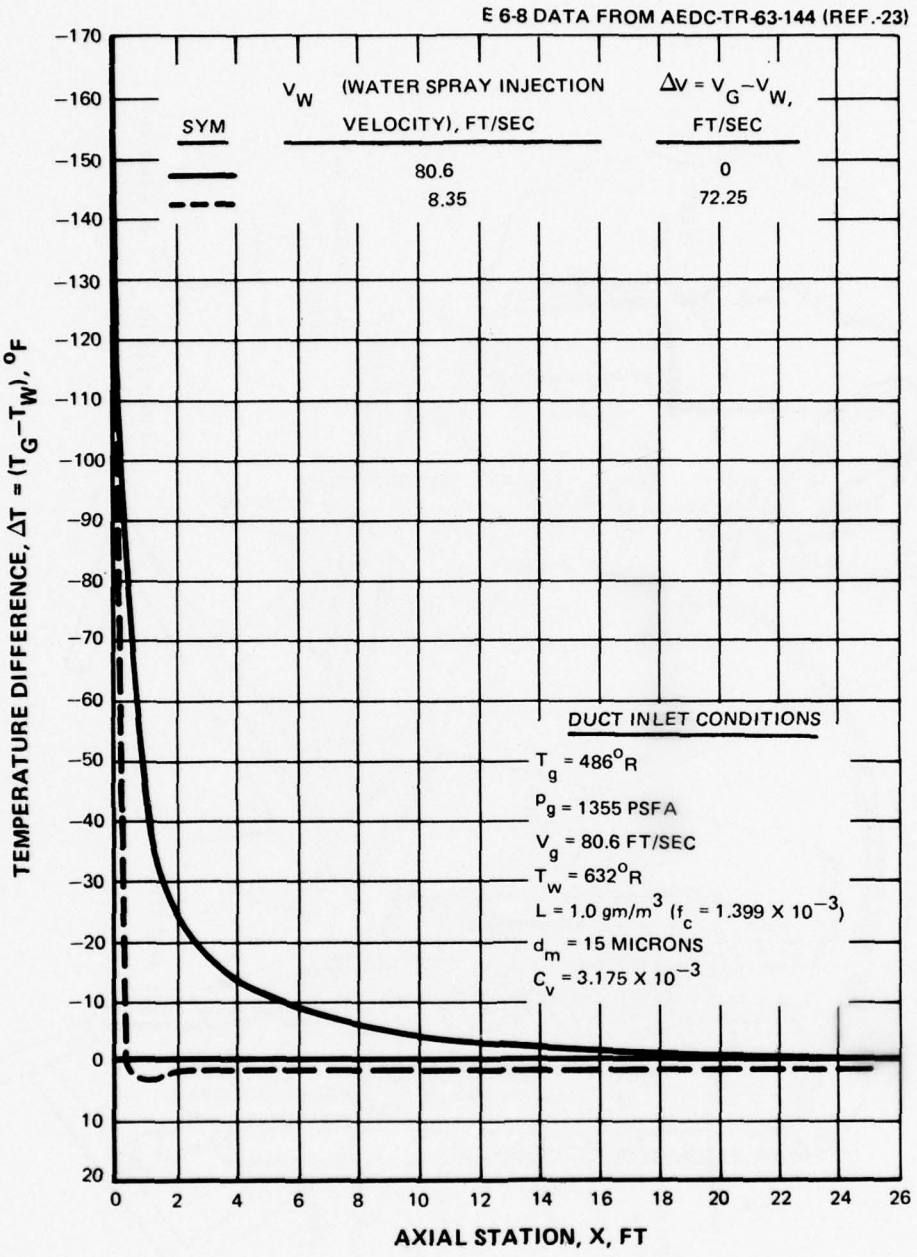

Figure 6-9 *Temperature Difference Between Gas and Water Droplets Versus Axial Location in a Ducted Simulation: Effect of Initial Velocity Difference Between Phases*

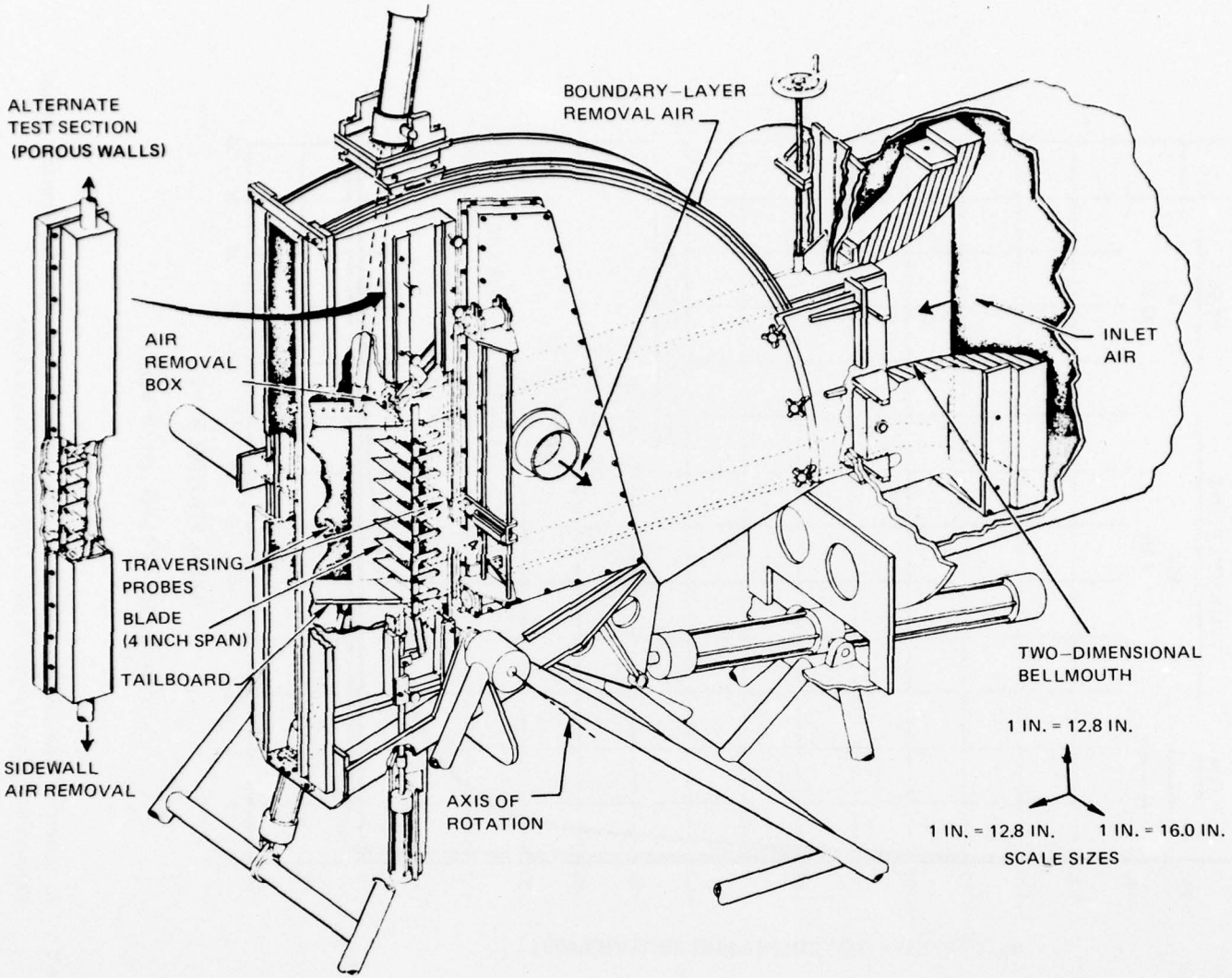

Figure 6-10 UTRC Variable Geometry High Speed Cascade Tunnel

(UNITED TECHNOLOGIES RESEARCH FACILITY)

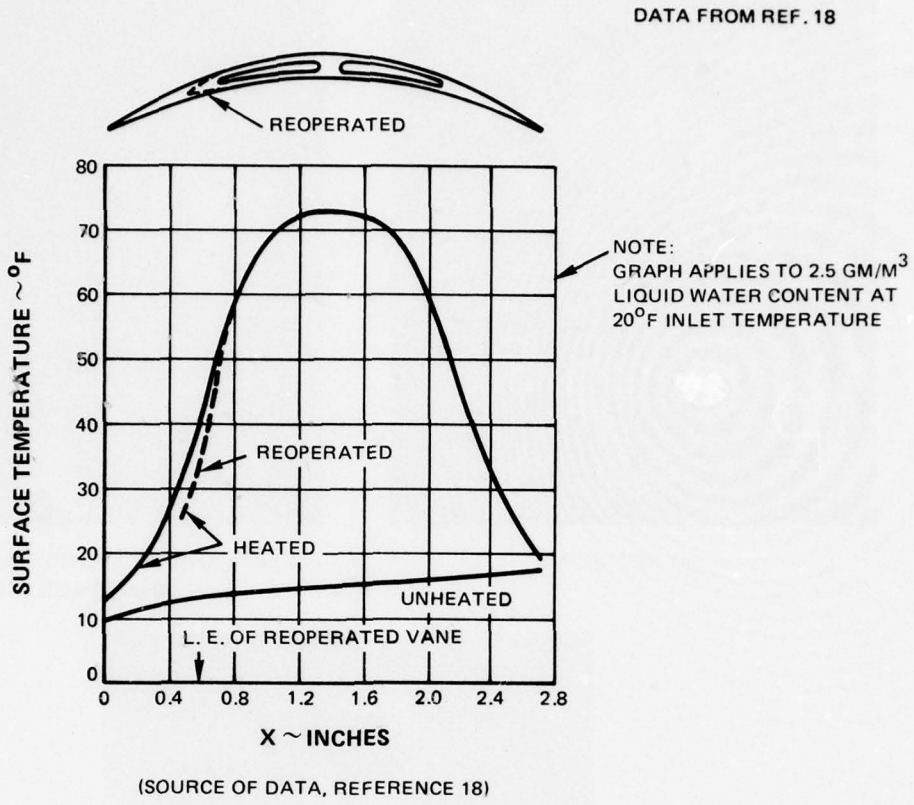

Figure 6-11 Predicted Mid-Span Temperature Distribution for a Thin Stator

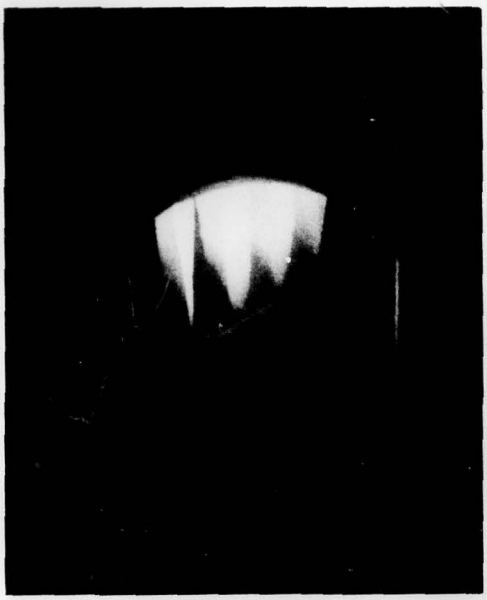

NO ANTI-ICING

HOT AIR ANTI-ICING, ONE PERCENT
9TH STAGE AIR

CUT BACK VANE, ONE PERCENT 9TH STAGE AIR

FIRST STATOR AFTER 100 SECONDS EXPOSURE TO SIMULATED 1800 N_1 AT 20° F INLET AIR TEMPERATURE AND 2.5 GM/M^3 LWC. (FROM REF. 18)

Figure 6-12 Photographs of Ice Buildup on Stator During Cascade Test

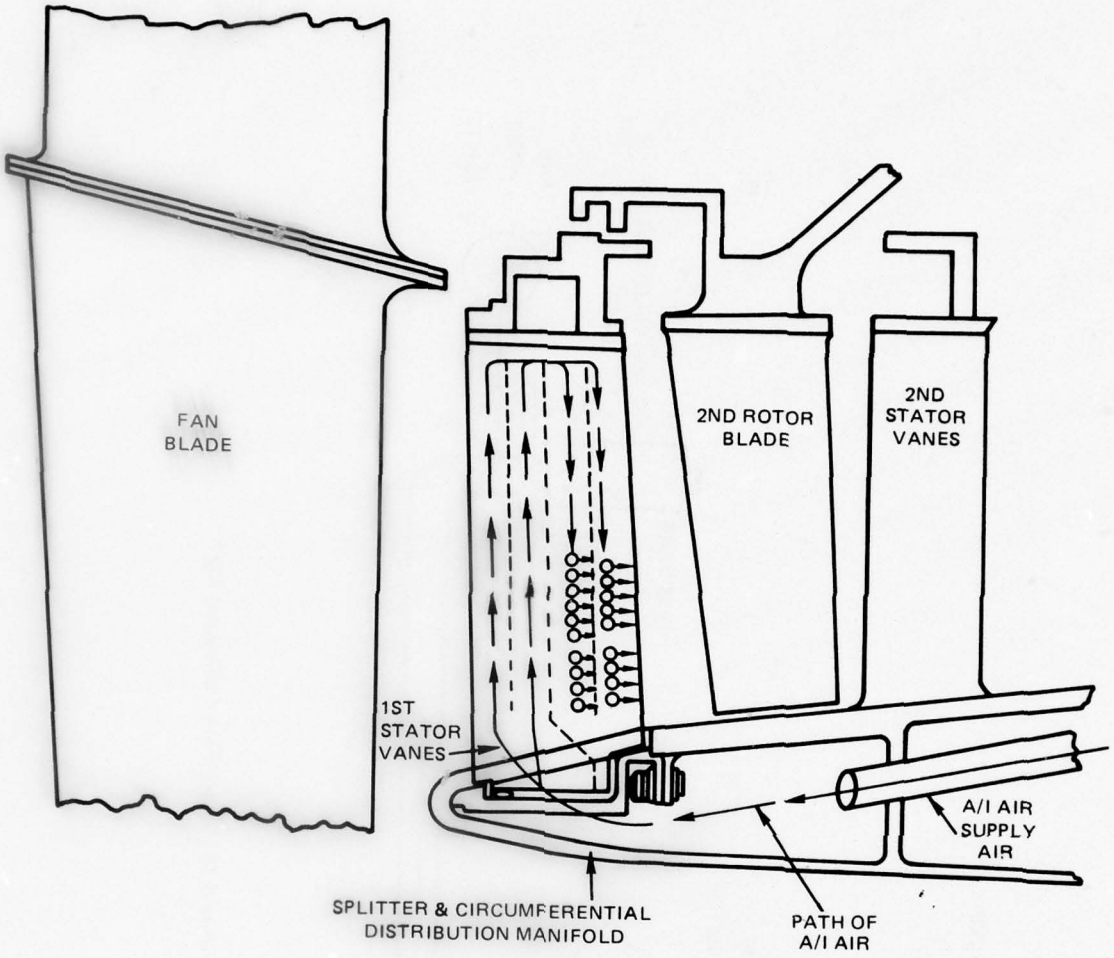

Figure 6-13 Schematic of Anti-Iced 1st Stator

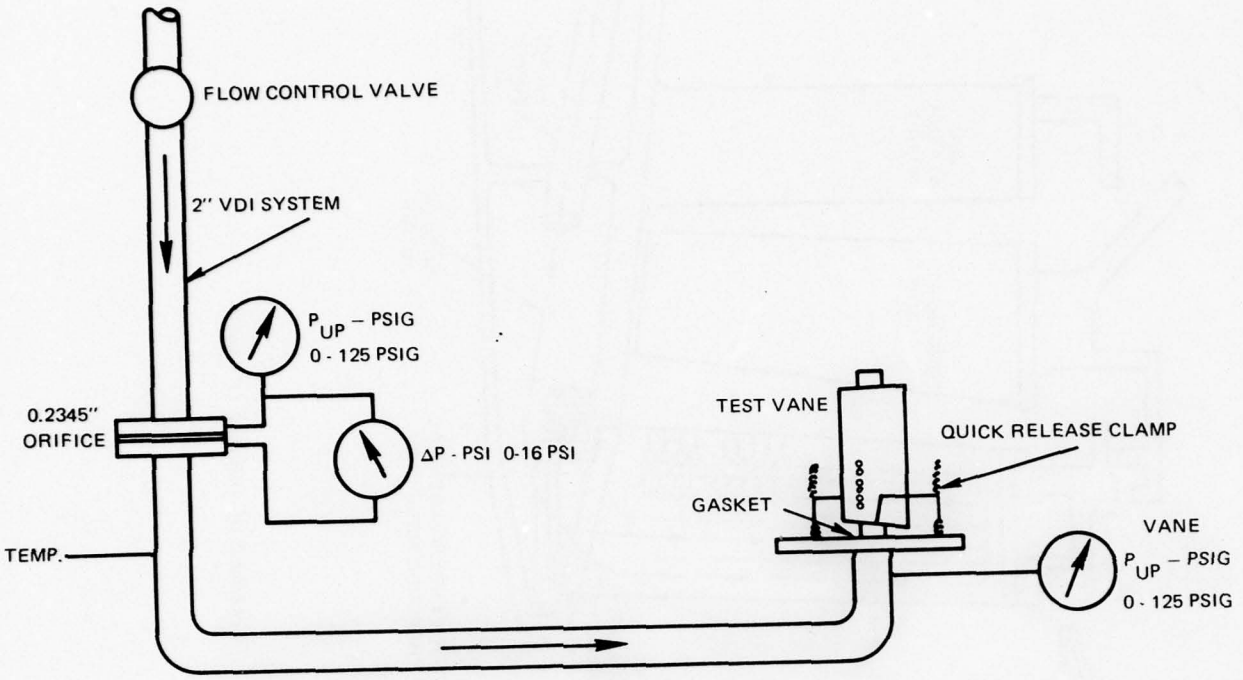

Figure 6-14 Vane Flow Calibration Rig

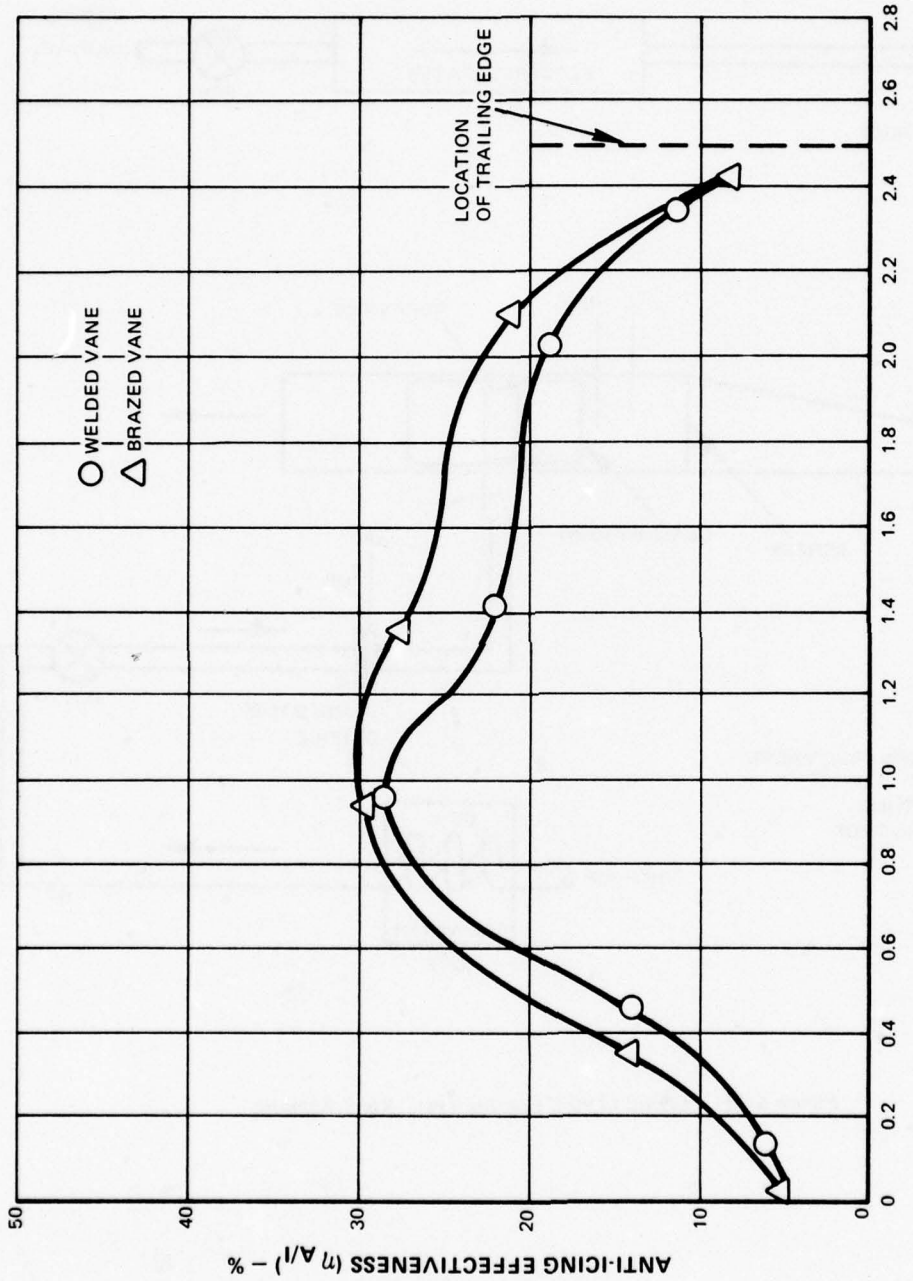

Figure 6-15 Relative Anti-Icing Effectiveness of Mid-Span Vane Section

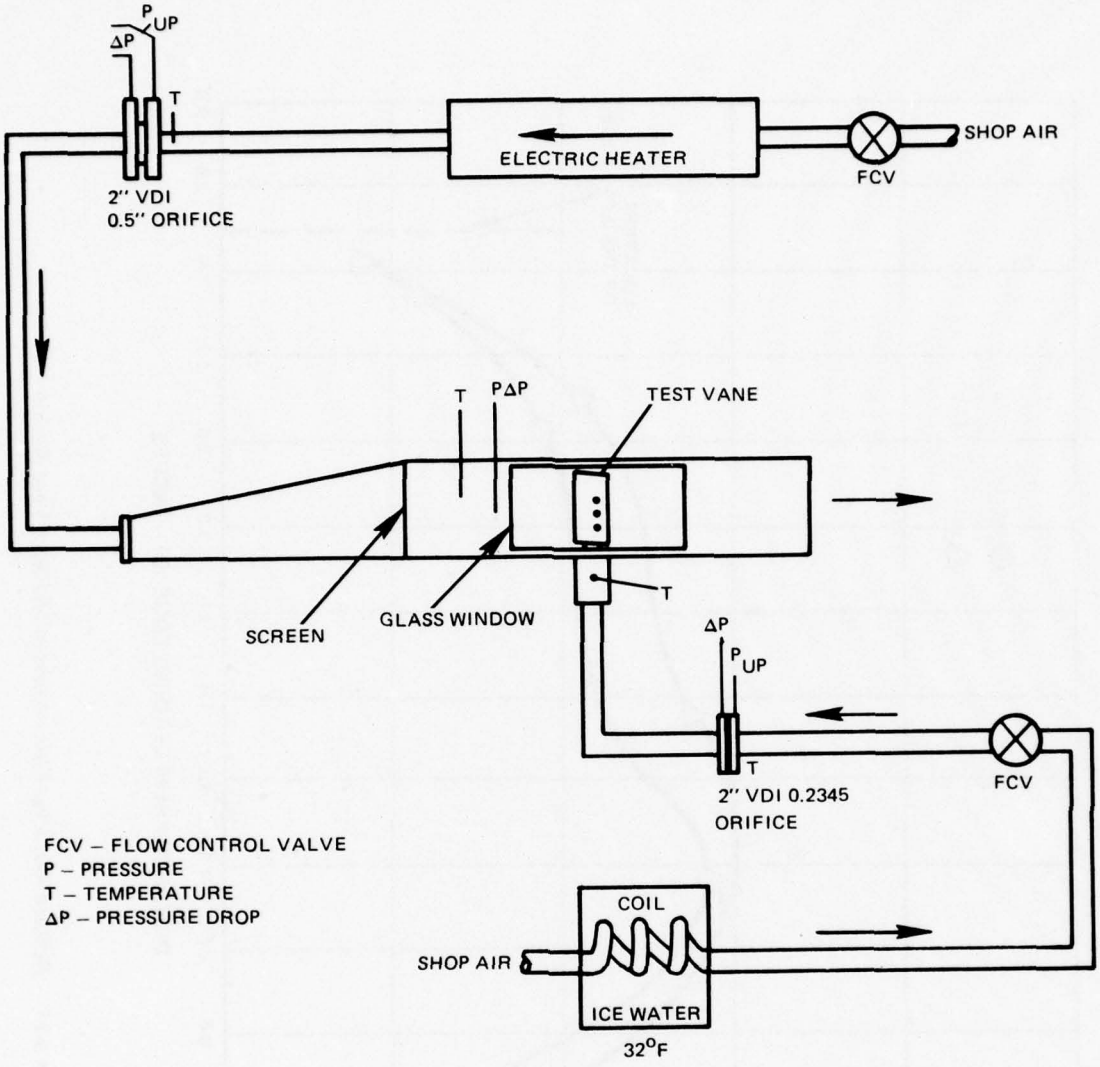

Figure 6-16 Liquid Crystal Coating Test: Rig Schematic

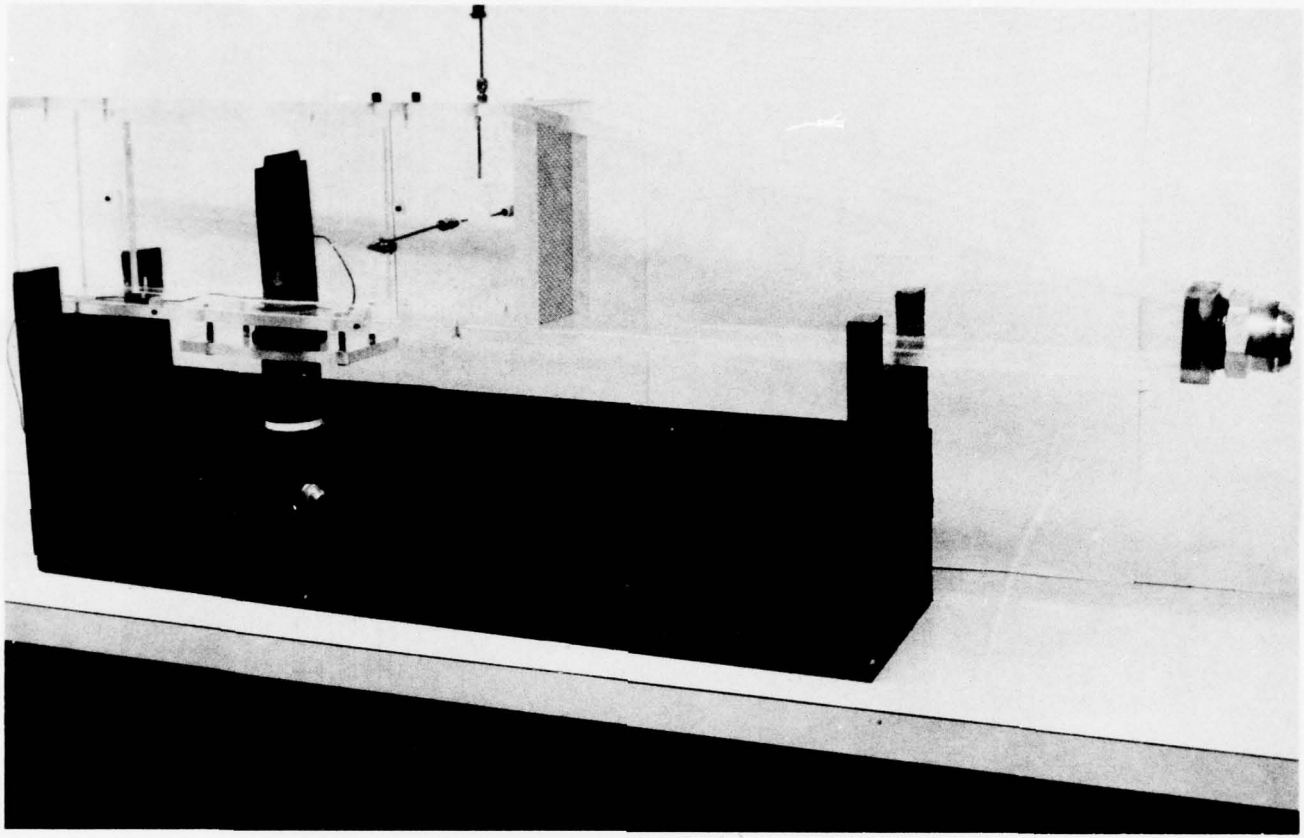

Figure 6-17 Photograph of Air Flow Rig for Liquid Crystal Test

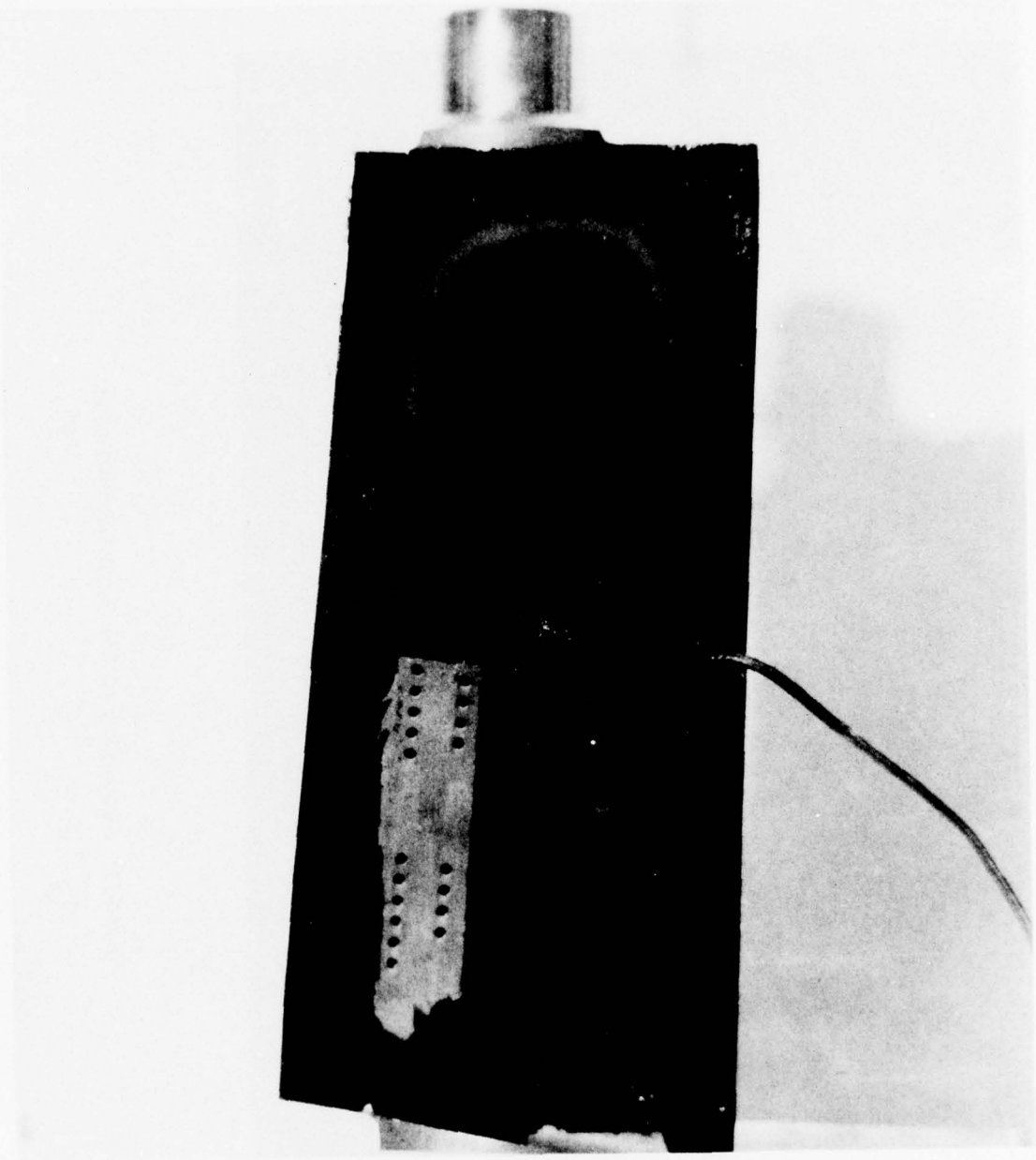

Figure 6-18 Photograph of Isotherm Zones in a Liquid Crystal Test: Anti-Iced Stator

NOMENCLATURE

Symbol		Quantity	Dimensions
a, b	=	locations on airfoil surface as shown in Figure 3-18	----------
b	=	dimension shown on Figure 5-7	length
A	=	area	$(\text{length})^2$
A_1, A_E, A_R	=	areas defined in Figure 3-3	$(\text{length})^2$
A_{FLOW}	=	flow area for an internal passage	$(\text{length})^2$
A_i	=	inlet projected area	$(\text{length})^2$
A_o, A_O	=	free stream tube area	$(\text{length})^2$
A'_{oI}, A'_{oII}, A'_{oIII}	=	inlet stream tube areas defined on Figure 3-3	$(\text{length})^2$
A'_{ox}, A'_{Ox}	=	denotes, whichever is appropriate of A'_{oI}, A'_{oII}, A'_{III}	$(\text{length})^2$
C_D	=	discharge coefficient for entire anti-icing flow system	dimensionless
C_p, $C_{p,a}$	=	specific heat of air at constant pressure	energy/(mass x temp)
$C_{p\ ice}$	=	specific heat of ice at constant pressure	energy/(mass x temp)
$C_{p\ w}$	=	specific heat of water at constant pressure	energy/(mass x temp)
C_t	=	total concentration factor (also called inlet catch efficiency and water catch efficiency)	dimensionless
C_{te}	=	water catch efficiency of core engine (i. e. inside splitter duct)	dimensionless
D	=	diameter (2 x LER) of leading edge of an airfoil; or the diameter of an equivalent sphere of the foremost section of a nose cap	length

NOMENCLATURE (Cont'd)

Symbol		Quantity	Dimensions
D_e	=	equivalent diameter of internal flow passage (also known as hydraulic diameter	length
da_o	=	differential stream tube area shown in Figure 3-5a	$(\text{length})^2$
dA	=	differential of A	$(\text{length})^2$
d_m, or dm	=	mean effective droplet diameter defined such that one-half the volume water in the sample is contained in droplets of diameters smaller than d_m while the other half volume is of droplets larger than d_m	length
dr	=	differential of r	length
ds, or dS	=	differential of s, or S	length
$d\theta$	=	differential of θ	radians
E_m	=	overall impingement efficiency on a solid object	dimensionless
	E_m =	$\dfrac{\text{actual total water impingement on an object}}{\text{water contained in the approaching stream tube of object projected area}}$	
FP	=	flow parameter defined in Figure 4-11	$\dfrac{\text{mass}\sqrt{\text{temp abs}}}{\text{time x force}}$
g_c	=	conversion factor	$\dfrac{(\text{length})(\text{mass})}{(\text{force})(\text{time})^2}$
h, h_θ, h_ℓ	=	local heat transfer coefficient	energy/(time x length^2 x temp)
H	=	projected blockage height of an airfoil	length
i	=	enthalpy	energy/mass

NOMENCLATURE (Cont'd)

Symbol		Quantity	Dimensions
IGV	=	inlet guide vane	– – – – – – – – – –
I	=	(N_{st}) modified/N_{st}	dimensionless
J	=	conversion factor (mechanical equivalent of heat)	– – – – – – – – – –
k	=	air thermal conductivity	energy/(time x length x temp)
k_{sk}	=	airfoil skin thermal conductivity	energy/(time x length x temp)
K	=	inertia parameter defined by Equ 3-10	dimensionless
K_o	=	modified inertia parameter defined by Equ 3-13	dimensionless
LWC	=	liquid water content	mass H_2O/volume of air
L, L_c	=	airfoil chord length or object dimension	length
LER	=	leading edge radius of airfoil shown in Figure 3-19	length
L_s	=	latent heat of vaporization	energy/mass
m''	=	mass evaporation rate per unit area	mass/(time x area)
M_n	=	Mach number	dimensionless
M_a	=	air molecular weight	mass/mole
M_v	=	vapor molecular weight	mass/mole
$\dot{m}_{H_2O}$, $\dot{M}_{H_2O}$	=	water droplet flow rate	mass/time
n	=	fraction of impinging water W″ that freezes on a surface at 32°F	dimensionless
N_1	=	fan rotational speed	RPM or $\% N_{1_{max}}$

NOMENCLATURE (Cont'd)

Symbol		Quantity	Dimensions
$N_{Nu,D}$	=	Nusselt number defined by Equ 3-26	dimensionless
$N_{Nu,S}$	=	Nusselt number defined by Equ 3-29	dimensionless
$N_{Nu,De}$	=	Nusselt number defined by Equ 3-30	dimensionless
N_{pr}	=	Prandtl number	dimensionless
$N_{Re,D}$	=	Reynold's number defined by Equ 3-26	dimensionless
$N_{Re,De}$	=	Reynold's number defined by Equ 3-30	dimensionless
$N_{Re,S}$	=	Reynold's number defined by Equ 3-29	dimensionless
N_{st}	=	Stanton number for heat transfer	dimensionless
(N_{st}) MODIFIED	=	modified Stanton number for mass transfer	dimensionless
P_v	=	vapor pressure (satured)	force/area
$P_{v,s}$	=	absolute vapor pressure evaluated at surface temperature	force/area
$P_{v,\ell}$	=	absolute local vapor pressure evaluated at outer edge of boundary layer	force/area
P_ℓ	=	local absolute static air pressure at outer edge of boundary layer	force/area
P_{BLEED}, P_{SOURCE}	=	compressor gaspath air pressure at the bleed location	force/area
P_T	=	total pressure	force/area
P_{SINK}	=	discharge pressure of anti-icing system	force/area
$P_{COMP\ IN}$, $P_{COMP\ OUT}$	=	entrance and exit gaspath pressures for the compressor module	force/area
P_{RAM}	=	air total absolute pressure at engine inlet	force/area

NOMENCLATURE (Cont'd)

Symbol		Quantity	Dimensions
q''	=	heat transfer rate per unit area	energy/(area x time)
Q''_{AVAIL}	=	heat available from anti-icing air	energy/(area x time)
R, R_{BASE}	=	maximum radius or semi-minor axis of nose cap	length
R	=	gas constant for air	$(\frac{\text{length x force}}{\text{mass x temperature}})$
r	=	local radius of axi-symmetric surface of revolution	length
$Re_{o,d}$	=	approach free-stream Reynold's number for droplet	dimensionless
r_{MAX}, r_{max}	=	radius at the location of S_{max}	length
$r_{o,\,MAX}$, $r_{o,\,max}$	=	stream line dimension shown in Figure 3-5a	length
s,S	=	arc length distance along airfoil from leading edge	length
s_u, S_u, S_U s_ℓ, S_ℓ, S_L	=	upper and lower impingement limits on 2 dimensionlal objects	length
$\lvert S_u - S_\ell \rvert$	=	denotes absolute value of total arc length dimension from S_u to S_ℓ	length
S_{MAX}, S_{max}	=	impingement limit for axi-symmetric surface of revolution	length
t	=	surface temperature; static air temperature	degrees
T	=	absolute static air temperature	degrees absolute
t_T, T_T	=	total air temperature	degrees, degrees absolute
t_{DATUM}, t_{datum}	=	temperature defined by Equ 3-34	degrees

NOMENCLATURE (Cont'd)

Symbol		Quantity	Dimensions
T_{BLEED}, T_{SOURCE}	=	compressor gaspath air temperature at the bleed location	degrees absolute
T_{RAM}	=	air total temperature at engine inlet	degrees absolute
T_{SINK}	=	temperature of discharge location for anti-icing system	degrees absolute
$T_{COMP\ IN}$ $T_{COMP\ OUT}$	=	entrance and exit gaspath temperatures for compressor module	degrees absolute
V	=	velocity	length/time
V_i	=	inlet air velocity	length/time
V_∞	=	free stream flight velocity	length/time
V_o	=	denotes the uniform approach velocity upstream of any object	length/time
$\dot{W}, \dot{w}, \dot{\omega}$	=	air flow rate	mass/time
$\dot{W}_i, \dot{w}_i, \dot{\omega}_i$	=	total engine air flow rate crossing basic inlet plane ($\dot{w}_i = \dot{w}_e + \dot{w}_f$)	mass/time
$\dot{W}_E, \dot{We}, \dot{\omega}_e, \dot{w}_e$	=	core engine air flow rate inside splitter duct	mass/time
$\dot{W}_F, \dot{Wf}, \dot{\omega}_f, \dot{w}_f$	=	fan duct air flow rate	mass/time
w'	=	local water film flow rate per unit length of the invariant dimension	mass/(time x length)
W	=	total water impingement rate on a solid object	mass/time
W'	=	total water impingement rate per unit length of the invariant dimension (for 2-D objects $W' = W$ per unit length of span; for surface of revolution $W' = W$ per unit circumferential length)	mass/(time x length)

NOMENCLATURE (Cont'd)

Symbol		Quantity	Dimensions
W''	=	average of total water impingement wetted surface area	mass/(time x area)
W_ℓ, W'_ℓ, W''_ℓ	=	local values of W, W′, W″ (i.e. values for a differential surface area)	mass/(time x area)
y_o, $y_{o,u}$, $y_{o,\ell}$	=	streamline dimensions defined on Figures 3-4, 3-5	length
y_{SK}	=	airfoil skin thickness shown on Figure 3-20	length
Z	=	denotes the invariant dimension of a 2-dimensional object	length
β	=	local impingement efficiency on a differential area of a solid object; as shown in Figure 3-5	dimensionless
	β =	$\frac{\text{actual impingement rate on differential area}}{\text{maximum possible impingement rate on differential area}}$	
$\in$	=	surface wetness fraction	dimensionless
γ	=	ratio of specific heats; equal to C_p/C_v	dimensionless
η_r	=	local recovery factor	dimensionless
θ	=	measure of an angle	radians
λ/λ_s	=	dimensionless ratio of true droplet range to Stokes Law range	dimensionless
μ	=	absolute viscosity of air	mass/(time x length)
ρ	=	air density	mass/volume
ρ_o	=	ambient air density	mass/volume

NOMENCLATURE (Cont'd)

Symbol		Quantity	Dimensions
ρ_{ICE}	=	ice density	mass/volume
ρ_{H_2O}	=	liquid water droplet density	mass/volume

SUBSCRIPTS

1 = denotes inlet plane of basic engine inlet

2 = denotes inlet region immediately upstream of inlet guide vane or 1st fan blade

3 = denotes inlet region immediately behind 1st fan blade

A/I = anti-icing air

D. P. = denotes the value for the design point conditions

F. C. = denotes the value for a particular Flight Cycle condition

ι = denotes the inlet plane of basic engine inlet

ISEN = denotes a value characteristic of isentropic flow

0 = denotes uniform flow field approaching any object

∞ = denotes free stream ambient atmosphere

ℓ = denotes a local value

S = denotes evaluation at the surface

REFERENCES

1. Bowden, D. T., Gensemer, A. E., and Speen, C. A.: Engineering Summary of Airframe Icing Technical Data. Federal Aviation Agency, FAA Technical Report ADS-4, 1964.

2. Department of Transportation, Federal Aviation Administration: Federal Aviation Regulations (FAR). October 31, 1974.

3. FAA Advisory Circular AC No. 20-73: Aircraft Ice Protection. April 21, 1971.

4. Gelder, T. F.: Droplet Impingement and Ingestion by Supersonic Nose Inlet in Subsonic Tunnel Conditions. NACA TN 4208, 1958.

5. Brun, R. J: Cloud-Droplet Ingestion in Engine Inlets with Inlet Velocity Ratios of 1.0 and 0.7. NACA Report 1317 (supercedes NASA TN 3593), 1956.

6. Jones, A. R. and Lewis, Wm.: Recommended Values of Meterological Factors to be Considered in The Design of Aircraft Ice Prevention Equipment. NACA TN 1855, 1949.

7. Hacker, P. T. and Dorsch, R. G.: A Summary of Meteorological Conditions Associated with Aircraft Icing and a Proposed Method of Selecting Design Criterions for Ice Protection Equipment. NACA TN 2569, 1951.

8. Bergrun, N. R. and Lewis, Wm.: A Probability Analysis of The Meteorological Factors Conducive to Aircraft Icing in The United States. NACA TN 2738, 1952.

9. VanDriest, E. R.: The Problem of Aerodynamic Heating. North American Aviation Inc., 1956.

10. United States Department of Defense: Military Specification MIL-E-5007D. October 15, 1973.

11. Civil Aviation Authority: British Civil Airworthiness Requirements. Paper No. 625, Section C; August 18, 1975.

12. Lewis, J. P. and Ruggeri, R. S.: Experimental Droplet Impingement on Four Bodies of Revolution. NACA TN 4092, 1957.

13. Sogin, Harold H.: A Design Manual for Thermal Anti-Icing Systems. Wright Air Development Center. WADC Technical Report 54-313, December 1954.

14. Gray, V. H.: Simple Graphical Solution of Heat Transfer and Evaporation from Surface Heated to Prevent Icing. NACA TN 2799, 1952.

15. Hardy, J. K.: Kinetic Temperature of Wet Surfaces, A Method of Calculating The Amount of Alcohol Required to Prevent Ice, and The Derivation of The Psychrometric Equation. NACA ARR #5G13, 1945.

REFERENCES (Cont'd.)

16. Messinger, B. L.: Equilibrium Temperature of an Unheated Surface as a Function of Airspeed. Journal of Aeronautical Sciences, Vol. 20, No. 1, January 1953.

17. Brun, T. L., Gallagher, H. M., and Vogt, D. E.: Impingement of Water Droplets on NACA 651-208 and 651-212 Airfoils at 4° Angle of Attack. NACA TN 2952, 1953.

18. Striebel, E. E.: Ice Protection for Turbine Engines. FAA Report of Symposium on Aircraft Ice Protection, April 28-30, 1969.

19. Stallabrass, J. R. and Price, R. D.: On The Adhesion of Ice to Various Materials. National Research Laboratories, Ottawa, Canada; Aeronautical Report LR-350, July 1962.

20. Grabe, W. and Vanslyke, G. K.: Icing Tests on The JT15D Turbofan Engine. Proceedings of The Tenth National Conference on Environmental Effects on Aircraft and Propulsion Systems, Sponsored by Naval Air Propulsion Tests Center; May 18-20, 1971.

21. Gall, E. S. and Floyd, F. X.: Icing Test Capability of The Engine Test Facility Propulsion Development Test Cell (J-1). Arnold Engineering Development Center, Report AEDC-TR-71-94 (AD729205), August 1971.

22. Lazelle, B. D.: Conditions to Prevent Freeze-Out During Atomization of Water Sprays for Icing Cloud Simulation. Reference DEV/TN/262/778, D. Napier and Son Limited, August 1958.

23. Willbanks, C. E. and Shulz, R. J.: Analytical Study of Icing Simulation for Turbine Engines in Altitude Test Cells. Arnold Engineering Development Center, Report AEDC-TR-73-144 (AD770069), November 1973.

24. Lowel, H. H.: Maximum Evaporation Rates of Water Droplets Approaching Obstacles in The Atmosphere. NACA TN 3024, 1953.

25. Sikorsky Aircraft, Division of United Aircraft Corporation: Functional Cold Weather Test of The HSS-2 Helicopter, S/N 148035. Report No. SER-61523, October 1961.

26. Dostal, Captain George C.: Adverse Weather Testing of The CH-3C Helicopter. Aeronautical Systems Division, Air Force Systems Command, Wright-Patterson Air Force Base; Technical Report ASD-TR-64-92, April 1965.

27. Reilly, Captain Donald A.: Adverse Weather Tests of The HH-53C Helicopter. Aeronautical Systems Division, Air Force Systems Command, Wright-Patterson Air Force Base; Technical Report ASD-TR-70-51, December 1970.

APPENDIX A

FEDERAL AVIATION REGULATIONS (REF 2)
APPENDIX C OF PART 25

(a) Continuous maximum icing. The maximum continuous intensity of atmospheric icing conditions (continuous maximum icing) is defined by the variables of the cloud liquid water content, the mean effective diameter of the cloud droplets, the ambient air temperature, and the interrelationship of these three variables as shown in Figure 1 of this Appendix. The limiting icing envelope in terms of altitude and temperature is given in Figure 2 of this Appendix. The inter-relationship of cloud liquid water content with drop diameter and altitude is determined from Figures 1 and 2. The cloud liquid water content for continuous maximum icing conditions of a horizontal extent, other than 17.4 nautical miles, is determined by the value of liquid water content of Figure 1, multiplied by the appropriate factor from Figure 3 of this Appendix.

(b) Intermittent maximum icing. The intermittent maximum intensity of atmospheric icing conditions (intermittent maximum icing) is defined by the variables of the cloud liquid water content, the mean effective diameter of the cloud droplets, the ambient air temperature, and the inter-relationship of these three variables, as shown in Figure 4 of this Appendix. The limiting icing envelope in terms of altitude and temperature is given in Figure 5 of this Appendix. The inter-relationship of cloud liquid water content with drop diameter and altitude is determined from Figures 4 and 5. The cloud liquid water content for intermittent maximum icing conditions of a horizontal extent, other than 2.6 nautical miles, is determined by the value of cloud liquid water content of Figure 4 multiplied by the appropriate factor in Figure 6 of this Appendix.

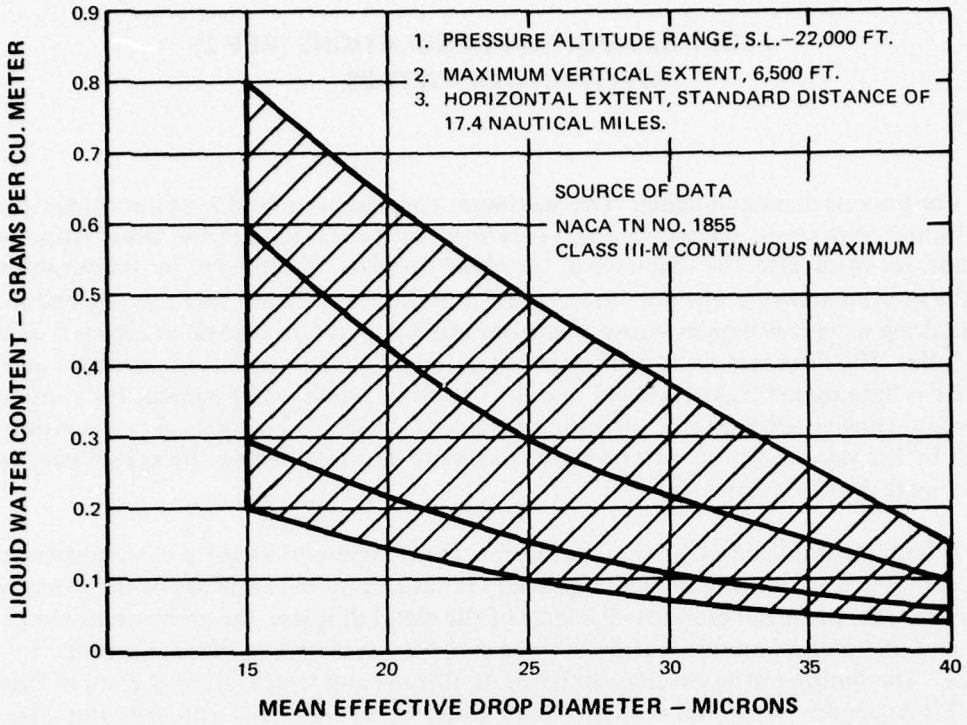

FIGURE A-1

CONTINUOUS MAXIMUM (STRATIFORM CLOUDS)
ATMOSPHERIC ICING CONDITIONS
LIQUID WATER CONTENT vs. MEAN EFFECTIVE DROP DIAMETER

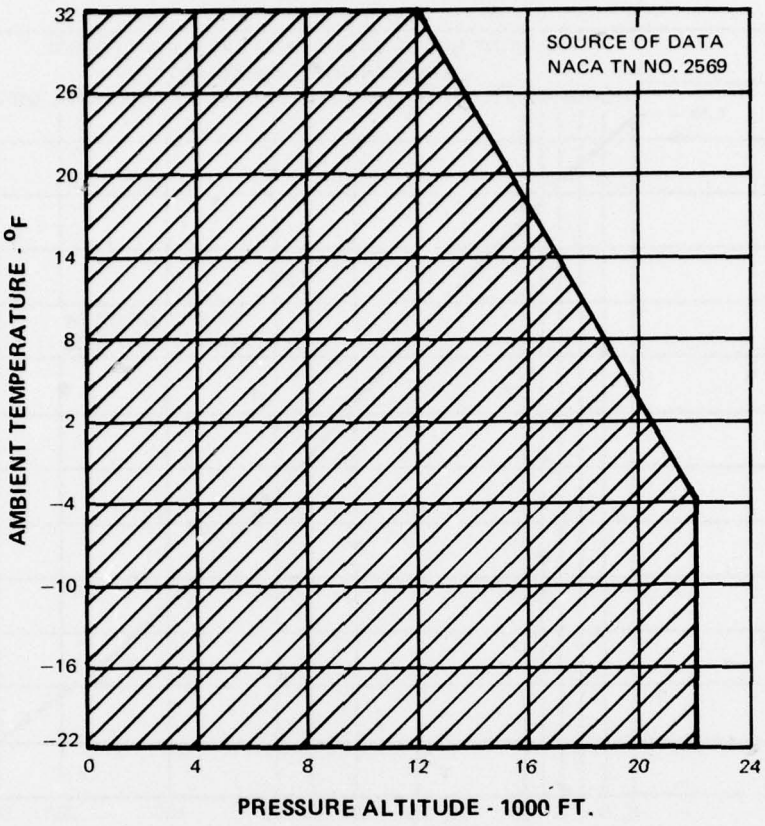

FIGURE A-2

CONTINUOUS MAXIMUM (STRATIFORM CLOUDS)
ATMOSPHERIC ICING CONDITIONS
AMBIENT TEMPERATURE VS. PRESSURE ALTITUDE

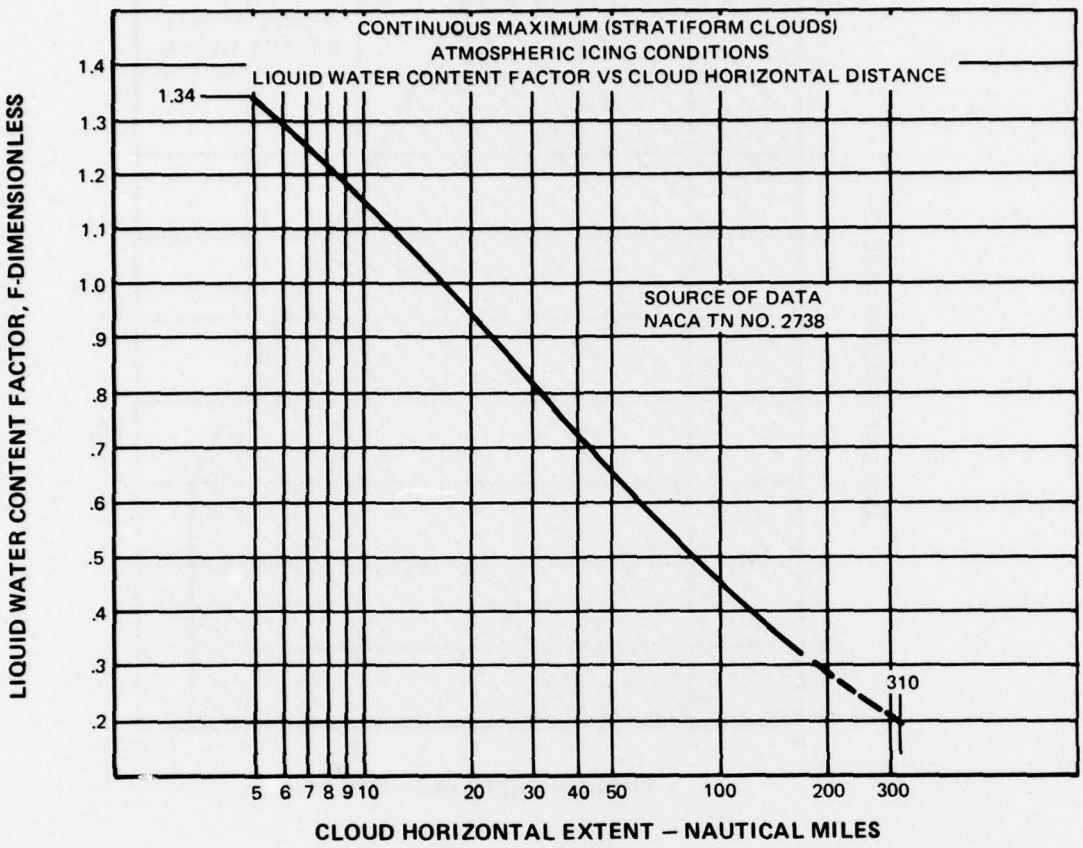
CONTINUOUS MAXIMUM (STRATIFORM CLOUDS)
ATMOSPHERIC ICING CONDITIONS
LIQUID WATER CONTENT FACTOR VS CLOUD HORIZONTAL DISTANCE
1.34
SOURCE OF DATA
NACA TN NO. 2738
310
LIQUID WATER CONTENT FACTOR, F-DIMENSIONLESS
1.4
1.3
1.2
1.1
1.0
.9
.8
.7
.6
.5
.4
.3
.2
5 6 7 8 9 10 20 30 40 50 100 200 300
CLOUD HORIZONTAL EXTENT – NAUTICAL MILES

FIGURE A-3

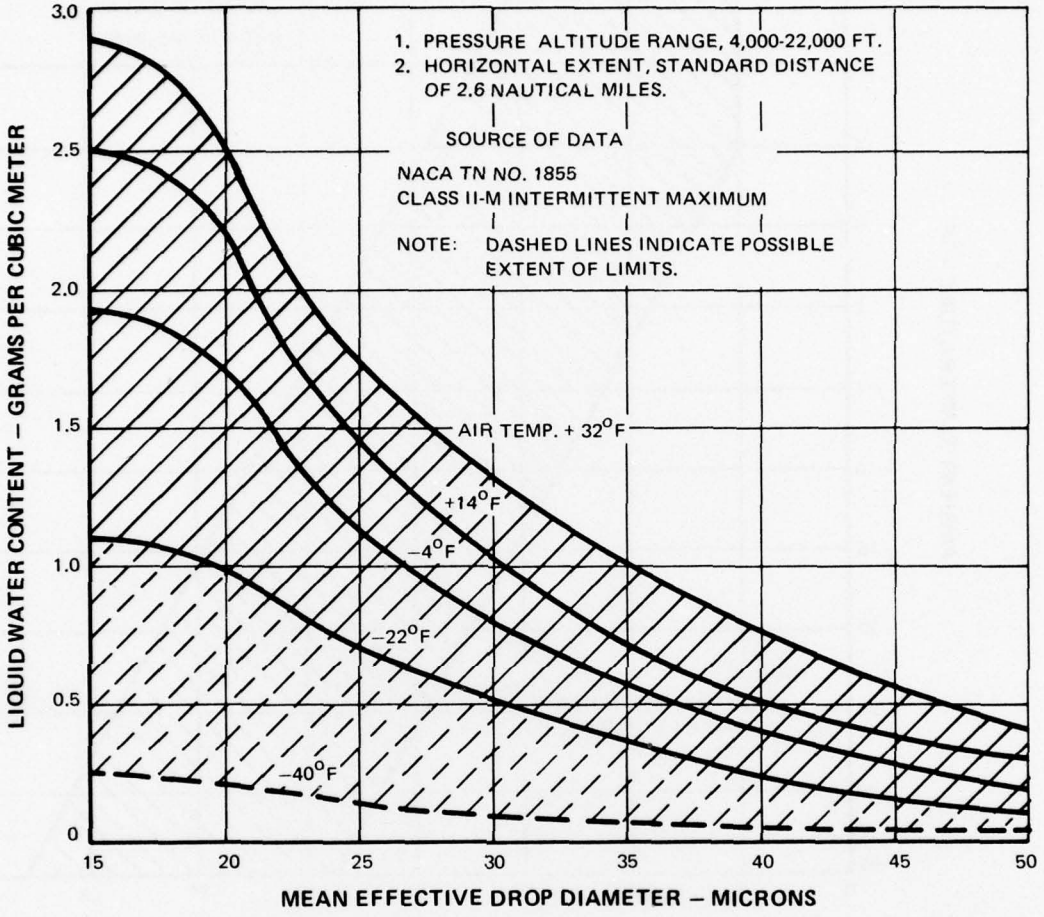

FIGURE A-4

INTERMITTENT MAXIMUM (CUMULIFORM CLOUDS)
ATMOSPHERIC ICING CONDITIONS
LIQUID WATER CONTENT VS. MEAN EFFECTIVE DROP DIAMETER

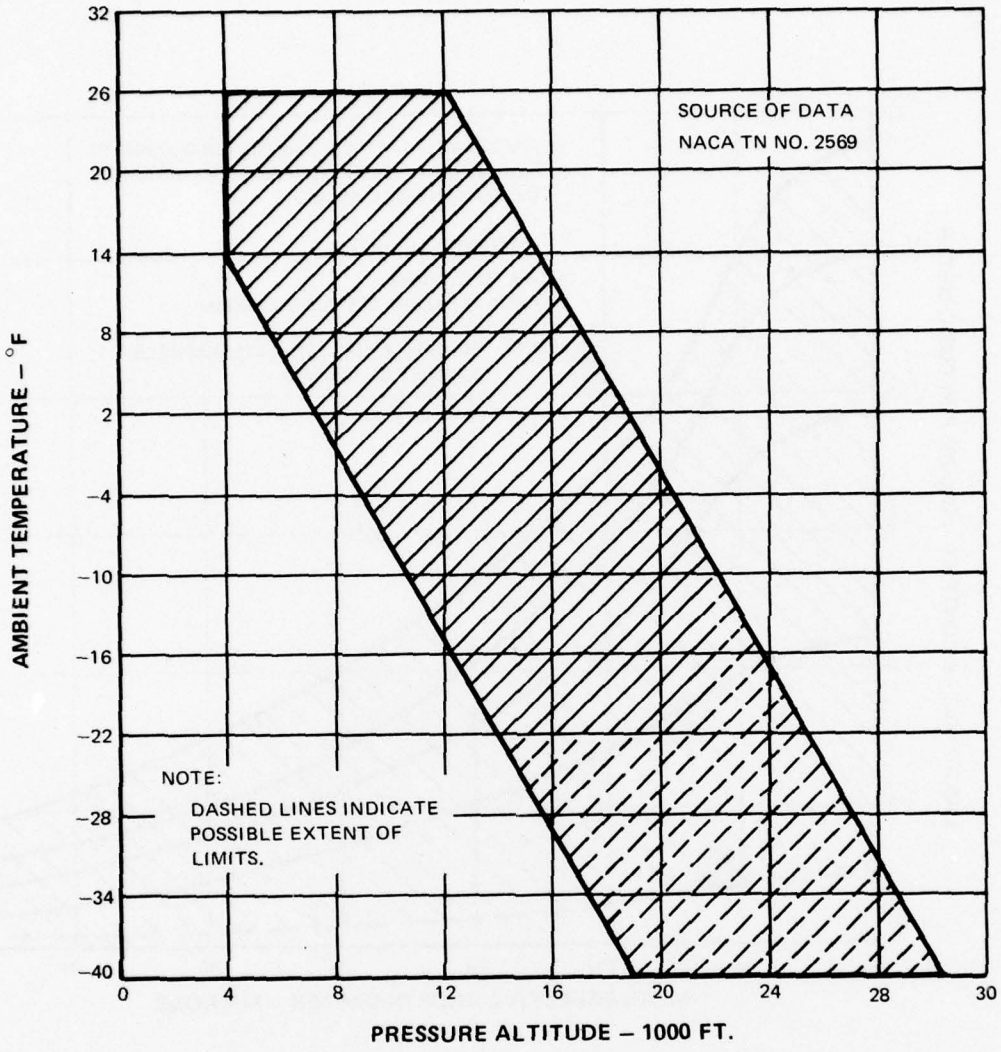

FIGURE A-5

INTERMITTENT MAXIMUM (CUMULIFORM CLOUDS)
ATMOSPHERIC ICING CONDITIONS
AMBIENT TEMPERATURE VS. PRESSURE ALTITUDE

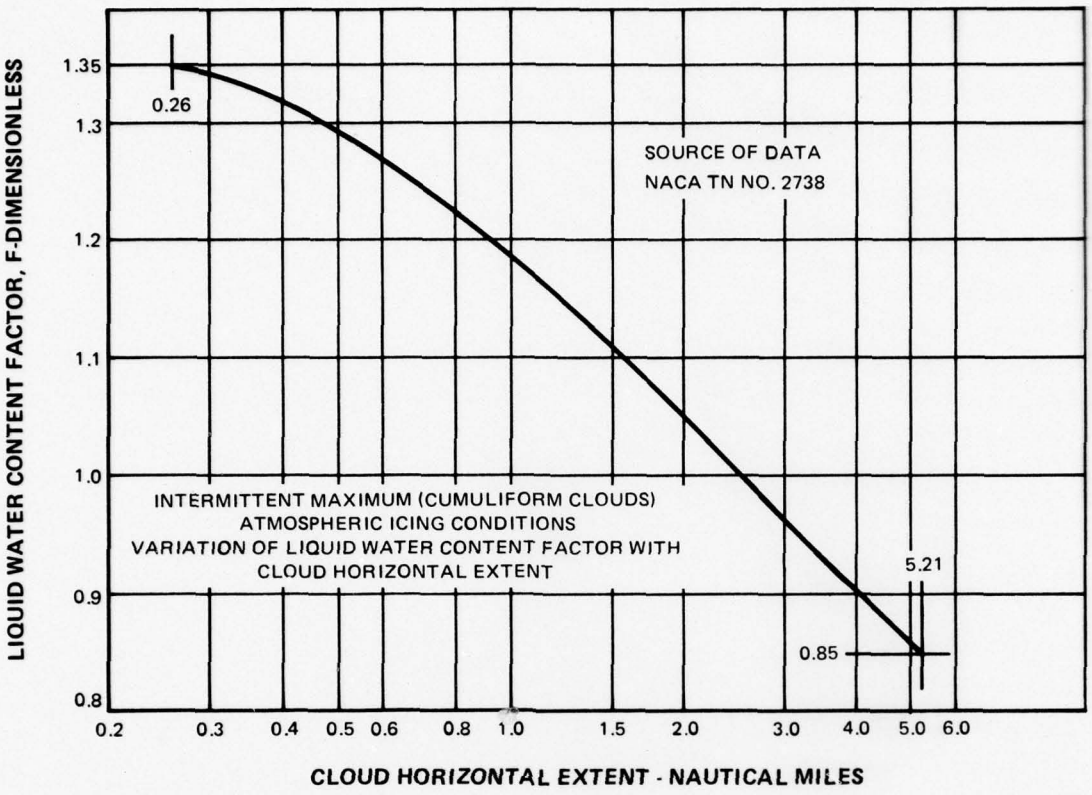
LIQUID WATER CONTENT FACTOR, F-DIMENSIONLESS
1.35
1.3
1.2
1.1
1.0
0.9
0.8
0.26
SOURCE OF DATA
NACA TN NO. 2738
INTERMITTENT MAXIMUM (CUMULIFORM CLOUDS)
ATMOSPHERIC ICING CONDITIONS
VARIATION OF LIQUID WATER CONTENT FACTOR WITH
CLOUD HORIZONTAL EXTENT
5.21
0.85
0.2
0.3
0.4
0.5
0.6
0.8
1.0
1.5
2.0
3.0
4.0
5.0
6.0
CLOUD HORIZONTAL EXTENT - NAUTICAL MILES

FIGURE A-6

APPENDIX B

EXCERPTS FROM "ICING TESTS ON THE JT15D TURBOFAN ENGINE" (REF. 20)

Liquid water droplets in the inlet air stream were obtained by spraying a measured flow of water through an array of pneumatic spray nozzles into the duct, see Fig. 5. Matching the computed water flow rate with a proper nozzle atomizing air pressure, which had been established in previous calibration work, yielded droplets with a volume median diameter of 20 microns. In order to prevent freeze-out of the water droplets as a result of the decrease in static temperature with adiabatic expansion in the nozzle, this atomizing air was heated according to the recommendations by Lazelle[4]. A series of nozzle arrays ranging from 3 to 27 nozzles permitted water flow rates between 25 and 550 lbm/hr. During a limited number of tests, ice particles were added to the water droplets in the inlet air stream. These ice particles were generated by feeding blocks of ice into a 12-inch wide bank of multiple 8¼ inch diameter circular saws stacked together. The ice cuttings were transported pneumatically into the inlet duct, see Fig. 4.

During the first part of the 1968/69 icing season, the engine was provided with two typical inlet cowls. For positioning the stagnation streamline at a representative location on the cowl lip, the cowls were encased in a shell, thus forming a narrow annular passage through which external flow was induced by a 50 HP centrifugal blower, see Fig. 6. A section of the inlet ducting was removed immediately after a test for inspection.

Since the cowls were found to have no effect on the engine's icing pattern and since they imposed limitations on engine test conditions and inlet inspection, subsequent testing was carried out with the cell ducting connected directly to the engine front flange.

A typical survey test extended over 30 minutes and followed closely the icing schedule specified in the British Civil Airworthiness Requirements[1]. While most tests were terminated in a normal engine shut-down, followed by a thorough inspection of the inlet, some runs ended in a rapid acceleration to maximum take-off power, testing the engine's ability to accelerate from an iced condition and to ingest any ice which had formed at this lower power setting. During an icing run, critical inlet areas were monitored by closed-circuit TV with the option of taping phases of special interest. After-test recording of iced inlet components consisted of photographic pictures, hand-drawn sketches, and notes of observations. Engine operating and icing environment parameters were logged manually and with a trace recorder.

TEST HIGHLIGHTS

During the course of the JT15D icing program, some 240 tests were carried out, covering the full engine operating range from flight idle to Maximum Continuous, at temperatures down to −33°C.

The anti-icing system that evolved provided the engine with excellent protection under expected icing conditions. Typically, Figs. 7, 8, and 9 show the engine intake after three of the most severe certification tests (Canadian Civil) simulating various flight maneouvres at an inlet temperature of −22°C. In the course of development testing, the engine operated

successfully in icing atmospheres of varying severity up to 30-min. periods of Intermittent Maximum liquid water concentrations[2].

Subsequent to the ground tests, the JT15D was flown in the Cessna Citation aircraft in simulated icing environments behind a tanker. No engine icing problems were revealed in a program which covered the icing envelope up to 23,000 feet altitude with ambient temperatures down to -32°C and liquid water concentrations in excess of Intermittent Maximum .

NOSE CONE

The original engine design did not incorporate nose cone heating. It was hoped that ice accretions on its surface would be controlled by self-shedding because of the action of centrifugal and aerodynamic forces on them. Since the decision "to heat or not to heat" would effect the engine design, a test program was carried out in the winter of 1967/68 on an early engine model with the aim of settling this question.

The test facilities immediately available could not provide sufficient icing environment for the total intake flow. Only one third of the inlet mass flow was conditioned and then ducted to the centre of the engine intake bellmouth. This arrangement provided a completely representative icing environment for the nose cone, with acceptable simulation on the fan blade root and primary flow stator.

Three stainless steel nose cones were designed and built to evaluate the effect of shape on ice accretions. The cones differed only in length to diameter ratio which varied from just over 1.0 to 0.6. Very limited testing showed that, regardless of shape, the unheated nose cones accululated unacceptable ice build-ups on the tip and forward section under moderate icing conditions. In Fig. 10, a close-up view of the classic "flower" formation on the tip of the longest cone is given. On other test runs, where ice did not form on the tip, excessive run back icing occurred at the rear of the nose cone, as can be seen in Fig. 11. This rather strange phenomenon, run back icing on an unheated surface, was the result of heat transfer forward from the fan shaft. Although insufficient tests were carried out to conclusively determine the merits of nose cone shape, it became apparent at this point that de-icing the cone by centrifugal and aerodynamic forces alone would be rather difficult if not impossible.

On the basis of the above tests, the decision was made to heat the nose cone's forward section with compressor bleed air. In the first approach, the cone was heated from the tip approximately halfway along its length. This partial heating resulted in the formation of substantial run back ice aft of the heated section.

It was concluded, at the end of the test program at UACL, that nothing short of a fully heated nose cone would provide acceptable protection against substantial ice formations in this area.

Before continuing with the discussion of subsequent testing, a brief review of some of the factors influencing the design of the nose cone is perhaps in order. The shortest cone tested had a half pound weight advantage over the longest one and, in addition, was calculated to require 23 percent less bleed air. Tests showed, however, that the short cone's aerodynamic performance was inferior to that of the long one. The final nose cone has a length to diameter ratio of 0.86.

Out of the preliminary icing tests on a variety of nose cones described above evolved the one which remained virtually unchanged throughout the icing program at NRC. This final version was protected against icing by compressor bleed air flowing through an annular passage formed by an outer and inner skin, see Fig. 12. As can be seen, the complete surface of the nose cone was heated with bleed air entering at the most critical part, the tip. The air flow was continuous during engine operation, whether in icing or not, and its rate was controlled by a fixed area metering hole. The bleed flow, which also served as a pneumatic bearing seal, was about 0.17% of the gas generator air flow. This air was extracted from behind the high pressure compressor impeller and passed through holes in the high and low pressure rotor shafts. The anti-icing and sealing requirements were so matched that no performance penalty was associated with the nose cone heating. The nose cone bolt was provided with a 0.080-inch bleed hole which was counterbored to 0.150 inch on the outside, see Fig. 12. The purpose of this arrangement was to prevent the formation of an ice cap on the bolt or, at least, induce its shedding. De-icing of the nose cone, once ice had accreted to its surface, was enhanced by centrifugal and aerodynamic forces acting on the ice.

Nose cone icing followed the usual pattern, in that ice accretions increased in size with decreasing speeds and temperatures. At fan speeds (N_1) above 65% or temperatures above -7C, the cone surface was completely free of ice. Moderate accretions of rime ice were recorded at 50% N_1 and -24°C inlet temperature. Prolonged operation at lower power settings, particularly near flight idle (31%), and low temperature (-24°C), produced a large "corona" of rime ice approximately one inch from the nose cone bolt, see Fig. 13. Dangerous as they may have appeared, these coronas have been shed and ingested by the fan on numerous occasions without detrimental effects to the engine.

The history of the bleed hole development through the nose cone bolt will be recounted briefly. Initially, rime ice caps of about 1 inch diameter and 3/4 inch thickness formed on the nose cone bolt, see Fig. 14. A 0.040-inch hole was drilled axially through the bolt with the result that in the subsequent test a hole of approximately equal size was found melted through the ice cap. Enlarging the bleed hole to 0.080 inch increased the size of the hole through the ice cap, but also reduced the size of the cap considerably. Finally, the 0.080-inch hole was counterbored on the outside to 0.150 inch in order to enhance heat diffusion. The ice cap was now of insignificant size, see Fig. 15, and no further modifications were undertaken.

In summary, one can state that while centrifugal and aerodynamic forces undoubtedly furthered the shedding of ice accretions from the nose cone surface, they did not de-ice this surface on their own. The anti-icing system which evolved prevented significant ice build-ups over most of the operating range. Rime ice accretions at low speeds and temperatures were successfully ingested by the fan. Most important, the protective system prevented the formation of hard glaze ice which could have endangered the fan.

PRIMARY FLOW STATOR

Downstream of the fan, the air flow is divided into a primary stream, leading into the gas generator, and a bypass stream. The bypass ratio is 3.2:1. At the beginning of the icing program at NRC, the primary as well as the bypass flow passages were provided with unheated, twin-row fan exit stators.

During the early part of survey testing, occasional jet pipe temperature (JPT) rises well in excess of 100°F were monitored, usually under test conditions at which icing, in general, was light, say a fan speed of 75 to 80% and an inlet temperature of between -11° and -19°C. An investigation into this phenomenon revealed that whenever substantial JPT increases took place, very heavy hammerhead glaze ice formations had formed on the primary flow stator. These formations seemed to start at the splitter ring and extend over part or the whole length of the span of a stator blade. A few typical build-ups projecting from the blades' leading edges are shown in Fig. 16.

Excerpts from "Icing Tests on the JT15D Turbofan Engine" (Ref 20)

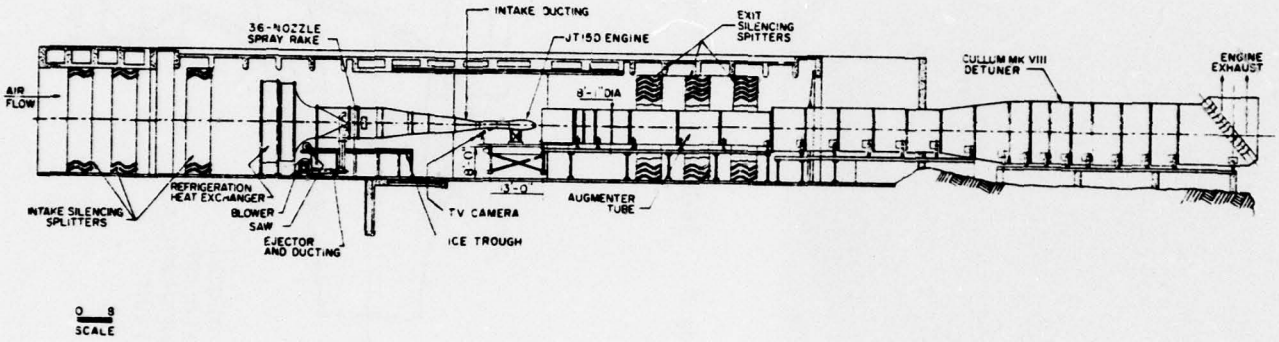

Fig. 4 United Aircraft JT15D Turbofan In No. 4 Test Cell

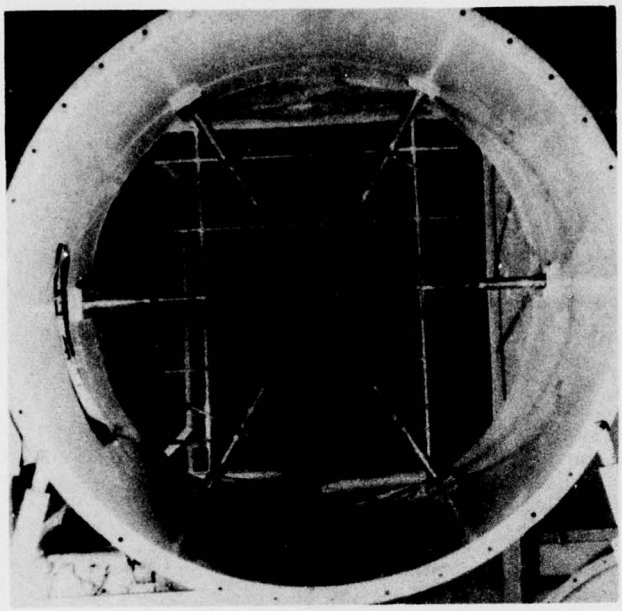

Fig. 5 36-Nozzle Spray Frame

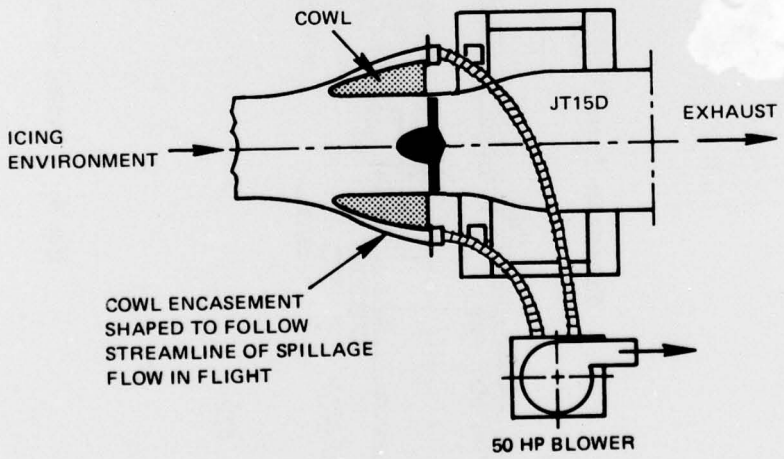

Fig. 6 Schematic of Engine Inlet With Cowl and Blower

Fig. 7 Engine Inlet After Cruising, Descent, and Stand Off Test At CM Concentration, $T_{in} = -22°C$

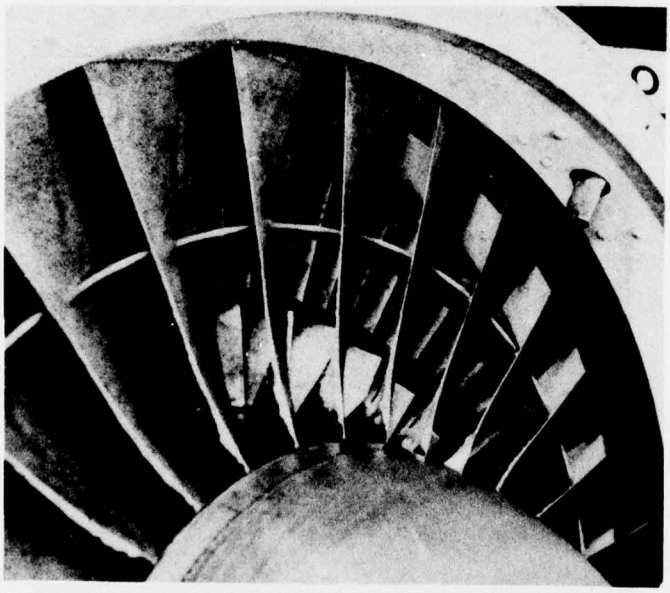

Fig. 8 Engine Inlet After Cruise At IM Concentration, $T_{in} = -22°C$

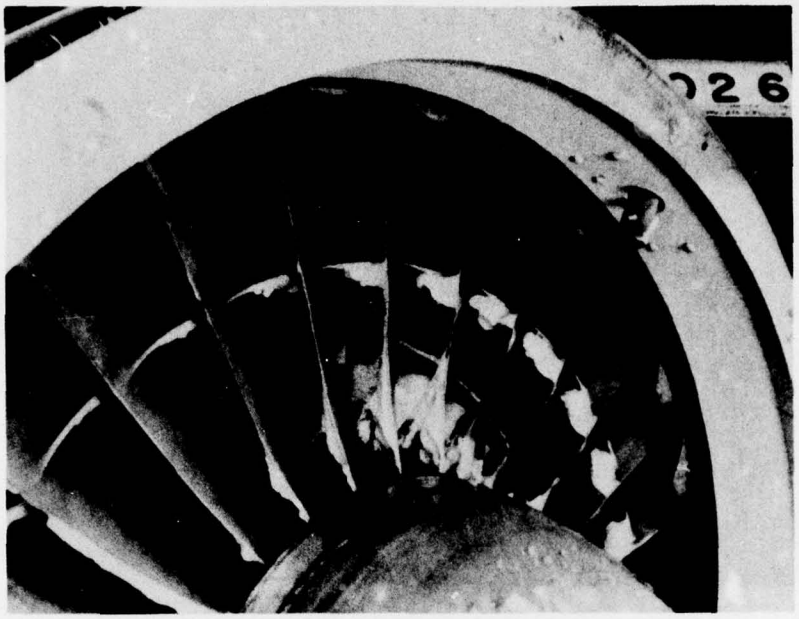

Fig. 9 Engine Inlet After Hold At IM Concentration, $T_{in} = -22°C$

Fig. 10 Glaze "Flower" At Tip of Unheated Nose Cone

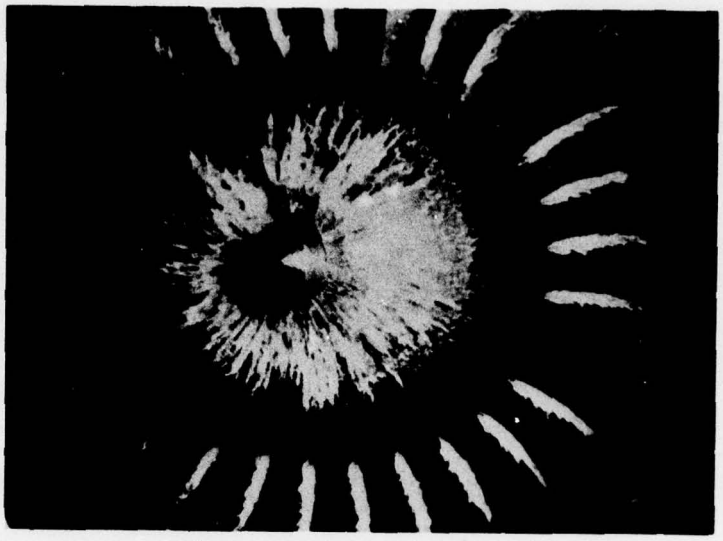

Fig. 11 Run Back Ice On Unheated Nose Cone

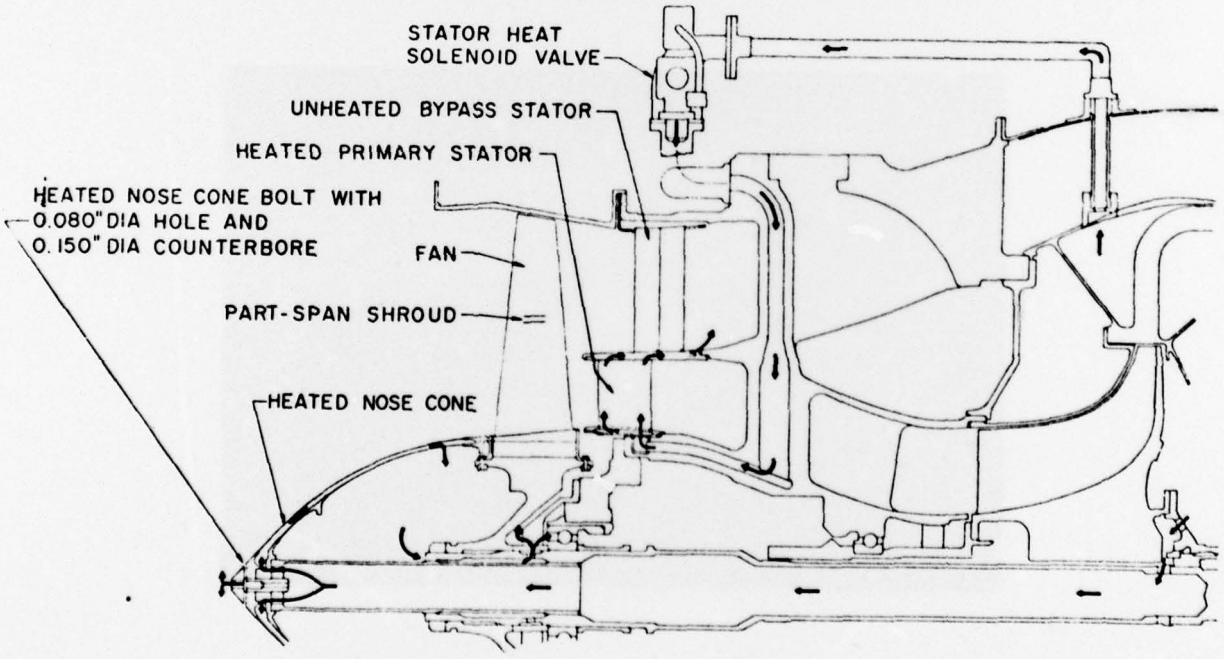

Fig. 12 Schematic of JT15D Anti-Icing System

Fig. 13 Rime Ice "Corona" On Heated Nose Cone

Fig. 14 Rime Ice Cap From Unprotected Nose Cone Bolt

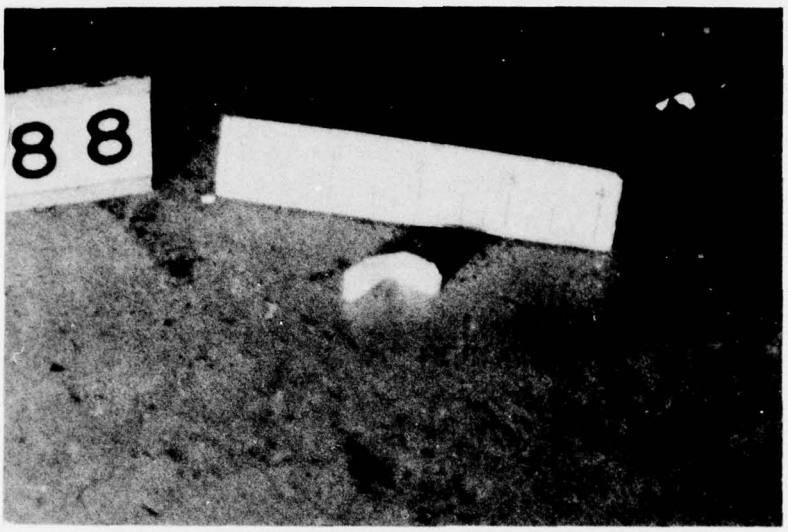

Fig. 15 Reduced Ice Cap From Drilled and Counter-bored Bolt

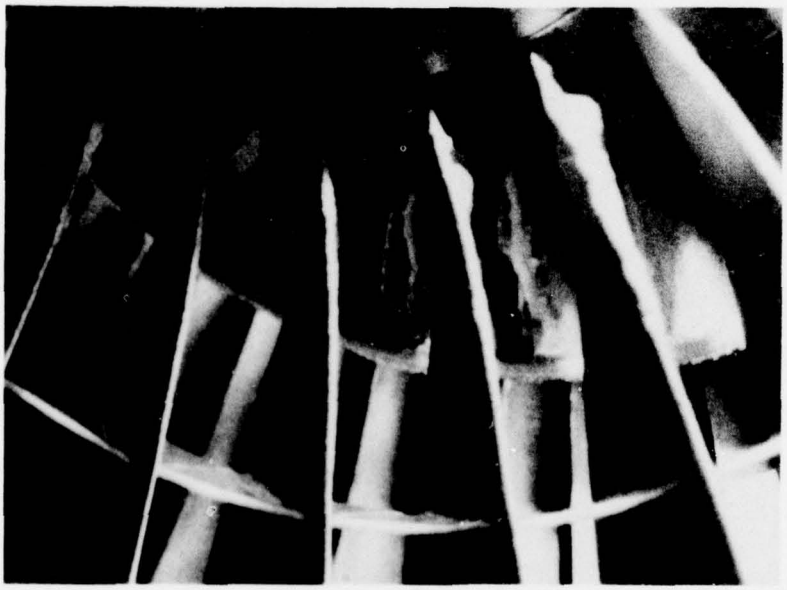

Fig. 16 Glaze Ice Build-Ups On Unheated Primary Flow Stator

APPENDIX C

FAR PART 25.1093
AND
FAR PART 33.67

25.1093 INDUCTION SYSTEM DEICING AND ANTI-ICING PROVISIONS

(a) Reciprocating engines. Each reciprocating engine air induction system must have means to prevent and eliminate icing. Unless this is done by other means, it must be shown that, in air free of visible moisture at a temperature of 30°F., each airplane with altitude engines using–

(1) Conventional venturi carburetors has a preheater that can provide a heat rise of 120°F. with the engine at 60 percent of maximum continuous power; or

(2) Carburetors tending to reduce the probability of ice formation has a preheater that can provide a heat rise of 100°F. with the engine at 60 percent of maximum continuous power.

(b) Turbine engines. Each turbine engine must–

(1) [illegible]te throughout its flight power range (including idling) without adverse effect o[illegible] operation or serious loss of power or thrust under the icing conditions specified in Appendix C of this Part, and in snow, both falling and blowing, within the limitations established for the airplane; and

(2) Idle for 30 minutes on the ground with the air bleed available for engine icing protection at its critical conditions, without adverse effect, in an atmosphere that is at a temperature of 29°F and has a liquid water content of 0.6 grams per cubic meter in the form of drops having a mean effective diameter of 40 microns, followed by a momentary operation at takeoff power or thrust.

33.67 FUEL AND INDUCTION SYSTEM.
(Obsolete: Updated in 1974 by 33.68)

(a) The fuel system must be designed and constructed to supply an appropriate mixture of fuel to the combustion chamber throughout the complete operating range of the engine under all flight and atmospheric conditions.

(b) Each intake passage of the engine through which air, or fuel in combination with air, passes for combustion purposes, must be designed and constructed to minimize the danger of ice accretion in those passages and to allow for a means of ice prevention.

(c) Each engine, with all icing protection systems operating, must be capable of operation throughout the flight power range without the accumulation of ice on the engine components that adversely affects engine operation or that causes a serious loss of power or thrust in continuous maximum and intermittent maximum icing conditions as defined in Appendix C of this chapter.

(d) The type and degree of fuel filtering necessary for protection of the engine fuel system against foreign particles in the fuel must be specified. The applicant must demonstrate that foreign particles passing through the specified filtering means do not critically impair engine fuel system functioning.

(e) If air is bled from the compressor for protection of the engine in icing conditions, provisions must be made for positive indication that air is being directed to the proper passages.

APPENDIX D

FAR PART 33.68

33.68 INDUCTION SYSTEM ICING.

Each engine, with all icing protection systems operating, must–

(a) Operate throughout its flight power range (including idling) without the accumulation of ice on the engine components that adversely affects engine operation or that causes a serious loss of power or thrust in continuous maximum and intermittent maximum icing conditions as defined in Appendix C of Part 25 of this chapter: and

(b) Idle for 30 minutes on the ground, with the available air bleed for engine icing protection at its critical condition, without adverse effect, in an atmosphere that is at a temperature of 29 degrees F and has a liquid water content of 0.6 grams per cubic meter in the form of drops having a mean effective diameter of 40 microns. followed by a momentary operation at takeoff power or thrust.

APPENDIX E

FAR PART 33.77

33.77 FOREIGN OBJECT INGESTION.

(a) Ingestion of a 4-pound bird, a piece of tire tread, or a broken rotor blade, under the conditions set forth in paragraph (f) of this section, may not cause the engine to–

(1) Catch fire;

(2) Burst (penetrate its case);

(3) Generate loads greater than those specified in § 33.23; or

(4) Lose the capability of being shut down.

(b) Ingestion of 3-ounce birds, 1½-pound birds, or mixed gravel and sand, under the conditions set forth in paragraph (f) of this section, may not cause more than a sustained 20 percent power or thrust loss or require the engine to be shut down.

(c) Ingestion of water, ice, or hail, under the conditions set forth in paragraph (f) of this section may not cause a sustained power or thrust loss or require the engine to be shut down.

(d) For an engine that incorporates a protective device, compliance with this section need not be demonstrated with respect to foreign objects sought to be ingested under the conditions set forth in paragraph (f) of this section, if it is shown that–

(1) Such foreign objects are of a size that will not pass through the protective device;

(2) The protective device will withstand the impact of the foreign objects; and

(3) The foreign object or objects stopped by the protective device will not obstruct the flow of induction air into the engine.

(e) In showing compliance with paragraphs (a) and (b) of this section, the engine need be tested by ingesting only that foreign object specified in paragraph (a) which the applicant shows has the most severe effect on the engine and by ingesting the mixed gravel and sand specified in paragraph (b) and either the 3-ounce birds or the 1½-pound birds, as specified in paragraph (f) of this section.

(f) The prescribed foreign object ingestion conditions are as follows:

Foreign object	*Test quantity*	*Speed of foreign object*	*Engine operation*	*Ingestion*
Ice	Maximum accumulation on inlet cowl and engine face resulting from a 30-second delay in actuating anti-icing system.	Sucked in	Maximum cruise.	To simulate an intermittent maximum icing encounter at 25 degrees F.
Hail:				
(0.8 to 0.9 specific gravity).	For subsonic and supersonic engines: With inlet areas of not more than 100 sq. in.: one 1-in. hailstone. With inlet area of more than 100 sq. in.: one 1-in. and one 2-in. hailstones for each 150 sq. in. of inlet area or fraction thereof.	Rough air flight speed of typical aircraft.	Maximum cruise at 15,000 ft. altitude.	In a volley to simulate a hailstone encounter. One half the number of hailstones aimed at random areas over the face of the inlet area and the other half aimed at the critical face area.
	For supersonic engines (in addition): 3 hailstones each having a diameter equal to that in a straight line variation from 1 in. at 35,000 ft. to ¼ in. at 60,000 ft. using diameter corresponding to the lowest supersonic cruise altitude expected.	Supersonic cruise velocity. Alternatively use subsonic velocities with larger hailstones to give equivalent kinetic energy.	Maximum cruise	Aimed for critical engine face area.
Water	4 percent of engine airflow by weight.	Sucked in	Takeoff and flight idle.	For 3 minutes at each engine operation condition as spray to simulate rain.

APPENDIX F

MIL-E-5007D

ICE INGESTION TEST SPECIFICATION

4.6.4.6 Ice Ingestion Test. The test engine shall be subjected to an ice ingestion test to demonstrate compliance with the requirements of 3.2.5.6.3. The type of ice and the conditions for ingestion shall be as follows:

a. One, two (2) inch diameter hailstone and two, one (1) inch diameter hailstones of 0.80 to 0.90 specific gravity for each 400 square inches, or fraction thereof, of inlet area at the engine face at typical takeoff (maximum), cruise, and descent conditions.

b. Sheet ice of 0.80 to 0.90 specific gravity in typical sizes, forms and thicknesses, as approved by the Using Service representative of inlet duct and lip formations in quantities likely to be ingested during takeoff and cruise conditions.

The contractor shall specify in the pretest data the procedures to be used for introduction of ice at the engine inlet and the engine power settings and speed at which the ice or hailstones are to be ingested. The time for engine power recovery shall be recorded. During the tests, high speed photographic coverage of the inlet is required. The test will be considered to be satisfactorily completed when, in the judgement of the Using Service, the performance criteria of 3.2.5.6.3 has been met and there is no evidence of major structural damage which could cause the engine to fail.